THE EXPRESSION AND DRUG TARGETING OF PARASITIC HYPOXANTHINE-GUANINE PHOSPHORIBOSYLTRANSFERASE (HGPRT)

A thesis presented in fulfilment of the requirement of the degree of

DOCTOR OF PHILOSOPHY

In the Division of Chemical Pathology

Faculty of Health Sciences

UNIVERSITY OF CAPE TOWN

University of Cape Town

OCTOBER, 2002

VUYISILE NTOSI PHEHANE

The copyright of this thesis vests in the author. No quotation from it or information derived from it is to be published without full acknowledgement of the source. The thesis is to be used for private study or non-commercial research purposes only.

Published by the University of Cape Town (UCT) in terms of the non-exclusive license granted to UCT by the author.

University of Cape Town

DECLARATION

The work contained in this thesis is original, except where indicated and acknowledged. No portion of this work has been submitted for another degree at this or any other University.

The University of Cape Town may reproduce the contents in whole or in part for the purpose of research.

V. N Phehane

October 2002

University of Cape Town

ABSTRACT

We have expressed and purified human, two forms of *P. falciparum*, and *Toxoplasma gondii* hypoxanthine-guanine phosphoribosyltransferase (HPRT) in *E. coli* using the pET expression system. The cDNA encoding the ORF of HPRT was amplified by PCR and transformed into *E. coli* cells using standard methods. Expression was induced by IPTG and reached about 13% of the total cell protein for all four proteins.

The HPRTs were purified by nickel affinity chromatography. Most of the expressed protein could be isolated from the crude supernatant fraction in a soluble form. Human HPRT was active, with activity levels in the region of 38 μmoles GMP min^{-1} mg^{-1} at 37 °C, which is comparable to published literature values. One of the malarial clones ($HPRT_{pfmet}$) was inactive, and attempts were made to obtain active protein. These included (i) removal or lowering the concentration of imidazole, (ii) inclusion of PRPP, (iii) induction of expression at lower temperatures, (iv) inclusion of reducing agents, (v) expression of $HPRT_{pfmet}$ without the 6x histidine tag. All these attempts failed.

A second malarial HPRT clone ($HPRT_{pfthr}$) was obtained that differed from the $HPRT_{pfmet}$ clone by one base change (Methionine (ATG) to Threonine (ACG) at position 101 of the protein). The $HPRT_{pfthr}$ and *T. gondii* HPRTs purified using standard protocols showed poor activity compared to the published literature values. The purification protocol was modified according to published procedures, but no improvement in $HPRT_{pfthr}$ or *T. gondii* HPRT activity was observed.

$HPRT_{pfthr}$, but not $HPRT_{pfmet}$ or *T. gondii* HPRT, could be activated several fold by incubation with MgPRPP. However, the enzyme was very unstable in the absence of PRPP, and inactivation even occurred during activity assays at pH 8.5 in the presence of PRPP and purine due to the transient formation of unstable intermediates. A new activity assay based on changes in intrinsic tryptophan fluorescence of $HPRT_{pfthr}$ and *T. gondii* HPRT at alkaline pH was developed. Inactivation of $HPRT_{pfthr}$ was accompanied by a 5-10% quenching of the fluorescence.

We synthesised 8-azido xanthine, 8-azido xanthosine and 2',3'-O-(2,4,6-trinitrophenyl) derivatives of 8-azido xanthosine, GMP, IMP and XMP. It was hoped to use the reactivity of the

University of Cape Town

light-activated azido group to generate a diversity of analogues. The key intermediate 8-azido xanthosine has not been synthesised before, and it was achieved in NaN_3-saturated dimethyl sulfoxide spiked with H_2O_2. Light activation of TNP-8-azido xanthosine, but not 8-azido xanthine, yielded the expected diversity of products. Only TNP-GMP inhibited the activity of the malarial HPRT in the micromolar range, and the inhibition was tentatively ascribed to competition with PRPP. None of a library of 38 flavonoids was inhibitory. Light dependent conjugates between TNP-8-azido xanthosine and two flavonoids were not inhibitory.

However, it was found that one flavonoid, 4-iodo-2',4',6'-trihydroxychalcone in the micromolar range activated $HPRT_{pfthr}$ 2 to 3-fold. No effect was observed with the human and *T. gondii* HPRTs. We suggest in this study based on IMP effects and simulations of the HPRT catalytic cycle that 4-I-chalcone may accelerate turnover mainly by activating release of nucleotide by binding to the vacant PPi site, although binding to a vacant IMP site, or an allosteric site, cannot be ruled out. The TNP group of TNP-GMP and the trihydroxy ring of the chalcone may occupy the same position in the PPi site. As far as we are aware this is the first time an activator of any HPRT has been found. The finding that 2,4,6-substituted aromatic compounds may be able to be accommodated at the PPi site offers a new direction for the design of HPRT inhibitors

University of Cape Town

ACKNOWLEDGEMENTS

I wish to express my gratitude to Prof David McIntosh for his supervision, guidance and teaching throughout this study.

I wish to express my sincerest thanks to Dr Anthony Marinaki (King's College London, University of London) for help with the Molecular Biology aspects.

I wish to acknowledge my indebtedness to the following:
Dr Patricia Owen of the Inherited Metabolic Diseases Laboratory, Faculty of Health Sciences, for the generous use of the Molecular Biology laboratory and facilities.
Ms Peggy Mobo for the technical assistance with the glutaraldehyde cross-linking studies
Mr Abduraman Mahomed for the technical assistance in the intrinsic tryptophan fluorescence studies;
Mr David Woolley for technical assistance and laboratory support;
Professor Denis Barron (Laboatorie de Produits Naturels, UMR 5013 CNRS/ Université Claude Bernard-Lyon I, Villeurbanne, France), Dr Attilio Di Pietro (Institut de Biologie et Chimie des Protéines, UMR 5086 CNRS/ Université Claude Bernard-Lyon I, France), and Dr Ahcène Boumendjal (Département de Pharmacochimie Moléculaire, UMR 5063 CNRS/ Université Joseph Fourier, de Grenoble, La Tronche, France) for the flavonoids used in this study;
Dr David Borhani, Dr Geetha Vasanthakumar and Dr Adelaine Leung (Southern Research Institute, Birmingham, Alabama) for the *P. falciparum* G11 and *T. gondii* HPRT C1 cDNA clones;
Dr David Melton (Edinburgh University, Edinburgh) for the *P. falciparum* 7-3g cDNA;
Prof Beverly Davidson (University of Michigan at Ann Harbor), Dr D. J. Jolly (University of California at San Diego, California) for the human HPRT cDNA clone;
Ms Di James (Department of Microbiology, University of Cape Town), Ms Gené Harms, Dr Gene Rousseau (Core Facility, Faculty of Health Sciences, University of Cape Town), Mr Carel Van Heerden and Ms René van Zyl (Stellenbosch University, Cape Town) for automated sequencing;
Ms Hajira Karjiker of the Department of Medical Biochemistry, University of Cape Town, for the PCR primer synthesis.

University of Cape Town

Support from AECI Ltd, the National Research Foundation, the Medical Research Council, and the University of Cape Town is gratefully acknowledged.

University of Cape Town

ABBREVIATIONS

ACN	acetonitrile
ADP	adenosine 5'-diphosphate
AMP	adenosine 5'-monophosphate
ANS	8-anilino-1-naphthalenesulfonic acid
Arg	Arginine
Asn	Asparagine
Asp	Aspartate
ATPase	adenosine 5'-triphosphatase
ATP	adenosine 5'-triphosphate
bp	base pairs
cDNA	complementary DNA
cfu	colony-forming units
CIAP	calf intestinal alkaline phosphatase
Cys	Cysteine
DMSO	dimethlysulfoxide
DNA	deoxyribonucleic acid
DNase	deoxyribonuclease I
dNTP	deoxynucleotide triphosphate
DTE	dithioerythritol
DTNB	5,5'-dithiobis-(2-nitrobenzoic acid)
DTT	dithiothreitol
EPPS	N-[2-hydroxyethyl]piperazine-N'-[3-propanesulfonic acid]
EDTA	ethylenediaminetetraaaecetic acid (disodium salt)
Glu	Glutamate
HCT-15	human colon adenocarcinoma cell line
HPLC	high performance liquid chromatography
HPRT	hypoxanthine (-guanine) phosphoribosyltransferase
HRMS	High Resolution Mass Spectrometry
Ile	Isoleucine
ImmucillinGP/immGP	(1*S*)-1-(9-deazaguanin-9-yl)-1,4-dideoxy-1,4-imino-D-ribitol 5-phosphate
ImmucillinHP/immHP	(1*S*)-1-(9-deazahypoxanthin-9-yl)-1,4-dideoxy-1,4-imino-D-ribitol 5-phosphate

University of Cape Town

IPTG	β-D-isopropyl-thiogalactopyranoside
KPi	KH_2PO_4/ K_2HPO_4
LB	Luria-Bertani medium (Luria broth)
Leu	Leucine
Lys	Lysine
MCF-7	human breast adenocarcinoma cell line
MDR	multidrug resistance
MgPPi	magnesium pyrophosphate
MOPS	3-[N-morpholino]propanesulfonic acid
MS	Mass Spectrometry
N_3	azide
Ni-NTA	nickel nitrilotriacetic acid
NMR	Nuclear Magnetic Resonance
ORF	Open reading frame
PBS	phosphate buffered saline
PCR	polymerase chain reaction
P-gp	P-glycoprotein
Phe	Phenylalanine
PMSF	phenylmethylsulfonyl fluoride
PPi	inorganic pyrophosphate
PRPP	5-phosphorylribose 1-pyrophosphate
PRTase	phosphoribosyltransferase
RNase	ribonuclease
Ser	Serine
SDS-PAGE	sodium dodecyl sulfate polyacrylamide gel electrophoresis
TAE	Tris-acetate buffer
TE	Tris-EDTA buffer
Thr	Threonine
TNBS	2,4,6-trinitrobenzenesulfonic acid
TNP	2',3'-*O*-(2,4,6-trinitrophenyl)
TNPGMP	TNP-guanosine 5'-monophosphate
TNPIMP	TNP-inosine 5'-monophosphate
TNPXMP	TNP-xanthosine 5'-monophosphate
Trp	Tryptophan

University of Cape Town

Tyr	Tyrosine
U	Unit
Val	Valine
X-gal	5-bromo-4-chloro-3-indolyl-β-galactopyranoside
λDNA	lambda DNA

University of Cape Town

TABLE OF CONTENTS

ABSTRACT	i
ACKNOWLEDGEMENTS	iii
ABBREVIATIONS	v
CHAPTER 1 INTRODUCTION	**1**
1.1 The pathology of malaria	1
1.2 The biology of *P. falciparum*	4
1.3 Chemotherapy	6
1.4 Purine salvage pathway	9
1.5 Reaction and kinetics of kinetics of the phosphoribosyltransferases	12
1.6 The structure and catalytic mechanism of HPRT	17
1.7 Drug targeting of parasitic HPRTs	31
1.8 Photolabile ligands	34
1.9 Trinitrophenyl-nucleosides/nucleotides	40
1.10 Flavonoids	44
1.11 The approach taken in this study	46
CHAPTER 2 MATERIALS AND METHODS	**53**
2.1 Molecular biology methods for human HPRT	53
2.2 Molecular biology methods for malarial HPRT	59
2.3 The expression and purification of human and malarial HPRT	62
2.4 The molecular biology of malarial HPRT cDNA clone G11	67
2.5 The molecular biology of *Toxoplasma gondii* HPRT cDNA clone C1	68
2.6 Reactivation studies	69
2.7 Stability studies on $HPRT_{pfthr}$	71
2.8 Chemical syntheses	72
2.9 Drug screening	75
2.10 Fluorescence studies	81

University of Cape Town

CHAPTER 3 RESULTS **84**

3.1 The molecular biology of human HPRT 84

3.2 The molecular biology of malarial HPRT 92

3.3 The expression and purification of human and malarial HPRT 96

3.4 The expression and purification of malarial HPRT clone G11 107

3.5 The expression and purification of Toxoplasma gondii clone C1 110

3.6 Reactivation studies 114

3.7 Stability studies on $HPRT_{pfthr}$ 119

3.8 Chemical syntheses 131

3.9 Drug screening 157

3.10 Fluorescence studies 165

CHAPTER 4 DISCUSSION **176**

4.1 Sequencing and expression 177

4.2 Purification 180

4.3 Activity 180

4.4 Inactivation during turnover 185

4.5 Fluorescence studies 193

4.6 Chemical syntheses and inhibition studies 195

4.7 Activation of $HPRT_{pfthr}$ by a flavonoid 203

APPENDIX **210**

BIBLIOGRAPHY **231**

University of Cape Town

CHAPTER 1 INTRODUCTION

Malaria is Africa's third most infectious disease after pneumococcal respiratory infections and tuberculosis. About 90% of the world's malaria cases occur in Africa. To date, 90 countries worldwide are defined as malarious, and about 50% of these are in sub-Saharan Africa. Up to 500 million people per annum are infected, and 1.5 to 2.7 million die from malaria. Approximately 90% of these deaths occur in sub-Saharan Africa, mostly amongst children less than five years of age (WHO report, 1996).

1.1 The pathology of malaria

In Africa, the Anopheles gambiae mosquito upon feeding on human blood transmits malaria. This vector occurs in tropical and subtropical regions, as well as in regions of temperate climate.

The causative agent of malarial infection is *Plasmodium falciparum, P. vivax, P. ovale or P. malariae.* Infection by *P. falciparum* leads to anaemia, cerebral malaria or death. Disease is caused by the asexual blood stages of the parasite, when erythrocytes are destroyed and cell debris, lipids, and proteins are released into the blood upon schizont rupture (Jacobsen *et al.*, 1995). Symptoms and features of malaria infection include headache, back and limb pain, chills, nausea, vomiting diarrhoea, dehydration and elevated body temperature. Renal failure is common in acute malaria, affecting about 50% of patients (Trang *et al*, 1992). Anaemia (Achidi *et al.*, 1996), spleen enlargement (Looareesuwan *et al.*, 1987) hepatic dysfunction, acidosis (English *et al.*, 1996), hypoglycaemia (White *et al.*, 1983) are other conditions caused by severe malaria. Infected erythrocytes may become sequestered in the capillaries and venules of vital organs such as the brain, heart, kidney, intestines and adipose tissue (MacPherson *et*

University of Cape Town

al., 1985) and obstruct blood flow. Oxygen and substrate availability become limited, resulting in anaerobic glycolysis and lactic acidosis (White and Ho, 1992).

There are other infectious protozoan organisms, and these include *Tritrichomonas foetus Trypanosoma cruzi*, *Trypanosoma brucei* and *Toxoplasma gondii*. *T.foetus* is an anaerobic flagellated organism that causes embryonic death and infertility in bovines by infection of the urogenital tract (Parsonson *et al.*, 1974; Fitzgerald, 1986; Williams *et al.*, 1987). *T cruzi* and *T. brucei*, the etiological agents of Chaga's disease and African sleeping sickness, are both fatal in humans. Nagana is also caused by *T. brucei*, and is fatal in humans as well as domestic animals (Garcia-Zapata *et al.*, 1991; Allen and Ullman, 1993).

T. gondii (a member of the Apicomplexa) is an obligate intracellular parasite. In some conditions in humans, toxoplasmosis can result in pneumonia, hepatitis and blindness. A common manifestation is lymphadenitis of the deep cervical nodes in humans, commonly associated with the progression of AIDS (Seitz and Trammer, 1998; Roullet, 1999). Cerebral toxoplasmosis-induced encephalitis and brain absces are caused by *T. gondii* infection, and are the second-leading causes of death amongst immunocompromised AIDS patients (Levy *et al.*, 1985; Murray, 1991; Luft *et al.*, 1994). Toxoplasmosis can be transmitted via the placenta, resulting in spontaneous abortion, or physically and/or mentally challenged newborn children (Carruthers, 2002), or pulmonary infection (Campagna, 1997). Infection by *T. gondii* is a primary cause of abortion in livestock.

The life cycle of *T. gondii* occurs in two phases. The first is the intestinal (or enteroepithelial) phase, for which the cats (Felidae) are the definitive host. The second is the extraintestinal

University of Cape Town

phase, where mammals, rodents and other animals are the intermediate host. Cats are not excluded from the latter phase. The life cycle is given below in Figure 1.1.

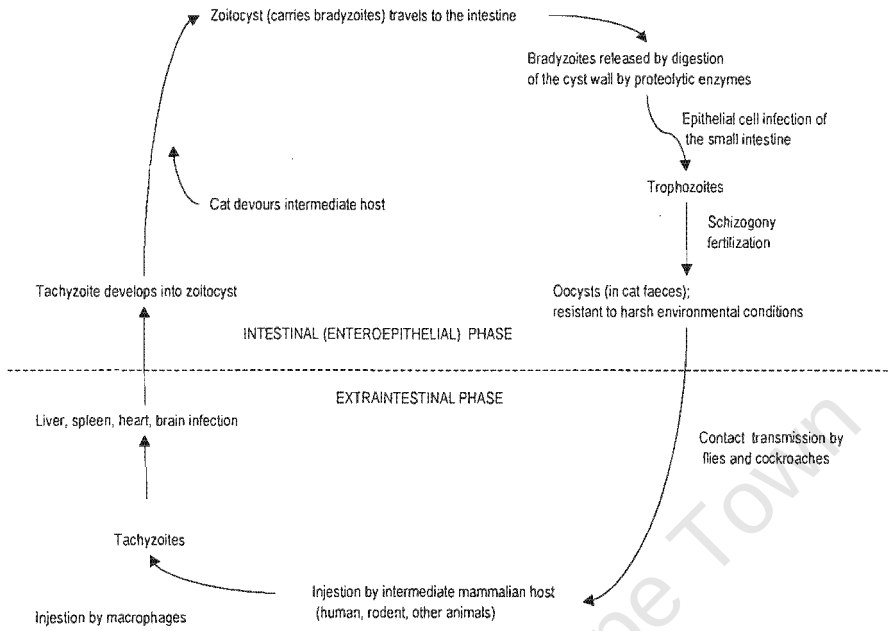

Figure 1.1 Life cycle of *T. gondii* (Adapted from Dubey, 1986; 1998)

Rodents infected with zoitocysts are devoured by cats, and digestion of the cyst by proteolytic enzymes releases bradyzoites. The bradyzoites develop into trophozoites, which in turn undergo schizogony and fertilisation to form oocysts. The resistant oocysts (which are resistant to harsh environmental conditions) are released in the faeces of cats, and transmission is through contact of the faeces with flies or insects. Oocysts can be injested by intermediate hosts like humans, where they are taken up by macrophages. Once an immune response is evoked, tachyzoites are released, and are capable of infecting almost any organ such as the liver, brain, spleen and heart. The tachyzoites develop into zoitocysts, for re-infection (Dubey, 1998).

University of Cape Town

The sulfonamides (sulfadiazine, sulfamethazine, sulfamerazine) and pyrimethamine are used together to treat toxoplasmosis in humans, by inhibiting the *p*-aminobenzoic acid and the folic-folinic acid cycle. An emerging approach is the use of immunotherapy (interleukin-2, -6, and –12, as well as interferon-gamma and alpha-tumour necrosis factor) to restore the immune system (Fung and Kirschenbaum, 1996).

1.2 The biology of *P. falciparum*

The life cycle of *P. falciparum* is shown in Figure 1.2, and illustrates the three stages of the life cycle, namely the vector (*Anopheles* host), tissue and erythrocytic stages. The exogenous sexual phase (sporogony) occurs in the Anopheles mosquito. The endogenous asexual phase (schizogony) occurs in the host liver parenchyma cells (exoerythrocytic) and in the red blood cell (intraerythrocytic).

University of Cape Town

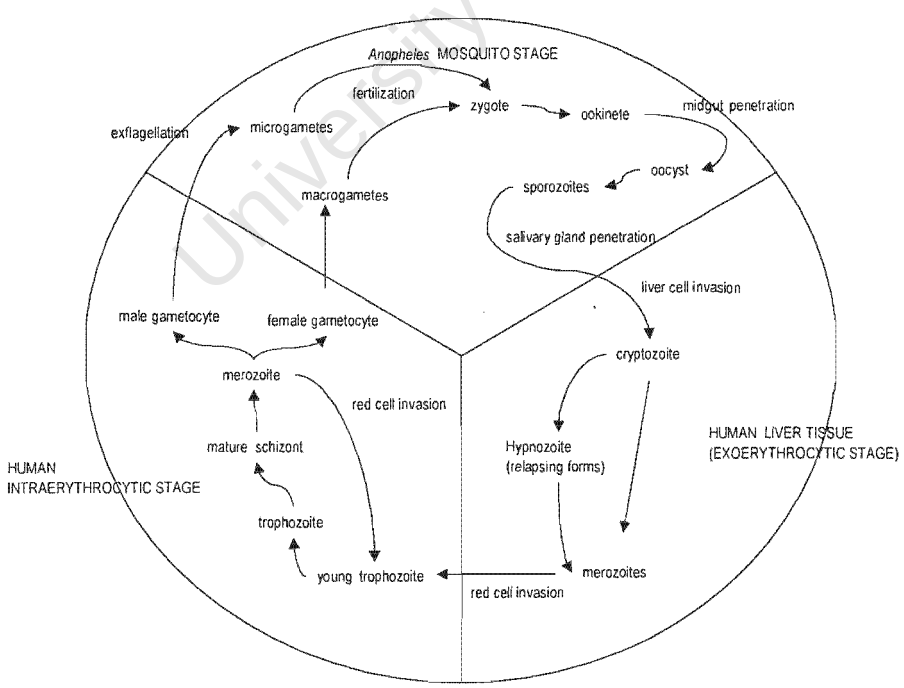

Figure 1.2 The life cycle of *P. falciparum* (adapted from Sherman, 1998)

As shown in Figure 1.2, the male gametocyte sheds its flagella (exflagellation) in the mosquito vector. The male microgametocyte and the female macrogametocyte fuse in the mosquito stomach and the fusion event or fertilization, results in a zygote. The zygote elongates within 24 hours to form a mobile oökinete. The oökinete settles on the outer surface of the stomach and assumes a spherical shape. At this stage it is called an oöcyst. The oöcyst becomes enlarged and pigmented. Its nucleus and cytoplasm undergo subdivision. Subdivision of the cytoplasm forms interconnected lobes. Elongated sporozoites are released from the oöcyst and migrate to the salivary glands. Once in the salivary glands, the sporozoites can be transmitted to the human host blood stream upon mosquito feeding. Sporozoites invade the parenchymal cells of the host liver, where they develop into the cryptozoite and hypnozoite forms, the latter occurring in relapsing forms of malaria. The crypotozoites can develop directly into exoerythrocytic merozoites that invade the red blood cell. Invasion involves invagination of the red blood cell surface via rhoptries and micronemes found at the apex of the merozoite. Development proceeds from the young trophozoite form to the intraerythrocytic merozoite form. The merozoites infect uninfected red blood cells and this cyclic event leads to more merozoites being formed. The merozoites differentiate into male and female micro- and macrogametocytes respectively (Bruce-Chwatt, 1985).

University of Cape Town

The intraerythrocytic phase is of interest from the point of view of this study because DNA replication occurs during schizont maturation (Janse *et al.*, 1986), and there is a greatly increased demand for nucleotides and their precursors. Antimalarial intervention in these anabolic pathways is particularly attractive.

1.3 Chemotherapy

A number of drugs are used as antimalarials. They fall into six general categories, namely, (1) inhibitors of the folate pathway (pyrimethamine, sulphonamides, sulphones), (2) inhibitors of mitochondrial electron transport and pyrimidine synthesis (atovaquone), (3) inhibitors of haeme polymerisation into haemazoin (chlororquine, quinine, amodiaquine, pyronaridine, mefloquine, halofantrine), (4) free radical alkylators (artemisinin, artesunate), (5) inhibitors of protein synthesis (tetracyclin, doxycyclin, azithromycin), and (6) inhibitors of DNA gyrase (quinolones). However, the use of many of these antimalarials has been limited in recent years by the development of resistance. Other limitations relate to their toxicity. Table 1.1 lists some of these drugs together with mode of action and limitations.

University of Cape Town

Table 1.1 Some antimalarial drugs currently in use, and their associated disadvantages (Adapted from Rosenthal, 1998)

Drug	Some disadvantages	Mode of action
Maloprim (dapsone/pyirimethamine)	Resistance; causes skin rashes	Inhibit the DHPS and DHFR of the folate pathway
Fansidar (pyrimethamine/sulfadoxine)	Slow-acting; dermatological activity	
Atovaquone	Recurrence; resistance when used alone	Inhibits mitochondrial electron transport and pyrimidine synthesis
Quinine/ quinidine	Cardiac toxicity	Inhibit haeme polymerisation to haemozoin
Chloroquine	Resistance, except in Central America	
Amodiaquine	Resistance; liver and bone marrow toxicity	
Halofantrine	Inconsistent bioavailability; cardiac toxicity	
Pyronoradine	Limited studies conducted	
Mefloquine	Resistance in South East Asia and Africa; CNS toxicity	
Primaquine	Resistance; cannot be administered to patients with G6PD deficiency	
Proguanil	Resistance; causes mouth ulcers	
Artemisinin and derivatives (Artelinate, Arteether, Artesunate, Artemether)	Recurrence; metabolised to dihydroartemisinin, a neurotxin	Alkylate free radicals
Tetracyclines	Slow-acting; skin toxicity; gastrointestinal Toxicity	Antibiotic inhibitors of protein synthesis
Doxycyclin	Phototoxicity; unsafe for children and pregnant women; not tolerated by the gastrointestinal system	
Azithromycin	Limited studies conducted	

CNS, central nervous system; DHFR, dihydrofolate reductase; DHPS, dihydropteroate synthase; G6PD, glucose 6-phosphate dehydrogenase

Mechanisms of resistance include mutations in the target protein and drug efflux. An example of the first mechanism is resistance to antifolates such as pyrimethamine and cycloguanil. A number of point mutations in the *dhfr-ts* gene have been found, and were demonstrated to confer resistance of *P. falciparum* to these antifolates (Cowman *et al.*, 1988; Peterson *et al.*, 1988, 1990; Zolg *et al.*, 1989; Foote *et al.*, 1990a). The primary mutation in the DHFR domain leading to antifolate resistance (especially resistance to pyrimethamine) was Ser-108 to Asn. Others included the double mutations, Ser-108 to Asn and Cys-59 to Arg, or Ser-108 to Asn and Asn-51 to Ile, and triple mutations. The double and triple mutations conferred higher levels of resistance to the pyrimethamine component of the combination. Strains with the double mutation Ser-108 to Asn, and Ile-164 to Leu were found to be resistant to both pyrimethamine

University of Cape Town

and cycloguanil, while it was the Ala-16 to Val and Ser-108 to Thr double mutation that conferred resistance to cycloguanil only (Peterson *et al.*, 1990; Foote *et al.*, 1990a). There is an indication that the mutations interact co-operatively to confer resistance (Sirawaraporn *et al.*, 1997).

Increased drug export is a second possible mechanism of resistance. Direct evidence of the export of chloroquine, mefloquine and halofantrine in *P. falciparum* by the P-glycoprotein homologue 1 (Pgh1) protein was provided by Reed and co-workers (2000). Verapamil (a calcium channel blocker) and other compounds known to reverse MDR (multidrug resistance) in neoplastic cells were shown to reverse chloroquine resistance. It is on the basis of these experiments that ABC (ATP-binding cassette) transporters were suggested to be involved in chloroquine resistance in malarial parasites (Martin *et al.*, 1987; Kyle *et al.*, 1990, Foot *et al.*, 1990b). Resistance to mefloquine and halofantrine by *P. falciparum* has been associated with increased gene copy number and expression of the *pfmdr*1 gene of *P. falciparum* (Wilson *et al.*, 1993).

More recently, chloroquine resistance has been linked to multiple mutations in the *Plasmodium falciparum* Chloroquine Resistance Transporter (PfCRT), which seems to be a chloroquine transporter in the parasite's digestive vacuole membrane (Wellems and Plowe, 2001; Carlton *et al.*, 2001; Nomura *et al.*, 2001).

The development of resistance has increased the urgency to find new protein targets and drugs. The identification of enzymes that are unique to the parasite and vital for its existence needs to be hastened. Specific inhibitors of such enzymes using structure-based drug design and molecular modelling could be developed.

University of Cape Town

1.4 Purine salvage pathway

Two pathways are used for the synthesis of nucleotides. These are the *de novo* pathway and the salvage pathway. *De novo* synthesis begins with the precursors amino acids (glycine, aspartate and glutamine), carbon dioxide, ammonia and ribose 5-phosphate, whereas the salvage pathway recovers free bases and nucleotides of nucleic acid degradation.

Most protozoan parasites including *P. falciparum* appear to be incapable of *de novo* purine synthesis. This was demonstrated for *P. falciparum* by the lack of radiolabelled formate and glycine uptake (Sherman, 1979). Purine and purine nucleosides are however salvaged from the host (Sherman, 1979; Hassan and Coombs, 1988), and the parasite relies completely on the salvage pathway to obtain purines. Figure 1.3 shows the purine salvage pathway in *P. falciparum*, and the enzymes that are involved in this pathway.

University of Cape Town

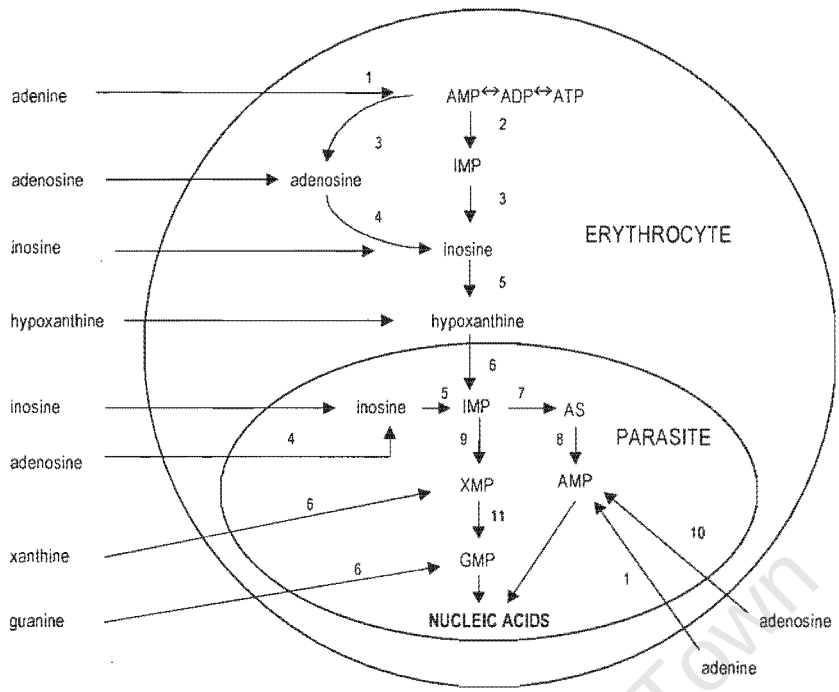

Figure 1.3 Purine salvage pathway of intraerythrocytic *P. falciparum* (Sherman, 1998)
ATP, adenosine 5'-triphosphate; ADP, adenosine 5'-diphosphate; AMP, adenosine 5'-monophosphate; IMP, inosine 5'-monophosphate; XMP, xanthosine 5'-monophosphate; GMP, guanosine 5'-monophosphate; 1, APRT, adenine phosphoribosyltransferase; 2, adenosine monophosphate deaminase; 3, 5' nucleotidase; 4, ADA, adenosine deaminase; 5, nucleoside kinase; 6, HPRT, hypoxanthine-guanine phosphoribosyltransferase; 7, ASS, adenylosuccinate synthetase; 8, ASL, adenylosuccinate lyase; 9, IMPDH, inosine monophosphate dehydrogenase; 10, AK, adenosine kinase; 11, GMPS, guanosine monophosphate synthetase

The purines hypoxanthine, guanine, xanthine and adenine enter the parasite and become phosphoribosylated through PRPP (phosphoribosyl-1-pyrophosphate), a reaction catalysed by HPRT and APRT respectively. This reaction affords nucleoside 5'-monophosphates IMP, GMP, XMP and AMP respectively. The figure indicates inosine or adenosine may also be a source of nucleoside 5'-monophosphates. A supply of hypoxanthine from the host is critically important as depletion of medium hypoxanthine using xanthine oxidase inhibited the growth of *P. falciparum* in erythrocytes cultured in vitro (Berman *et al.*, 1991).

University of Cape Town

Since the malarial parasite (as well as other protozoan parasites) relies heavily on the HPRT enzyme for salvage hypoxanthine, guanine and xanthine, inhibition of this enzyme may be a means of control. The HPRT enzyme is discussed below in some detail.

University of Cape Town

1.5 Reaction and kinetics of the phosphoribosyltransferases

Phosphoribosyltransferases (PRTs) are involved in the synthesis of pyrimidine, pyridine and purine nucleotides, as well as the amino acids tryptophan and histidine (Musick, 1981). Purine PRTs are specific for a nitrogenous (aromatic) base, divalent metal ions and α-D-5-phosphoribosyl 1-pyrophosphate (PRPP), and all three are necessary for catalysis. During catalysis, the phosphoribosyl group is transferred from PRPP to the N9 position of the purine base to form purine nucleotides and inorganic pyrophosphate, and this is represented in Figure 1.4.

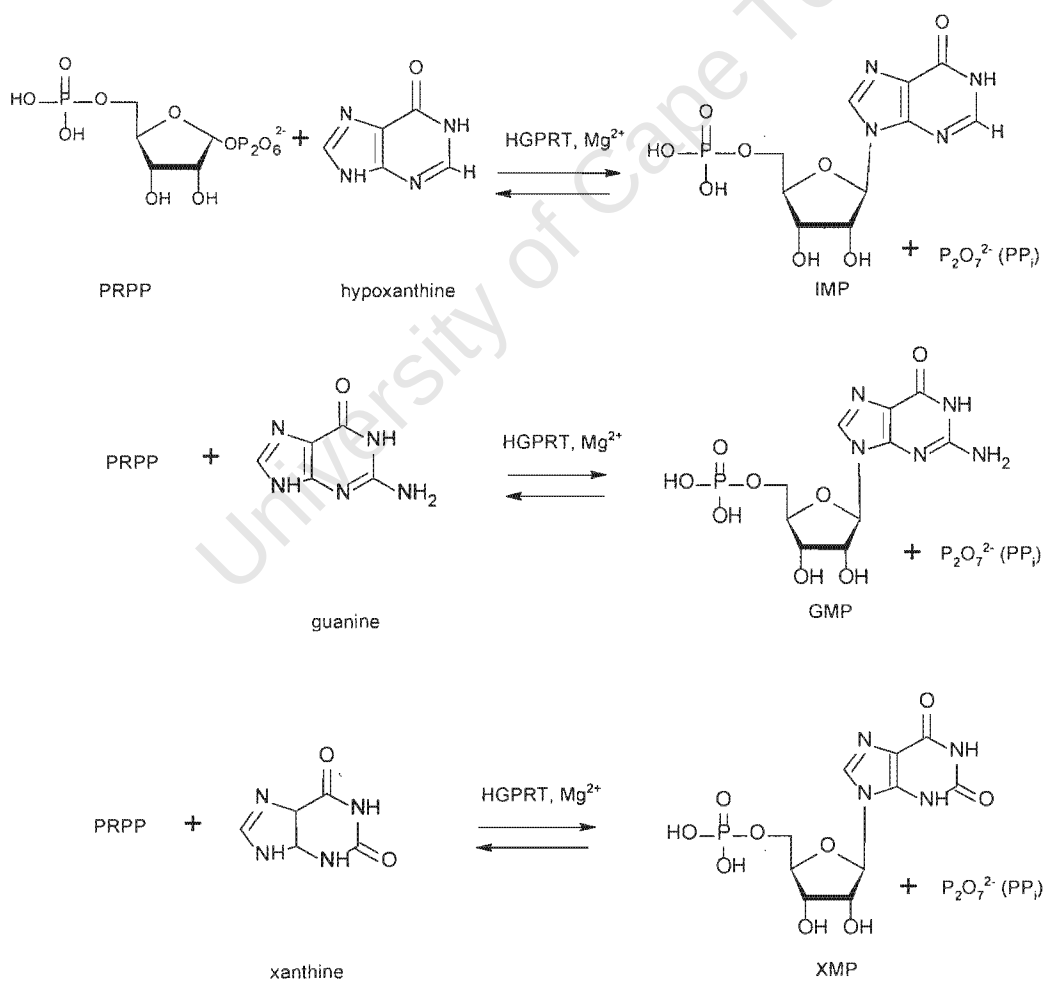

Figure 1.4 Ribose 5-phosphate transfer in HPRT (Eads *et al.*, 1994; Héroux *et al.*, 1999a)

University of Cape Town

The forward reaction occurs by ordered binding of PRPP first, followed by the purine (Hendersen *et al.*, 1968; Giacomello and Salerno, 1978). PPi is released first, and then nucleotide (Yuan *et al.*, 1992; Xu *et al.*, 1997; Munagala *et al.*, 1998). Nucleotide and PPi either bind in a random equilibrium manner in the reverse direction (Giacomello and Salerno, 1978), or the nucleotide binds first (Xu *et al.*, 1997)

The reaction mechanism could follow dissociative mechanism chemistry (S_n1), in which the bond between PPi and the ribose 5'-phosphate breaks before attack by the N9 nucleophile on the C1' of the ribose 5'-phosphate. In this scenario, an unstable oxocarbenium cation forms as a distinct entity. It could also follow an associative mechanism (S_n2), where the breaking of the bond between PPi and ribose 5'-phosphate occurs at the same time as the glycosidic N9-C1' occurs. The pathways are shown in Figure 1.5.

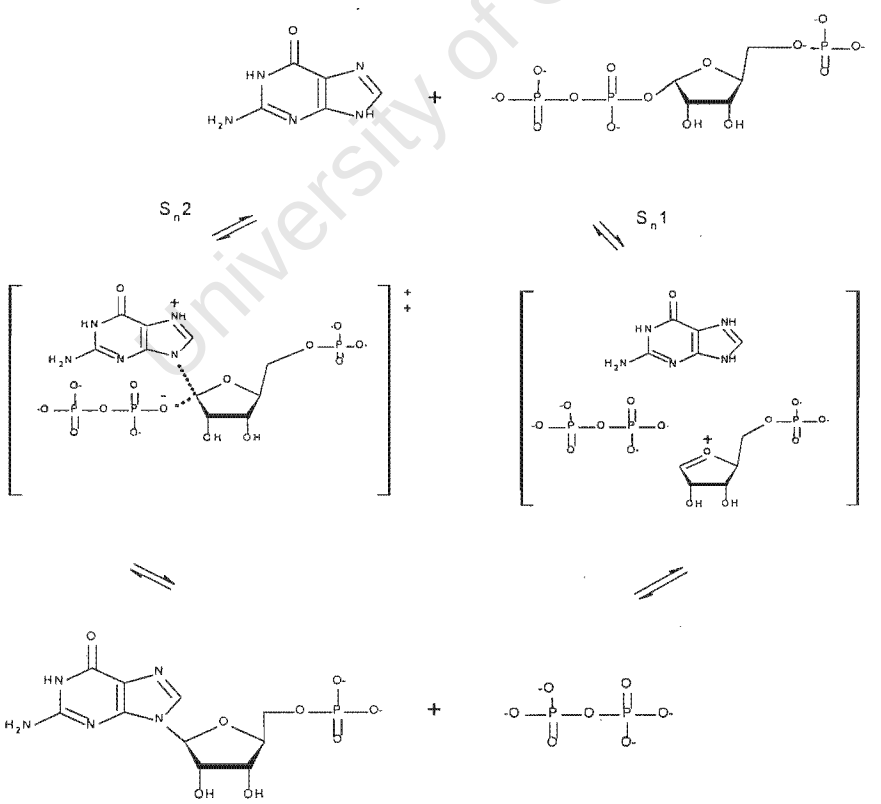

Figure 1.5 Illustration of dissociative and associative chemistry (Craig and Eakin, 2000). The transition state is in square brackets

University of Cape Town

Evidence for an S_n1 type of reaction has come from two kinetic isotope studies of PRTs (Goiten *et al.*, 1978) and OPRT from *Salmonella typhimurium* (Tao *et al.* 1996). Large α secondary ^3H and small primary ^{14}C effects were found, and are indicative of a separate oxocarbenium cation with double bond formation between O4' and C1'. The extremely tight binding of transition state-like nucleotides where the O4' of the ribosyl moiety is replaced by a protonatable nitrogen to yield an iminocarbenium cation (Shi *et al.*, 1999a; 1999b; see later for detailed structure), is compatible with an S_n1 mechanism. However, an S_n2 mechanism, with transient cation formation during the course of concerted bond breaking and formation, is not ruled out. The identification of water molecules in the active site of the *T. gondii* $HPRT_{XMP,\ PPi}$ complex suggests that a distinct, highly reactive oxocarbenium cation is unlikely to form (Héroux *et al.*, 1999b). Further, the geometry of the complex in the region of the chemical reaction is such that no major shifts in the position of the XMP or PPi need to occur for PRPP and xanthine to form, suggesting a concerted S_n2 reaction.

Xu and colleagues (1997) detailed the kinetic mechanism of human HPRT using equilibrium gel filtration, rapid quench and isotope trapping. Their findings from equilibrium gel filtration and isotope trapping experiments suggest that PRTs follow an ordered bi-bi mechanism, with PRPP binding first before purine base in the presence of Mg^{2+}. Release of product is also ordered, with the release of PPi before nucleotide. In the reverse direction, GMP or IMP binds first. Phosphoribosyl transfer was monitored using rapid quench techniques, and it was shown that transfer was very rapid under pre steady-state conditions. Kinetic studies in the reverse direction showed that release of the product PRPP is partially rate limiting. These authors proposed a scheme for the kinetic mechanism of human HPRT, which is shown in Figure 1.6 below.

University of Cape Town

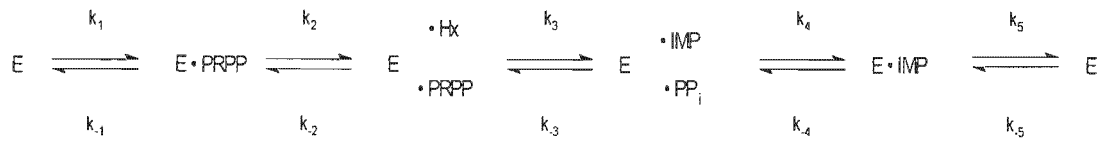

Figure 1.6 Kinetic mechanism of human HPRT (Xu *et al.*, 1997)

PRPP binds first before the hypoxanthine, and PPi is released before IMP release. The transfer of the phosphoribosyl group is rapid in both the forward and reverse directions. Hypoxanthine dissociation is rapid in the reverse direction, whereas the release of PRPP is partially rate limiting. The kinetic constants for the illustration in Figure 1.5 are presented in Table 1.2.

Table 1.2 Kinetic constants for human HPRT (Xu *et al.* (1997)

Rate constant	Value	Rate constant	Value
k_1	$0.2 \times 10^6\ M^{-1}s^{-1}$	k_{-3}	$9s^{-1}$
k_{-1}	$0.24s^{-1}$	k_4	$>12s^{-1}$
k_2	$1.97 \times 10^7\ M^{-1}s^{-1}$	k_{-4}	$>0.09 \times 10^6\ M^{-1}s^{-1}$
k_{-2}	$9.5s^{-1}$	k_5	6.05^{-1}
k_3	$131s^{-1}$	k_{-5}	$0.09 \times 10^6\ M^{-1}s^{-1}$

Several studies report on the kinetic parameters of HPRTs from different sources, and some of these are presented in Table 1.3 below.

University of Cape Town

Table 1.3 The kinetic parameters of human and protozoan PRTs

HPRT reaction

		K_m (μM)		k_{cat}/K_m ($\mu M^{-1}s^{-1}$)		
	k_{cat} (s^{-1})	Hx	PRPP	Hx	PRPP	
human	15.7	2.4	15.2	6.48	1.03	(Héroux *et al.*, 1999b)
P. falciparum	**0.6**	0.9	59.8	0.75	**0.01**	(Keough *et al.*, 1999)
T. gondii	7.59	1.6	42.9	4.6	0.18	(White *et al.*, 2000)

GPRT reaction

		K_m (μM)		k_{cat}/K_m ($\mu M^{-1}s^{-1}$)		
	k_{cat} (s^{-1})	Gua	PRPP	Gua	PRPP	
human	70.3	4.2	32.8	16.8	2.1	(Héroux *et al.*, 1999b)
P. falciparum	**2.4**	1.4	362	1.5	**0.007**	(Keough *et al.*, 1999)
T. gondii	12.7	2.1	74.6	6.02	0.17	(White *et al.*, 2000)

XPRT reaction

		K_m (μM)		k_{cat}/K_m ($\mu M^{-1}s^{-1}$)		
	k_{cat} (s^{-1})	Xan	PRPP	Xan	PRPP	
human	0.27	20	237	0.013	0.001	(Héroux *et al.*, 1999b)
P. falciparum	**1.3**	420	168	0.005	**0.008**	(Keough *et al.*, 1999)
T. gondii	31.0	14.4	146.0	2.15	0.21	(White *et al.*, 2000)

k_{cat} and k_{cat}/K_m for *P. falciparum* (shown in bold) were calculated using the molecular mass of 26229 Da (Keough *et al.*, 1999). Hx, hypoxanthine; Gua, guanine, Xan, xanthine.

The k_{cat} values for human and two protozoan PRTs reveal that the human enzyme is the fastest with hypoxanthine and guanine as substrates, and is worst with xanthine. The enzyme from the malarial parasite performs poorly, being 5 to 30-fold slower than the *T. gondii* enzyme, depending on the substrate. The catalytic efficiency as encompassed in k_{cat}/K_m is also poor for the malarial enzyme. This is surprising in view of its importance for the parasite. The K_m with respect to hypoxanthine and guanine is similar in all three enzymes, but that with respect to PRPP when guanine is substrate is higher, although how this occurs in an ordered mechanism where guanine binding follows PRPP binding is unclear. The K_m for xanthine is very high with the malarial enzyme.

University of Cape Town

1.6 The structure and catalytic mechanism of HPRT

The ORFs of human, *T. gondii, P. falciparum and T. cruzi* HPRTs range from 650 to 690 bp, and the polypeptide sizes from 24.5 to 26.6 kDa (Jolly *et al.*, 1983; Vasanthakumar *et al.*, 1994; Vasanthakumar *et al.*, 1990; Allen and Ullman, 1994). The amino acid sequences of Human, *T. gondii*, *P. falciparum*, *T. cruzi* and *T. foetus* HGPRTases are aligned in Figure 1.7. The amino terminal end is somewhat variable with the first conserved residues (Arg and Ala, shown in bold) being associated with a large helix spanning the whole of one side of the protein. Other conserved amino acid residues are largely associated with the active site (underlined). The most conserved stretch is the PRPP binding motif, the end of which constitutes a P-loop (DTGKT), common in ATP-utilising enzymes. The proteins end with a highly polar segment.

University of Cape Town

human
gondii
P. fal.
T. cru.
T. foetus.

Figure 1.7 Sequence alignment of a selection of HPRTs (Héroux *et al.*, 1999a). Absolutely conserved residues are shown in bold, while active site residues are underlined. The PRPP binding motif is shaded. Dimer interfaces in malarial HPRT are shown boxed. T.gon (*T. gondii*), P.falc (*P. falciparum*), T.cruz (*T. cruzi*), T. foet (*T. foetus*).

Eads and colleagues (1994) were the first to publish a 3-D structure of an HPRT (shown in Figure 1.8), and it was the human HPRT with bound GMP. The protein consisted of a dimer along the non-crystallographic 2-fold symmetry and a tetramer along the crystallographic symmetry axis. The two axes are nearly perpendicular to each other.

University of Cape Town

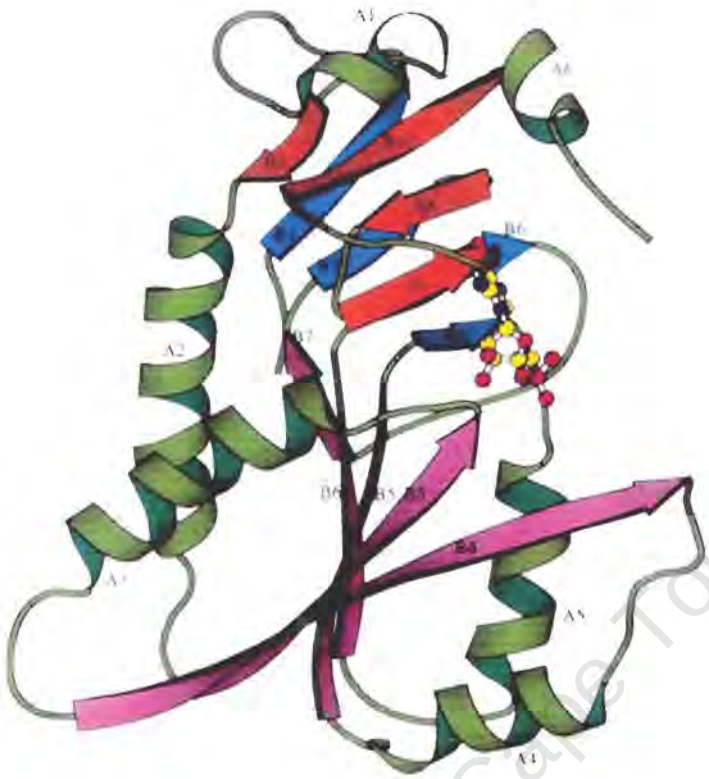

Figure 1.8 Ribbon diagram of Human HGPRT complexed with GMP (Eads *et al.*, 1994)

University of Cape Town

Each subunit consists of a core region and a secondary lobe, or hood region. The core region is composed of five-stranded twisted parallel β-sheet (B3-B7, shown in pink) surrounded by four α–helices (A2-A5, shown in green). The core is similar to those of other HPRT crystal structures (Scapin *et al.*, 1994; Smith *et al.*, 1994). The first half of the sheet is made up of α-helix (A2), β-strand (B3), α-helix (A3) and β-strand (B4), which then crosses over to the second half via an α-helix (A4) to a β-strand (B5), α-helix (A5) and finally two β-strands (B6 and B7). This second half of β-strands forms a flattened ledge at one edge of the sheet upon which the bound GMP sits (B5', B6' B7', shown in blue). A secondary lobe or hood region composed of residues from close to the amino terminal and carboxy terminal ends occurs above the core. It consists of four β-strands (B2, B10, B8, B9 shown in orange) in a twisted anti-parallel β-

sandwich and two α-helices (A1 and A6). Hydrophobic, interdigitated amino acid side chains from the two sheets join the core and hood domains.

The guanine base of GMP apparently distorts the interaction of the β-strands in the hood region. Both sheets make contributions to ligating the base. For example, the side chain carbonyl of Ile-135 in the core sheet interacts with the guanine from below, and Phe-186 of the hood region overlays the base, locking it in place.

GMP is bound in the anti conformation about the glycosidic bond (which means that the 8-H is above the 2'-H of the ribose). The Glu and Asp residues of the PRPP-binding motif (129-VLIVEDIIDTGK-140) form the floor of the active site cleft, below the ribose entity. Residues Asp-137 to Thr-141 form the phosphate-binding loop that encircles the 5'-phosphate. The main chain nitrogens of Asp-137 to Lys-140 are pointed towards the phosphate oxygens for hydrogen bonding. Phosphate oxygens also make hydrogen bond contacts with Thr-138 and Thr-141. Glu-133 and Asp-134 carboxylate side chains are placed below the ribose groups. The hydrophobic side chains of Ile-135 and Phe-186 (mentioned above) are found above and below the plane of the guanine moiety. Further contacts are made between the exocyclic oxygen of the guanine ring and the main chain nitrogen of Val-187 and the side chain of Lys-165. The exocyclic nitrogen of the guanine ring hydrogen bonds with the main chain oxygens of Val-187 and Asp-193. Base binding and substrate specificity therefore reside in the edge of the hood region.

This first crystal structure provided a single static picture of the active site with one product bound. Since then, several more structures in the HPRT family of proteins with substrates or products or transition state analogues bound have been published. The crystal structure of the

University of Cape Town

HPRT from the protozoan parasite *T. foetus* also revealed an asymmetric dimer, however with GMP bound to only one subunit (Somoza *et al.*, 1996). The structure was very similar to that of the human enzyme, with GMP bound between the core and the hood region. Interestingly, differences between the unbound and bound subunits showed that a flexible hinge joined the two regions, and that binding of GMP brings the core and hood closer together by a 5° rotation. This in effect means that the residues ligating the nucleotide on either side of the cleft are drawn 1 Å closer on nucleotide binding. This could be important in the design of antiparasitic drugs.

Another point of interest is that the loop presumed to interact with MgPPi (absent in the structure) has a very different conformation compared with the human enzyme. This loop contains a cis peptide bond between Leu-46 and Thr-47. The parasite enzyme lacks the critical lysine that was predicted to interact with MgPPi.

The crystal structure of the protozoan parasite *T. gondii* grown in the presence or absence of XMP highlighted the movement of a long flexible loop (residues 115 to 126) on XMP binding. The movement brings absolutely conserved Ser and Tyr residues into the catalytic site, and covers the catalytic pocket (Schumacher *et al.*, 1996). A further feature was that the asymmetrical crystal was the tetramer. In all four subunits of the apoenzyme, Glu-146 and Asp-147 complex a magnesium ion. In the XMP-bound form, magnesium was absent, suggesting that the pair of acidic residues may play a role in stabilizing the oxocarbenium transition state when and if magnesium is not present.

The structural features of the transition state were revealed when the human enzyme was crystallised with immucillin GP and MgPPi (Shi *et al.*, 1999b). The structure of the nucleotide

University of Cape Town

analogue is shown in Figure 1.9, and possesses a ribosyl nitrogen in place of O4', which can be protonated (pKa ~6.5) to mimic the positive charge of the oxocarbenium transition state. The N9 of the purine base was substituted with a carbon atom, which provided a chemically stable carbon-carbon ribosidic bond, and increased the pKa of N7 by at least six pH units. Protonation of N7 may occur in the transition state to stabilise the build-up of negativity over the imidazole ring of the purine. The compound exhibited a K_D of 4.6 nM, which is 14000 times tighter than the binding for IMP (Xu *et al.*, 1997).

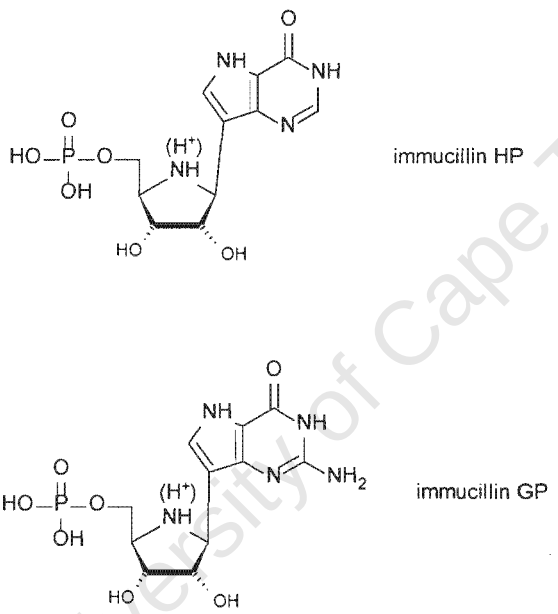

Figure 1.9 Transition state inhibitors of malarial and human HPRT (Shi *et al.*, 1999a, Shi *et al.*, 1999b)

The human enzyme was crystallised as a tetramer with each catalytic site occupied with the inhibitor. Active site interactions between human HPRT, ImmGP and MgPPi are shown in Figure 1.10. MgPPi binds beneath the inhibitor very close to C1' and N4' of the iminoribitol ring. The inhibitor occupies the same position as GMP of the earlier structure. Surprisingly, the imino entity of the oxocarbenium mimic does not interact with a protein residue directly, and the nearest neighbours are the O5' of the inhibitor itself, and an oxygen from pyrophosphate below

University of Cape Town

it. The latter oxygen also coordinates a magnesium ion. The 5'-phosphate, the purine base and PPi all seem to be tightly bound, whereas the ribitol ring is loosely bound, which would permit the latter to move during the transition state from the purine to the pyrophosphate. The movement appears to be guided by linkage of the two ribitol oxygens, O2' and O3', to the conserved Glu and Asp doublet of the PRPP binding motif, and two bound magnesium ions.

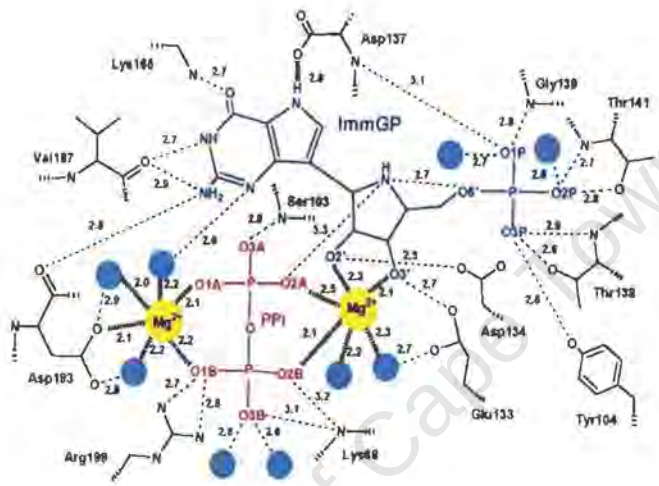

Figure 1.10 Active site interactions of human HPRT with ImmGP and MgPPi. (Shi *et al.*, 1999b; cartoon reproduced from Wang *et al.*, 2001). ImmGP is purple. Magnesium ions are shown as yellow spheres. Blue spheres represent water molecules. PPi is shown in red. Contacts are shown by the dotted lines.

There are numerous contacts between the 5'-phosphate and the long flexible loop of the active site (mentioned above for *T. gondii* HPRT) that could be important for the design of analogues.

A new feature of the structure is the presence of two magnesium ions positioned on either side of the PPi group. One of the magnesium ions does not make direct contacts with the protein, and is coordinated by the PPi, the inhibitor, and one water molecule. This magnesium is in a similar position to that of the *T. gondii* enzyme commented on earlier, except that the conserved acidic residue pair Glu and Asp were direct ligands. The second magnesium

University of Cape Town

coordinates aspartate, PPi and three water molecules. This magnesium ion had previously been seen in a *T. cruzi* HPRT structure (Focia *et al.*, 1998).

Another point of interest in the human enzyme is Lys-68, which orients away from the active site and hydrogen bonds Glu-196 and Val-96 of another subunit. This serves to change the peptide backbone geometry to an unfavourable cis configuration. Similar findings have been reported in other HPRTs. This orientation allows for the backbone amide nitrogen of Lys-68 to interact with two oxygens of PPi. PPi also hydrogen bonds to Arg-199, Asp-193, and the Ser-103-Tyr-104 doublet from the flexible catalytic loop.

The catalytic loop in human HPRT undergoes a large conformational change to seal off the active site from the solvent, sequestering ten water molecules within. The loop becomes ordered, and some secondary structure appears in the form of two anti-parallel twisted β-sheets. The loop interacts directly with PPi and the 5'-phosphate of the inhibitor.

University of Cape Town

The development of tight-binding transition state inhibitors allowed the crystallisation of the relatively unstable malarial HPRT (Shi *et al.*, 1999a). The structure revealed many similarities to the human structure detailed above, including evidence for substrate-assisted formation of a ribooxocarbenium cation, a dissociative mechanism where a relatively mobile ribosyl moiety moves between fixed base and pyrophosphate moieties, and a trans to cis peptide bond change in one of the loops to permit interaction with a main chain amide and PPi.

Details of the reaction chemistry were derived from the structure of malarial HPRT complexed with ImmHP. An oxygen of the pyrophosphate ligated weakly to a magnesium ion was identified as the likely attacking nucleophile, and, in order to bond with the reactive C1' atom of

the ribooxocarbenium state, needs to rotate 10 ° to bring the C1' and an oxygen of PPi within 2.5 Å of one another for nucleophilic attack. Several interactions serve to lock the 5'-phosphate and 2'- and 3'-hydroxyls in place. Additional interactions prevent the PPi group from being translocated towards C1', and anchor it within the PPi binding region. The C1' and O4' atoms of the ribosyl group are not tightly anchored, which allows the C1' atom to descend 0.5 Å towards the oxygen of PPi. The bond with the purine base would need to be broken. If this were the case, the chemistry would be characteristic of a two-step S_n1 dissociative mechanism, and would be in agreement with large secondary α-secondary ^3H kinetic isotope effects observed in yeast OPRT (Goiten *et al.*, 1978), and *Salmonella typhimurium* OPRT with the with the PRPP analogue, phosphonoacetic acid (Tao *et al.*, 1996).

It is of note that the protein contacts between the inhibitor and MgPPi in the human and malarial enzymes were almost identical. A significant difference found by proton NMR was in the hydrogen bond distance of the protonated N7 in the human and malarial HPRTs complexed with ImmHP-Mg^{2+}, and suggested that the hydrogen-bonding properties of the immucillins could be altered by chemical modification. Such changes could allow for drug specificity. However, the striking similarities between the two HPRTs in complex with the transition state analogue suggest that it would be difficult to find transition state inhibitors that would be specific for the malarial HPRT over the human enzyme.

The crystal structures of *T. gondii* HPRT complexed with GMP, IMP and XMP-MgPPi were subsequently published (Héroux *et al.*, 1999a; 1999b), and show that the enzyme is a tetramer, with secondary structure similar to the human and malarial enzymes (see Figure 1.11 and compare with Figure 1.8).

University of Cape Town

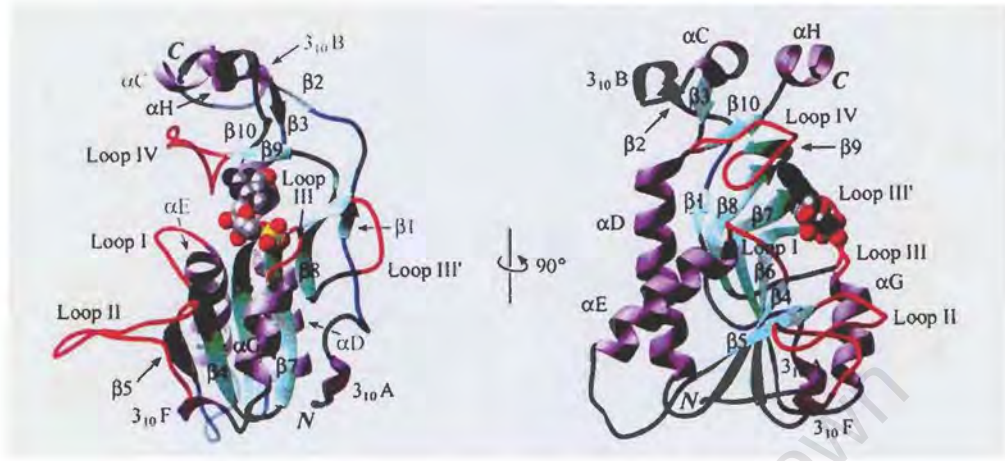

A

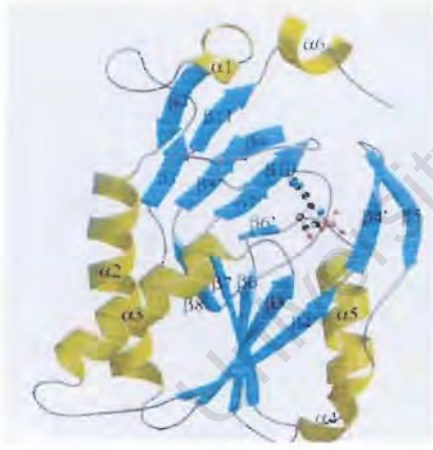

B

C

Figure 1.11 Monomers of (A) *T. gondii* HPRT (Héroux *et al.*, 1999a), (B) human HPRT (Shi *et al.*, 1999b) and (C) *P. falciparum* HPRT (Shi *et al.*, 1999a);

Comparison of the three HPRTs gave insights to the purine-binding specificity. This is of interest because the PRTs from protozoans utilize xanthine much faster than the human

University of Cape Town

enzyme (Table 1.3). However, it appears that purine binding interactions of the human and protozoal HPRTs are very similar, and that the differences in the substrate specificity are due to subtle structural variations. The interactions between most residues and the N1, O6 and N7 of the purine ring, including an aromatic amino acid-purine-hydrophobic amino acid sandwich or clamp are very similar in the enzyme-nucleotide complexes discussed previously. The specificity changes appear to be related to changes in the interaction between Trp-199 and Asp-206. In the *T. gondii* $HPRT_{GMP}$ complex, Trp-199 hydrogen bonds via a water molecule to the main chain carbonyl of Asp-206. This allows it to interact with the N2 of the purine base. In the $HPRT_{T.gondii \cdot XMP \cdot PPi}$ complex, the hydrogen bond from Trp-199 is directly attached to Asp-206, and this changes the position of the backbone such that interaction of the xanthine O2 with the main chain amide of Asp-206 is favourable.

Mutation of the Trp-199 to Phe still allowed for xanthine use (White *et al.*, 1999), and in fact, the malarial HPRT, which has Phe in this position, is able to use xanthine. Thus Trp is not critical for xanthine use. Correct positioning of the loop IV by an aromatic residue in this position may contribute to xanthine use. However after careful analysis of the structures, Héroux and colleagues are of the view that global changes in the hood domain and packing of hydrophobic residues determine whether the configuration of residues around the base is compatible with xanthine use.

A comparison of the structures of the *T. gondii* apoenzyme, the GMP or IMP complexes and the XMP·PPi ternary complexes allowed Héroux and colleagues (1999b) to propose a detailed reaction pathway for catalysis. This pathway is likely to be applicable to most of the HPRTs as the active site structures and ligations are very similar. For example, the coordination of the two magnesium ions on either side of PPi is almost identical between the human and *T. gondii*

University of Cape Town

HPRTs. Small differences are probably due to the structures representing different phases along the reaction coordinate.

Trans-cis isomerisation of the Leu-78-Lys-79 peptide bond in Loop 1 appears to play a fundamental role in catalysis, as mentioned above in respect of the human HPRT complexed with ImmGP, PPi and magnesium. All apoprotein and nucleotide-complexed HPRTs, except for the *T. gondii* HPRT complexed with IMP, have the normal trans configuration at this peptide bond. However, all ternary-complexed proteins occur in the cis configuration. The peptide bond in the cis configuration serves to (a) hydrogen bond with a pyrophosphate oxygen via the peptide NH, (b) position Gly-80 for hydrogen bonding with a pyrophosphate oxygen and (c) position the side chain of Lys-79 for hydrogen bonding with atoms at the base of the active site, and at a dimer interface. However, in the *T.gondii* $HPRT_{Apo}$, *T.gondii* $HPRT_{GMP}$, Human $HPRT_{GMP}$ and Human $HPRT_{IMP}$ (Schumacher *et al.*, 1996; Héroux *et al.*, 1999a; Eads *et al.*, 1994; Xu *et al.*, 1997), the peptide bond was found to be in the trans configuration. PRPP and pyrophosphate are incapable of binding to HPRT when the peptide bond is in the trans configuration for two reasons (a) Lys-79 occupies the pyrophosphate site and (b) hydrogen bonds to Lys-79 and Gly-80 are prevented. It was therefore concluded that since both (cis and trans) configurations are found, and that the cis form seems to be required for catalysis, isomerisation between the two forms occurs during the catalytic cycle.

Héroux and colleagues (1999b) proposed that binding of PRPP releases energy, which is used to reconfigure the peptide bond from trans to cis, in preparation for catalysis. Following product formation, the unstable cis form reverts to trans, and released energy may drive PPi dissociation.

University of Cape Town

The crystal structures of the apoenzyme and the various complexes allow the reaction pathway to be delineated as shown in Figure 1.12 (Héroux *et al.*, 1999b).

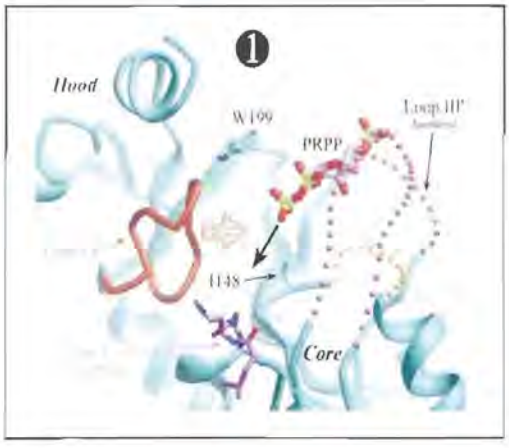

Figure 1.12 Active site events during HPRT catalysis
1: The apoenzyme in an open state, ready to bind PRPP and magnesium. The loop I Leu-Lys peptide bond is in the trans configuration. Loops II, III and III' are also open. Purine cannot bind tightly as the Ile-148 and Trp-199 clamp is open and displaced, and the interactions between them and other residues are not sufficient to close the hood region on the core without PPRP being bound.

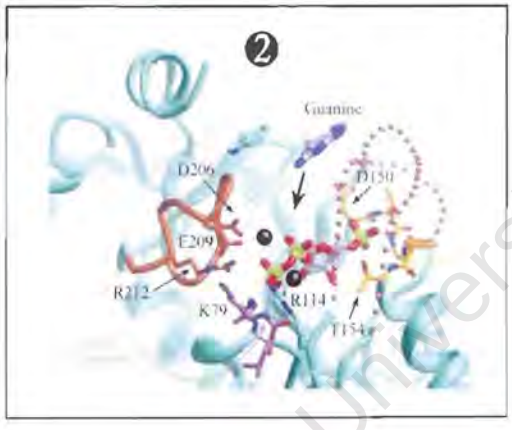

2: PRPP binds with magnesium ion and salt bridges and hydrogen bonds form to draw loop I, the hood and loop IV together. The Leu-Lys peptide bond of loop I adopts the cis configuration. Magnesium ions position the pyrophosphate moiety for phosphoribosyl transfer to occur. The hood is tied down only at the lower side of the active site, leaving the upper region open for guanine to approach the active site. Loop III is ordered by the 5'-phosphate and orientates Asp-150 to form the active site base.

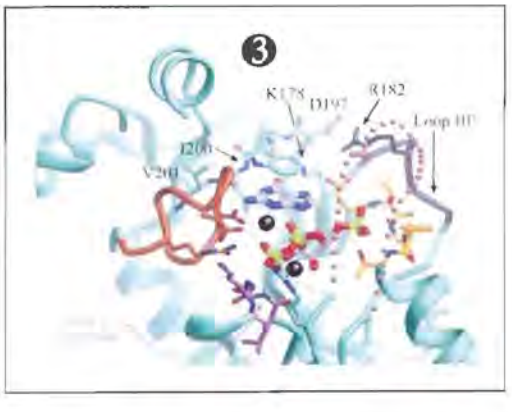

3: The purine binds, and the hood closes over the core to form the bi-substrate complex. Loop III is ordered, resulting in the ordering of loop III' so that a double salt bridge or sandwich is formed, placing Arg-182 between Asp-150 and Asp-197, helping to lock the hood onto the core.

University of Cape Town

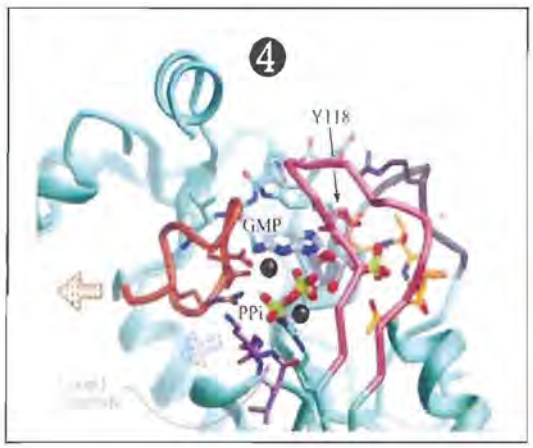

4: Loop II closes over the ribose ring and allows the conserved doublet Ser-117 and Tyr-118 to interact with the 5'-phosphate and increases PRPP hydrogen bonding. This final closure forces the two substrates together to gain the transition state and effect phosphoribosyl transfer.

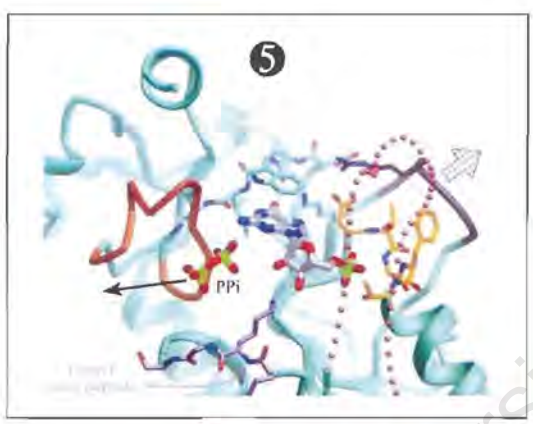

5: Loops I and IV open, followed by opening of loop II. Hydrogen bonds between the core domain and the hood domain are disrupted. The interaction between loop IV and the purine is lost. This, together with the isomerisation of the peptide bond to the trans configuration results in the release of the pyrophosphate group from the active site. This dissociation breaks up the hydrogen bonding network in that region of the active site and weakens the interaction between the core and hood regions, and in turn that between the hood and the purine.

University of Cape Town

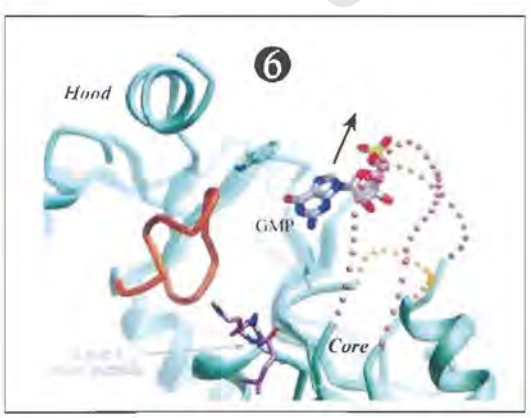

6: Loop III' and hood domain open to release GMP. Loop III becomes disordered. The enzyme returns to the apoenzyme state.

1.7 Drug targeting of parasitic HPRTs

Since protozoan parasites are incapable of *de novo* synthesis of purines, they depend primarily on the HPRT enzyme for the salvage of purines. Inhibition of HPRT may be a means of controlling malaria, toxoplasmosis and trypanosomiasis.

The inhibition of protozoan HPRT has to be specific, as there is also the host HPRT, which, if partially inhibited, or is completely deficient, leads to the condition known as gouty arthritis (or uric acid nephrolithiasis) (Sculley *et al.*, 1992), or the Lesch-Nyhan syndrome. The latter is characterised by abnormal movements, retardation and self-mutilation (Lesch and Nyhan, 1964).

As mentioned previously, the most potent inhibitors found thus far are the transition state analogues (1*S*)-1-(9-deazahypoxanthin-9-yl)-1,4-dideoxy-1,4-imino-D-ribitol 5-phosphate (immucillins HP) and (1*S*)-1-(9-deazaguanin-9-yl)-1,4-dideoxy-1,4-imino-D-ribitol 5-phosphate (immucillins GP) (Shi *et al*, 1999a; 1999b; Li *et al.*, 1999).

The screening of 64 known inhibitors of nucleotide synthesis produced two compounds, namely 6-mercaptopurine and 6-thioguanine, that potently inhibited malarial growth and malarial HPRT in particular (Queen *et al.*, 1990). These two compounds as well as 8-azahypoxanthine had been predicted to be possible inhibitors of the *P. falciparum* HPRT enzyme (Smith and Matthews, 1957; Krenitsky et al., 1969; Walter and Königk, 1974).

The HPRT crystal structures of human and *T. foetus* have been used to generate lead inhibitors using computer-assisted methods (Aronov *et al.*, 2000). The docking algorithm

University of Cape Town

yielded several potential inhibitors of which eighteen were tested *in vitro* in HPRT assays. The two most active compounds were a phthalic anhydride and an indole 2-one. Further computer-assisted refinements led to another series of related compounds of which one, called [4-(3-nitroanilino)phthalic anhydride] was shown to be a competitive inhibitor of the isolated HPRT, and inhibited parasite growth. Further structure-based drug design of combinatorial libraries of phthalimidocarboxanilides produced the more potent [(4'-phthalimido)carboxamido-3-(4-bromobenzyloxy) benzene], or TF2 (Figure 1.13).

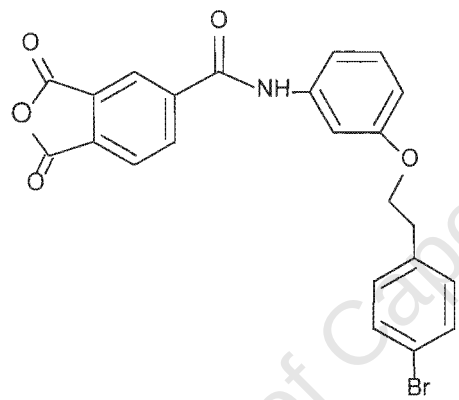

Figure 1.13 [(4'-phthalimido)carboxamido-3-(4-bromobenzyloxy) benzene], or TF2, an inhibitor of *T. foetus* HPRT (Aronov *et al.*, 2000)

University of Cape Town

This compound was found to exhibit an IC_{50} of 1.5 μM, and had 30-fold selectivity for *T. foetus* over human HPRT. The 4-bromobenzyloxy moiety was hypothesised to interact with the flexible loop II (Figure 1.11A).

These two studies illustrate how subtle differences in the active site between parasite and human enzymes can result in specificity changes towards purine analogues and how regions or loops outside of the substrate-binding region may be used to gain extra ligand binding energy. Presumably the additional benzoyl moiety prevents loop II ordering and closure over the active site.

In this study a rather similar strategy is explored in that a large trinitrophenyl moiety attached to the ribose hydroxyls or a flavonoid is covalently stacked on the purine ring may potentially interact with disordered loops, and prevent loop closure. In the first case, the trinitrophenyl group is expected to bind in the cleft between loops II and IV, where the PPi binds. In the latter case, the stacked structure will prevent the hood region with the critical aromatic residue closing over the active site (see Figure 1.14 below).

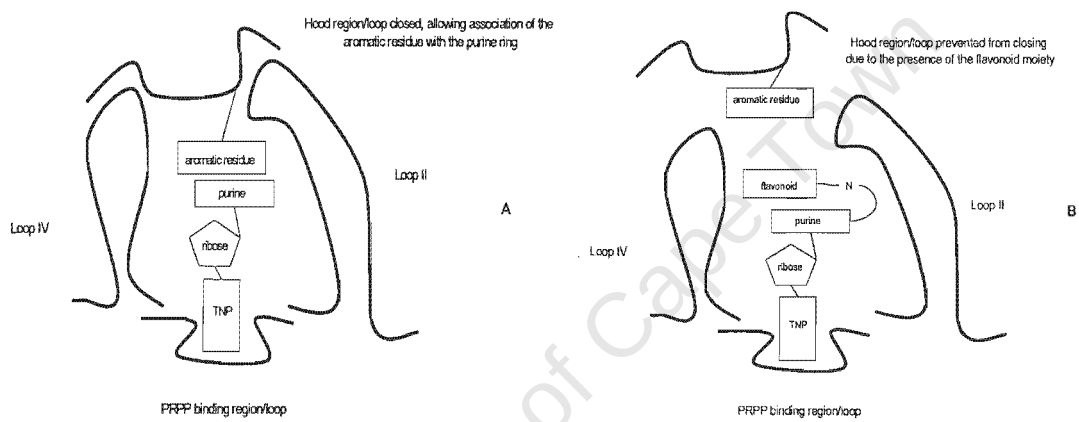

Figure 1.14 A schematic representation of the expected interactions of TNP and flavonoid groups with the active site loops in HPRT. A, PRPP binding region occupied by TNP; B, the presence of the flavonoid moiety prevents association of the aromatic group with the purine ring, and therefore preventing hood region closure over the active site

There are strong interactions between the imidazole entity of the purine base, the 5'-phosphate and PPi. The only entity that is loosely held is the ribose, which is hypothesised to move in the transition state (Shi *et al.*, 1999a), and this flexibility may allow the trinitrophenyl to assume part of the PPi site.

We chose to derivatise the 8-position of the purine ring in order to preserve the selective specificity and favourable protein-purine interactions around the C1, N2 and C3 positions of the purine.

University of Cape Town

1.8 Photolabile ligands

Light-activatable compounds are being increasingly used to study ligand-protein interactions through identifying target proteins and the mapping of active or effector sites. The technique, which is usually referred to as photoaffinity labelling, depends on chemically introducing a photoactivatable group into a ligand or potential ligand (for reviews see Knowles, 1972; Bayley and Knowles, 1977; Kotzyba-Hibert *et al.*, 1995; Dormán and Prestwich, 2000). In the absence of light, the compound is stable and can interact with the target protein in the usual manner. However, on irradiation, a highly reactive species is produced which can covalently insert in neighbouring amino acid residues, forming a stable complex. If the ligand is radiolabelled, fluorescent or immunoreactive, the protein is tagged, and can be identified. Alternatively, some ligand-binding amino acid residues may be identified following digestion of the protein, and isolation of the labelled peptides and sequencing.

Specific photolabelling of a binding site can be used to screen for other compounds or ligands that bind to the same site. This could be particularly valuable in the case of a soluble protein like HPRT where measurement of ligand binding is time-consuming and usually, as in equilibrium dialysis, requires large amounts of protein.

A third possible use of photolabile ligands is to use the reactive intermediate as a means to generate a diversity of compounds, as will be elaborated on later.

Several stable, but photoactivatable groups have been developed for photolabelling purposes. These include azides, diazo compounds, diazonium salts, diazirines and benzophenones. Ideally the photoprobe should be reasonably stable under ambient light in water and be light-

University of Cape Town

activated above 295 nm to prevent damage to the protein. The photochemically generated reactive species should have a short half-life (it is in the region of 10^{-4} s for nitrenes (Reiser *et al.*, 1968; Reiser and Leyshon, 1970)) so that an insertion reaction occurs before the probe diffuses from the binding site. A favoured reaction pathway that produces a single product should occur, and the photoprobe should react with C-H bonds, as well as with nucleophiles. The photoactivatable group should be small so as not to deviate significantly from the size and shape of the true substrate. Finally, the ligand should be reasonably easy to synthesise.

Probably no photoprobe satisfies all these criteria. Aryl azides exhibit many favourable characteristics such as ease of synthesis, stability in the dark, small size, short half-life of the nitrene (about 10^{-6} s) and irradiation by light above 300 nm. Aryl azides have the disadvantage of being selective – reacting strongly with nucleophiles, and poorly with alkyl groups.

University of Cape Town

1.8.1 Arylazide/ nitrene chemistry

The reaction of arylazides with proteins has been known since 1969 (Fleet *et al.*, 1969), and since then, a number different of aryl azides have been synthesised as precursors of nitrenes. Aryl azides usually need activation at wavelengths less that 280 nm, but the introduction of a nitro group in the ring allows longer wavelengths (even greater than 350 nm) to be used. Irradiation of an aryl azide results in activation either to a triplet azide, which loses nitrogen to produce a triplet nitrene, or to a singlet azide that also loses nitrogen to yield a singlet nitrene (see Figure 1.15 and reviewed in Schuster and Platz, 1992).

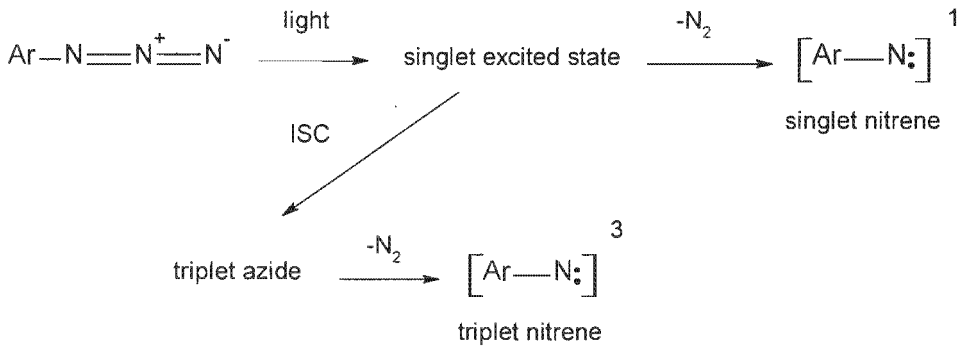

Figure 1.15 Nitrene generation. Ar, arylazide; ISC, intersystem crossing

The reactions of the nitrenes are complex and either (i) didehydroazepines with ring expansion can result followed by reaction with a nucleophile, or (ii) the triplet nitrene can abstract a hydrogen and lead to coupling and covalent linkage, or (iii) the singlet nitrene can react with nucleophiles and result in insertion (Figure 1.16). The pathway depends on the nature of the substituents on the ring (Li *et al.*, 1988). Insertion reactions by the singlet nitrene seem less favoured, except in the case of azido nucleotides and fluorinated azides.

University of Cape Town

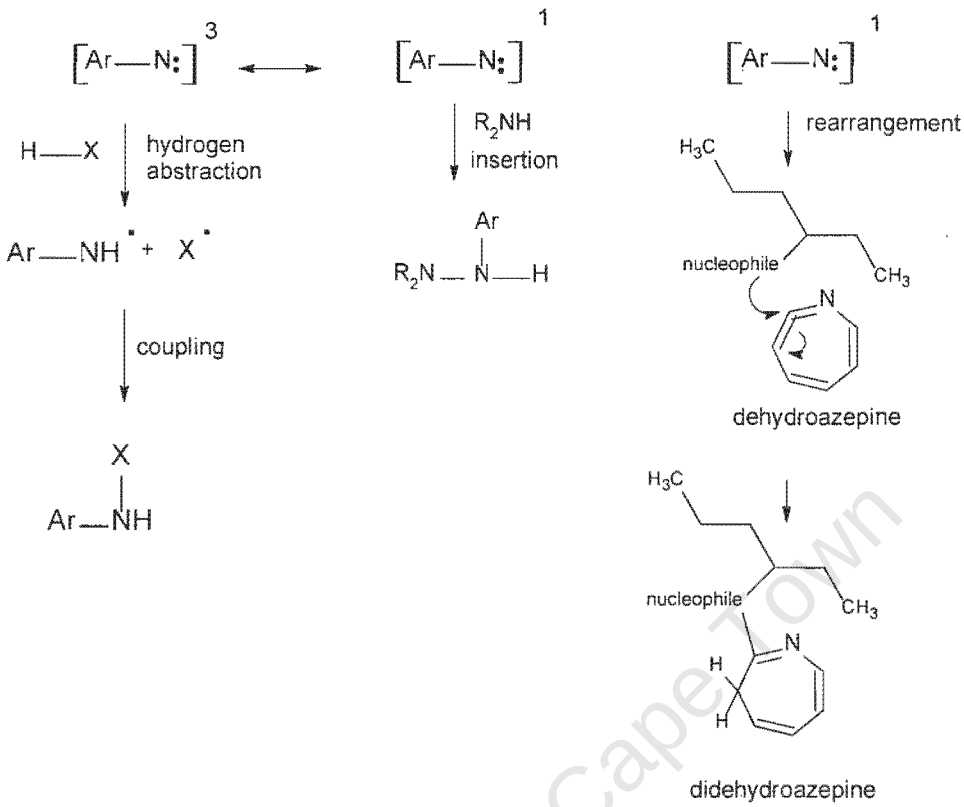

Figure 1.16 Aryl nitrene chemistry. Ar, arylazide; ISC, intersystem crossing

University of Cape Town

If the azide group is ortho to a ring nitrogen, then rearrangement is possible so that the precursor is a mixture of aryl azide and the tetrazole isomer, the latter being much less sensitive to photolysis (Hyatt and Swenton, 1972a; 1972b; Sasaki *et al.*, 1971) (Figure 1.17).

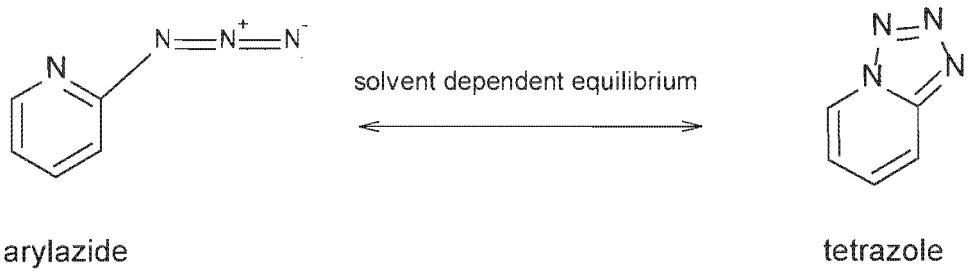

arylazide tetrazole

Figure 1.17 Tetrazole isomer formation

The isomerization was found to complicate photolabelling studies using 2-azido ADP as the photoprobe. The UV spectra of 2-azido ADP under strongly alkaline and acidic conditions were reportedly due to changes in the azidomethine-tetrazole equilibrium, and could be reversed by alterations in the medium acidity/ alkalinity (Czarnecki, 1984).

Azidonucleotides, particularly 8-azido ATP have been used successfully in photolabelling studies (Xue *et al.*, 1987; Garin *et al.*, 1986; Knight and McEntee, 1985). A number of amino acid residues from different biological receptors have been labelled using azidonucleotides (Mayinger and Klingenberg, 1992; Grammer *et al.*, 1993; Shoemaker and Haley, 1993). The most labelling reported however is of tyrosine, and this is due to the possibility of insertion on the tyrosine side chain by both nitrene triplet (deficient in one electron) and nitrene singlet (deficient in two electrons) species. Figure 1.18 shows the possible ways that this can occur.

University of Cape Town

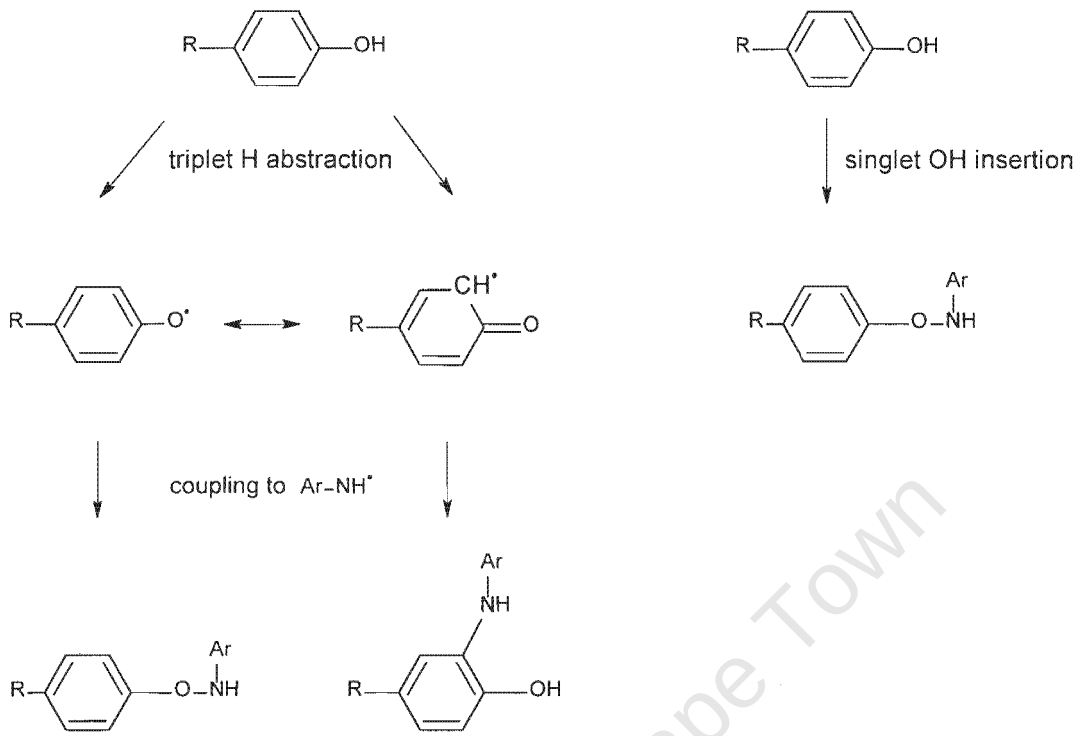

Figure 1.18 Insertion of singlet or triplet nitrenes into the tyrosine side chain.
Ar, arylazide

University of Cape Town

One potential disadvantage of 8-azido ATP as a photoprobe is its unusual structure. ATP exists in the anti conformation with respect to the orientation of the purine ring about the glycosidic bond, which means that the 8-position is pointing over the 2'-hydroxyl. In contrast, 8-azido ATP should be structured in the syn conformation (8-position pointing away from the 2'-hydroxyl group) due to steric hindrance of the usual positioning by the bulky 8-azido group (Ikehara *et al.*, 1972). The anti and syn conformations for ATP and 8-azido ATP respectively are shown in Figure 1.19.

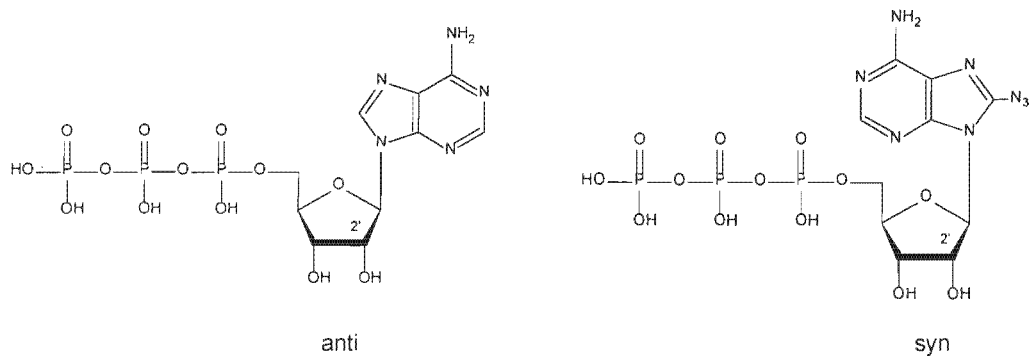

Figure 1.19 Anti and syn conformations of ATP and 8-azido ATP.

As elaborated on in the next section, 2',3'-*O*-(2,4,6-trinitrophenyl) may be introduced into nucleotides in order to possibly increase affinity and allow easier monitoring through its absorbance and fluorescence properties. TNP-8–azido ATP has been used to photolabel the ATP site(s) of Ca^{2+}-ATPase of sarcoplasmic reticulum and, the linkage between the probe and the lysine residue labelled at the active site was found to be unstable with a half-life of 9 h at room temperature (Seebregts and McIntosh, 1989; McIntosh *et al.*, 1992). The high specificity of the reaction was subsequently demonstrated by mutational analysis, where mutating the lysine to leucine completely eliminated photolabelling. However, mutation to tyrosine enhanced the labelling, and formed a stable adduct (McIntosh *et al.*, 1996; unpublished results).

University of Cape Town

1.9 Trinitrophenyl-nucleosides/nucleotides

Azegami and Iwai (1964) first showed that reaction of 2,4,6-trinitrobenzenesulfonate (TNBS) with nucleosides produced 2',3'-*O*-(2,4,6-trinitrophenyl)-nucleosides that had properties of Meisenheimer complexes, i.e. absorbance maxima at about 410 and 475 nm, and were orange at alkaline pH and colourless at acidic pH. The structure of spiro Meisenheimer complexes is shown in Figure 1.20.

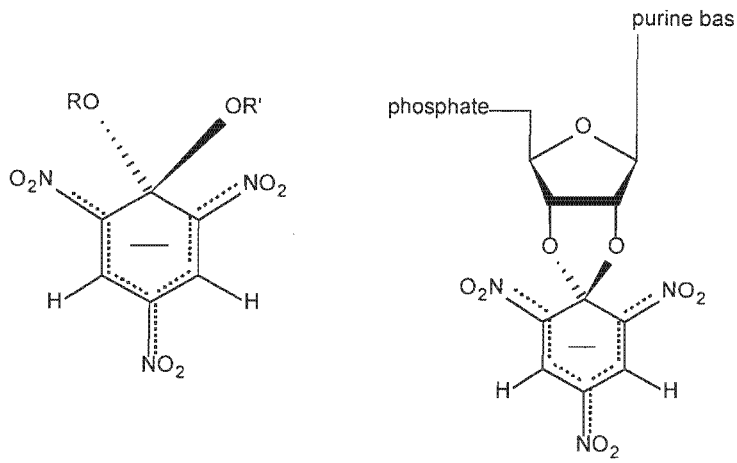

Figure 1.20 The structure of spiro Meisenheimer complexes

The alkoxy groups at the sp^3-hybridised C1 lie in a plane perpendicular to the ring (spiro linkage). In the case of TNP-nucleotides, the plane of the TNP ring is at right angles to the approximate plane of the ribose ring. The TNP ring has a negative charge that is delocalised as shown. The delocalisation of the electrons produces the intense colours of the Meisenheimer complexes, and makes them fluorescent. The pH dependence of the colour in the case of the nucleosides is due to protonation of the 2'oxygen and opening of the dioxolane ring to produce 3'-*O*-(2,4,6-trinitrophenyl)-nucleoside, shown in Figure 1.21 (Ah-Kow *et al.*, 1980). The formation of the 2'-*O*-isomer is not favoured, possibly due to steric hindrance between the *o*-nitro groups of the picryl ring and the purine moiety.

University of Cape Town

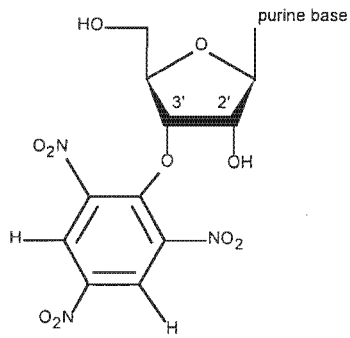

Figure 1.21 Protonation and opening of the dioxolane ring in spiro Meisenheimer complexes (Ah-Kow *et al.*, 1980)

TNP-ATP, first described by Hiratsuka and Uchida (1973), has been widely used as an ATP analogue. It often binds much tighter than ATP. Examples include the P-type ATPases, where, in the case of the Ca^{2+}-ATPase of sarcoplasmic reticulum, the binding affinity is increased approximately 100-fold ($K_{D\ TNP\text{-}ATP}$= 20 nM (DuPont *et al.*, 1982)), and the multidrug resistance P-glycoprotein where the change is about 1000-fold (Dayan *et al.*, 1996). The nucleotide has been extensively used to understand the properties of ATP binding site(s) of Ca^{2+}-ATPase of sarcoplasmic reticulum (Watanabe and Inesi, 1982; Nakamoto and Inesi, 1984). A useful feature has been the large increase in fluorescence on phosphorylation of the pump. TNP-ATP has found use with a number of other enzymes, for example adenylate kinase, adenosine dearninase, F1-ATPase, myosin, DNA polymerase IV.

Azido derivatives of TNP-ATP at the 8-position of the adenine ring were first synthesised in this laboratory (Seebregts and McIntosh, 1989). The derivatives behave much like the parent with respect to fluorescent and binding properties. On irradiation with sarcoplasmic reticulum Ca^{2+}-ATPase it covalently attaches to Lysine 492 with 50% efficiency (McIntosh *et al.*, 1992). As mentioned, the TNP group as a Meisenheimer complex with the ribose ring often allows the

University of Cape Town

nucleotide to bind tighter to ATP sites. The only atomic structure of a TNP nucleotide with a protein is that of the recently solved structure of Ca^{2+}-ATPase complexed with TNP-AMP (Toyoshima *et al.*, 2000). The crystals were grown in the absence of TNP-AMP, and the nucleotide was floated into the preformed crystal. The interactions of the TNP-group with the protein seem weak, and Arg-560 is the only residue that may be involved. It is possible that specific TNP-protein interactions were not optimised due to crystal packing constraints.

One observation in this laboratory is that TNP-nucleotides bind irreversibly to strong anion exchange resins, and very strongly to weak anion exchange resins. These resins consist of polyamines, and this suggests that trinitro-aromatic/ amine interaction, over and above the favourable charge effects, are involved. In this context, it is interesting that a new type of intermolecular interaction has been described between amines and aromatic rings (Burley and Petsko, 1986; Sussman *et al.*, 1991; Rodham *et al.*, 1993, Waksman *et al.*, 1992). It appears that amine groups make energetically favourable interactions with the π-electrons of aromatic rings ("amino-aromatic" interactions, where the side chain of NH groups was shown to have a tendency to be positioned near aromatic residues), contributing bond strengths equivalent to a hydrogen bond. It can be imagined that the interaction between an amino group and the TNP-nucleoside Meisenheimer complex with formal but delocalised negative charge could be considerably stronger.

Related to this phenomenon is the observation of cation-π interactions: a non-covalent force, where the face of an aromatic ring provides a surface of negative electropotential so that cations can bind strongly and influence protein folding (Dougherty, 1996; Ma and Dougherty, 1997). This interaction would occur in addition to hydrogen-bonds, salt bridges and hydrophobic effects. In proteins, it is usually the side chains of Asp and Glu that bind cations,

University of Cape Town

but the hydrophobicity of the side chains of Phe, Tyr and Trp make them better candidates for cation-binding. Although these amino acids bind polar cationic substances, they are found in hydrophobic environments (Dougherty, 1996), and their aromatic side chains can take part in cation-π interactions (Zhong *et al.*, 1998). The indole ring of Trp has enhanced cation-π binding over the benzene and phenol rings of Phe and Tyr respectively, as it provides a larger and more intense region of negative electrostatic potential (Dougherty, 1996; Gullivan and Dougherty, 1999). Cation-π interactions involving protein side chains can be angled to take advantage of favourable electrostatic interactions, and in turn influence protein folding (Gullivan and Dougherty, 1999).

1.10 Flavonoids

The number of known flavonoids was 6500 in 1999 (Harborne and Williams, 2000). Over 4000 flavonoid compounds have been isolated from plants (Middleton and Kandaswami, 1994), and are widely distributed in vegetables and fruit, but especially abundant in citrus fruit, wine and tea (Pierpont, 1986; Scalbert and Williamson, 2000). Flavonoids may be grouped into different classes as illustrated in Figure 1.22.

University of Cape Town

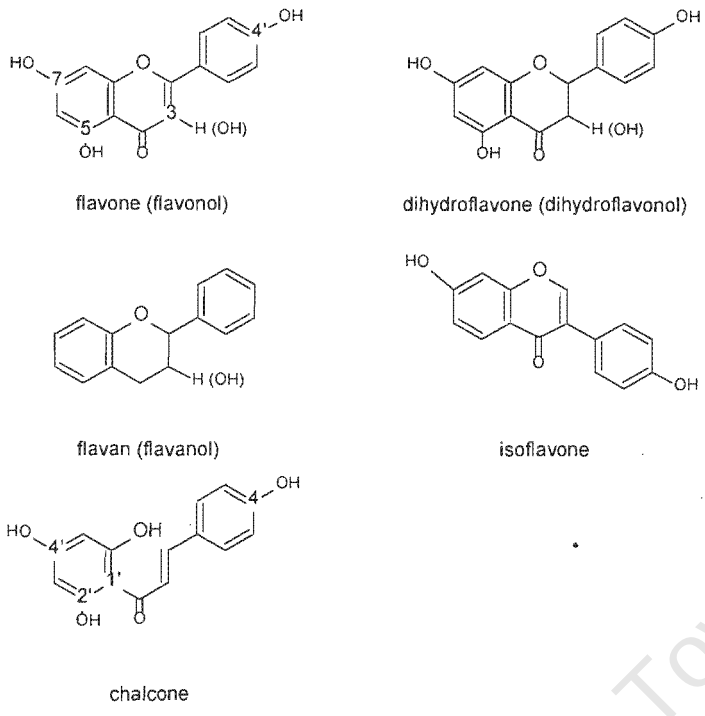

Figure 1.22 Different classes of flavonoids (Adapted from Bois *et al.*, 1998, Bloor, 2001)

A range of functions for the flavonoids have been reported, and include antioxidant, free radical scavenging, anti-inflammatory, antiviral, enzyme inhibition/ activation, redox regulation in cells and anticancer functions (reviewed in Pietta, 2000; Rice-Evans, 2001). In other studies, flavonoids prevented cancer cell proliferation and the growth of the *Leishmania* parasite (Cassady *et al.*, 1990; Chen *et al.*, 1993).

A mechanism by which cancer cells achieve resistance to structurally diverse drugs is through the over expression of the transmembrane protein, P-glycoprotein (Gottesman and Pastan, 1993). P-gp, about 170 kDa in size, is a member of the ATP-binding cassettes superfamily of transporter proteins, that binds and transports drugs out of cells through the hydrolysis of ATP. This allows the levels of drugs inside the target cells to remain at levels that are not cytotoxic (Higgins, 1992).

University of Cape Town

The role of flavonoids in multidrug resistant (MDR) cells has been debated. For example, flavonoids were reported to increase the efflux of adriamycin from HCT-15 colon cells (Critchfield *et al.*, 1994), or to block the efflux of rhodamine 123 from MCF-7 breast cells (Scambia *et al.*, 1994). Quercetin was found to inhibit the ATPase activity of P-gp (Shapiro and Ling, 1997a) and the efflux of Hoechst 33342, or to increase the efflux of rhodamine 123 (Shapiro and Ling 1997b). Several mechanisms of the effect of flavonoids on drug efflux have been proposed, and include interaction with membrane phospholipids, changes in the lipid packing density of membranes, and diffusion rates of drugs (Clarke *et al.*, 1990), or effects on the expression of the multi drug transporter (Kioka *et al.*, 1992).

1.11 The approach taken in this study

Photoactivatable purines and nucleosides were developed in this study for several reasons. The foremost among these was to try to use the reactivity of the activated azido nucleotides to produce a diversity of 8-substituted purines, 2',3'-*O*-(2,4.6-trinitrophenyl)-nucleosides and purine or nucleoside/ flavonoid conjugates. 8-azido ATP was first synthesised by Haley and co-workers in 1979, and since then has been used widely to label and map ATP sites. Many different amino acids have been labelled and include tyrosine, tryptophan, lysine, threonine, leucine, isoleucine, proline and glycine (Tran *et al.*, 1994; reviewed in Kotzyba-Hibert *et al.*, 1995). Since triplet or singlet pathways may be followed, irradiating azido purines or azido nucleotides in a variety of different solvents or mixtures may produce a huge diversity of compounds. In this study we largely focussed on 8-azido xanthosine and 8-azido xanthine because the malarial enzyme, can utilize xanthine much more efficiently than the human enzyme. The synthesis of 8-azidoxanthine has not been described before.

University of Cape Town

TNP nucleotides, where the trinitrophenyl grouping is attached to the 2', 3' hydroxyls of the furanose ring, have some remarkable properties, which have been discussed above. The spectral characteristics of the Meisenheimer complex make monitoring simpler. Photolabelling of protein offers a way to measure binding of different compounds through competitive inhibition, as an alternative to equilibrium dialysis, and other methods, which are generally difficult and usually tedious. Photolabelling can yield information on the amino acids in the binding site of an inhibitor.

The potential for the azido nucleotides to yield a diversity of compounds is illustrated in Figure 1.23, where TNP-8-azido AMP was irradiated MOPS/ TMAH buffer, pH 7, and the products were separated by reverse phase HPLC. At least seven prominent species with distinct spectral characteristics different from the parent compound (Figure 1.24) are evident. Changing the buffer, pH or the addition of magnesium chloride or co-solvents like glycerol results in a new range of species (not shown). The novel nucleoside, TNP-8-azido xanthosine synthesised in this study, will be shown to exhibit similar characteristics.

University of Cape Town

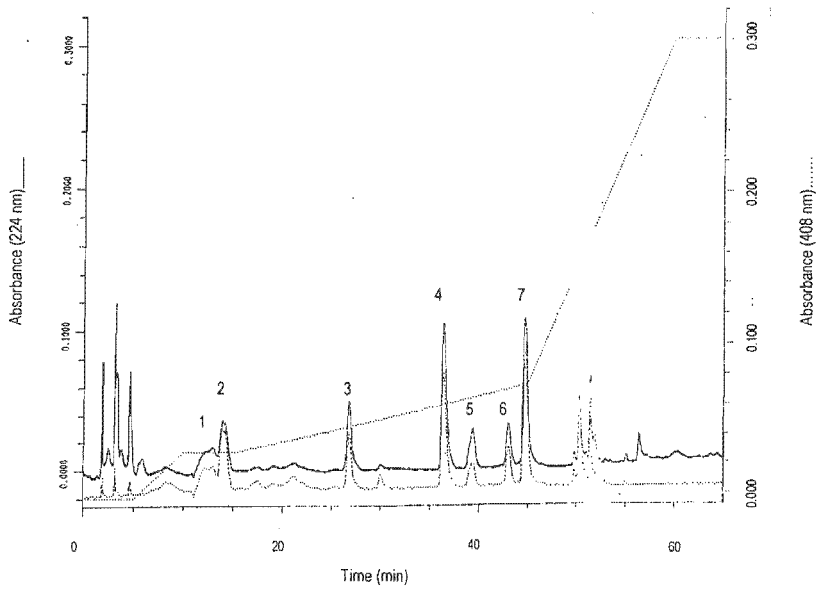

Figure 1.23 Reverse phase HPLC analysis after irradiation of TNP-8-azido AMP (McIntosh and Woolley, unpublished results). TNP 8-azido AMP (10 μM) was irradiated for 4 min in 1 mM MOPS/ TMAH buffer, pH 7. Mobile phase A= 10 mM KPi, pH 6, mobile solvent B= 10 mM KPi, pH 6, 60% (v/v) acetonitrile. Gradient for mobile phase B: 0% for 5 min, 0-10% over 5 min, 10% for 5 min, 10-40% over 30 min, 40-100% over 15 min, 100% for 5 min. Detection was at 224 nm and 408 nm. A Vydac ™ C18 reverse phase column was used for HPLC analysis.

University of Cape Town

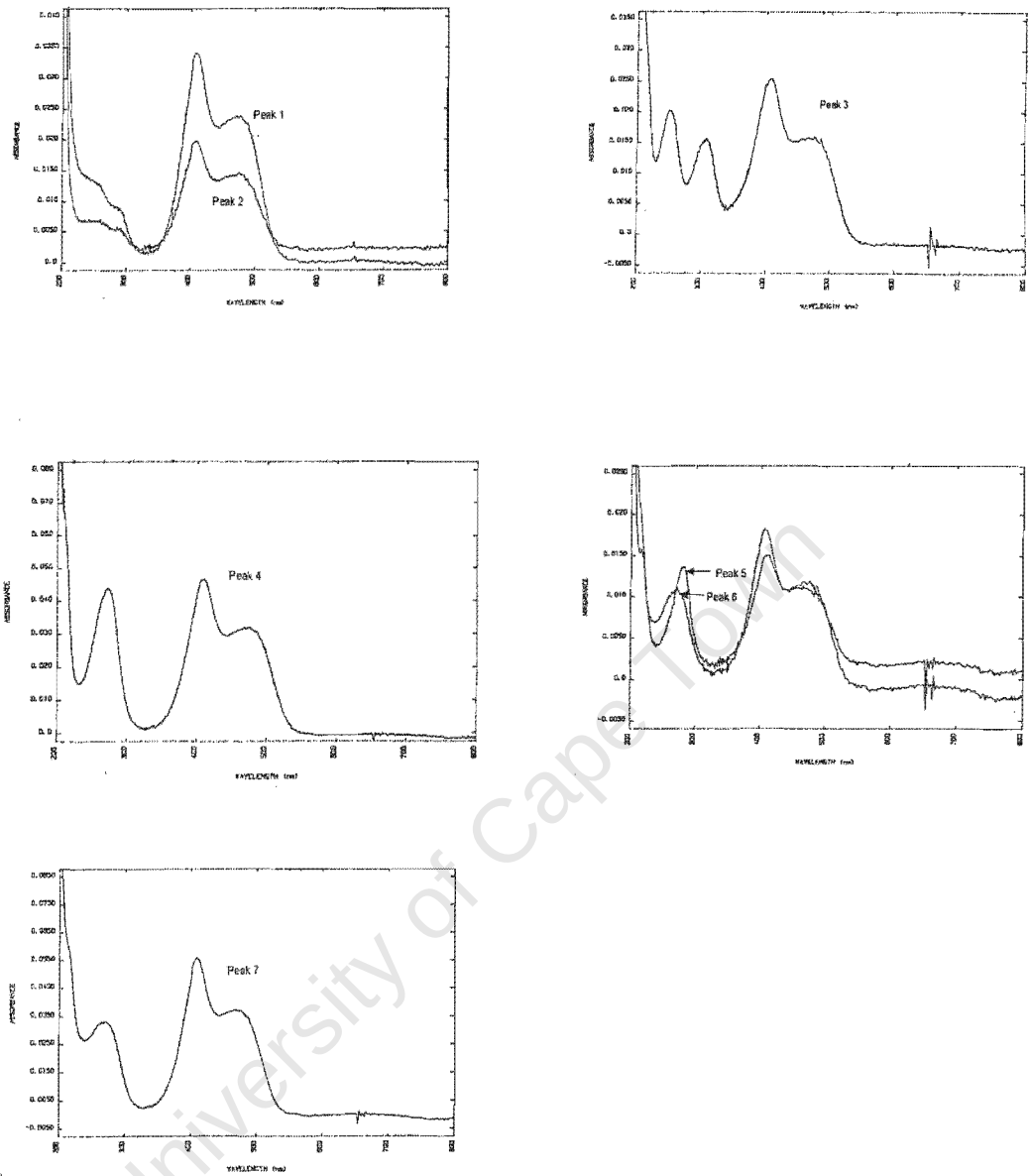

University of Cape Town

Figure 1.24 The spectral characteristics of the products from irradiation of TN8-azido AMP (McIntosh and Woolley, unpublished results). TNP 8-azido AMP (10 μM) was irradiated for 4 min in 1 mM MOPS/ TMAH buffer, pH 7. The absorbance spectra of the products formed were obtained by Diode Array spectrophotometry, and show the presence of the TNP group with absorbance maxima at approximately 408 nm and 480 nm. Each compound has a unique spectrum. The peaks refer to those shown in Figure 1.23.

Flavonoids interact with both the ATP site and a vicinal hydrophobic/steroid-binding region on mouse P-gp (Conseil *et al.*, 1998; Pérez-Victoria *et al.*, 1999), and could be usefully screened for binding to other nucleoside or nucleotide binding proteins like HPRT. Thirty-eight flavonoids were obtained from Professor Denis Barron (Laboatorie de Produits Naturels, UMR 5013 CNRS/ Université Claude Bernard-Lyon I, Villeurbanne, France), Dr Attilio Di Pietro (Institut de Biologie et Chimie des Protéines, UMR 5086 CNRS/ Université Claude Bernard-Lyon I, France), and Dr Ahcène Boumendjal (Département de Pharmacochimie Moléculaire, UMR 5063 CNRS/ Université Joseph Fourier, de Grenoble, La Tronche, France), and were tested for inhibition of malarial HPRT.

An approach explored in this study is the possibility of obtaining TNP-nucleoside/ flavonoid conjugates by utilizing the tendency of purines to form π-π aromatic stacking interactions (Hunter, 1993) via the attractive interactions of polar exocyclic groups with delocalised electrons of the aromatic rings (Bugg *et al.*, 1971 cited in Sponer *et al.*, 1996). The latter arises when a permanent dipole induces a dipole in a neutral species alongside, and this in turn induces dipole moments in another neutral molecule. The goal would be to obtain various heterodimer conjugates, as illustrated schematically in Figure 1.25.

University of Cape Town

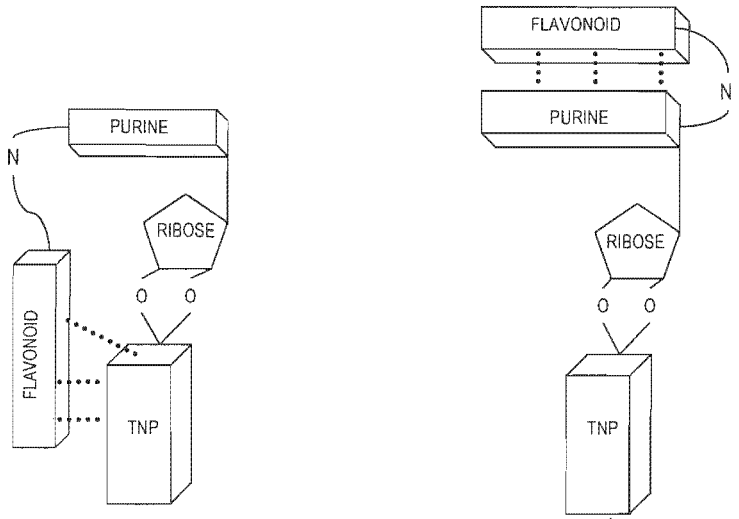

Figure 1.25 A schematic representation of how two types of TNP-nucleoside/ flavonoid conjugates may be structured. TNP, 2',3,-*O*-(2,4,6-trinitrophenyl)

Crude modelling suggests that flavonoid stacking on the TNP group may still allow reaction with the azido in the 8-position. Preliminary studies conducted in this laboratory with TNP-8-azido ATP and several classes of flavonoids indicated that efficient light-induced coupling could occur in aqueous solutions (unpublished results).

As mentioned earlier, the reaction mechanism of HPRT occurs by ordered sequential binding of substrates, and their envelopment by mobile loops to form a closed active site. These events facilitate attaining the transition state for chemical transfer. Following PRPP binding, a dimeric covalent conjugate may be accommodated in the open site, but would inhibit folding over of a loop that would normally place an aromatic side chain over the purine (Figure 1.26). The flavonoid on top may provide extra binding energy through the exocyclic hydroxyl groups contained in flavonoids. These flavonoid conjugates could inhibit parasitic HPRTs by exploiting the mechanism of catalysis. The conjugates could serve as mechanistic probes of the HPRT reaction.

University of Cape Town

CHAPTER 2 MATERIALS AND METHODS

2.1 Molecular biology methods for human HPRT

Taq polymerase, $MgCl_2$ and 10X PCR buffer (200 mM Tris/HCl, pH 8.4, 500 mM KCl) were obtained from Gibco BRL. dNTPs were obtained from Roche Molecular Biochemicals. The human HPRT cDNA clone (p4aA8) was a gift from Dr D. J. Jolly, University of California at San Diego, La Jolla, California. Primers for amplification of human HPRT (EX1 and EX2) were obtained from Dr A. M Marinaki, Cape Town. The pGEM®-T vector system, Lambda DNA, T7 and SP6 promoter primers, and the 100 bp marker were purchased from Promega. IPTG was purchased from Amresco®, Ohio. X-gal was obtained from Biosolve, Ltd, Netherlands. The Fast-Link™ DNA ligation and screening kit was obtained from Epicentre Technologies. Restriction endonucleases *Nco*1, *Nde*1 and *Bam*H1 were purchased from Amersham™ Lifescience. Yeast extract and tryptone were purchased from Merck Biolab. SuRE/Cut™ restriction buffers B and H, and Ampicillin were obtained from Boehringer Mannheim. Whitehead Scientific supplied D1 LE agarose. The 100 bp marker was obtained from Promega. The Plasmid Midi/Maxi kit, and the QiaexII gel extraction kits were purchased from Qiagen. The expression vector pET-15b was obtained from Novagen. Oligonucleotide primers were synthesised at the Department of Microbiology, or the Department of Medical Biochemistry, University of Cape Town. Automated DNA sequencing was performed at the Department of Microbiology, University of Cape Town, the Core Facility, Health Sciences Faculty, University of Cape Town, or at the DNA Sequencing Unit, University of Stellenbosch, Cape Town. All other reagents used were of analytical grade.

University of Cape Town

2.1.1 The amplification of human HPRT cDNA

Human cDNA was amplified by PCR using 5'CGGCTCCCATATGGCGACCCGCAG3' and 3'CTCAAGTTCAACTCAAACCCTAGGCGT5' as the forward (EX1) and reverse (EX2) oligonucleotide primers respectively. The forward and reverse primers were synthesised to generate *Nde*1 and *Bam*H1 recognition sites (underlined) respectively, and flanked the coding region of human HPRT cDNA. The primers were diluted to 50 pmol μl^{-1} in TE buffer, pH 8 and were stored as aliquots at –20 °C. The 100 µl amplification reaction consisted of 50 pmol of each primer in TE buffer, 200 µM of each dNTP, 20 mM Tris/HCl, pH 8.4, 50 mM KCl, 1.5 mM $MgCl_2$, and 2.5 U *Taq* polymerase in sterile deionised water. The amount of template used was 10 ng. A control for contamination of the reagents was included, and consisted of all the reaction components except the template. A Techne Gene-E thermocycler (Techne, UK) was used, and the temperature profile was as follows:

denaturation 93.5 °C for 30 s

denaturation 93.5 °C for 45 s, 30 cycles

annealing 52 °C for 30 s, 30 cycles

extension 72 °C for 1 min, 30 cycles

final extension 72 °C for 10 min.

The PCR reaction (15 µl) was analysed on a 1.5% agarose gel, incorporating ethidium bromide. DNA was visualised using a long wavelength UV light box.

University of Cape Town

2.1.2 The concentration of amplified human cDNA

Standard ethanol precipitation was used to concentrate the PCR product. Sterile deionised water (100 µl) was added to 100 µl PCR reaction. Sodium acetate (0.1 volume of 3 M solution at pH 5.2) and two volumes cold absolute ethanol were added. Mixing was by tapping the side of the tube, and incubation was at –80 °C for 15-20 min. The contents were then inverted and microcentrifuged at 9000 rpm for 5 min. The supernatant was carefully removed and discarded, taking care not to disturb the pellet. The pellet was washed in 70% ethanol by microcentrifugation for 1 min. The supernatant was discarded, and the pellet was dissolved in 15 µl of 10 mM TE buffer.

2.1.3 The extraction of human HPRT cDNA from agarose

The entire cDNA pellet in TE buffer (15 µl) was extracted from a 1.5% agarose gel using the QIA ExII gel extraction kit (Qiagen). This procedure was used to separate amplified cDNA from all other components of the amplification reaction.

2.1.4 The ligation of cDNA into pGEM®-T vector

The ligation of cDNA to pGEM®-T vector was performed according to the manufacturer's instructions, with the following exceptions. The ligation buffer and DNA ligase were from the Fast-Link™ DNA ligation and screening kit. The ligation reaction was incubated for 1 h at 16 °C. Ligation was stopped by incubation at 70 °C for 15 min.

University of Cape Town

2.1.5 The transformation of *E. coli* cells

Competent *E. coli* XL1 blue cells were prepared by the rubidium chloride method (Hanahan, 1985) for a transformation efficiency of 10^6 or greater, and stored at –80 °C. The cells were thawed in icy water and 50 µl was used for each transformation. Ligation reaction (3 µl) was added to the cells and incubated on ice for 45 min. pUC 18 vector (0.03 ng) was used to determine transformation efficiency. The transformation reaction was incubated for 30 s at 37 °C, and was immediately incubated on ice for 2 min. Sterile 2X TY medium (16 g/l tryptone, 10 g/l yeast extract, 5 g/l NaCl) was added to 1 ml, and the cells were incubated for 1 h at 37 °C with gentle shaking. Cell pellets were collected by brief centrifugation, resuspended in residual medium (about 50 µl), and aseptically plated out onto Luria plates (10 g/l tryptone, 5 g/l yeast extract, 5 g/l NaCl, 1 mM NaOH, 15 g/l agar) supplemented with 100 µg/ml ampicillin, 20 mg/ml X-gal and 100 mM IPTG. X-gal and IPTG were included for blue/white selection by insertional inactivation of the α-peptide coding region of β-galactosidase. Plates were incubated overnight at 37 °C. The control transformation (10 or 25 µl of cells that were not pelleted) were plated out onto ampicillin-supplemented Luria plates and incubated as for the transformations.

University of Cape Town

2.1.6 The preparation of plasmid DNA extracts

The alkaline lysis method of plasmid DNA preparation was conducted on a selection 13 colonies, as described in Current Protocols (1991), with the exception that 3 ml of cells grown to saturation was used for the extraction. In addition, 1 µl 10 mg/ml DNase-free RNase was added to the supernatant from cell debris and chromosomal DNA removal, and was incubated at room temperature for 30 min before nucleic acid precipitation with absolute ethanol. Plasmid DNA extractions were analysed by agarose gel electrophoresis.

2.1.7 Restriction digests of plasmid DNA

Each of the plasmid DNA extractions was digested with 10 U restriction enzymes *Nde*1 and *Bam*H1 in the presence of SuRE/Cut™ restriction buffer B (10 mM Tris/HCl, pH 8, 5 mM $MgCl_2$, 100 mM NaCl, 1 mM 2-mercaptoethanol). Digestion was performed overnight at 37 °C. Control digests were conducted on lambda DNA using *Bam*H1 or *Nde*1, and in the presence or absence of a mixture of the plasmid DNA extracts. The result of the digestion was analysed on 1.5% agarose or 0.8% agarose gel for the digests or the digestion controls respectively.

2.1.8 The sequencing of positive clones

The colonies corresponding to the positive clones were cultured and the plasmid DNA from each colony was prepared by a modification of the protocol by Kraft *et al.* (1988) for sequencing. A total of 6 possible clones were submitted for sequencing in the forward and reverse directions. Each plasmid DNA extraction (3 µl) was mixed with 1 µl of either T7 or SP6 promoter primer for sequencing (see Technical Appendix, 1J for sequencing details).

University of Cape Town

2.1.9 The large-scale preparation of the expression vector, pET-15b

The expression vector, pET-15b, was transformed into *E. coli* XL1 blue competent cells as in Section 2.1.5. Plasmid DNA was prepared in bulk using the Qiagen Plasmid Maxi kit according to the manufacturer's instructions.

2.1.10 The cloning of human HPRT cDNA into pET15-b

2.1.10.1 The sequential digestion of pET-15b

The sequential digestion of pET-15b was performed first with 10 U *Nde*1 and then with 10 U *Bam*H1. Digestion with *Nde1* was conducted overnight at 37 °C in the presence of SuRE/Cut™ buffer H (50 mM Tris/HCl, pH 7.5, 10 mM $MgCl_2$, 100 mM NaCl, 1 mM DTE). The digested vector was analysed on a 1.5% agarose gel, and extracted using QIAExII gel extraction kit (Qiagen) according to the manufacturer's instructions. TE buffer was added to the extracted vector to a volume of 200 µl. An equal volume of phenol:chloroform:isoamyl alcohol (25:24:1) was added and the mixture was vortexed. The contents were centrifuged at 9000 rpm for 5 min, and the clear aqueous phase was transferred to a fresh tube. TE buffer (200 µl) was added to the organic phase, and the extraction was repeated. The aqueous phase was added to that from the first extraction for a total of about 400 µl. The standard ethanol procedure was used to concentrate the DNA in 20 µl deionised water. pET-15b digested with *Nde*1 (15 µl) was digested overnight with 10 U *Bam*H1 at 37 °C in the presence of SuRE/Cut™ buffer B. The digested pET-15b was extracted from agarose gel, treated with phenol:chloroform:isoamyl alcohol solution and concentrated by standard ethanol precipitation to a volume of 20 µl in TE buffer.

2.1.10.2 Test for linearity of digested pET-15b

In order to test the linearity of the sequentially digested pET-15b vector, 50 µl *E. coli* XL1 blue competent cells were transformed with 0.03 ng pUC 18 vector or 50 ng of the digested pET-

University of Cape Town

15b, as before. X-gal and IPTG were omitted in the Luria agar plates used to culture transformants.

2.1.10.3 The ligation of human HPRT to digested pET-15b and transformation into *E. coli* XL1 blue competent cells

Human HPRT cDNA was excised from pGEM®-T using *Bam*H1 and *Nde*1. The 654 bp fragment was extracted from agarose gel using the QiaEXII gel extraction kit according to the manufacturer's instructions, and was ligated to digested pET-15b as before. The ligation reaction was transformed into *E. coli* XL1 blue competent cells. A single colony was selected for plasmid DNA extraction.

2.1.10.4 The transformation of *E. coli* expression strains with human HPRT/pET-15b plasmid DNA and test for plasmid stability

E. coli BL21, *E. coli* BL21(DE3) and *E. coli* BL21(DE3)pLysS were transformed with the human HPRT/pET-15b plasmid DNA. Plasmid stability was tested following instructions as laid out in the pET system manual (Novagen). Glycerol stocks of *E. coli* BL21(DE3)pLysS transformed with human HPRT/pET-15b were prepared according to the manufacturer's instructions.

2.2 Molecular biology methods for malarial HPRT

The materials used for the molecular biology studies of malarial HPRT were essentially the same as for human HPRT. Malarial HPRT cDNA (clone 7-3g) was a gift from Dr D.W Melton, Edinburgh University, Edinburgh.

University of Cape Town

2.2.1 The design of primers for the amplification of malarial HPRT

Primers were designed using computer software, Oligo Version 3.4 (National Biosciences Inc, Pymouth MN, USA). The primers synthesised were 5'TATAATATTAGCATATGCCAATACC3' (MALP1, forward primer) and 3'GTTGAAGTAATATTCCTAGGAATAA5' (MALP2, reverse primer), and flanked the coding region of malarial HPRT cDNA. The primers were diluted to 50 pmol μl^{-1} in TE buffer for storage in aliquots at -20 °C. As for the human HPRT amplification primers, the forward primer was synthesised to generate *Nde*1 recognition site (underlined), while the reverse primer was synthesised to generate a *Bam*H1 recognition site (underlined) on amplified malarial HPRT cDNA. These primers were checked for possible dimer formation and primer secondary structure, both of which would limit amplification. The template (50 ng malarial HPRT cDNA clone 7-3g) was used for the amplification. The thermocycler temperature profile was as follows:

denaturation 93.5 °C for 30 s

denaturation 93.5 °C for 1 min, 30 cycles

annealing 45 °C for 30 s, 30 cycles

extension 72 °C for 1 min, 30 cycles

final extension 72 °C for 10 min.

The PCR product was analysed on 1.5% agarose gel. Amplified cDNA was concentrated using standard ethanol precipitation, and extracted from the agarose gel as before. A subsequent amplification of malarial HPRT cDNA was conducted using Expand™ High Fidelity PCR system according to the manufacturer's instructions.

University of Cape Town

2.2.2 The cloning of malarial HPRT cDNA into pET-15b

2.2.2.1 Restriction endonuclease digestion of malarial HPRT cDNA

The purified PCR product was digested with both *Nde*1 and *Bam*H1 in the presence of SuRE/Cut™ buffer B overnight at 37 °C. As for the human HPRT cDNA digest, controls for the efficiency of *Nde*1 and *Bam*H1 digestion were included.

2.2.2.2 The ligation of malarial HPRT cDNA in pET-15b and transformation into *E. coli* XL1 blue

Ligation and transformation reactions were conducted as before. Ten colonies were selected for extraction of plasmid DNA by the alkaline lysis method.

2.2.2.3 Confirmation of the presence of insert in pET-15b

A selection of plasmid DNA preparations was made for digestion with *Nde*1 and *Bam*H1. Digestion was conducted overnight at 37 °C. Digestion controls were run simultaneously, and the digests were analysed on a 1% agarose gel, while the controls were analysed on a 0.8% agarose gel. A single clone was selected for automated sequencing (see Technical Appendix, 1J for sequencing details).

Glycerol stocks of *E. coli* BL21(DE3)pLysS transformed with malarial HPRT/pET-15b were prepared according to the manufacturer's instructions.

University of Cape Town

2.3 The expression and purification of human and malarial HPRT

Molecular weight standards were purchased from Bio-Rad Laboratories. The protease and phosphatase inhibitor cocktail, pepstatin A, soybean trypsin inhibitor, PRPP and 1,10-phenanthroline were purchased from Sigma. PMSF was obtained from Fluka. The Ni-NTA resin was purchased from Qiagen, and Sephadex™ G-25 M columns were purchased from Amersham Pharmacia Biotech. DNase 1 was purchased from Roche Molecular Biochemicals. Bovine albumin (fraction V) was obtained from BDH Biochemicals, and lysozyme was purchased from Boehringer Mannheim.

2.3.1 Time course of induction of HPRT expression

The glycerol stock of *E. coli* BL21(DE3)pLysS containing human or malarial HPRT cDNA in the expression plasmid pET-15b was streaked onto a Luria agar plate supplemented with 100 µg/ml ampicillin and incubated overnight at 37 °C. A single colony was inoculated into 50 ml Luria broth (10 g/l tryptone, 5 g/l yeast extract, 5 g/l NaCl, 1 mM NaOH) supplemented with 100 µg/ml ampicillin, and grown at 37 °C in an orbital shaker at 220 rpm. Incubation was continued until an OD_{600nm} of 0.6 was reached, at which point IPTG (1 mM) was added for induction of HPRT expression. A 500 µl aliquot was taken immediately, and the cell pellet of the aliquot was collected by microcentrifugation at 9000 rpm for 5 min. All purification steps were conducted at 4 °C. The cells were resuspended in 50 µl water, and an equal volume 2X SDS-PAGE solubilisation buffer (125 mM Tris/HCl, pH 6.8, 20% (w/v) glycerol, 4% (w/v) SDS, 300 mM 2-mercaptoethanol, 0.1 mg bromophenol blue) was added. The contents were mixed by vortexing, and stored at –20 °C. Samples taken at 15 min, 30 min, 45 min, 1 h, 2 h, 3 h, 4 h, 5 h were treated the same. A control where no IPTG was added to a second culture was

University of Cape Town

included. All samples were heated at 70 °C for 15 min to denature the protein. Each sample (10 µl) was loaded onto a 15% polyacrylamide gel for analysis according to Laemmli (1970.

2.3.2 The purification of human and malarial HPRT

2.3.2.1 Purification

The glycerol stock of *E. coli* BL21(DE3)pLysS containing human or malarial HPRT cDNA in pET-15b was cultured on Luria plates and grown in 100 ml Luria broth supplemented with 100 µg/ml ampicillin. Cells were grown to OD_{600nm} of 0.6, and expression was induced with 1 mM IPTG for 3 h at 37 °C in an orbital shaker at 200 rpm. Cells were pellets by centrifugation at 8000 rpm at 4 °C, and resuspended in ice-cold 5 mM imidazole, 500 mM NaCl, 20 mM Tris/HCl, pH 7.9. Lysozyme was added to 1 mg/ml, and the cells were incubated on ice for 1 h. $MgCl_2$ (10 mM) and DNase 1 (20 µg/ml) were added, followed by a 20 min incubation at room temperature. Cells were frozen in liquid nitrogen, and thawed in water at room temperature. Freeze-thaw was repeated twice. Subsequent purification steps were conducted at 4 °C. The cell lysate was centrifuged at 21000*g* for 20 min at 4 °C, and the supernatant was passed through a 0.45 µm filter before loading onto a nickel affinity resin column equilibrated with 5 mM imidazole, 500 mM NaCl, 20 mM Tris/HCl, pH 7.9. The column was washed with 10 column volumes of equilibration buffer, and 6 column volumes of equilibration buffer containing 60 mM imidazole. Elution of HPRT was in 6 column volumes of equilibration buffer containing 1 M imidazole.

University of Cape Town

2.3.2.2 Assays for activity

The eluant was assayed for enzyme activity with the purine bases guanine, hypoxanthine or xanthine using a continuous spectrophotometric assay at 25 °C unless otherwise specified. Assays were performed on a Hewlett Packard 8450A Diode Array Spectrophotometer, and the standard assay consisted of 100 mM Tris/HCl, pH 8.5, 100 mM $MgCl_2$, 1 mM PRPP, 60 µM purine base and an aliquot of enzyme. The rate of increase in absorbance at 257, 245 and 255 nm was a measure of HPRT activity, and was used to calculate specific activities using extinction coefficients of 5817, 2283 and 4685 $M^{-1} cm^{-1}$ for guanine, hypoxanthine and xanthine respectively. Protein concentration was determined by the Bio-Rad protein microassay procedure according to the manufacturer's instructions, using bovine albumin as the standard.

2.3.3 Procedures to obtain active malarial HPRT

2.3.3.1 The removal of imidazole from purified malarial HPRT

E. coli BL21(DE3) plysS containing the pET-15b/malarial HPRT expression vector was cultured in 100 ml Luria broth supplemented with 100 µg/ml ampicillin, and was purified as described in section 2.3.2. The eluant (2.5 ml) from nickel column affinity chromatography was immediately passed through a Sephadex™ G-25 M column equilibrated with 25 mM Tris/HCl, pH 8, 10 mM $MgCl_2$, and was eluted with 3.5 ml of the equilibration buffer. Malarial HPRT was assayed for activity using substrates guanine, hypoxanthine and xanthine as before.

University of Cape Town

2.3.3.2 The inclusion of PRPP in the lysis medium

Cells containing the expression plasmid with the insert were cultured, and centrifuged as before. Cells were resuspended in the lysis medium supplemented with 1 mM PRPP. Purification was conducted as described previously.

2.3.3.3 The induction of expression at low temperature

An *E. coli* BL21(DE3) plysS culture was cultured at 37 °C in the presence of 100 µg/ml ampicillin to an OD_{600nm} of 0.6. The culture flask was allowed to equilibrate to in a water bath set at 20 °C. IPTG (1 mM) was added, and expression was conducted at 20 °C in an orbital shaker at 200 rpm.

2.3.3.4 The assay of crude supernatant in the presence and absence of imidazole

An *E. coli* BL21(DE3) plysS culture induced for expression of malarial HPRT was divided into two portions of 50 ml each. The cells in both portions were collected by centrifugation and were resuspended in 3.5 ml 20 mM Tris/HCl, pH 7.9 containing 20 mM imidazole, or in the absence of imidazole. The preparation of cell lysate and supernatant was conducted as before. The supernatant was assayed for activity using guanine, hypoxanthine and xanthine as substrates as described previously.

University of Cape Town

2.3.3.5 The effect of DTT or 2-mercaptoethanol on crude supernatant HPRT activity

Crude supernatant was obtained from the *E. coli* culture described above. DTT was added (1 or 10 mM) or 2-mercaptoethanol (750 mM) was added. Assays for activity using guanine as the substrate in the presence of 1 or 10 mM DTT, or 15 mM 2-mercaptoethanol were conducted.

2.3.3.6 The expression of malarial HPRT without the histidine tag

Malarial HPRT cDNA was amplified using the forward primer 5'ATTAGACCATGGCAATACCAAATAAT3' and the reverse primer 3'GTTGAAGTAATATTCCTAGGAATAA5' (MALP2). The forward primer had the *Nco*1 restriction site (underlined) engineered into the 5' end region, whereas the reverse primer had the *Bam*H1 restriction site (underlined) engineered into the 5' end region. $MgCl_2$ was varied from 1 mM to 3 mM in separate reactions. The thermocycler temperature profile was as follows:

denaturation 93.5 °C for 30 s

denaturation 93.5 °C for 1 min, 30 cycles

annealing 42 °C for 30 s, 30 cycles

extension 72 °C for 1.5 min, 30 cycles

final extension 72 °C for 10 min.

The PCR reaction was analysed on 1.5% agarose gel and extracted from agarose gel as before.

University of Cape Town

The PCR product was ligated to pGEM®-T vector as described previously. Positive clones were selected for plasmid DNA extraction. Plasmid DNA was digested overnight at 37 °C in the presence of SuRE/Cut™ buffer B with 10 U *Nco*1 and 12 U *Bam*H1 to excise the 693 bp fragment corresponding to malarial HPRT cDNA. In a separate digestion, pET-15b was digested with the same restriction enzymes. Digested malarial cDNA and pET-15b were ligated as described in previous experiments, and transformed into *E. coli* XL1 blue competent cells. The plasmid DNA of the transformants was extracted for transformation into *E. coli* BL21(DE3)pLysS cells. A single *E. coli* BL21(DE3)pLysS colony containing malarial HPRT without the histidine tag was induced for expression with IPTG. The crude supernatant extract was obtained as before, and was assayed for activity using guanine, hypoxanthine and xanthine as substrates.

2.4 The molecular biology of malarial HPRT cDNA clone G11

2.4.1 Transformation, expression and purification of a malarial HPRT clone G11

Malarial HPRT (G11) cloned into pET-15b was a gift from Drs D. Borhani and G. Vasanthakumar, Southern Research Institute, Birmingham, Alabama. This clone has threonine in place of methionine in position 101 of the malarial HPRT protein, and is henceforth referred to as $HPRT_{pfthr}$ (*Plasmodium falciparum* threonine). The methionine-containing clone (the gift from Dr D.W. Melton, and used thus far in this study) will be referred to as malarial $HPRT_{pfmet}$ (*Plasmodium falciparum* methionine) to distinguish between the two clones

The $HPRT_{pfmet}$ clone in pET-15b was submitted for automated sequencing in order to verify its nucleotide sequence, and the sequencing details are in the Technical Appendix, 1J.

University of Cape Town

$HPRT_{pfthr}$/pET-15b was transformed into *E. coli* BL21(DE3) pLysS and was induced for HPRT expression with IPTG. The expressed protein was purified by nickel affinity chromatography, and was assayed for activity using guanine, hypoxanthine and xanthine as substrates.

2.5 The molecular biology of *Toxoplasma gondii* HPRT cDNA clone C1

2.5.1 The transformation, expression and purification of *T. gondii* HPRT clone C1

T. gondii HPRT (C1) cloned into pET-15b was also a gift from Drs D. Borhani and G. Vasanthakumar, Southern Research Institute, Birmingham, Alabama). The clone in pET-15b was submitted for automated sequencing to verify its nucleotide sequence (see Technical Appendix 1J for sequencing details). The cDNA clone was transformed into *E. coli* BL21(DE3)pLysS and was expressed as for $HPRT_{pfthr}$. The expressed protein was eluted from a nickel affinity column using 1 M imidazole, and was assayed for activity as described for before. Purified enzyme was stored in 50% (w/v) glycerol at –20 °C. A glycerol stock of *E. coli* BL21(DE3)pLysS containing *T. gondii* HPRT/pET-15b was prepared and stored at –80 °C.

University of Cape Town

2.5.2 The assay of *T. gondii* HPRT

T. gondii HPRT was purified and assayed using conditions reported by Héroux *et al.* (1999a). The assay medium consisted of 100 mM Tris/HCl, pH 8, 0.1 mM EDTA, 0.1 mg/ml bovine serum albumin and 20 mM $MgCl_2$. Assays were conducted at 37 °C. The conditions used by Keough *et al.*(1999) to assay $HPRT_{pfthr}$ were used as a comparison.

2.6 Reactivation studies

2.6.1 The reactivation of purified human HPRT, $HPRT_{pfmet}$, $HPRT_{pfthr}$, and *T. gondii* HPRT

All four HPRTases were purified using an adaptation of the protocol for *T. gondii* HPRT purification reported by Héroux *et al.* (1999a).

The glycerol stock of *E. coli* BL21(DE3)pLysS containing human HPRT, $HPRT_{pfmet}$, $HPRT_{pfthr}$, or *T. gondii* HPRT cDNA in pET-15b were each cultured on Luria agar plates and in 100 ml Luria broth as before. The Luria broth was supplemented with 10 mM sodium phosphate to suppress phosphatase expression. HPRT expression was induced with 1 mM IPTG when cell cultures reached an OD_{600nm} of 0.4. Induction was at 37 °C over 3 h, after which cells were collected by centrifugation at 8000 rpm at 4 °C. The pellet was washed in sterile PBS, and frozen overnight at –80 °C, or used immediately. Frozen pellet was thawed before use. The cell pellet was resuspended in buffer containing 50 mM Tris/HCl, pH 8, 10 mM $MgCl_2$, 2 mM PMSF, 4 µg/ml pepstatin A, 20 µg/ml soybean trypsin inhibitor, protease and phosphatase inhibitor cocktail (used according to the manufacturer's instructions), 100 µg/ml lysozyme, 20 µg/ml DNase 1, 1 mM PRPP and 10% (w/v) glycerol. Cells were frozen in liquid nitrogen, and thawed by incubation in water at room temperature. The freeze-thaw procedure was repeated twice. The cell extract was sonicated using a Branson Sonifier 250 (30% duty cycle) for 10 min, at 1 min intervals on icy water. The cell extract was centrifuged at 27000*g* for 20 min at 4 °C. The supernatant was passed through a 0.45 µm filter and loaded onto a 2.5 ml Ni-NTA resin column equilibrated with 20 mM sodium phosphate, pH 7.5, 0.5 M NaCl, 10 mM imidazole. The column was washed with 6 column volumes of equilibration buffer containing 60 mM imidazole. Elution of HPRT was in 2 column volumes of equilibration buffer containing 250 mM imidazole.

University of Cape Town

PMSF and 1,10-phenanthroline were added to 2 mM, and 2.5 ml of this solution was immediately loaded onto a Sephadex™ G-25 M column equilibrated with 25 mM Tris/HCl, pH 8, 10 mM $MgCl_2$, 0.1 mM EDTA, 1 mM DTT. Elution was in 3.5 ml equilibration buffer. When required, the protein was concentrated using a Centriplus® YM-100 centrifugal filter device (Amicon® Bioseparations). PRPP and glycerol were added to 1 mM, and 50% (w/v) respectively. Purified protein was assayed immediately, and incubated at 4 °C. Assays at 16, 40, 64, 88, 112, 136, 160 h time intervals were conducted as before at 37 °C, in the absence of EDTA and bovine serum albumin. Protein concentration was determined as before.

2.6.2 The effect of DTT and PRPP on $HPRT_{pfthr}$ reactivation at low temperature

Purified $HPRT_{pfthr}$ was incubated with 50% glycerol at 4 °C in the absence of additives DTT and PRPP, or in the presence of 1 mM DTT, or 1 mM PRPP, or 1 mM DTT and 1 mM PRPP. An aliquot of protein was assayed for activity using guanine as substrate after 48 h and 72 h incubation at 4 °C.

2.6.3 The effect of glycerol on the reactivation of $HPRT_{pfthr}$ at low temperature

Purified $HPRT_{pfthr}$ was incubated as in Section 2.6.2, in the presence of 50% or 10% glycerol.

2.6.4 The effect of freezing on reactivated $HPRT_{pfthr}$

Reactivated $HPRT_{pfthr}$ was frozen in liquid nitrogen, and incubated at -80 °C for 10 days. Thawed protein was assayed for activity.

University of Cape Town

2.7 Stability studies on $HPRT_{pfthr}$

2.7.1 Studies on $HPRT_{pfthr}$ inactivation during turnover

In the following series of experiments, enzyme was pre-incubated with or without substrates, and in the presence of a high or low concentration of $MgCl_2$. Activity was monitored by a continuous spectrophotometric assay.

2.7.1.1 Purified $HPRT_{pfthr}$ was pre-incubated in 100 mM Tris/HCl buffer, pH 8.5 and 10 or 100 mM $MgCl_2$ for 5 min at 25 °C. Substrates PRPP and Guanine were added at 1 mM and 60 µM respectively, and incubation was continued for a further 5 min.

2.7.1.2 Protein was pre-incubated for 5 min at 25 °C in the presence of 100 mM Tris/HCl buffer, pH 8.5, 10 or 100 mM $MgCl_2$ and 1mM PRPP. Guanine (60 µM) was added, and incubation was continued for 5 min.

2.7.1.3 Protein was pre-incubated for 5 min at 25 °C in the presence of 100 mM Tris/HCl buffer, pH 8.5, 10 or 100 mM $MgCl_2$ and 60 µM guanine. PRPP (1 mM) was added, and incubation was continued for 5 min.

2.7.2 Establishing of whether substrate depletion or enzyme inactivation occurs during turnover

Purified $HPRT_{pfthr}$ was assayed in at 25 °C in the presence of 100 mM Tris/HCl buffer, pH 8.5, 100 mM $MgCl_2$, 1 mM PRPP and 60 µM guanine for 100 s. Guanine (40 µM) was added, and

University of Cape Town

incubation was allowed to proceed for a further 100 s. PRPP (1 mM) was added to the reaction, and incubation was continued for a further 100s.

2.7.3 Histidine tag cleavage by thrombin

$HPRT_{pfthr}$ was pre-incubated in 25 mM Tris/HCl, pH 8 containing 500 µM PRPP for 5 min at 20 °C and was added to 10 U thrombin in 25 mM Tris/HCl, pH 8, 0.1 mM EDTA, 10 mM $MgCl_2$, 1 mM DTT, and 1 mM $CaCl_2$. The cleavage reaction was incubated at 20 °C, and at time intervals 30 s, 1 min, 3 min, 5 min, 10 min, 15 min, 30 min and 1 h, cleavage was stopped by the addition of 1 mM PMSF. The extent of cleavage was monitored by SDS-PAGE. The enzyme activity of the samples was measured at each time interval using guanine as substrate.

2.8 Chemical syntheses

Xanthosine was purchased from Sigma. Aluminum oxide (activated, neutral) was obtained from Aldrich Chemical Co, Ltd). Sep-Pak® Plus C18 cartridges were purchased from Waters Associated. DE52 DEAE cellulose was purchased from Whatman®. A Beckman System Gold 126 pump mechanism/168 diode array detector HPLC system was used for analysis and purification of compounds on a Vydac™ C18 column (0.45 x 25 cm), at ambient temperature. HPLC conditions are presented in the legend of HPLC traces in the results section. Absorption spectra were obtained on a Hewlett Packard 8450A Diode Array Spectrophotometer. TNBS was purchased from Fluka, and DTNB was purchased from Sigma. All other reagents used were of analytical grade.

University of Cape Town

2.8.1 The synthesis of 8-azidoxanthine

8-bromoxanthosine was synthesised according to Long *et al.* (1967). Xanthosine (100 mg) was suspended in 500 µl water. Bromine water (80 µL bromine dissolved in 4 ml water) was added over 10 min with constant stirring at room temperature. The reaction was allowed to proceed for about 5 min longer, after which a white precipitate had formed. An aliquot was taken for HPLC analysis of the extent of bromination. The reaction solution was filtered through Whatman® 2.5 cm GF/F Glass microfibre filters and the residue crystals were washed with cold water. The white crystals were dried in a dessicator at room temperature. The product (8-bromoxanthosine) was confirmed by diode array spectrophotometry. 8-bromoxanthosine (4 mg) was dissolved in 10 ml DMSO pre-saturated with sodium azide. Sodium azide (500 mg) and 30% H_2O_2 (20 µl) were added, and the reaction was allowed to proceed in the dark for 16 h at room temperature with stirring. An aliquot was taken for analysis by HPLC. Excess sodium azide was removed by filtration on Whatman® 2.5cm GF/F Glass microfibre filters. The residue was washed with 500 µl DMSO. The mixed DMSO solutions were passed through an aluminum oxide (activated, neutral) resin. The column was washed with water to remove DMSO and sodium azide. 8-azidoxanthosine was eluted from the aluminum column with 0.5 M ammonium acetate, pH 7, and lyophilised to dryness at room temperature. The end product was reconstituted in minimal water and purified by HPLC to remove an undesirable side product. HPLC fractions were concentrated by lyophilisation and reconstituted in water. 8-azidoxanthosine (2 mM) was incubated overnight at 25 °C with 2 M HCl. The acid cleavage reaction was diluted 1:10 in 1 mM KPi, pH 3 and was analysed and purified by HPLC.

University of Cape Town

2.8.2 The synthesis of TNP-GMP, TNP-IMP and TNP-XMP

TNP-GMP, TNP-IMP and TNP-XMP were synthesised using a method of TNP-8-azido-nucleotide synthesis by Seebregts and McIntosh (1989). A suspension was made by adding 600 µl sodium carbonate buffer (218 mg Na_2CO_3, 151 mg $NaHCO_3$ in 2.4 ml water) to 90 mg TNBS. The remainder of the buffer was added to the suspension and dissolved by warming in water at 37 °C if necessary. 100 µmoles GMP, IMP or XMP were added, and the reaction was allowed to proceed with stirring overnight at 37 °C. In crude separation, an acetonitrile step-wise gradient (1 ml portions of 5, 10 and 30% acetonitrile) was used to separate TNP-GMP or TNP-IMP from picrate and any remaining TNBS using Sep-Pak® Plus C18 cartridges. TNP-XMP, however, was purified from the reaction mixture by HPLC. Acetonitrile-eluted fractions containing TNP-GMP or TNP-IMP were identified from their spectra, and pooled. Acetonitrile was removed using a gentle nitrogen gas stream, before lyophilisation to dryness. Lyophilised fractions were reconstituted in water. TNP-GMP and TNP-IMP were purified by HPLC.

2.8.3 The synthesis of TNP-8-azido-xanthosine

TNP-8-azido-xanthosine was synthesised using a method of TNP-8-azido-nucleotide synthesis by Seebregts and McIntosh (1989). Sodium carbonate buffer, pH 9.5 was made by dissolving 910 mg Na_2CO_3 and 630 mg $NaHCO_3$ in 10 ml distilled water. TNBS (6 mg) and DTNB (12 mg) were dissolved in 500 µl sodium carbonate buffer, pH 9.5 by warming in water if necessary. The TNBS/DTNB solution in buffer (83 µl) was immediately added to 670 nmoles 8-azido-xanthosine in 100 µl water. The reaction was incubated with stirring for 4 h in the dark at room temperature. TNP-8-azido-xanthosine was purified by HPLC.

University of Cape Town

2.8.4 The synthesis of conjugates between TNP-8-azido-xanthosine or 8-azido-xanthine and a selection of flavonoids

2.8.4.1 The synthesis of a conjugate between TNP-8-azido-xanthosine and kaempferide

TNP-8-azido-xanthosine and kaempferide (both at 10 μM concentration) were irradiated in water for 5 min. The irradiation products were analysed by HPLC. Controls included the irradiation of kaempferide alone or TNP-8-azido-xanthosine alone under the same conditions.

2.8.4.2 The synthesis of a conjugate between 8-azido-xanthosine and kaempferide

8-azido-xanthosine and kaempferide were irradiated together and the analysis of the irradiation products was analysed as in section 2.8.4.1.

2.8.4.3 The synthesis of a conjugate between 8-azido-xanthine and kaempferide

8-azido-xanthine and kaempferide were irradiated together and the irradiation products were analysed in section 2.8.4.1.

2.9 Drug screening

The compounds synthesised were tested for inhibitory properties on human HPRT, $HPRT_{pfthr}$ and *T. gondii* HPRT.

University of Cape Town

2.9.1 Pre-incubation with TNP-GMP, TNP-IMP or TNP-XMP

All three TNP-nucleotides were tested for inhibition of $HPRT_{pfthr}$ as a start. Enzyme was pre-incubated for 5 min in the presence of 100 mM Tris/HCl, pH 8.5 and 100 mM $MgCl_2$ and 6 µM (1/10th purine base substrate) TNP-nucleotide at 25 °C. PRPP (1 mM) and guanine (60 µM) were added, and incubation was continued for a further 5 min. A control for activity after pre-incubation in the absence of TNP-nucleotide was conducted. The reaction was monitored by continuous spectrophotometry, and enzyme activity was expressed as before.

2.9.2 Continuous assays in the presence of TNP-GMP

TNP-GMP was the only TNP-nucleotide that showed inhibition after pre-incubation with enzyme. Tests for inhibition by TNP-GMP were performed on human HPRT, $HPRT_{pfthr}$, and *T. gondii* HPRT, and were designed so that competition between TNP-GMP and PRPP could be studied.

The HPRTases were assayed in the presence of 100 mM Tris/HCl, pH 8.5, 100 mM $MgCl_2$, 1 mM PRPP, 20 µM guanine and up to 60 µM TNP-GMP at 25°C. The reaction was started by the addition of enzyme.

University of Cape Town

2.9.3 The characterisation of inhibition of $HPRT_{pfthr}$ by TNP-GMP

Inhibition studies of $HPRT_{pfthr}$ by TNP-GMP were conducted in the presence of either substrate. The data obtained was fitted to a Michaelis-Menton curve for characterisation of inhibition.

2.9.4 Test of flavonoids as inhibitors of $HPRT_{pfthr}$ activity

A selection of flavonoids (Figure 2.1) obtained from Professor D Barron (Laboatorie de Produits Naturels, UMR 5013 CNRS/ Université Claude Bernard-Lyon I, Villeurbanne, France), Dr A Peitro (Institut de Biologie et Chimie des Protéines, UMR 5086 CNRS/ Université Claude Bernard-Lyon I, France), and Dr A Boumendjal (Département de Pharmacochimie Moléculaire, UMR 5063 CNRS/ Université Joseph Fourier, de Grenoble, La Tronche, France) was tested for inhibition of $HPRT_{pfthr}$ under turnover conditions.

University of Cape Town

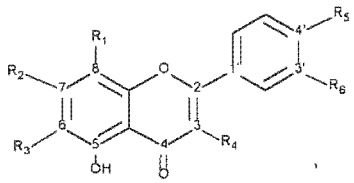

galangin: R_2=R_4=OH, R_1=R_3=R_5=R_6=H

6-prenyl-galangin: R_2=R_4=OH, R_3=A, R_1=R_5=R_6=H

8-prenyl-galangin:R_2= R_4=OH, R_1=A, R_3=R_5=R_6=H

kaempferide:R_2=R_4=OH, R_5=OMe, R_1=R_3=R_6=H

chrysin:R_2=OH, R_1=R_3=R_4=R_5=R_6=H

6,8(di-3,3-DMA)-chrysin:R_1=R_3=A, R_2=OH, R_4=R_5=R_6=H

tectochrysin:R_2=OMe, R_1=R_3=R_4=R_5=R_6=H

6(3,3-DMA)-chrysin:R_3=A, R_2=OH, R_1=R_4=R_5=R_6=H

7(3,3-DMA)-chrysin:R2=O-A, R1=R3=R4=R5=R6=H

8(1,1-DMA)-chrysin:R_1=B, R_2=OH, R_3=R_4=R_5=R_6=H

8(3,3-DMA)-chrysin:R_1=A, R_2=OH, R_3=R_4=R_5=R_6=H

6-geranyl-chrysin:R_3=C, R_2=OH, R_1=R_4=R_5=R_6=H

8-geranyl-chrysin:R_1=C, R_2=OH, R_3=R_4=R_5=R_6=H

4'-F-chrysin:R_5=F, R_2=OH, R_1=R_3=R_4=R_6=H

4'-I-chrysin:R_5=I, R_2=OH, R_1=R_3=R_4=R_6=H

F5OH-I: R_5=I, R_1=R_2=R_3=R_4=R_6=H

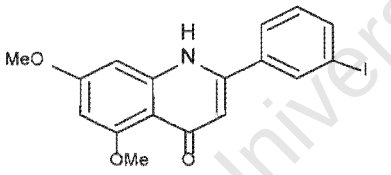

MH-48

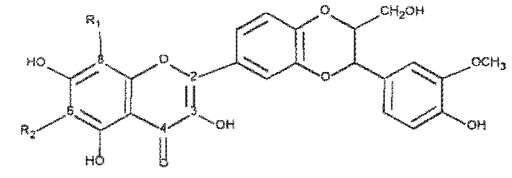

silybin:R_1=R_2=H; reduced 2,3 bond

dehydrosilybin:R_1=R_2=H

6-prenyl-dehydrosilybin:R_1=H, R_2=A

8-prenyl-dehydrosilybin:R_1=A, R_2=H

University of Cape Town

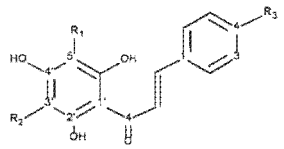

4-C_2H_5-chalcone:R_4=O-C_2H_5, R_1=R_2=R_3=H

4-C_4H_9-chalcone:R_4=O-C_4H_9, R_1=R_2=R_3=H

4-C_6H_{13}-chalcone:R_4=O-C_6H_{13}, R_1=R_2=R_3=H

4-C_8H_{17}-chalcone:R_4=O-C_8H_{17}, R_1=R_2=R_3=H

4-I-chalcone:R_4=I, R_1=R_2=R_3=H

4-F-chalcone:R_4=F, R_1=R_2=R_3=H

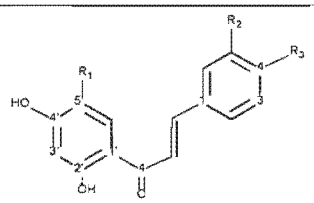

broussochalcone A: R_1=A, R_2=R_3=OH

2',4',4-trihydroxy chalcone: R_1=R_2=H, R_3=OH

2',4',4-trihydroxy-3-prenyl chalcone: R_1=H, R_2=A, R_3=OH

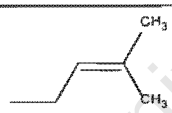

A (3,3-DMA)

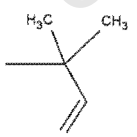

B (1,1-DMA)

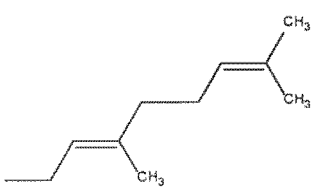

C (geranyl)

University of Cape Town

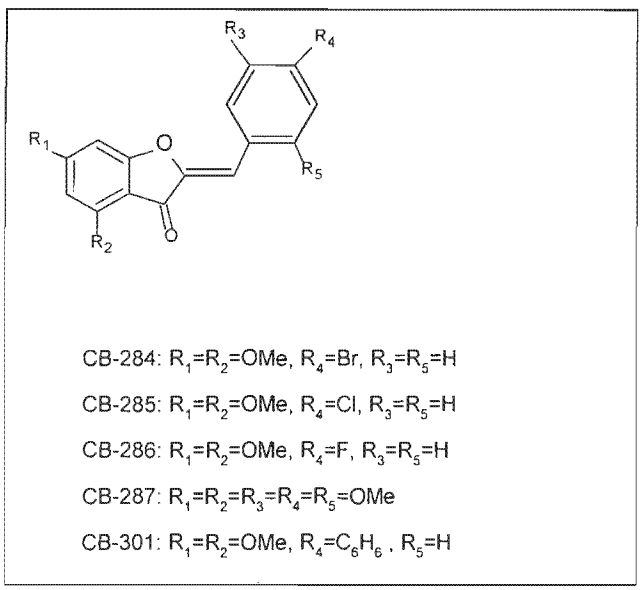

CB-284: R_1=R_2=OMe, R_4=Br, R_3=R_5=H

CB-285: R_1=R_2=OMe, R_4=Cl, R_3=R_5=H

CB-286: R_1=R_2=OMe, R_4=F, R_3=R_5=H

CB-287: R_1=R_2=R_3=R_4=R_5=OMe

CB-301: R_1=R_2=OMe, R_4=C_6H_6 , R_5=H

Figure 2.1 Flavonoids used to test for inhibitory properties against $HPRT_{pfthr}$
Flavonoid stocks of 5mM concentration were prepared in DMSO, and were used at 2 and 20µM concentration in the presence of 100 mM Tris/HCl, pH 8.5, 100 mM $MgCl_2$, 20 µM guanine and 1 mM PRPP at 25 °C. The appropriate blanks for spectrophotometric assays were prepared simultaneously.

University of Cape Town

2.9.5 Further studies on the effect of 4-I-chalcone on $HPRT_{pfthr}$

2.9.5.1 The activation of $HPRT_{pfthr}$ activity by 4-I-chalcone

The activation of $HPRT_{pfthr}$ (and not human nor *T. gondii* HPRT) by 4-I-chalcone (4-iodo-2',4',6'-trihydroxy chalcone) was observed, and was investigated further. Up to 60 µM 4-I-chalcone was used in the presence of 100 mM Tris/HCl, pH 8.5, 100 mM $MgCl_2$, 20 µM guanine and 1 mM PRPP at 25 °C.

2.9.5.2 The effect of conjugates between TNP-8-azido-xanthosine and 4-I-chalcone on $HPRT_{pfthr}$ activity

Conjugates between TNP-8-azido-xanthosine and 4-I-chalcone were synthesised. HPLC analysis of the reaction was conducted. TNP-8-azido-xanthosine (125 µl of 400 µM stock) was mixed with 20 µl of a 5 mM stock of 4-I-chalcone, and the mixture was irradiated for 5 min. Tris/HCl, pH 8.5 (100 mM), $MgCl_2$ (100 mM) and guanine (20 µM) were added. $HPRT_{pfthr}$ was assayed for activity at 25 °C. The effect of a conjugate between TNP-8-azido-xanthosine and kaempferide under the same conditions was tested as a comparison. Photolysis products from the irradiation of TNP-8-azido xanthosine and 8-azidoxanthosine were also tested for inhibitory properties.

2.10 Fluorescence studies

2.10.1 Probing for hydrophobic pockets formed during unfolding and inactivation

The anionic dye ANS (8-anilino-1-naphthalene-sulfonic acid) was used to probe for hydrophobic pockets formed upon unfolding and inactivation of $HPRT_{pfthr}$. Emission scans under the following conditions were conducted on a Spex Fluoromax® Spectrofluorimeter at 25 °C with constant stirring, and were analysed for evidence of ANS binding to hydrophobic sites:

(i) $HPRT_{pfmet}$ (10 µg protein/ml), 500 µM PRPP, 10 mM $MgCl_2$, 25 mM Tris/HCl, pH 8.5

(ii) conditions in (i) above + 40 µM ANS

(iii) conditions in (i) above + 40 µM ANS + 50 µM hypoxanthine

(iv) 40 µM ANS alone

University of Cape Town

2.10.2 pH-dependence of fluorescence changes during turnover

$HPRT_{pfthr}$ (50 µg protein/ml) was incubated in the presence of 50 mM Tris/maleate buffer (pH 6 to 8 range) or Tris/HCl (pH 8.5 to 9.5 range), 100 mM $Mgcl_2$, and 500 µM PRPP at 25 °C. Intrinsic Trp fluorescence was monitored at excitation and emission wavelengths of 290 and 340 nm respectively. Water (125 µl) was added for a 5% change in fluorescence, used to determine changes due to dilution upon the addition of hypoxanthine. The initial fluorescence signal was also determined at each pH for $HPRT_{pfthr}$ (50 or 15 µg protein/ml) and was plotted against pH.

2.10.3 Monitoring of HPRT inactivation

Changes in fluorescence corresponding $HPRT_{pfthr}$ inactivation were monitored by incubation of 50 µg protein/ml enzyme in the presence of 50 mM Tris/HCl, pH 9.5 and 100 mM $MgCl_2$, with or without PRPP as the stabilising agent. Changes were also observed under turnover conditions.

2.10.4 Fluorescence changes during turnover and an assay for the reversal of IMP inhibition of HPRT activity by 4-I-chalcone

$HPRT_{pfthr}$ or *T. gondii* HPRT (20 µg protein/ml) was incubated in the presence of 100 mM Tris/HCl, pH 8.5, 100 M $MgCl_2$, and 500 µM PRPP at 25 °C. Intrinsic Trp fluorescence was monitored using excitation and emission wavelengths of 290 and 340 nm respectively. Water (125 µl) was added for a 5% change in fluorescence, and this change was incorporated in the interpretation of dilution effects brought by subsequent additions of substrates and to determine

University of Cape Town

the extent change in fluorescence. The water addition was followed by increasing amounts of hypoxanthine up to 20 μM, with constant monitoring of fluorescence. Changes in fluorescence were monitored in the presence increasing concentrations of IMP (50 to 500 μM) and 20 μM 4-l-chalcone.

University of Cape Town

CHAPTER 3 RESULTS

3.1 The molecular biology of human HPRT

3.1.1 The amplification of human HPRT cDNA

Human HPRT cDNA was amplified by PCR to produce a 650 bp DNA fragment. The result is shown in Figure 3.1.

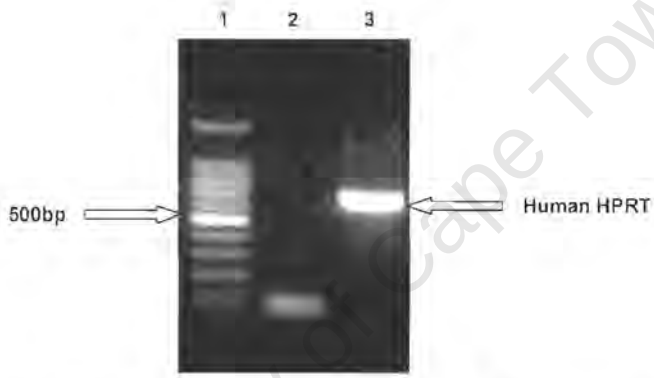

Figure 3.1 Amplified human HPRT cDNA analysed on a 1.5% agarose gel. Lane 1, 100 bp ladder; lane 2, contamination control (all components except for the template, 15 µl) showing primer dimer at the bottom of the lane; lane 3, PCR reaction (15 µl) showing amplified human HPRT cDNA. DNA was visualized by ethidium bromide staining.

University of Cape Town

3.1.2 The transformation of *E. coli* cells

Human HPRT cDNA amplified by PCR was concentrated by standard ethanol precipitation, and was purified by agarose gel extraction using the QiaexII gel extraction kit (Qiagen). The purified cDNA was cloned into the pGEM®-T vector using the 3'-terminal thymidine residues of the vector, and the corresponding adenosine residue from the PCR product (added in a template – independent manner by Taq polymerase). Competent *E. coli* XL1 blue cells were transformed by mixing and incubating on ice with human HPRT cDNA in pGEM®-T vector. A separate

aliquot of cells was transformed with 0.03 ng PUC18 vector to determine transformation efficiency. Transformation efficiency was usually approximately $3.5x10^7$ cfu (colony forming units) per µg DNA. Recombinants or positive clones were identified by blue/white screening using the α-peptide coding region of β-galactosidase enzyme in pGEM®-T vector (Figure 3.2).

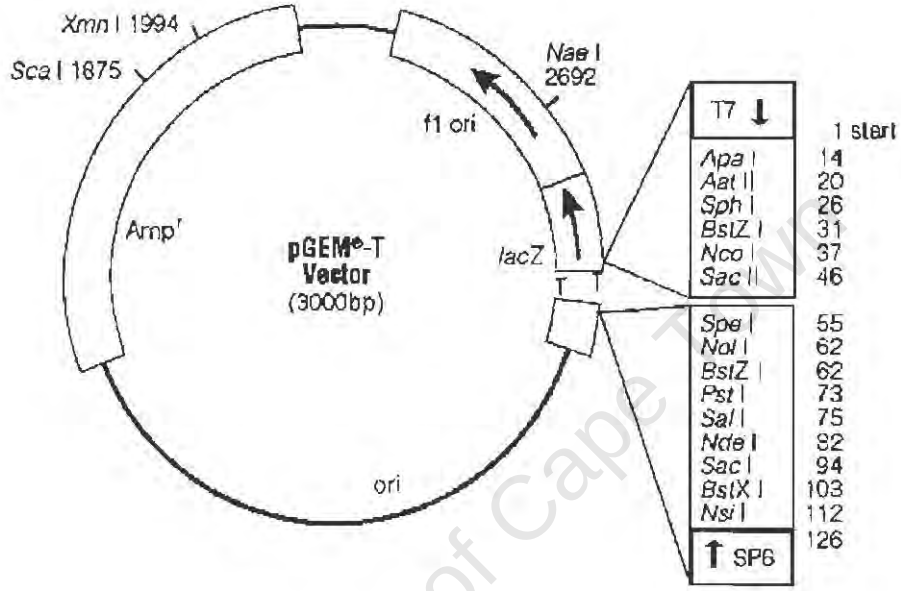

Figure 3.2 Map of pGEM®-T vector, showing the region used for cloning of PCR products. The 3' terminal thymidines (T) were used for inserting PCR products with a single 3' deoxyadenosine (A) added by Taq polymerase in a template-independent manner. Positive clones were selected by blue/white screening. This figure was taken from the Promega website (http://www.promega.com. © 1995-2001, Promega Corporation).

University of Cape Town

3.1.3 Transformation and selection of *E. coli* cells human cDNA insert in pGEM®-T

E. coli XL1 blue colonies transformed with purified pGEM®-T containing human HPRT cDNA were selected for and cultured for plasmid DNA extraction by the alkaline lysis method. The results of the extraction are shown in Figure 3.3.

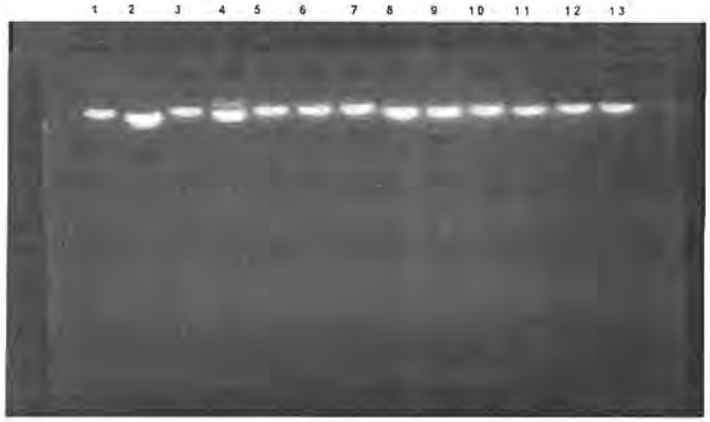

Figure 3.3 Plasmid DNA extraction from *E. coli* XL1blue colonies. Lanes 1-13, Plasmid DNA extractions from thirteen *E. coli* XL1 blue colonies with human HPRT cDNA in pGEM®-T. Plasmid DNA (10 µl) was analysed on a 0.8% agarose gel. DNA was visualized by ethidium bromide staining.

3.1.4 Restriction digests of plasmid DNA

A selection of plasmid DNA extracts was digested with restriction enzymes *Nde*1 and *Bam*H1 to confirm the presence of the human HPRT cDNA insert. The digests were analysed by agarose gel electrophoresis as shown in Figure 3.4.

University of Cape Town

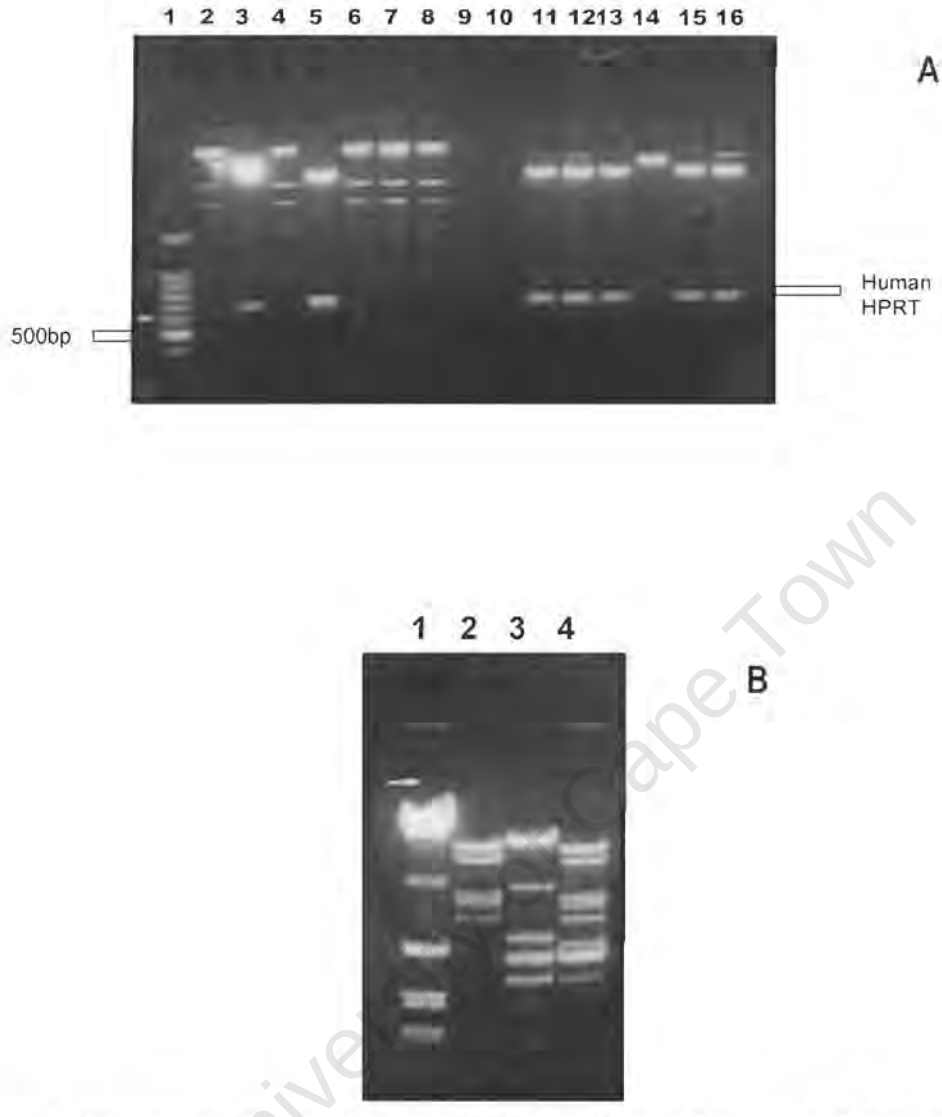

University of Cape Town

Figure 3.4 Restriction digests of plasmid DNA extracts. Panel A, lane 1, 100 bp ladder, lanes 2-8 plasmid DNA extracts digested with *Nde*1 and *Bam*H1. Lanes 9 and 10, unloaded wells. Lanes 11-16 plasmid DNA extracts digested with *Nde*1 and *Bam*H1. Plasmid DNA extracts were digested with *Nde*1 and *Bam*H1 overnight at 37 °C. Each lane contains 15 µl digest, analysed on a 1.5% agarose gel. Panel B, lane 1, digestion of λDNA by *Nde*1 (yields 7 bands); lane 2, digestion of λDNA by *Bam*H1 (yields 5 bands); lane 3, digestion of λDNA by *Nde*1 in the presence of plasmid DNA; lane 4 digestion of λDNA by *Bam*H1 in the presence of plasmid DNA. Digestion reaction (15 µl) was used as in Panel A. DNA was analysed on a 0.8% agarose gel, and was visualized by ethidium bromide staining.

Panel A in Figure 3.4 shows that 7 of the 13 plasmids contain the 650 bp fragment corresponding to human HPRT cDNA after digestion with *Nde1* and *Bam*H1. The fragment is clearly visible in lanes 3, 5, 11, 12, 13, 15 and 16. Panel B (lanes 1 and 2) shows that

restriction enzymes are active, as the expected number of bands after digestion of λDNA with either enzyme is observed: 7 bands for *Nde*1 (the last two bands are doublets), and 5 bands for *Bam*H1. Lanes 3 and 4 show a more complex pattern as expected with both λDNA and plasmid DNA present. The result indicates efficient digestion in the presence of plasmid DNA, and the absence of inhibitors such as phenol, chloroform, ethanol, SDS, salts or protein that could be carried through from the plasmid DNA extraction.

3.1.5 Sequence analysis of positive clones

Six of the plasmid DNA extractions showing the presence of the 650 bp fragment after digestion were selected for automated sequencing using the Sequenase® Version 2.0 DNA Sequencing Kit (United States Biochemical) or Thermo Sequenase dye terminator cycle sequencing pre-mix kit (Amersham Life Science) on a DNA sequencer (Applied Biosystems). The result of sequencing is shown aligned with the published sequence (Technical Appendix, 1A), and shows that the determined sequence is correct.

3.1.6 The preparation of pET-15b

The expression vector pET-15b was prepared using the Qiagen Plasmid Maxi kit from *E. coli* XL1 blue cells transformed with this vector. The result of the purification is presented in Figure 3.5. Lanes 11 and 12 show the purified pET-15b vector.

University of Cape Town

Figure 3.5 The purification of pET-15b. Two cultures (25 ml each) were used for the preparation of pET-15b, and the purification profile for each is presented. Lanes 1 and 2, supernatant from the first clarification. Lanes 3 and 4, supernatant from the second clarification. Lanes 5 and 6, flowthrough at column loading. Lanes 7 and 8, wash step to remove contaminants. Lanes 9 and 10, column eluant. Lanes 11 and 12, isopropanol/ ethanol-treated eluant. Each sample (2 µl) was analysed on a 0.8% agarose gel, except for the isopropanol/ ethanol-treated eluant (5 µl). DNA was visualized by ethidium bromide staining.

University of Cape Town

The cloning region for expression of DNA inserts is shown in Figure 3.6.

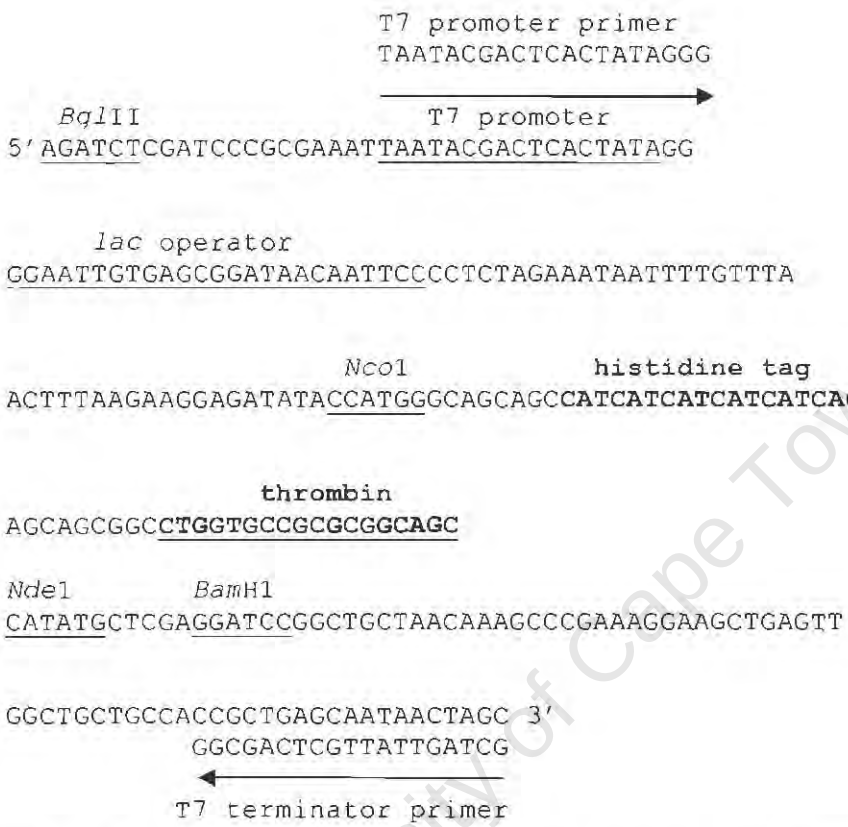

Figure 3.6 The cloning region of pET-15b, showing restriction sites, sequencing primer binding regions, His tag and thrombin cleavage regions. This figure was taken from the Promega website (http://www.promega.com. © 1995-2001, Promega Corporation).

University of Cape Town

3.17 The sequential digestion of pET-15b

The simultaneous digestion of pET-15b with *Nde*1 and *Bam*H1 was attempted. A control for efficiency of digestion (insert omitted during ligation) was included during the ligation of human HPRT cDNA to pET-15b, and transformation into *E. coli* XL1 blue. No colonies or a few colonies are expected from this control if digestion is complete or almost complete, since the ends produced by the restriction enzymes would be incompatible. The number of colonies

produced from this control was estimated to be 400, and strongly suggested re-ligation of pET-15b to itself. Re-ligation of pET-15b would result in a circular vector with ampicillin resistance that would be efficiently transformed. The cloning region of pET-15b shows that the distance between the *Nde*1 and *Bam*H1 restriction sites is only 12 bp apart. This short distance may not allow both enzymes to bind simultaneously. Consequently, sequential digestion, i.e. digestion with one enzyme first, and then the other was tried. Sequential digestion could be followed by calf intestinal alkaline phosphatase (CIAP) treatment to hydrolyse the 5'-phosphate groups from pET-15b, and prevent recircularization and religation of linearized pET-15b.

*Nde*1 was used first, followed by digestion with *Bam*H1. pET-15b digested by both enzymes was analysed on a 1% agarose gel. The gel was run for a long time to improve the separation of vector digested with both enzymes from that digested with *Nde*1 only. The bottom half of the pET-15b band was excised, as it was likely that removal of the 12 base-pair region would result in a pET-15b species that migrates slightly further. The control ligation, where insert was omitted, produced 2 colonies on Luria broth plates supplemented with 100 µg/ml ampicillin, suggesting efficient digestion of pET-15b.

Some of the sequentially-digested pET-15b was treated with CIAP according to the manufacturer's instructions. The control ligation produced no colonies. Transformation efficiency was calculated as 5.9×10^7 cfu/µg DNA.

Sequential digestion of pET-15b, with or without CIAP treatment, was thus shown to be a means of producing vector suitable for ligation with insert. A single colony from the ligation of pET-15b to human HPRT insert was cultured for plasmid DNA extraction. Extracted plasmid DNA was used to transform the *E. coli* expression strain, BL21(DE3)pLysS.

University of Cape Town

3.1.8 Test for plasmid stability

The test for plasmid stability was conducted as described in the pET System Manual (Novagen). In essence, the appropriate dilutions of a culture grown to saturation with *E. coli* BL21(DE3)pLysS strain containing the human HPRT cDNA insert in pET-15b were made, and were plated onto Luria agar plates supplemented with 100 µg/ml ampicillin, 1 mM IPTG, both, or neither. A total of 83 colonies were counted on the plate without additives (all viable cells) and 11 colonies on the plate with antibiotic only (cells that have retained plasmid). The colonies on plates supplemented with IPTG only, or IPTG and antibiotic were too small for accurate counting. The very poor growth of these colonies even after 16 h incubation at 37 °C suggested that these cells had not lost plasmid, or the ability to express target protein. The result was interpreted as a very strong inductive effect by IPTG.

3.2 The molecular biology of malarial HPRT

3.2.1 The design of oligonucleotide primers

Alignments for predicting the intracomplementarity as well as intercomplementarity of primers used to amplify malarial HPRT cDNA were conducted using the computer programme, Oligo Version 3.4.

Intercomplementarity of the two primers at their 3'ends was predicted. Steps were taken to reduce this intercomplementarity through the GC regions at the 3' end of MALP2: the 3' terminal C was removed. It is of note that 6 of the 12 bases at the 3' ends of MALP1 and MALP2 are complementary, but the extent of primer dimer formation was not considered to

University of Cape Town

have the potential of inhibiting amplification altogether. However, in the event of PCR failure, modification of the primers would be one of the options that could be considered.

3.2.2 The amplification of malarial HPRT cDNA

Amplified malarial HPRT cDNA is shown in Figure 3.7.

Figure 3.7 Agarose gel of amplified malarial HPRT cDNA. Lane 1, 100 bp ladder; lane 2, contamination control (all components of the reaction, except for the template) showing the faint primer dimer band at the bottom of the lane; lane 3, PCR reaction showing amplified malarial HPRT cDNA. Aliquots of 15 µl were analysed on a 1.5% agarose gel. DNA was visualized with ethidium bromide staining.

In view of the success of malarial HPRT cDNA amplification, further modification of the amplification primers and review of the amplification reaction was not necessary.

3.2.3 The cloning of malarial HPRT cDNA into pET-15b

Malarial HPRT cDNA purified from the PCR mix by gel extraction was digested with restriction endonucleases *Nde*1 and *Bam*H1. The digested PCR product was purified again by gel extraction and was ligated to pET-15b vector that had been digested with the same enzymes.

University of Cape Town

Plasmid DNA was extracted from *E. coli* XL1 blue transformants, and was digested with these enzymes to confirm the presence of the insert. The result is shown in Figure 3.8.

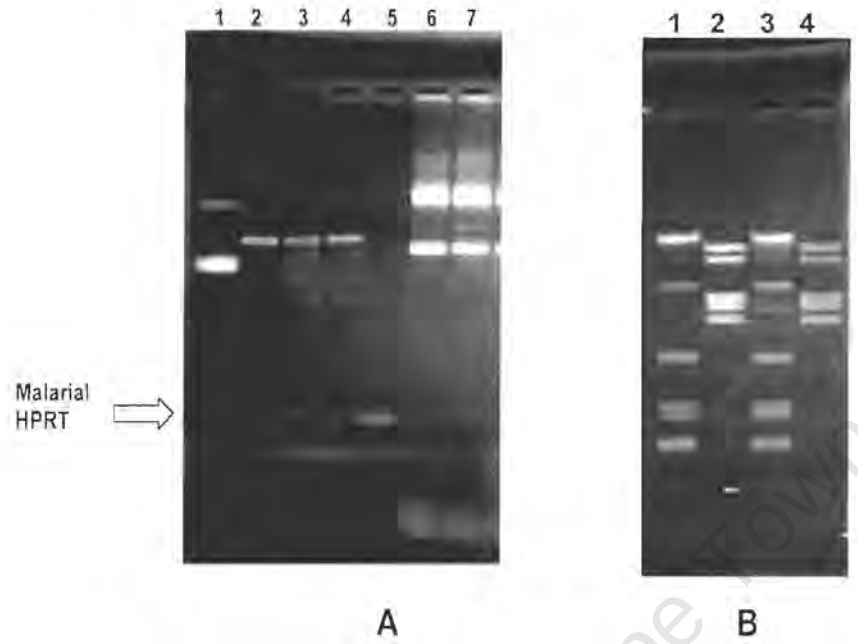

Figure 3.8 Agarose gel to confirm the presence of malarial HPRT cDNA insert in pET-15b. Panel A, lane 1, pET-15b vector (10 µl); lanes 2-4, plasmid DNA extract from 3 positive clones digested overnight with *Nde*1 and *Bam*H1 at 37 °C (10 µl); lane 5, digested malarial HPRT cDNA PCR product (10 µl); lanes 6-8, undigested plasmid DNA extracts (5 µl). Digests or controls were mixed with 4 µl loading buffer before analysis on a 1% agarose gel. Panel B, lane 1, digestion of λDNA by *Nde*1; lane 2, digestion of λDNA by *Bam*H1; lane 3, digestion of λDNA by *Nde*1 in the presence of plasmid DNA; lane 4 digestion of λDNA by *Bam*H1 in the presence of plasmid DNA. Digestion reaction (20 µl) was used. DNA was analysed on a 0.8% agarose gel, and was visualized with ethidium bromide.

Lanes 2 to 4 in Panel A of Figure 3.8 show the presence of the 693 base pair fragment corresponding to malarial HPRT cDNA after digestion with *Nde*1 and *Bam*H1. The DNA fragment in these lanes migrated parallel to the HPRT cDNA produced directly from PCR (lane 5), and this result confirms the presence of malarial HPRT cDNA in pET-15b. The undigested plasmid DNA fragments are included as a control. Panel B shows the efficient digestion of λDNA by *Nde*1 and *Bam*H1 and the expected number of fragments from λDNA digestion in the presence of a mixture of the plasmid DNA extracts is observed. This result compares favourably with that in Panel B, Figure 3.4.

University of Cape Town

The sequence of malarial HPRT cDNA in pET-15b is presented aligned with the published sequence in the Technical Appendix (1B), and analysis of the data suggests that the determined sequence is correct.

University of Cape Town

3.3 The expression and purification of human and malarial HPRT

3.3.1 The time course of induction

The time dependence for induction of HPRT expression with IPTG is shown in Figure 3.9.

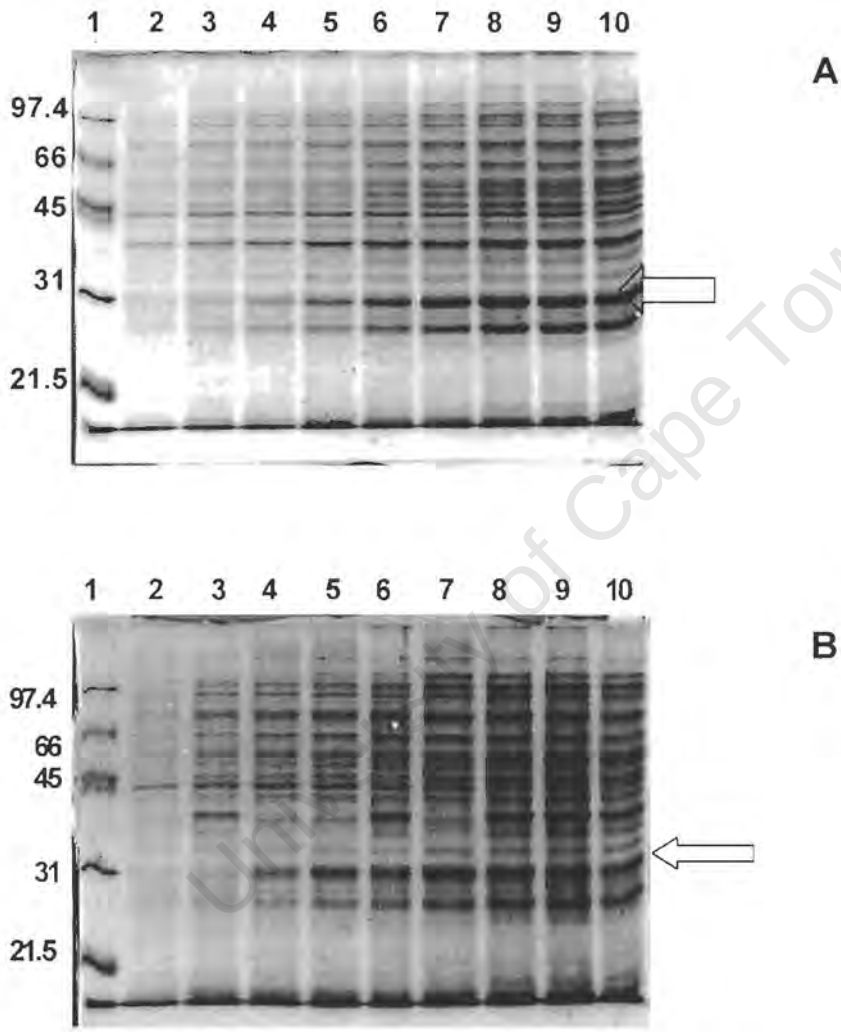

Figure 3.9 Time course of induction of (A) human and (B) malarial HPRT in *E. coli*. Lane 1, molecular weight marker (kDa); lanes 2-10, aliquots taken at times 0, 15, 30, 45 min, and 1, 2, 3, 4, and 5 h respectively. The arrows indicate putative expressed HPRT.

Putative expressed proteins (approximately 26 kDa) are both visible after approximately 30 min induction, and attained maximal levels after about 3 h.

University of Cape Town

3.3.2 The purification of human and malarial HPRT

Human and malarial HPRT were purified by nickel affinity chromatography, and the results are shown in Figure 3.10.

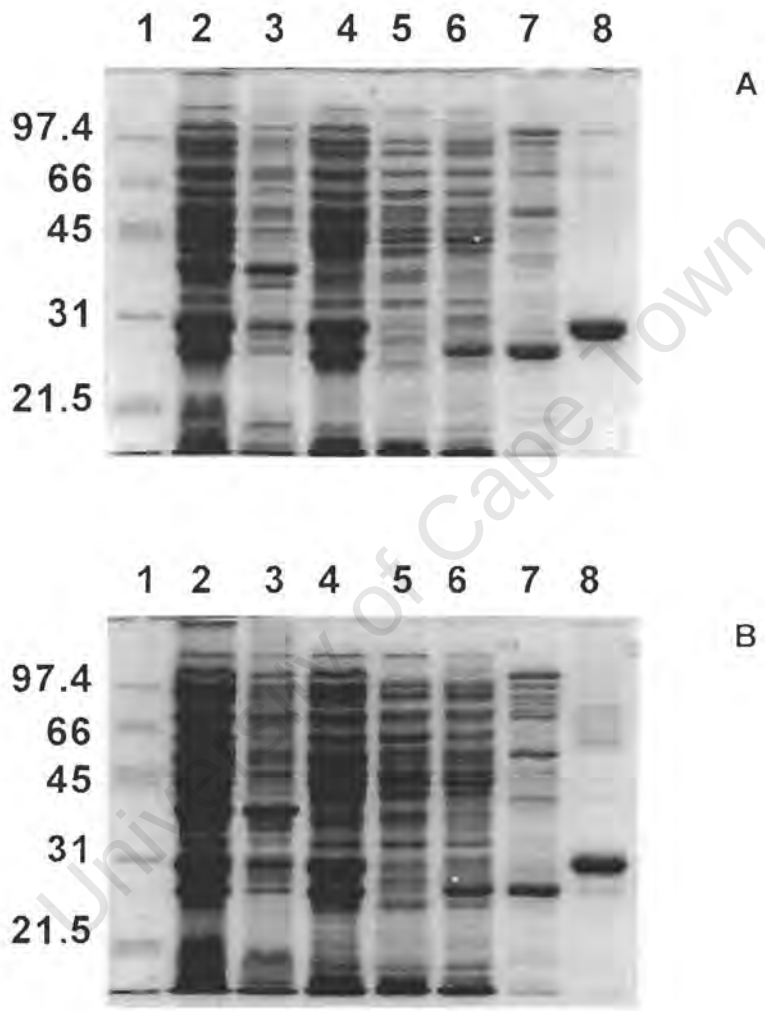

Figure 3.10 Nickel affinity chromatography purification of (A) human and (B) malarial HPRT. Lane 1, molecular weight marker (kDa); lane 2, total protein fraction; lane 3, pellet fraction after ultracentrifugation; lane 4, supernatant of crude cell lysate; lane 5, flow through fraction; lane 6, 5 mM imidazole wash fraction; lane 7, 60 mM imidazole wash fraction; lane 8, 1 M imidazole fraction. Fractions were resolved on a 15% denaturing polyacrylamide gel according to Laemmli, 1970.

University of Cape Town

3.3.3 Assays for activity

HPRT activity was determined using a continuous spectrophotometric assay. The products GMP, IMP and XMP have significantly different absorbance scans from the substrates guanine, hypoxanthine and xanthine respectively. The activity of the enzymes was monitored continuously by appropriate choice of wavelength (257 nm for GMP, 245 nm for IMP and 255 nm for XMP; see arrows in Figure 3.11)

University of Cape Town

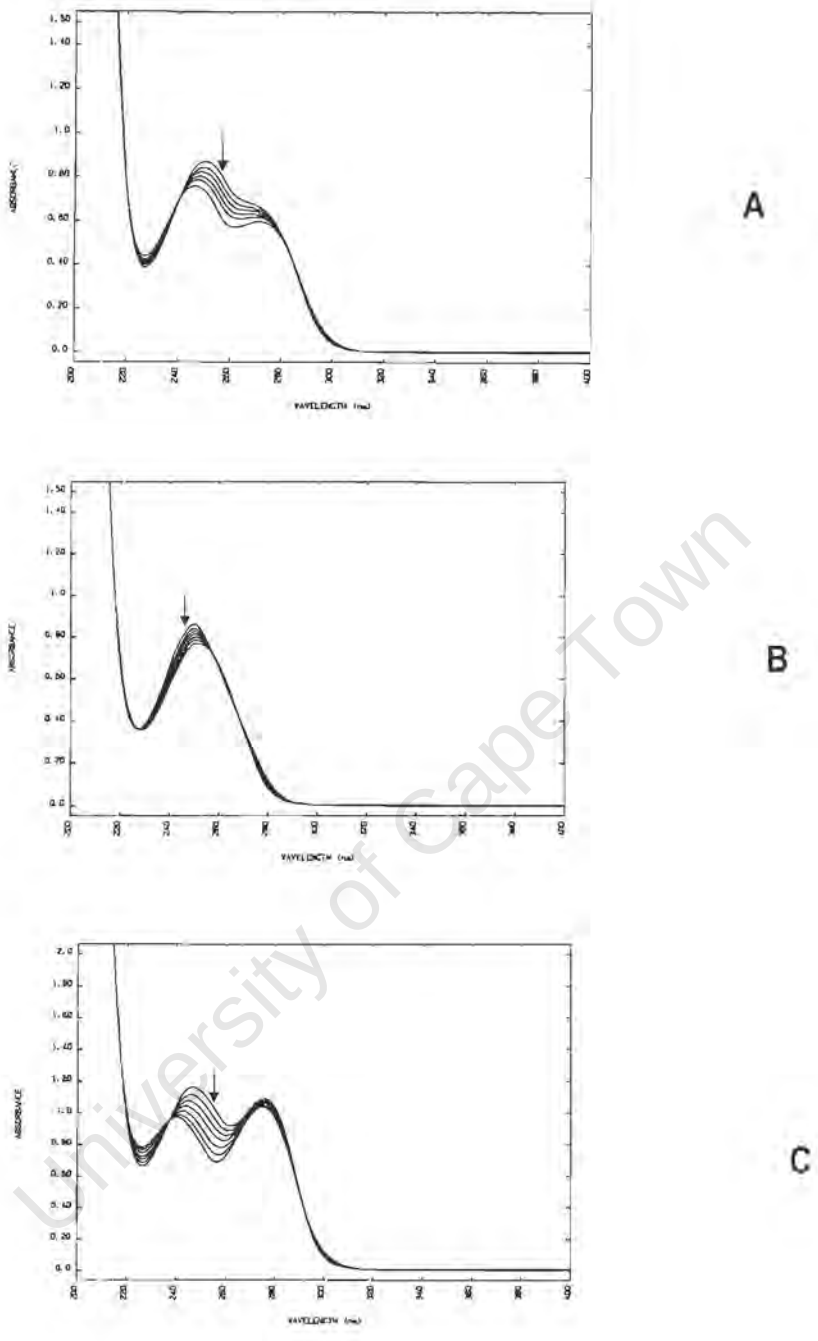

Figure 3.11 A spectrophotometric assay to determine HPRT activity. Panel A, Scans of the reaction mix containing 100 mM Tris/HCl pH 8.5, 100 mM $MgCl_2$, 1 mM PRPP, an aliquot of human HPRT, and 20 µM guanine at 10 s intervals, starting at time 0 s. Panel B, Scans of the reaction mix with the same components and scanning intervals as Panel A, with the exception that 20 µM hypoxanthine instead of guanine was used. Panel C, Scans of the reaction mix with the same components and scanning intervals as Panels A and B, with the exceptions that 20 µM xanthine and *T. gondii* HPRT were used. In all panels the production of the nucleotide is indicated by an increase in absorbance at the indicated wavelength (arrow).

University of Cape Town

Typical assay recordings of substrate conversion by human and malarial HPRT are illustrated in Figures 3.12 and 3.13 respectively. The human enzyme catalysed GMP and IMP production, but not XMP, as reported before (Kelley *et al.*, 1967; Krentisky *et al.*, 1969).

Addition of protein to the assay mix produced a change in absorbance, and the rates continued in a linear fashion until substrate depletion at 40-80 s. The sharp switch-off in activity is consistent with a high affinity for the purine.

University of Cape Town

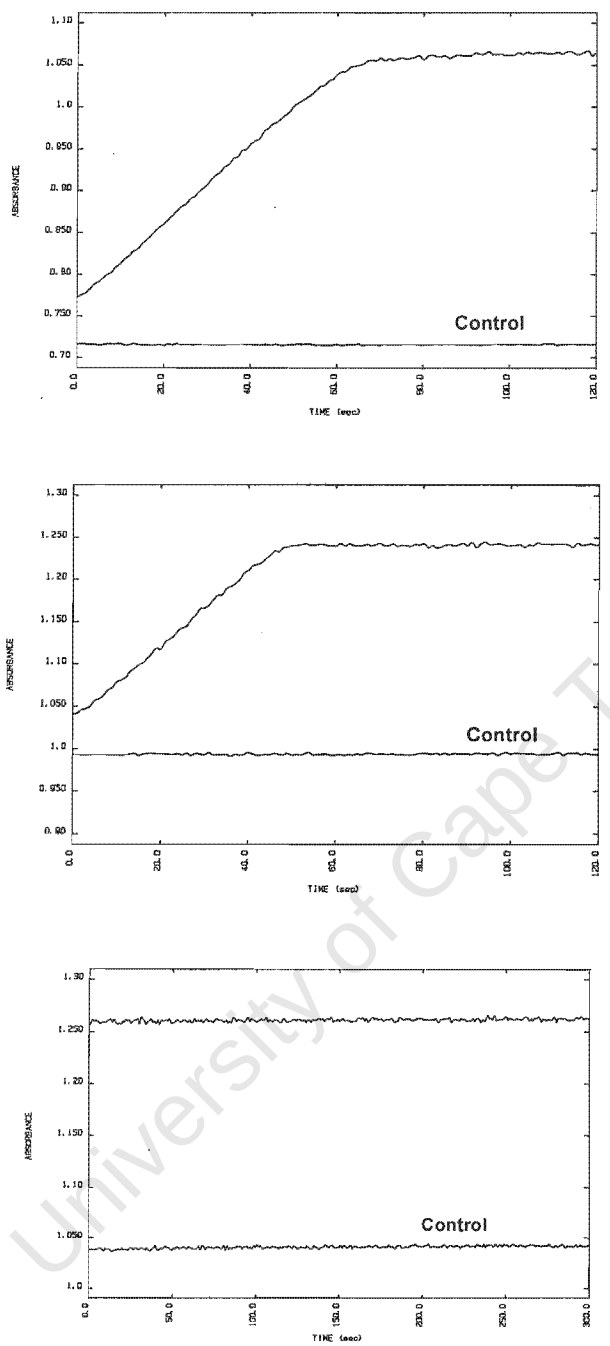

Figure 3.12 Continuous spectrophotometric assays to measure substrate conversion by human HPRT during turnover. A, The formation of GMP from guanine was monitored at 257 nm; B, The formation of IMP from hypoxanthine was monitored at 245 nm; C, The formation of XMP from xanthine was monitored at 255 nm. The controls were conducted in the absence of protein. The standard assay consisted of 100 mM Tris/HCl, pH 8.5, 100 mM $MgCl_2$, 60 μM purine base and 1 mM PRPP at 25 °C. The initial rates of activity were considered for the calculation of specific activity.

University of Cape Town

Typical assay recordings for the conversion of purine bases to the corresponding nucleotides by malarial HPRT are shown in Figure 3.13.

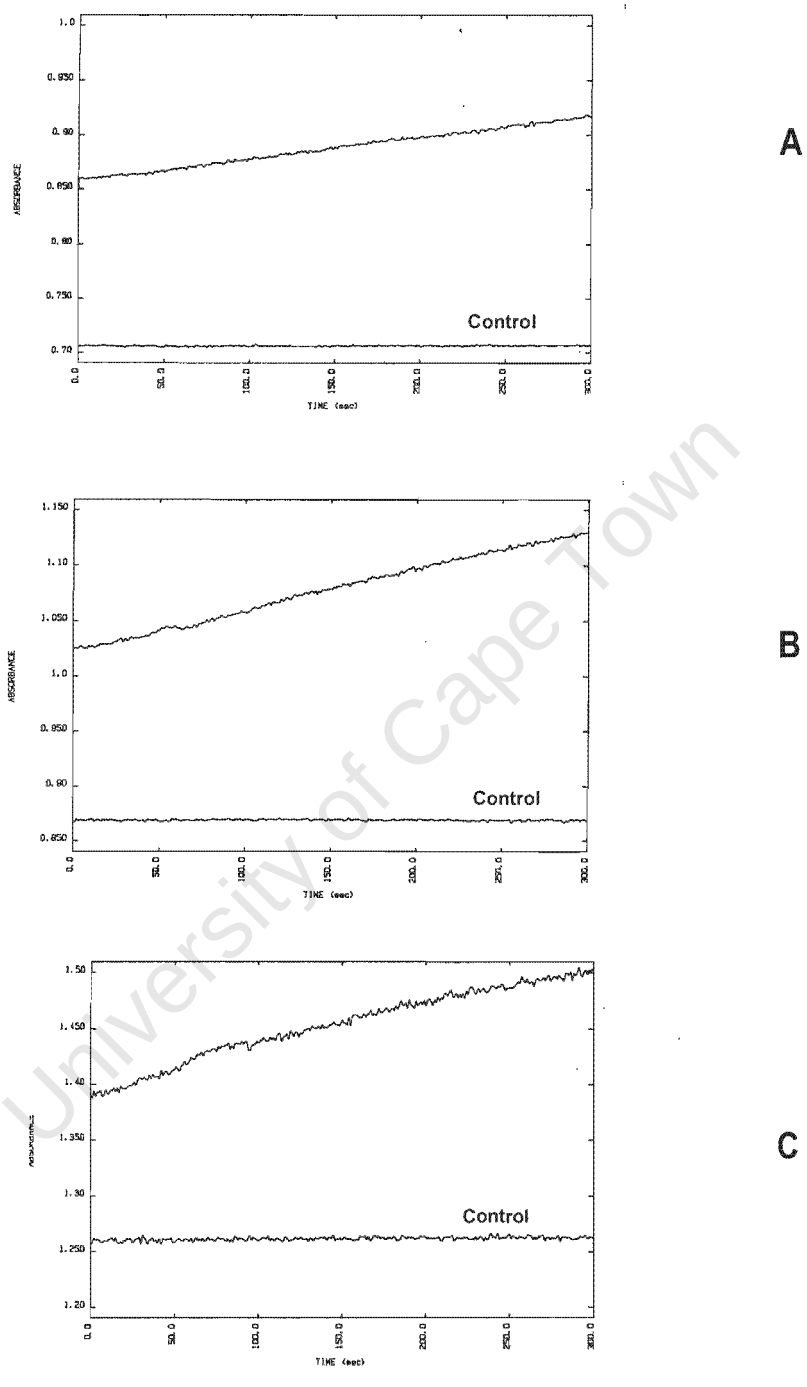

Figure 3.13 Continuous spectrophotometric assays to measure substrate conversion by malarial HPRT during turnover. A, The formation of GMP from guanine was monitored at 257 nm; B, The formation of IMP from hypoxanthine was monitored at 245 nm; C, The formation of XMP from xanthine was monitored at 255 nm. The controls were conducted in the absence of protein to show that the rates observed were due to enzyme activity. The standard assay consisted of 100 mM Tris/HCl, pH 8.5, 100 mM $MgCl_2$, 60 µM purine base and 1 mM PRPP at 25 °C. The initial rates of activity were considered for the calculation of specific activity.

University of Cape Town

The specific activity of the human and malarial HPRTases are shown in Table 3.1. Literature values are included as a comparison in Table 3.2.

Table 3.1 The specific activity of purified recombinant human and malarial HPRT

	Specific activity (μmoles product.min^{-1}.mg^{-1})		
	Guanine	Hypoxanthine	Xanthine
Human HPRT	37.8	17.9	nda
Malarial HPRT	0.03	1.4	0.07

nda, no detectable activity

Table 3.2 Published specific activity values for human and malarial HPRT specific activity

	Specific activity (μmoles product.min^{-1}.mg^{-1})[a]		
	Guanine	Hypoxanthine	Xanthine
Human HPRT	46	27	nda
Malarial HPRT	5.4	1.4	3.0

[a] Keough *et al.*, 1999
nda, no detectable activity

Human HPRT was purified on nine occasions, and the specific activity was found to be comparable with that of the literature. The result for malarial HPRT in Table 3.1 was the highest obtained in eight purifications. The specific activity value of 1.4 μmoles IMP min^{-1} mg^{-1} for malarial HPRT was not reproducible, and this fact, coupled with the very low activity generally found, made us conclude that the malarial enzyme was inactive.

Table 3.2 indicates that malarial HPRT should exhibit about one tenth the activity of the human enzyme with guanine and hypoxanthine as the substrates. In contrast to the human HPRT, the malarial enzyme exhibits activity with xanthine.

University of Cape Town

3.3.4 Attempts to obtain active malarial HPRT

A number of strategies were devised to try and obtain malarial HPRT in an active form. These included immediate removal of imidazole from purified enzyme, the purification and assay of crude supernatant extract in the absence of imidazole, the inclusion of PRPP in the lysis medium, and the induction of malarial HPRT expression at low temperatures (20 °C). In a separate series of experiments, the crude supernatant extract or purified enzyme extract was supplemented with dithiothreitol (DTT) or 2-mercaptoethanol, and was assayed for activity in the presence of either of these reducing agents. Finally, malarial HPRT was expressed without the histidine tail, to see if the histidine tag was interfering with the correct folding of recombinant protein. Eight purifications of malarial HPRT were conducted in an attempt to produce active enzyme using these approaches. The results of these experiments are presented below.

University of Cape Town

High concentrations of imidazole that may be needed for elution from the nickel affinity column (for example 1 M) could be inhibitory to proper malarial HPRT folding. Purified malarial HPRT was assayed for activity, and was then passed through a size exclusion column. Specific activity was determined to be 0.005 μmoles $GMP.min^{-1}.mg^{-1}$ before the size exclusion column. Protein that was passed through the size exclusion column was observed to form aggregates, and was not suitable for assay. The effect of removal of imidazole could thus not be assessed.

Instead, the crude supernatant, which had not been exposed to imidazole, was assayed for activity. Unfortunately, it too showed very low activity, suggesting that the problem lay with protein folding in the bacterium itself. The inclusion of PRPP in the lysis medium did not provide stabilisation, and induction at 20 °C did not produce active enzyme.

The formation of inter-subunit and/or intra-subunit disulfide bonds involving any of the seven cysteine residues (at positions 74, 117, 134, 157, 172, 215, 216 in the protein) was considered as a possible cause of malarial HPRT inactivation. Reducing agents DTT or 2-mercaptoethanol were therefore included during assay of crude supernatant or purified enzyme extract for activity. Neither DTT nor 2-mercaptoethanol inclusion in the assay medium resulted in appreciable malarial HPRT activity.

Interference by the histidine tag in optimal malarial HPRT folding, into the tertiary or quaternary structure was considered as a possible cause of inactivation. Figure 3.14 illustrates the PCR product of malarial HPRT cDNA for cloning into pET-15b modified for expression of target protein without the histidine tag.

University of Cape Town

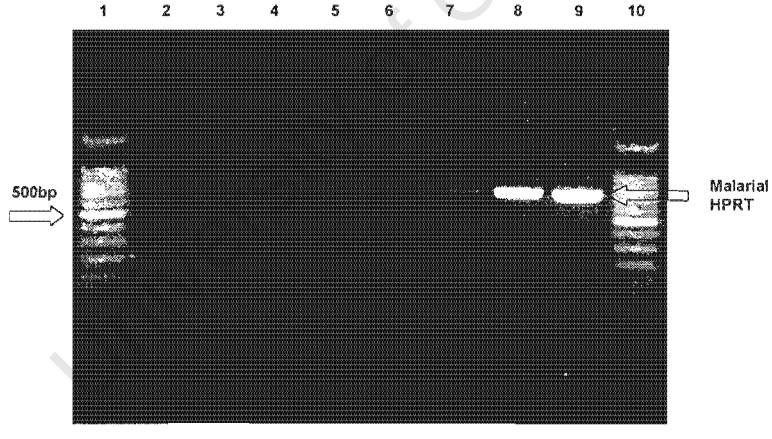

Figure 3.14 PCR amplification of malarial HPRT for expression without the histidine tag.
Lane 1, 100 base pair ladder marker; lane 2, contamination control for PCR in the presence of 1 mM $MgCl_2$; lane 3, contamination control for PCR in the presence of 1.5 mM $MgCl_2$; lane 4, contamination control for PCR in the presence of 2 mM $MgCl_2$; lane 5, contamination control for PCR in the presence of 3 mM $MgCl_2$; lane 6, PCR in the presence of 1mM $MgCl_2$; lane 7, PCR in the presence of 1.5 mM $MgCl_2$; lane 8; PCR in the presence of 2 mM $MgCl_2$; lane 9, PCR in the presence of 3 mM $MgCl_2$; lane 10, 100 base pair ladder marker. PCR reaction (15 µl) was analysed on a 1.5% agarose gel. DNA was visualized by ethidium bromide staining.

Significant PCR product was observed at 2 and 3 mM $MgCl_2$, and was visible as a DNA band of approximately 650 bp.

The PCR product was cloned into pGEM®-T. The plasmid DNA containing the insert was identified by digestion with Nco1 and BamH1. The resulting insert was extracted from agarose gel, and was cloned into pET-15b digested with *Nco*1 and *Bam*H1 to produce a linearised vector without the region encompassing the histidine tag, the thrombin cleavage site, and the Nde1 restriction site (see Figure 3.6). The expression of the malarial HPRT without the histidine tag was successfully conducted in *E. coli* BL21(DE3)pLysS, and the result is shown in Figure 3.15. It is apparent that total bacterial protein contained a broad extra band in the region of 26 kDa. The crude supernatant also contained the protein, but rather less

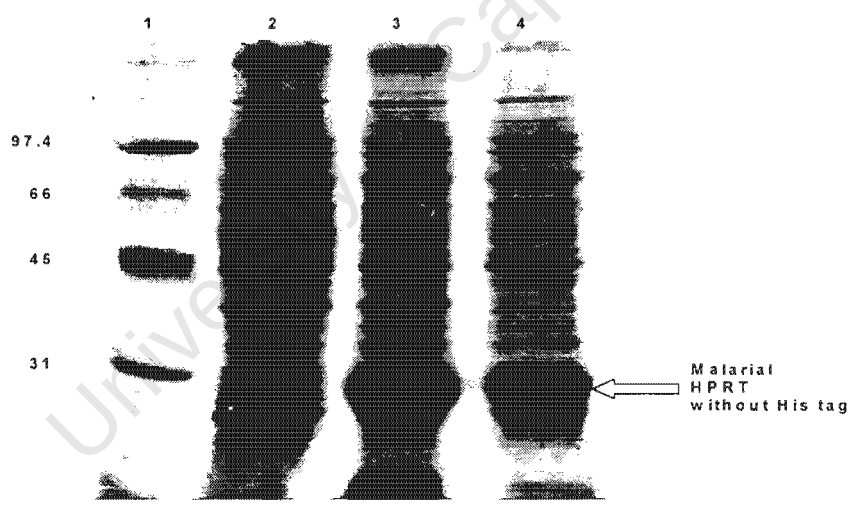

Figure 3.15 SDS-PAGE of malarial HPRT expressed without the histidine tag. Lane 1, molecular weight marker (kDa); lane 2, total protein fraction of uninduced cell culture; lane 3, total protein fraction of induced cell culture; lane 4, crude supernatant fraction of induced cell culture. The protein fractions were analysed on a 15% polyacrylamide gel according to Laemmli, 1970. The approximately 26 kDa protein is shown in lane 3 (compare lane 2, uninduced cell culture).

The crude supernatant extract of malarial HPRT expressed without the histidine tag was inactive with respect to HPRT activity. Several purifications of malarial HPRT were also carried

University of Cape Town

out in the presence of 1 mM PRPP (resullts not shown, but see Figure 3.20, later). Significant extra activity was not found.

3.4 The expression and purification of malarial HPRT clone G11

The malarial HPRT cDNA clone G11 was obtained form Drs D. Borhani and G. Vasanthakumar, Southern Research Institute, Birmingham, Alabama, as an alternative to the clone published by King and Melton (1987. The G11 clone codes for threonine (ACG) at position 427 of the of the nucleotide sequence, instead of methionine (ATG) (compare Technical Appendices 1G and 1H). The malarial HPRT G11 clone was sequenced for verification, and alignment with the published sequence showed the determined sequence to be correct (see Technical Appendix 1C). Malarial HPRT clone G11 in pET-15b, referred to in this study as $HPRT_{pfthr}$, was transformed into *E. coli* BL21(DE3)pLysS, expressed, and purified by nickel affinity chromatography as described in the previous section. The activity of the crude supernatant was assayed for activity, and was compared with that of purified enzyme. The crude supernatant extract from *E. coli* BL21(DE3)pLysS transformed with a non-inducible plasmid, pUC 18 was obtained and used as a control for endogenous HPRT activity. The purification is shown in Figure 3.16. Figure 3.17 shows the optimisation of imidazole concentration required for $HPRT_{pfthr}$ elution. Activity results for $HPRT_{pfthr}$ are shown in Table 3.3.

University of Cape Town

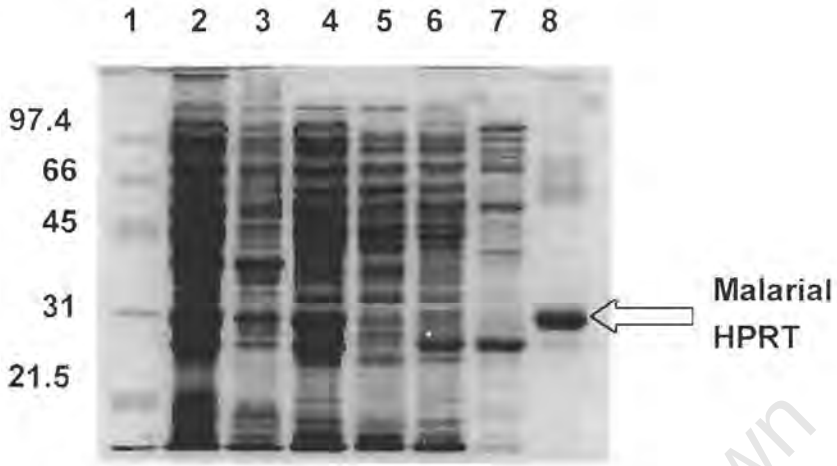

Figure 3.16 The purification of malarial HPRT ($HPRT_{pfthr}$). Lane 1, molecular weight marker (kDa); lane 2, total protein fraction from induced cell culture; lane 3, pellet fraction from induced culture; lane 4, crude supernatant fraction from induced cell culture; lane 5, flow through fraction; lane 6, 5 mM imidazole wash fraction; lane 7, 60 mM imidazole wash fraction; lane 8, 1 M imidazole fraction. Aliquots of 10 µl loaded onto 15% SDS-PAGE gel according to Laemmli, 1970.

University of Cape Town

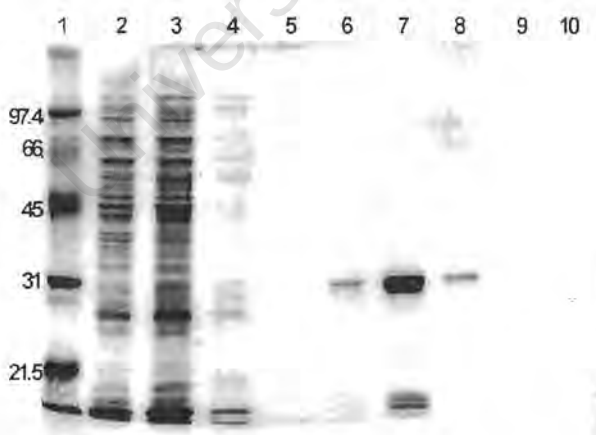

Figure 3.17 The optimisation of imidazole concentration required for HPRT elution.
Lane 1, molecular weight marker (kDa); lane 2, flow through fraction; lanes 3-10, fractions eluted with a step-wise imidazole gradient at 20, 40, 60, 100, 250, 500, 750 mM and 1 M imidazole respectively. Crude supernatant extract (1 ml) containing $HPRT_{pfthr}$ was loaded onto 2 ml Ni-NTA resin for this experiment. Fractions (10 µl) were loaded in each well, and analysis was conducted by 15% SDS-PAGE according to Laemmli, 1970.

As shown in Figure 3.16, $HPRT_{pfthr}$ was purified to close to homogeneity. The optimisation of imidazole concentration required for $HPRT_{pfthr}$ elution is shown in Figure 3.17. Most of the enzyme was eluted with 250mM imidazole, and this is the concentration adopted in subsequent experiments.

Table 3.3 shows the activity of $HPRT_{pfthr}$ in the crude supernatant extract compared to that of purified $HPRT_{pfthr}$.

Table 3.3 The specific activity of $HPRT_{pfthr}$ in crude supernatant extract compared to the specific activity of purified $HPRT_{pfthr}$

Fraction	Specific activity (μmoles.min^{-1}.mg^{-1}) [a]		
	GMP	IMP	XMP
Endogenous HPRT activity¶	0.02	0.06	0.04
Total HPRT activity in the crude supernatant extract¶	0.05	0.13	0.06
$HPRT_{pfthr}$ activity in the crude supernatant extract [b]	0.23	0.54	0.31
Purified $HPRT_{pfthr}$ activity	0.02	0.04	0.02

[a] Assays were conducted according to Keough *et al.*, 1999 (100 mM Tris/HCl, 110 mM $MgCl_2$, pH 8.5, 1 mM PRPP, 60 µM guanine at 25°C).
[b] The protein band corresponding to $HPRT_{pfthr}$ was calculated as 13% of the entire crude supernatant extract shown in lane 4, Figure 3.16 on a Shimadzu CS-9000 Dual-wavelength Flying-spot Scanner. The activity of the crude supernatant was increased to take this proportion into account.
¶Endogenous HPRT activity: activity measured in the supernatant of host cells that do not have the induced HPRT gene
¶ Total HPRT activity in the crude supernatant extract: activity measured in the supernatant of host cells carrying the induced HPRT gene

The results suggest that there was an approximately 10-fold loss in activity during the purification of $HPRT_{pfthr}$ from the crude supernatant extract. This finding suggested that $HPRT_{pfthr}$ was unstable.

University of Cape Town

3.5 The expression and purification of *Toxoplasma gondii* HPRT clone C1

T. gondii HPRT cDNA was obtained from Drs D. Borhani and G. Vasanthakumar, Southern Research Institute, Birmingham, Alabama for study as an additional parasitic HPRTase. The *T. gondii* HPRT (C1), cloned in pET-15b, was transformed into *E. coli*, and was expressed as for $HPRT_{pfthr}$. Sequencing was performed to confirm that this was the correct clone (Technical Appendix, 1D) when an alignment was performed with the published sequence. Figure 3.18 shows the purification of *T. gondii* HPRT by nickel affinity chromatography.

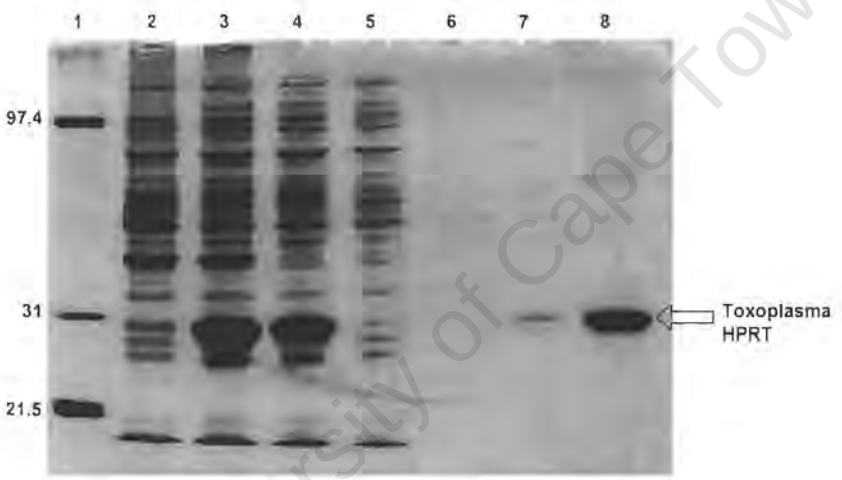

Figure 3.18 The purification of *T. gondii* HPRT Lane 1, molecular weight marker (kDa); lane 2, total protein fraction of uninduced cell culture; lane 3, total protein fraction of induced cell culture; lane 4, supernatant of crude cell lysate; lane 5, flow through fraction; lane 6, 5 mM imidazole wash fraction; lane 7, 60 mM imidazole wash fraction; lane 8, 1 M imidazole fraction. Fractions (5 µl) were resolved on a 15% SDS-PAGE gel according to Laemmli, 1970.

University of Cape Town

As shown in Figure 3.18, *T. gondii* HPRT was purified close to homogeneity as for human and malarial HPRT. The spectrophotometric assay data used to calculate specific activity is shown in Figure 3.19. It is apparent that the activity curves are not linear, and that the enzyme only attains maximal activity after approximately 30 s. After approximately 60 s, the activity declines to zero due to substrate depletion. Unlike the human enzyme (Figure 3.12, Panel C), *T. gondii* HPRT can utilize xanthine as substrate.

University of Cape Town

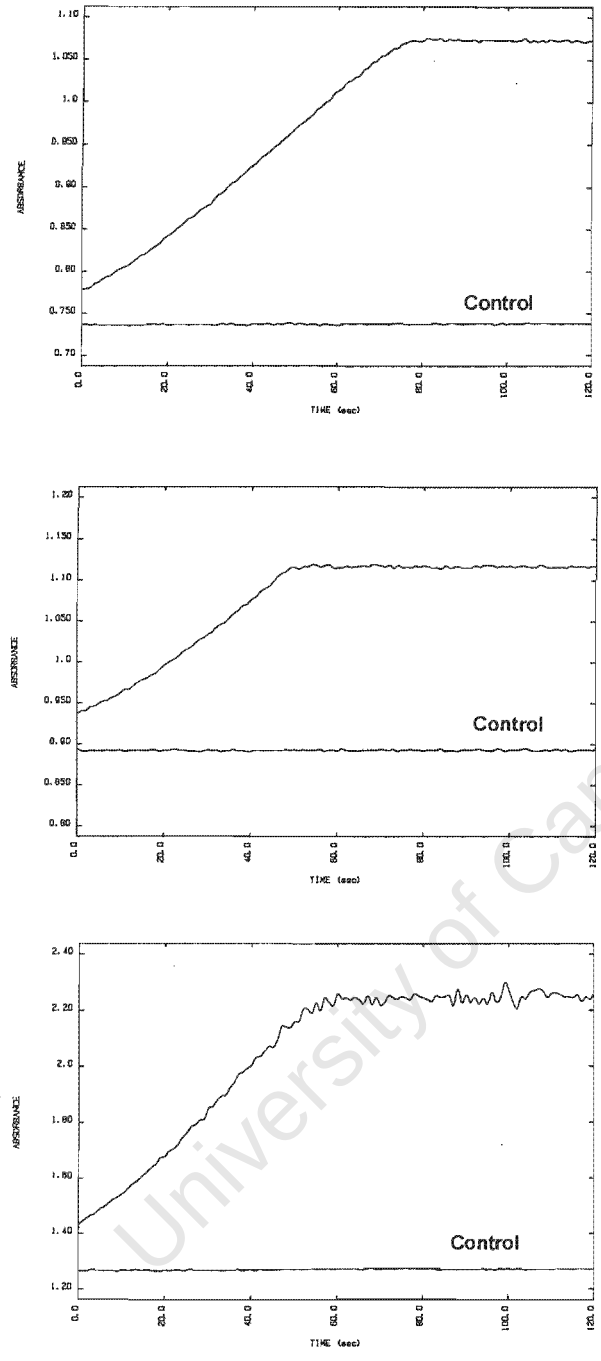

University of Cape Town

Figure 3.19 Continuous spectrophotometric assays to measure substrate conversion by *T. gondii* HPRT. Panel A, The formation of GMP from guanine was monitored at 257 nm; Panel B, The formation of IMP from hypoxanthine was monitored at 245 nm; Panel C, The formation of XMP from xanthine was monitored at 255 nm. The controls were conducted in the absence of protein. Assays were conducted according to an adaptation of the method by Keough and colleagues (1999): 100 mM Tris/HCl, pH 8.5, 100 mM $MgCl_2$, 1 mM PRPP, 60 µM purine base at 37 °C. Activity was initiated by the addition of protein.

Table 3.4 shows the specific activity of the *T. gondii* HPRT that was purified.

Table 3.4 The specific activity of purified *T. gondii* HPRT

	Specific activity (μmoles.min^{-1}.mg^{-1})		
	GMP	IMP	XMP
Toxoplasma HPRT [a]	7.0	3.3	nda
Toxoplasma HPRT [b]	3.7	4.4	8.6
Toxoplasma HPRT [c]	28.6	17.1	69.7

[a] Assayed using conditions similar to Héroux *et al.*, (1999a): 100 mM Tris/HCl, pH 8, 20 mM $MgCl_2$, 0.1 mM EDTA, 0.1 mg/ml BSA, 0.5 mM PRPP, 80 μM purine base) at 37 °C.
[b] Assayed using conditions similar to Keough *et al.*, (1999): 100 mM Tris/HCl, pH 8, 100 mM $MgCl_2$, 1 mM PRPP, 60 μM guanine and hypoxanthine, 200 μM xanthine) at 25 °C.
[c] Literature values (Héroux *et al.*, 1999a)
nda, no detectable activity

Table 3.4 shows that the activity measured for *T. gondii* HPRT is appreciable but lower than those published by Héroux *et al.*, (1999a). This result prompted us to change our purification to that adopted by (Héroux *et al.* (1999a). The changes in protocol included culture in the presence of sodium phosphate to suppress phosphatase expression, and the incorporation of protease and trypsin inhibitors during purification. Sodium phosphate was used in the nickel affinity chromatography buffers, and 250 mM imidazole was used to elute protein. These changes did not increase *T. gondii* HPRT activity.

University of Cape Town

3.6 Reactivation studies

3.6.1 Time dependence of reactivation

It has been shown previously that prolonged incubation of malarial HPRT with substrate can result in activation (Keough *et al.*, 1999). We tested whether our recombinant $HPRT_{pfmet}$, $HPRT_{pfthr}$, and *T. gondii* HPRT could be activated in similar manner by incubating the protein with PRPP, glycerol and DTT at 4 °C over several days. The results are shown in Figure 3.20. The activity of the human enzyme was unchanged, and remained high over 7 days. $HPRT_{pfmet}$ failed to show any activation, and remained inactive. $HPRT_{pfthr}$ slowly gained activity, up to 6 μmoles min^{-1} mg^{-1} of protein, and then returned within 24 h to low activity levels (presumably due to hydrolysis of PRPP). $HPRT_{pfthr}$ was reasonably active (about 2 μmoles min^{-1} mg^{-1} of protein) before incubation, and this could be ascribed to purification in the presence of 1 mM PRRP and 10% glycerol. The activity of $HPRT_{pfthr}$ after reactivation is as high as that reported in the literature for the recombinant enzyme purified from bacterial cells by Hg-Sepharose column chromatography (Keough *et al.*, 1999).

There is evidently a significant difference between the ability of $HPRT_{pfmet}$ and $HPRT_{pfthr}$ to fold into a structure capable of catalysing the transferase activity.

University of Cape Town

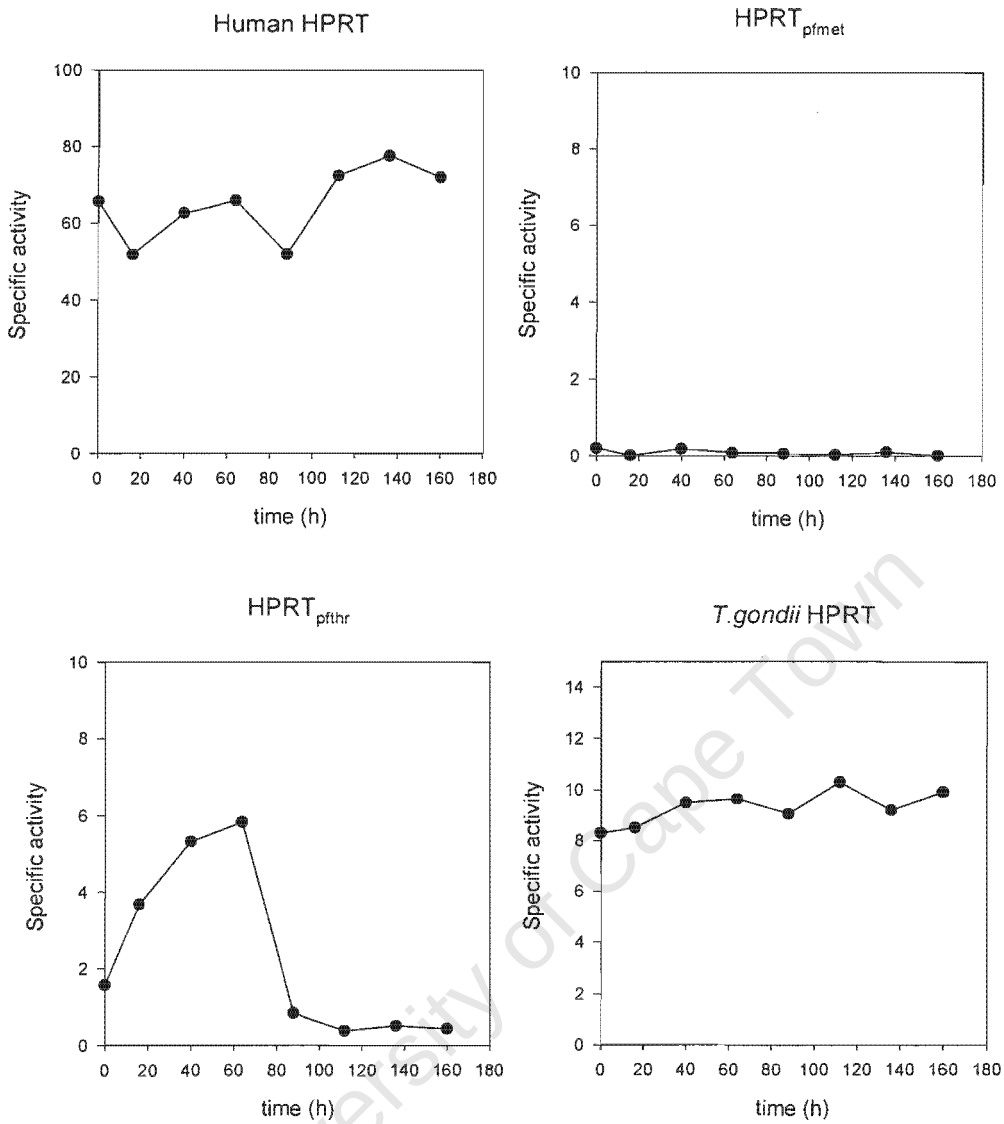

Figure 3.20 The reactivation studies of HPRTases. Protein was purified from cells cultured in the presence of sodium phosphate, and purified in the presence of protease and trypsin inhibitors, and was eluted from nickel affinity columns in sodium phosphate buffer containing 250 mM imidazole. Purified enzyme was incubated at 4 °C in the presence 50% glycerol and 1 mM PRPP in 2 5mM Tris/HCl pH 8, 10 mM $MgCl_2$, 0.1 mM EDTA, 1 mM DTT. Assays for activity were conducted at 37 °C in the presence of 100 mM Tris/HCl, pH 8.5, 100 mM $MgCl_2$, 1 mM PRPP, 60 µM guanine. The Specific Activity is given in µmoles GMP formed min^{-1} mg^{-1}.

University of Cape Town

3.6.2 The effects of DTT and PRPP on $HPRT_{pfthr}$ reactivation at low temperature

The effects of DTT and PRPP, alone and in combination, on the reactivation of $HPRT_{pfthr}$ are shown in Figure 3.21.

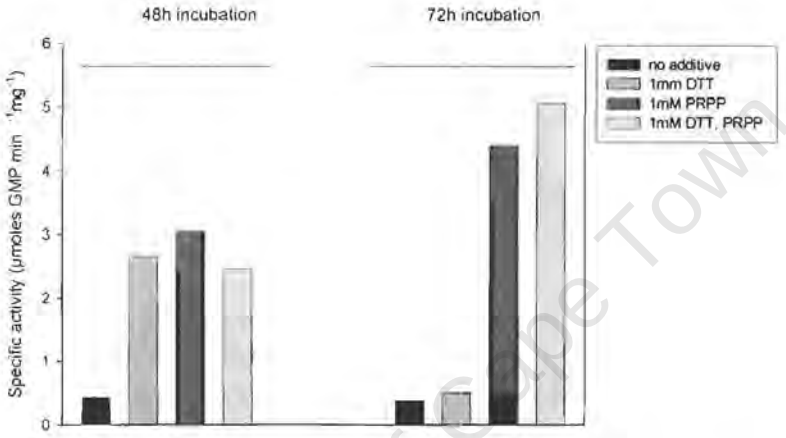

Figure 3.21 The reactivation of $HPRT_{pfthr}$ by DTT and PRPP at low temperature. $HPRT_{pfthr}$ eluted from a Sephadex™ G-25 M column in 25 mM Tris/HCl pH 8, 10 mM $MgCl_2$, and 0.1 mM EDTA was incubated at 4 °C over the period shown with no additives, or in the presence of one or both additives at 1 mM concentration. Assays were conducted at 37 °C in the presence of 100 mM Tris/HCl, pH 8.5, 100 mM $MgCl_2$, 1 mM PRPP, and 60 µM guanine.

The results show that reactivation was not achieved in the absence of additives. DTT alone yielded a 5-fold activation of activity after 48 h incubation, rather similar to PRPP. However, further incubation up to 72 h resulted in a decline in activity with DTT alone, and further activation in the case of PRPP alone. The combination of DTT and PRPP gave similar results as PRPP alone. It is concluded that PRPP is the best activator, while DTT alone provides some activation over shorter incubation times.

University of Cape Town

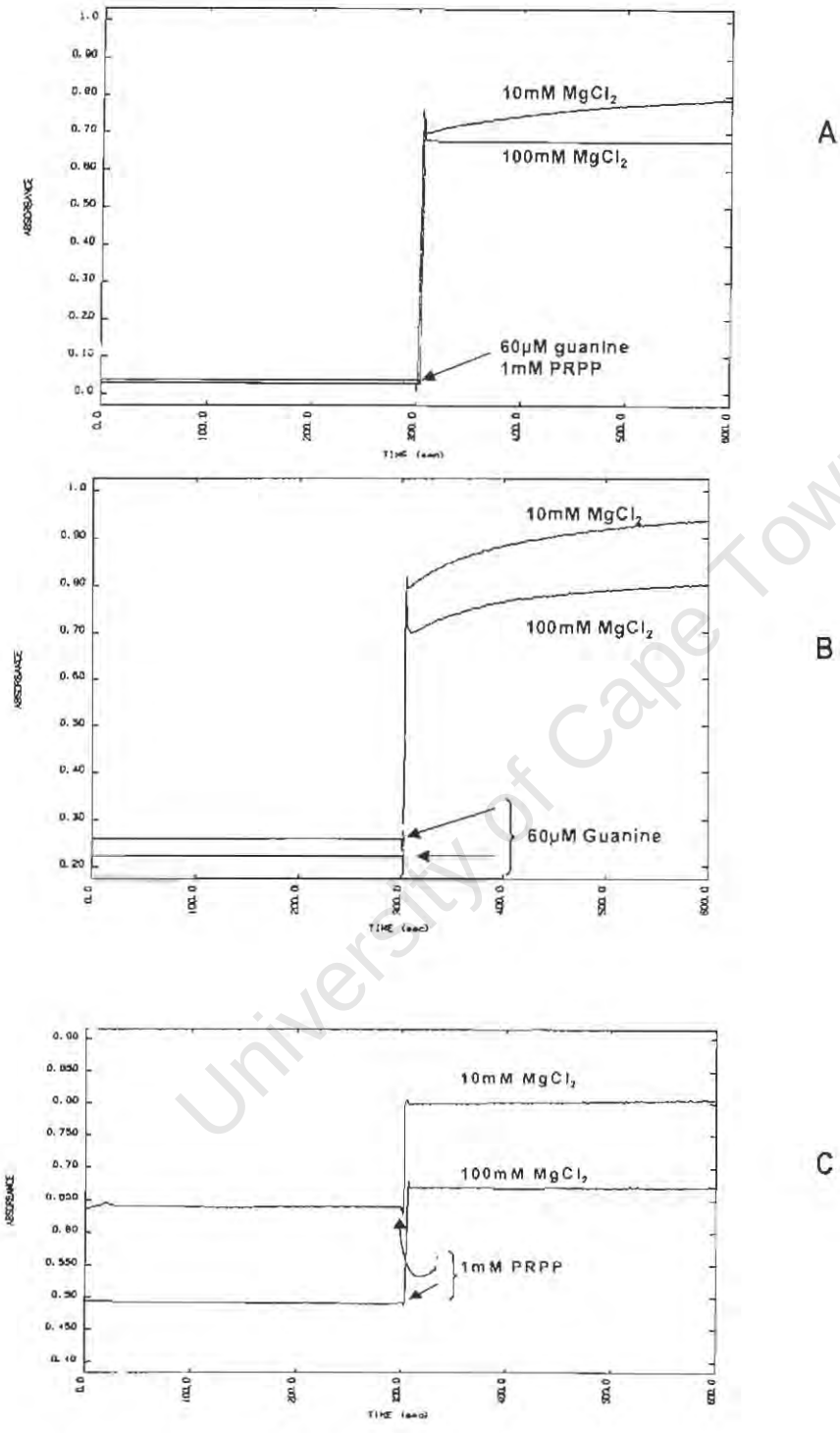

Figure 3.26 Stability studies on $HPRT_{pfthr}$ during assay. A, Pre-incubation in the absence of both guanine and PRPP; B, Pre-incubation in the presence of 1 mM PRPP only; C, pre-incubation in the presence of 60 µM guanine only. All assays were conducted in the presence of 100 mM Tris/HCl, pH 8.5, at 25 °C.

University of Cape Town

The results of Figure 3.26A suggest that there was slow inactivation over time if no additional PRPP is added. This inactivation was measured by assaying for activity after measured time intervals, and the results are shown in Figure 3.27. The results indicate a first-order decay of activity at approximately 30 μM PRPP (the concentration estimated after dilution of stock protein), with a $t_{1/2}$ of approximately 10 min, and provide additional evidence of PRRP stabilising the enzyme. If the protein was diluted into 60 μM guanine rapid inactivation ensued with a $t_{1/2} \approx 12$ s. Turnover evidently rapidly depleted the medium of PRPP and promoted destabilisation of the unligated enzyme

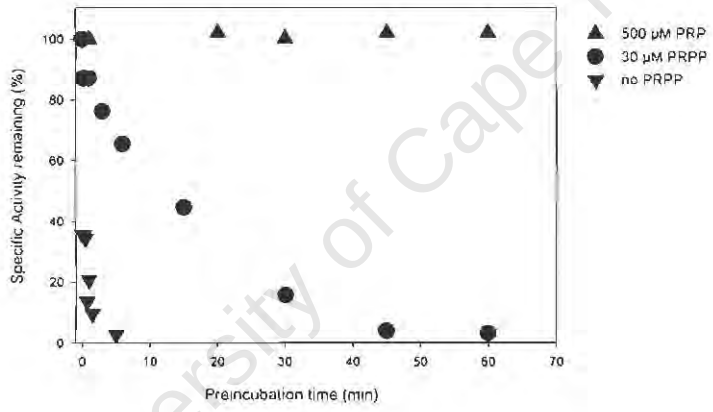

Figure 3.27 Time-dependent inactivation of $HPRT_{pfthr}$ by the removal of medium PRPP. Enzyme (4 μg/ml) was preincubated over the times shown at 25 °C in the presence of 100 mM Tris/HCl pH 8.5,10 mM $MgCl_2$ and 500 μM PRPP (▲), or 30 μM PRPP (●), or without PRPP (▼). In the last case, PRPP depletion was achieved by incubation in the presence of 60 μM guanine. The remaining activity of enzyme incubated in the presence of 500 μM PRPP or 30 μM PRPP, or in the absence of PRPP was assayed at 25 °C by adding 60 μM guanine, or guanine in combination with 500 μM PRPP, or 500 μM PRPP respectively.

University of Cape Town

3.7.2 Histidine tag cleavage by digestion with thrombin

We considered the possibility that the instability of $HPRT_{pfthr}$ may be due to the presence of the histidine tag. Accordingly, we attempted to cleave off the tag with thrombin. The extent of cleavage was monitored by SDS-PAGE, while assays for stability were conducted at specific time intervals. The results are shown in Figures 3.28 and Figure 3.29 respectively.

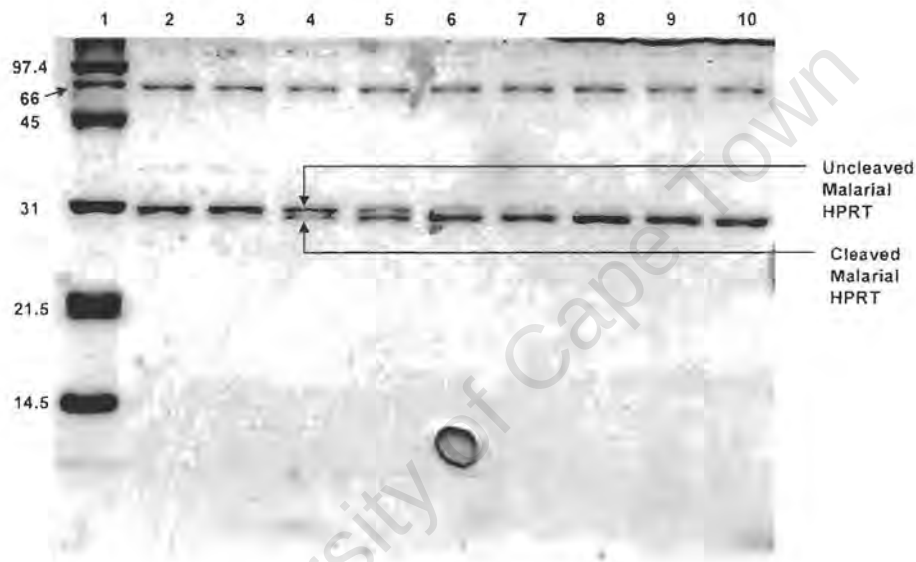

University of Cape Town

Figure 3.28 The extent of histidine tag cleavage by thrombin from $HPRT_{pfthr}$. Lane 1, molecular weight marker (kDa); lanes 2-10, 30 s, 1, 3, 5, 10, 15, 30, 45, 60 min cleavage reactions. The cleavage conditions are described in Materials and Methods (Section 2.7.1.6) Cleavage was stopped at specific time intervals by the addition of PMSF. Samples were analysed on a 15% SDS-PAGE gel according to Laemmli, 1970.

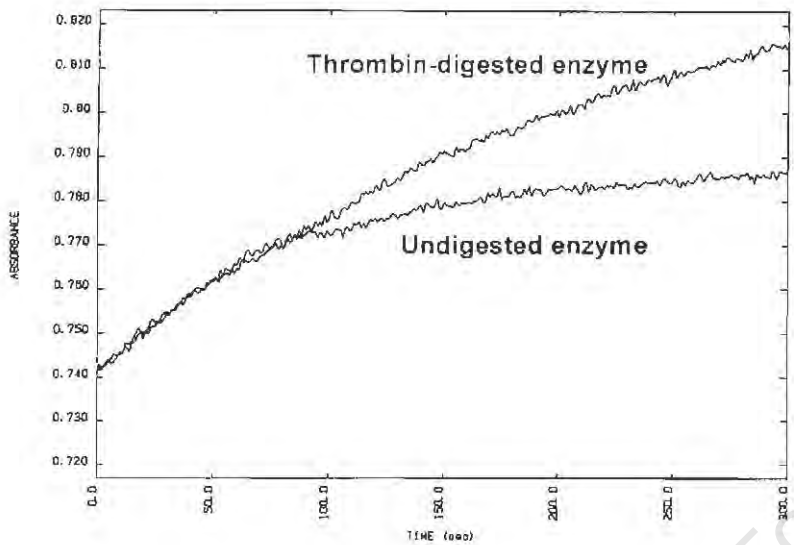

Figure 3.29 The effect of thrombin cleavage on $HPRT_{pfthr}$ stability during turnover. Samples were taken for assays after 30min cleavage (100% cleavage according to the SDS-PAGE result). The control (incubation in the absence of thrombin) was assayed for comparison.

The result in Figure 3.28 shows the appearance of a protein band with a lower molecular weight directly below the $HPRT_{pfthr}$ band (indicated with arrows), and is evidently the $HPRT_{pfthr}$ without the histidine tag. After 30 min digestion, only the untagged $HPRT_{pfthr}$ species is present, indicating 100% cleavage. In Figure 3.29, the cleaved $HPRT_{pfthr}$ species is shown to be somewhat more stable compared to the uncleaved species. Both cleaved and uncleaved species had the same initial rates of activity. It is concluded that the cause of the instability of $HPRT_{pfthr}$ is partly but not completely due to the histidine tag. In subsequent experiments the histidine tag was not removed, as it was not possible to measure maximal activity even with the unstable enzyme, and we wanted to investigate the nature of the instability.

Glutaraldehyde was used as a cross-linking agent to characterize the oligomeric form of active and inactive $HPRT_{pfthr}$ (Figure 3.30). Incubation of active (PRPP-stabilised) and inactive

University of Cape Town

(preincubated with guanine to deplete the medium of PRPP through turnover) with 20 mM glutaraldehyde caused the rapid formation of a species of $HPRT_{pfthr}$ that migrated with a lower molecular weight (indicated in Panel A with the longer arrow). Longer incubation times with glutaraldehyde resulted in the formation of a prominent cross-linked dimer band with both PRPP-stabilised and inactivated enzyme. The pH dependence of the cross-linking is shown by comparing Panels A, B and C (which were performed at pH 8, pH 8.5 and pH 9 respectively). At pH 8.5 a cross-linked tetramer band was clear for the PRPP-stabilised protein. Very little trimer is formed, consistent with a native tetrameric structure seen in the crystal structure (Shi et al., 1999). The amount of tetramer formed with the inactivated protein appeared to be less. There also seemed to be a difference in the proportion of monomeric protein that migrated normally or faster when comparing PRPP-stabilised and inactivated protein. For example, relative amounts at pH 8.5 and following 2 min glutaraldehyde reaction (lanes 5 and 11). The proportion of the two bands for PRPP-stabilised protein is approximately 1:1, whereas that for the inactivated protein is about 1:4. This trend is not as clear at the other pHs, but is nevertheless present (for example compare lanes 7 and 13 (pH 8), or lanes 3 and 9 (pH 9)).

In conclusion, the differences between the active and inactive $HPRT_{pfthr}$ are subtle. There is, however, a tendency for less cross-linked tetramer. This was not apparent when partially-active (recently purified) and fully active (activated over days at 4°C with PRPP) were compared. Human HPRT seemed slightly less susceptible to cross-linking to oligomers compared with $HPRT_{pfthr}$. $HPRT_{pfmet}$ readily cross-linked to high molecular weight species that did not enter the gel during denaturing electrophoresis, indicative of a denatured aggregated protein (results not shown).

University of Cape Town

There was also a tendency for more facile formation of a faster migrating monomeric species. The latter is probably the result of an intramolecular cross-link(s) that alters the hydrodynamic properties of the protein in SDS. We noticed that the formation of this species was more prominent at higher glutaraldehyde concentrations and did not occur with human or *T. gondii* HPRT (result not shown).

University of Cape Town

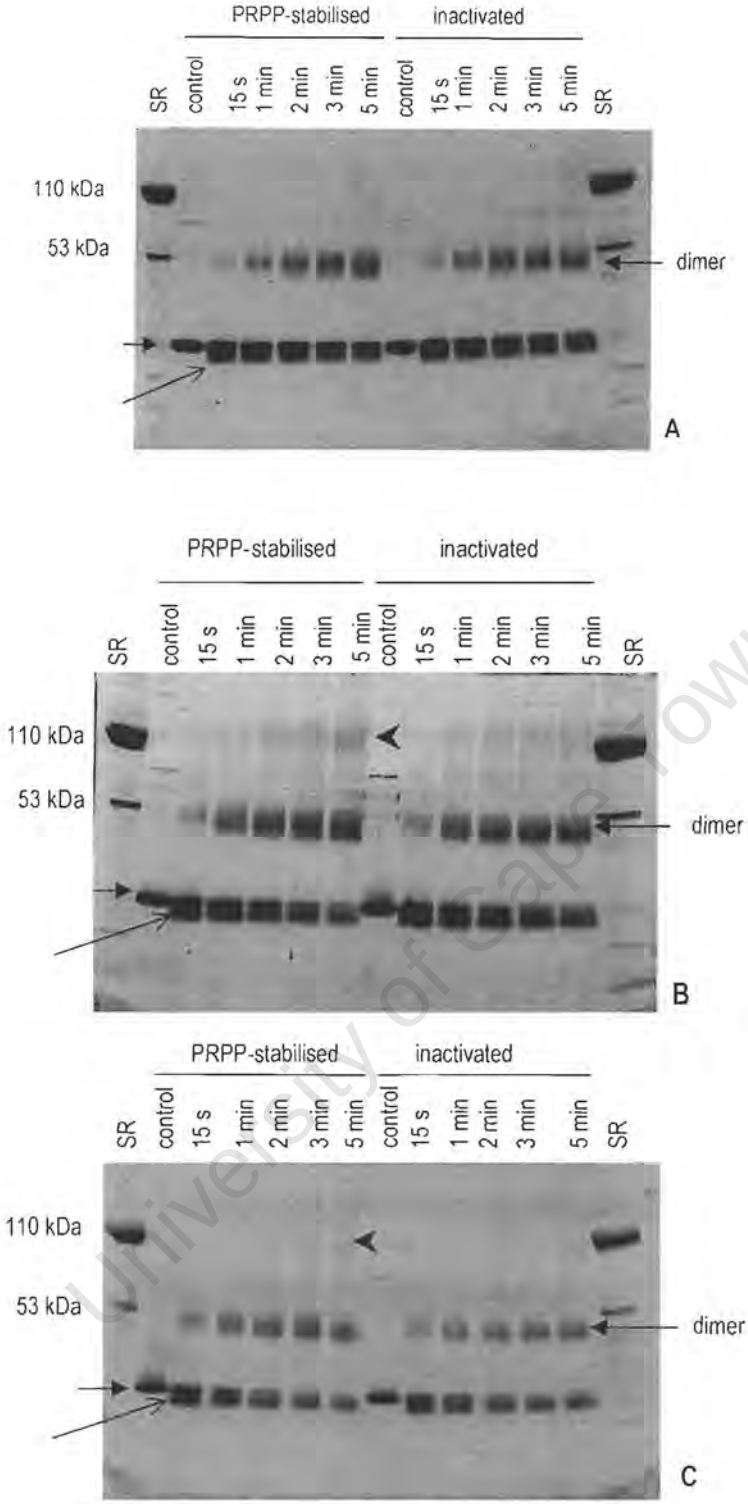

Figure 3.30 The pH dependence of glutaraldehyde cross-linking of PRPP-stabilised and inactive $HPRT_{pfthr}$ cross-linking with glutaraldehyde. Enzyme (0.17 mg protein/ml) was preincubated at room temperature for 1 min in 83 mM EPPS/TMAH pH 8 (Panel A), pH 8.5 (Panel B) or pH 9 (Panel C), 17 mM $MgCl_2$ and 1.7 mM PRPP (PRPP-stabilised) or for 6 min in the same medium except that PRPP was replaced with 0.3 mM guanine (inactivated). The reaction was initiated by the addition of glutaraldehyde (20 mM) and aliquots taken at the timed intervals shown, and mixed with solubilisation buffer. The marker used (first and last lanes) was Ca^{2+}-ATPase from sarcoplasmic reticulum (110 kDa) and also shows the calsequestrin (53 kDa). The tetramer is indicated with short arrow-heads, while the short and long arrows indicate the monomer and the putative intramolecular cross-link respectively.

University of Cape Town

The specific activity of different preparations of purified reactivated $HPRT_{pthr}$ was in the range of 3 to 5 µmoles GMP min^{-1}. mg^{-1}, 1.4 to 2.8 µmoles IMP min^{-1}. mg^{-1} and up to 1.2 µmoles XMP min^{-1}. mg^{-1} under standard assay conditions.

University of Cape Town

3.8 Chemical syntheses

Our goal in respect of chemical synthesis, for drug targeting of HPRT was three-pronged:

(i) The synthesis of 8-azido purines that could lead to a diversity of 8-substituted purine analogues. We focussed on the synthesis of 8-azido-xanthine due to the parasite enzyme's ability to utilize xanthine as substrate.

(ii) The synthesis of 2',3'-*O*-(2,4,6-trinitrophenyl)-nucleotides. Crude modelling suggested that TNP nucleotides might be accommodated at the active site. TNP-8-azido-nucleotides may be used to create a diversity of 8-substituted TNP-nucleotides.

(iii) The synthesis of TNP-nucleotide/flavonoid conjugates. This laboratory obtained evidence that light activation of TNP-8-azido- ATP in the presence of certain flavonoids results in conjugate formation, suggesting that the nucleotides and flavonoids stack together. We anticipated that if TNP-nucleotides bind tightly to the active site, additional binding might derive from a stacked conjugate.

The general pathways adopted for the syntheses of the various species are outlined in Figure 3.31. The products obtained in this thesis are boxed. Those never synthesised before are boxed and shaded.

University of Cape Town

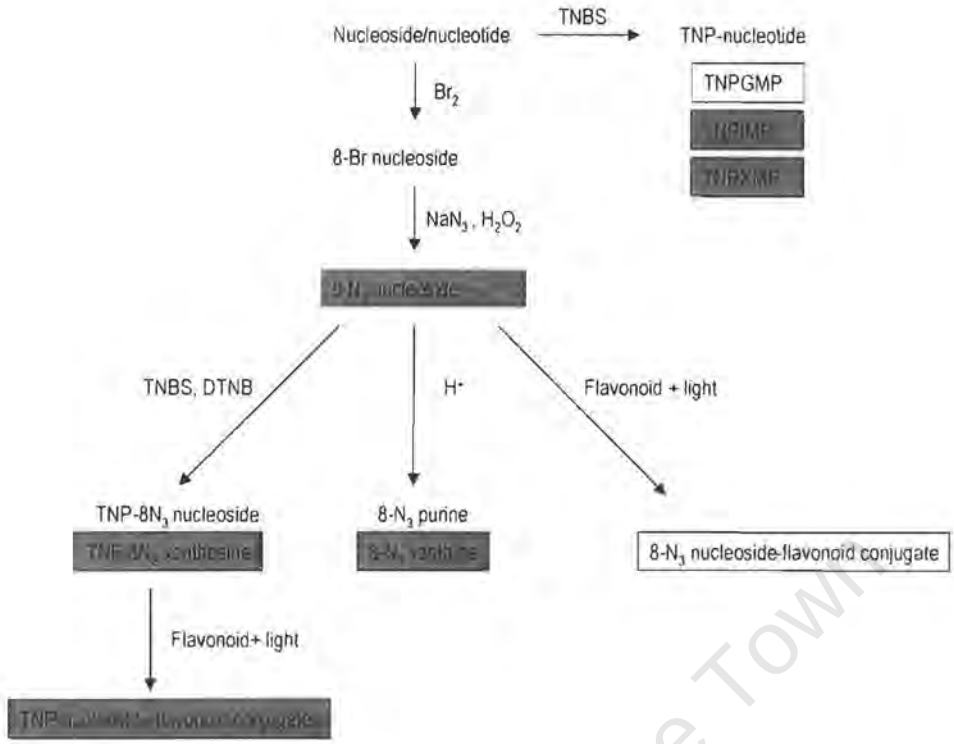

Figure 3.31 Pathways for synthesis

3.8.1 The synthesis of 8-azido xanthosine and 8-azido xanthine

The synthesis of 8-azido xanthosine and 8-azido xanthine is shown in Scheme 1 below.

University of Cape Town

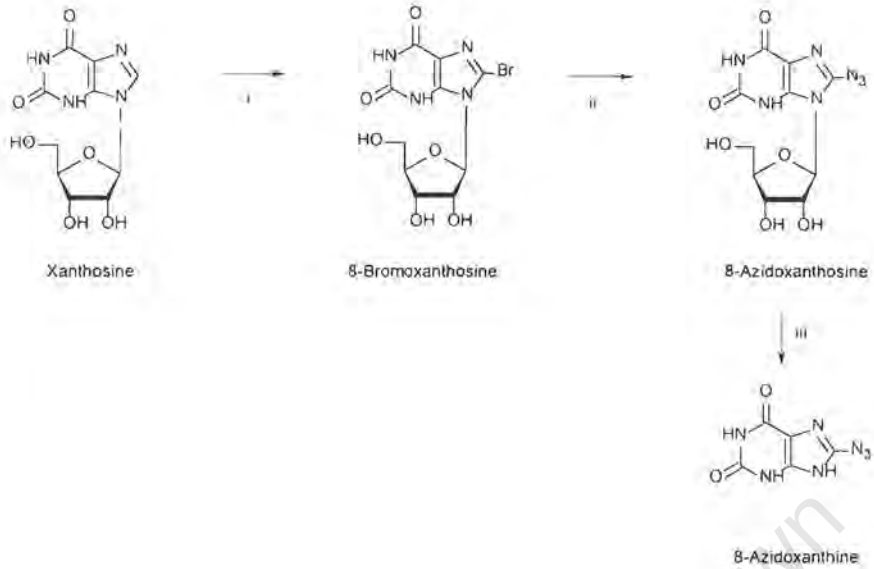

Scheme 1 Preparations of 8-azido xanthosine and 8-azido xanthine
i) Br_2/H_2O, 60% yield; ii) NaN_3/H_2O_2, 30% yield; iii) 2M HCl, 6% yield

The bromination of xanthosine was accomplished by the method of Long *et al.* (1967), and the composition of the reaction mix after 10 min, as determined by HPLC, is shown in Figure 3.32. It can be seen that approximately two thirds of the xanthosine is converted to 8-bromo xanthosine. Pure product was obtained by washing filtered material with water. The absorption spectra of the starting material and the pure product are shown in Figure 3.33 and 3.34 respectively. The absorption maxima at 255 nm for 8-bromo xanthosine is in agreement with that published (Holmes and Robins, 1964).

University of Cape Town

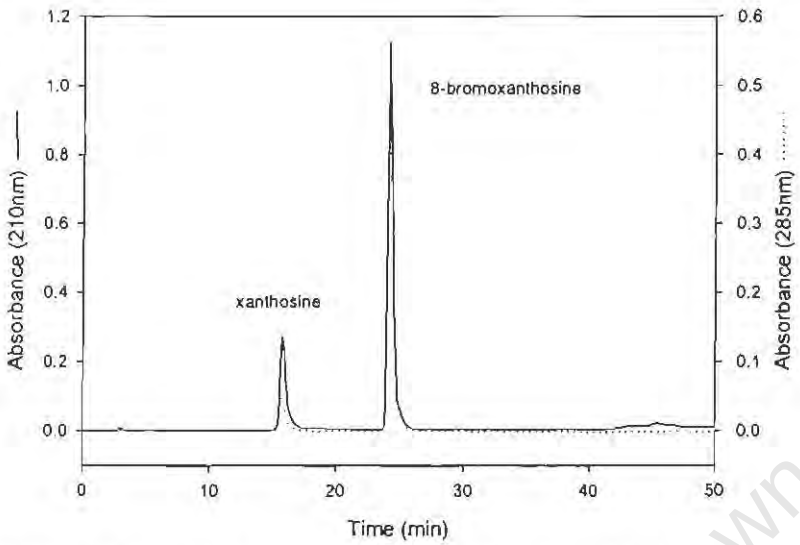

Figure 3.32 HPLC trace showing xanthosine and 8-bromoxanthosine
Mobile phase A= 1 mM KPi, pH3; Mobile phase B= 50% (v/v) acetonitrile. Detection was at 210 nm and 285 nm. Gradient (mobile phase B): 0% for 5 min, 0-30% over 30 min, 30-100% over 5 min, 100% for 5 min, 100-0% over 5 min. Flow rate: 1 ml/min.

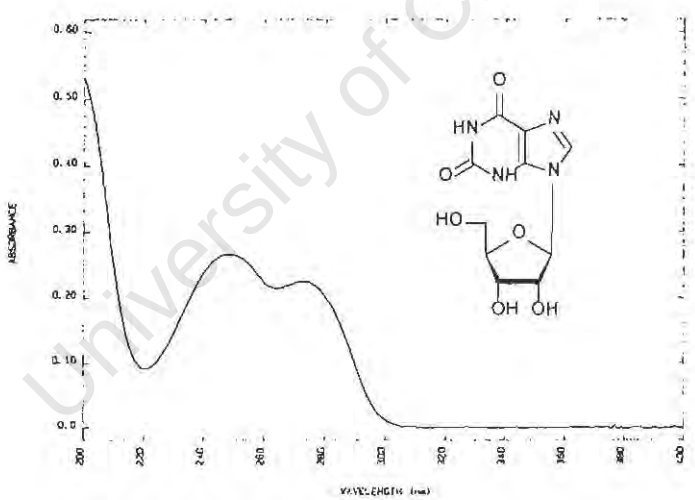

Figure 3.33 The absorption spectrum of xanthosine (with absorbance peaks at 248 and 287 nm)

University of Cape Town

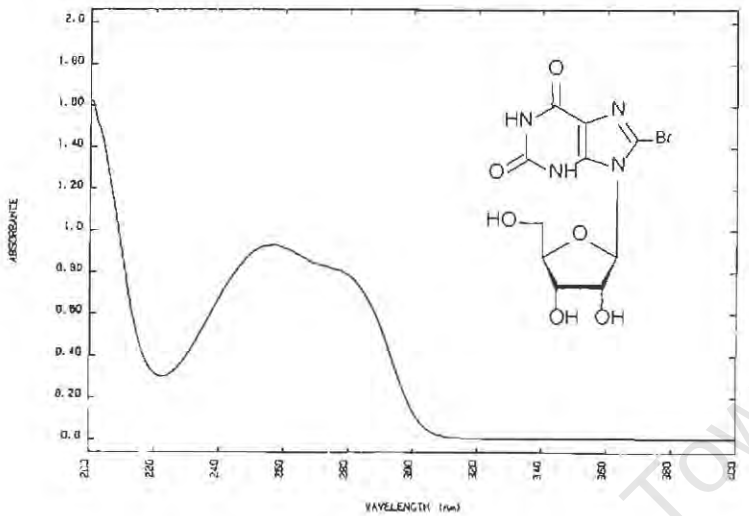

Figure 3.34 The absorption spectrum of 8-bromoxanthosine, with λmax at 255 nm.

The next step, namely replacing the bromo group with an azido group has not been published before, and proved to be extremely problematical. The synthesis was accomplished during the course of several Honours projects (Cox, 1993; Hacker, 1994; Phehane, 1995), and this thesis. Key factors to the successful synthesis were replacing the usual water solvent with DMSO, and saturating it with NaN_3, and the inclusion of H_2O_2. With the protocol described in the Materials and Methods, the yield of 8-azido xanthosine after 16 h is approximately 100% as judged by HPLC analysis (Figure 3.35). The product is light sensitive, indicative of an aryl azido group (Figure 3.36). The wavelength maximum is at 270 nm, and the red shift (15 nm) from 8-bromo xanthosine is consistent with the bromo group being replaced by an azido group.

University of Cape Town

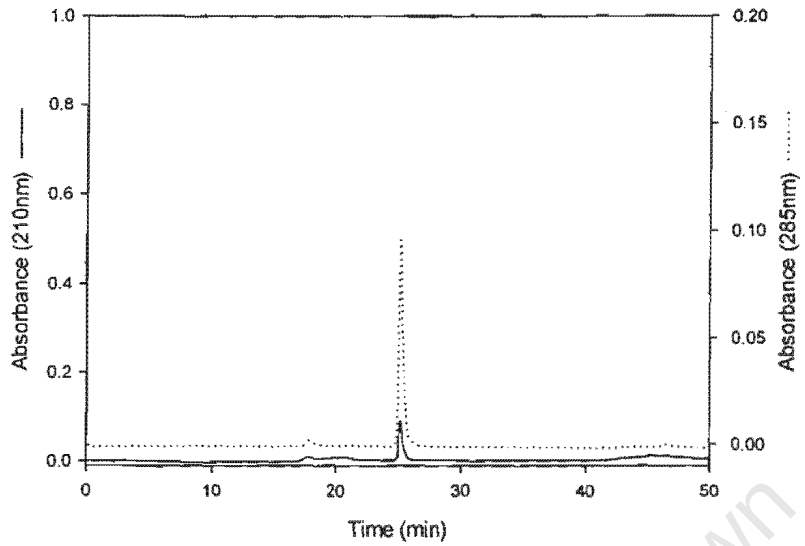

Figure 3.35 HPLC trace of the reaction mix for synthesis of 8-azidoxanthosine after 16 h. Mobile phase A= 1 mM KPi, pH 3; Mobile phase B= 50% (v/v) acetonitrile. Detection was at 210 nm and 285 nm. Gradient (mobile phase B): 0% for 5 min, 0-30% over 30 min, 30-100% over 5 min, 100% for 5 min, 100-0% over 5 min. Flow rate: 1 ml/min.

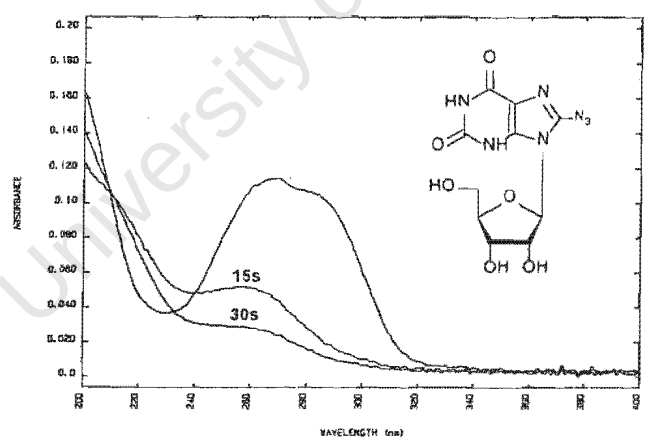

Figure 3.36 The absorption spectrum of 8-azidoxanthosine, with λmax 270 nm. Irradiation using a Xenon light source placed 10 cm from a quartz cuvette containing 8-azidoxanthosine results in the abolishment of the 270 nm peak, and this change is indicative of the presence of an azido group presumably at the 8-position of the purine ring. The times shown are the times of irradiation.

University of Cape Town

A major obstacle was the removal of DMSO and sodium azide from the completed 8-bromoxanthosine to 8-azidoxanthosine reaction. Repeated lyophilisation to remove DMSO resulted in the degradation of 8-azidoxanthosine. Both DMSO and sodium azide were eventually removed by aluminium oxide chromatography: nucleotides bind tightly to this resin, DMSO and sodium azide passed straight through the column, and the remainder could be washed off with water. Elution of 8-azidoxanthosine from the alumina column was achieved with 0.5 M ammonium acetate, pH 7. The elution profile is shown in Figure 3.37.

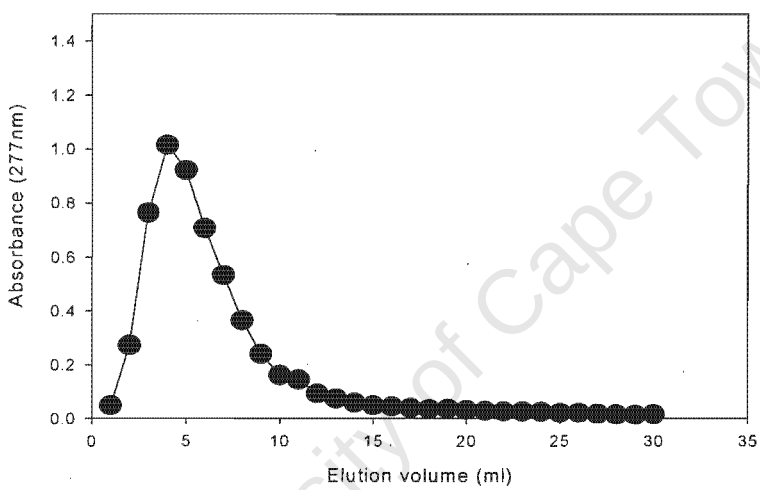

University of Cape Town

Figure 3.37 Elution profile of 8-azidoxanthosine from an aluminium oxide column. The 8-azidoxanthosine synthesis reaction (500 µl) was loaded onto 0.6 g aluminium oxide (activated, neutral) resin. The column was washed with 30 ml water, and the 8-azidoxanthosine was eluted with 30 ml 0.5 M ammonium acetate, pH 7. The eluant was collected in 1 ml aliquots. The absorbance of each aliquot at 277 nm was determined, and was plotted against elution volume.

HPLC analysis of the pooled first 10 ml after lyophilisation and dissolution in water indicated a contaminant eluting at 18 min in comparison to 8-azido xanthosine at 26 min (Figure 3.38). The earlier-eluting peak was not light sensitive. Its appearance depended on the presence of ammonium acetate, as prolonged incubation of purified 8-azido xanthosine without this salt failed to produce it. The yield of 8-azido xanthosine was approximately 30%. Pure product was obtained by HPLC, using the conditions described in Figure 3.38.

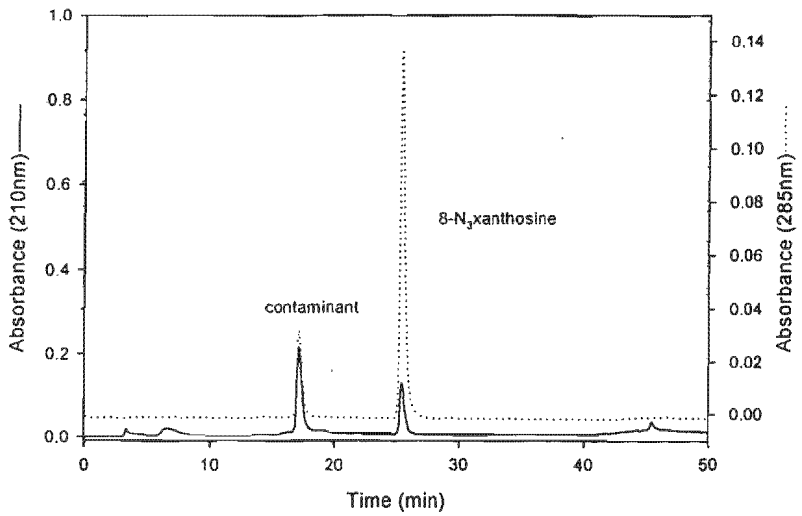

Figure 3.38 The formation of an impurity during 8-azidoxanthosine elution from an alumina column. The eluant (8-azidoxanthosine) from the alumina column was lyophilised, and reconstituted in water. An aliquot was analysed for purity by HPLC. Mobile phase A= 1 mM KPi, pH 3; Mobile phase B= 50% (v/v) acetonitrile. Detection was at 210 nm and 285 nm. Gradient (mobile phase B): 0% for 5 min, 0-30% over 30 min, 30-100% over 5 min, 100% for 5 min, 100-0% over 5 min. Flow rate: 1ml/min.

The incubation of 8-azido xanthosine in 2 M HCl yielded a light-sensitive compound eluting earlier than the parent compound, and was presumed to be 8-azido xanthine with an absorbance maximum of 290 nm (Figures 3.39 and 3.40). The yield of product was approximately 80% as judged by HPLC using the 285 nm trace in Figure 3.39.

University of Cape Town

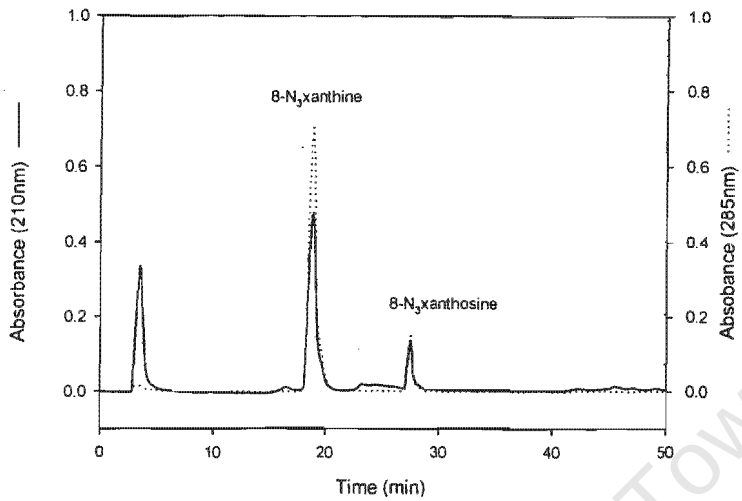

Figure 3.39 Acid cleavage of 8-azidoxanthosine to afford 8-azidoxanthine. The cleavage of 2 mM 8-azidoxanthosine was conducted with 2 M HCl overnight at 25 °C. Mobile phase A= 1 mM KPi, pH 3; Mobile phase B= 50% (v/v) acetonitrile. Detection was at 210 nm and 285 nm. Gradient (mobile phase B): 0% for 5 min, 0-30% over 30 min, 30-100% over 5 min, 100% for 5 min, 100-0% over 5 min. Flow rate: 1 ml/min.

University of Cape Town

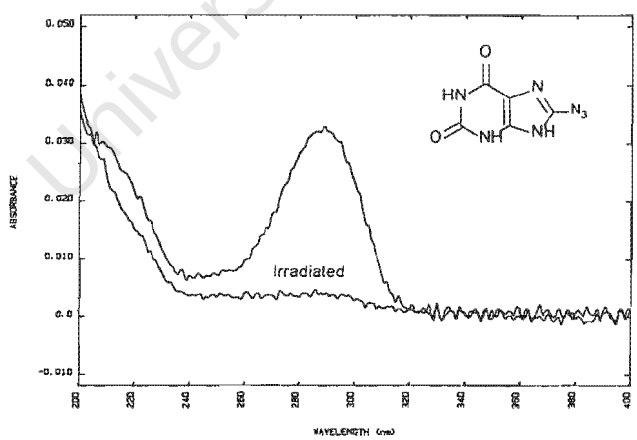

Figure 3.40 The absorption spectrum of 8-azidoxanthine in 1 mM KPi, pH 3, showing the spectral changes that occur upon irradiation with a Xenon light source.

3.8.2 The synthesis of 2',3'-O-(2,4,6-trinitrophenyl)- nucleotides

The synthesis of 2',3'-O-(2,4,6-trinitrophenyl)- nucleotides is shown in Scheme 2 below.

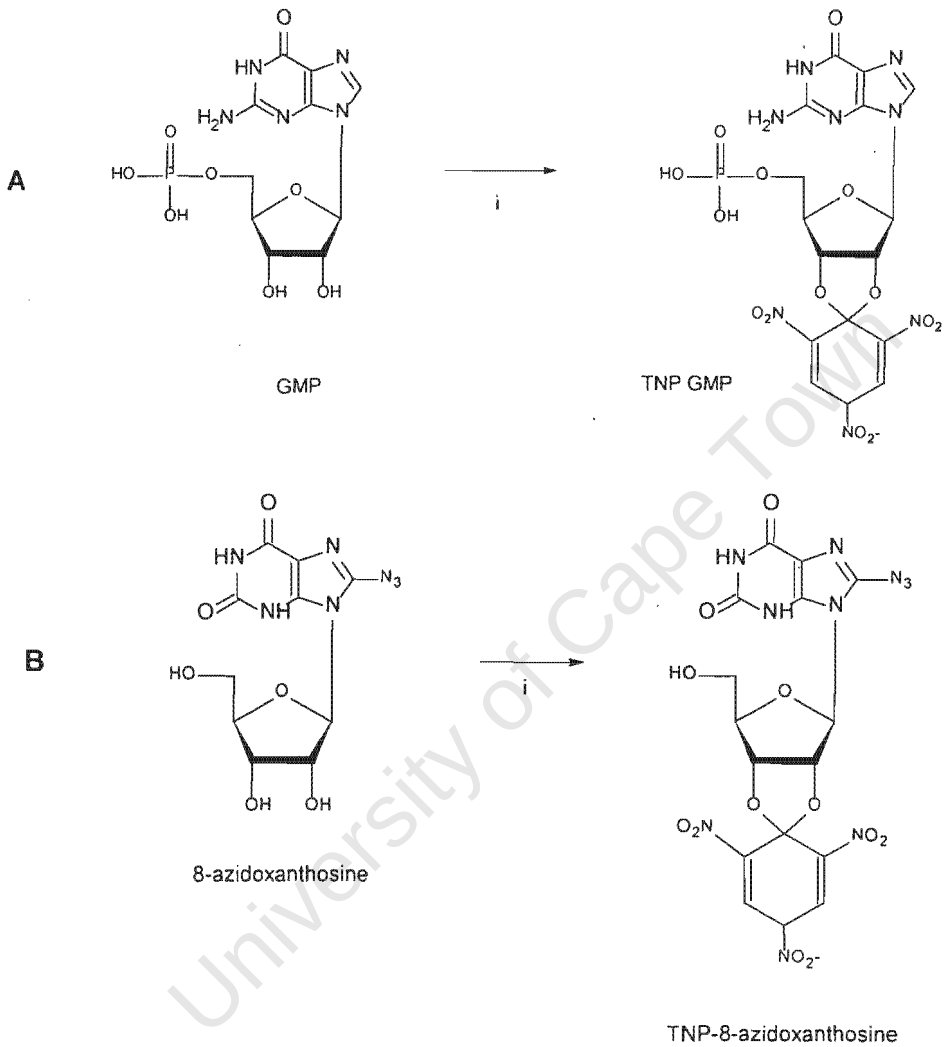

Scheme 2 The synthesis of 2',3'-O-(2,4,6-trinitrophenyl)-nucleotides. Panel A i) $Na_2CO_3/NaHCO_3$, TNBS. 1.2% TNP-GMP yield, 0.5% TNP-IMP yield, 0.8% TNP-XMP yield; Panel B i) $Na_2CO_3/NaHCO_3$, TNBS, DTNB. 9% TNP-8-azidoxanthosine yield

University of Cape Town

3.8.2.1 The synthesis of TNP-GMP

TNP-GMP was synthesised as described in Materials and Methods. Crude purification of TNP-GMP employed Sep-Pak® Plus C18 cartridges, and further purification was conducted by HPLC. The HPLC analysis of the product of the crude purification is shown in Figure 3.41.

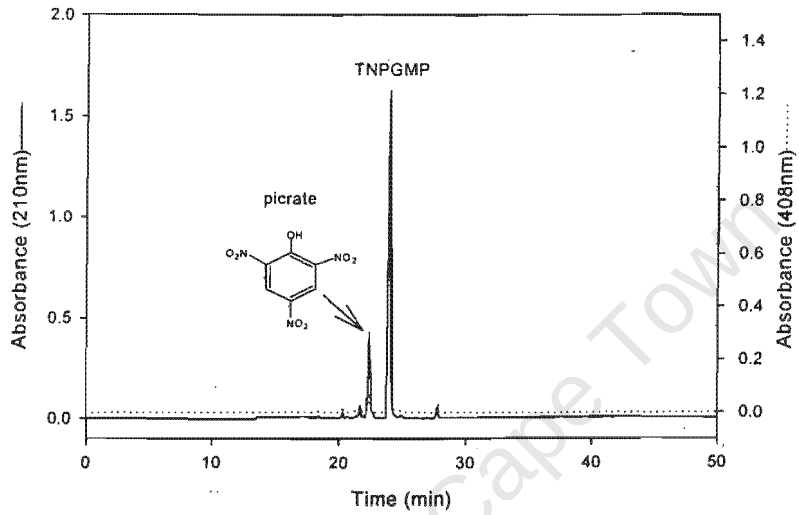

Figure 3.41 HPLC analysis following crude purification of TNP-GMP by Sep-Pak® Plus C18 cartridges. Mobile phase A= 10 mM KPi, pH 5.5; Mobile phase B= 10 mM KPi, 60% (v/v) acetonitrile. Detection was at 210 nm and 408 nm. Gradient (mobile phase B): 0% for 5 min, 0-100% over 30 min, 100% for 10 min, 100-0% over 5 min. Flow rate: 1ml/min.

University of Cape Town

Figure 3.41 shows an HPLC analysis of semi-purified TNP-GMP. The major contaminant is picrate with a retention time of 22 min. The major peak is that of TNP-GMP, as judged by its spectral properties, with a retention time of 24 min. TNP-GMP was collected by HPLC, lyophilised to dryness, and reconstituted in water. An aliquot was analysed by HPLC for purity, and the result is shown in Figure 3.42.

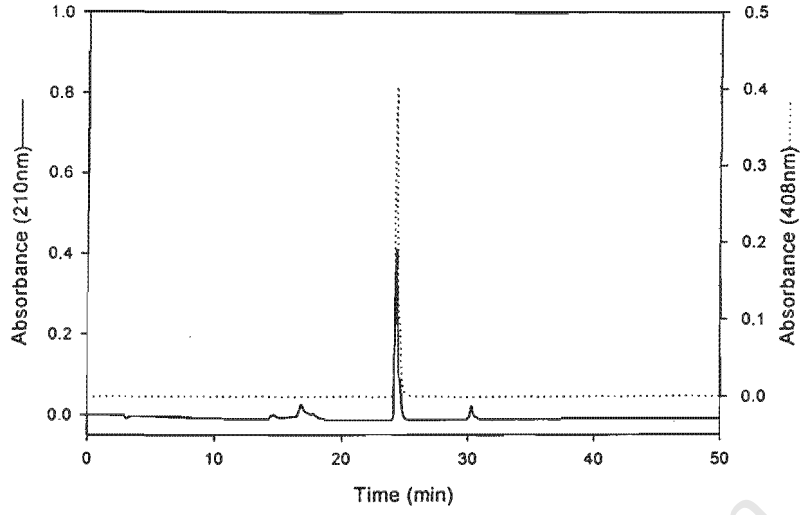

Figure 3.42 Purity of TNP-GMP synthesised. Mobile phase A= 10 mM KPi, pH 5.5; Mobile phase B= 10 mM KPi, pH 5.5, 60% (v/v) acetonitrile. Detection was at 210 nm and 408 nm. Detection was at 210 nm and 408 nm. Gradient (mobile phase B): 0% for 5 min, 0-100% over 30 min, 100% for 10 min, 100-0% over 5 min. Flow rate: 1ml/min.

The spectral properties of the TNP-GMP synthesised are shown in Figure 3.43. TNP derivatives can be identified spectrophotometrically by absorbance maxima at 408 nm and at 475 nm. This feature is characteristic of the TNP group attached via the 2' and 3' hydroxyl groups as a Meisenheimer complex (inset, Figure 3.43).

University of Cape Town

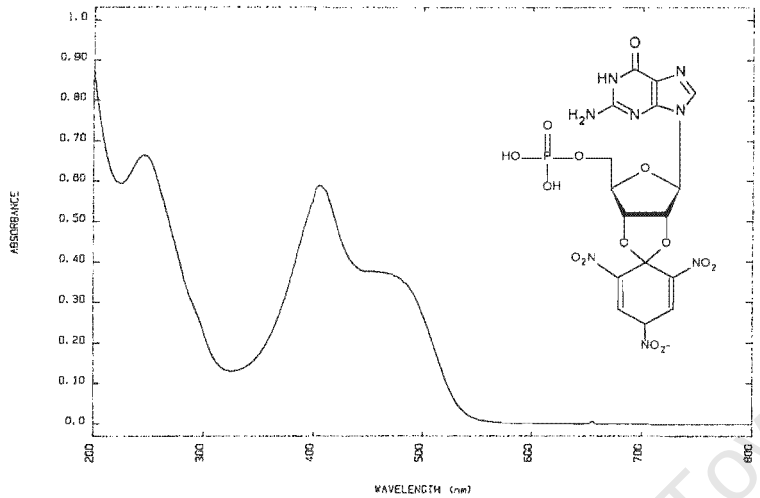

Figure 3.43 The absorption spectrum of TNP-GMP (pH 5). The inset shows the structure of TNP-GMP.

University of Cape Town

3.8.2.2 The synthesis of TNP-IMP

TNP-IMP was synthesised as in Scheme 2A, where IMP was used as the starting material. The purification of TNP-IMP was conducted as for TNP-GMP. HPLC analysis of the product of the crude purification is shown in Figure 3.44.

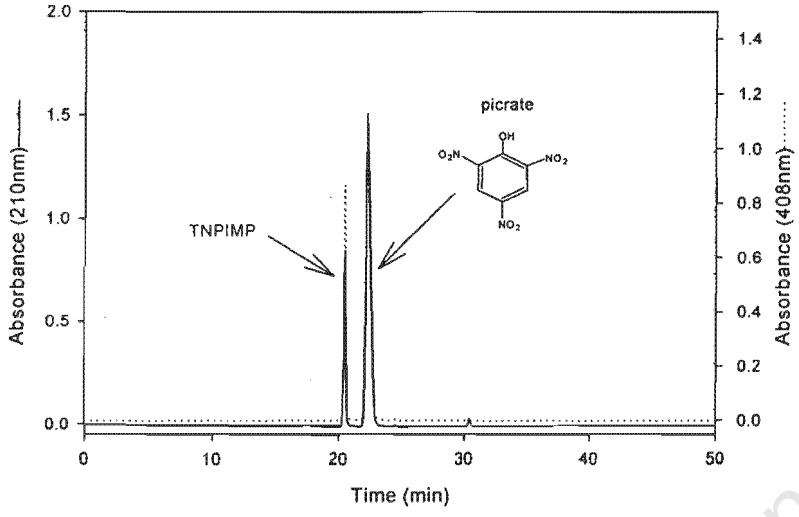

Figure 3.44 HPLC analysis following crude purification of TNP-IMP by Sep-Pak® Plus C18 cartridges. Mobile phase A= 10 mM KPi, pH 5.5; Mobile phase B= 10 mM KPi, pH 5.5, 60% (v/v) acetonitrile. Detection was at 210 nm and 408 nm. Gradient (mobile phase B): 0% for 5 min, 0-100% over 30 min, 100% for 10 min, 100-0% over 5 min. Flow rate: 1ml/min.

TNP-IMP (with retention time of 21min) was purified from pirate (with retention time of 23min) by HPLC, and the purity of the resulting TNP-IMP is shown in Figure 3.45. Figure 3.46 shows the spectral properties of TNP-IMP.

University of Cape Town

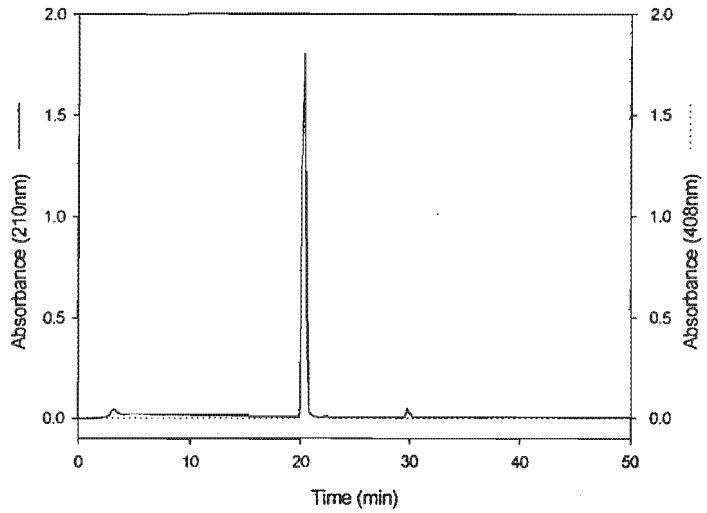

Figure 3.45 HPLC analysis of purified TNP-IMP. Mobile phase A= 10 mM KPi, pH 5.5; Mobile phase B= 10 mM KPi, pH 5.5, 60% (v/v) acetonitrile. Detection was at 210 nm and 408 nm. Gradient (mobile phase B): 0% for 5 min, 0-100% over 30 min, 100% for 10 min, 100-0% over 5 min. Flow rate: 1ml/min.

University of Cape Town

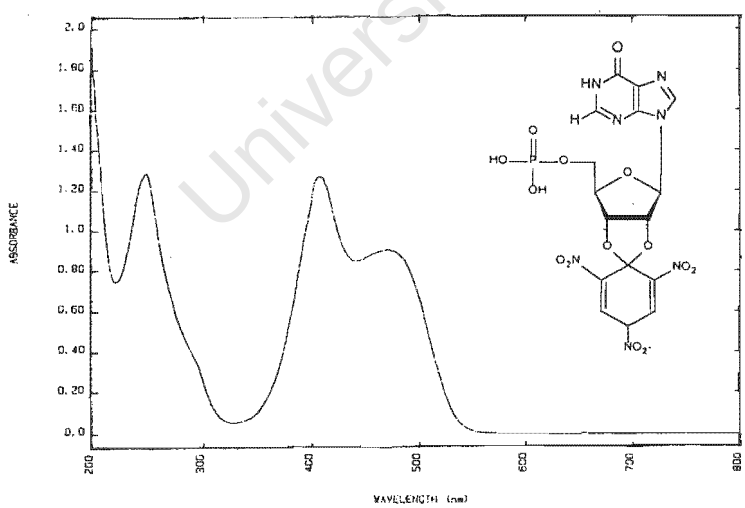

Figure 3.46 The absorption spectrum of TNP-IMP (pH 5). The inset shows the structure of TNP-IMP.

3.8.2.3 The synthesis of TNP-XMP

The synthesis of TNP-XMP proved not as straightforward as the synthesis of TNP-GMP and TNP-IMP as poor yields were obtained using the standard protocol (shown in Scheme 2A,using XMP as the starting material). HPLC analysis of the reaction mix over time is shown in Figure 3.47.

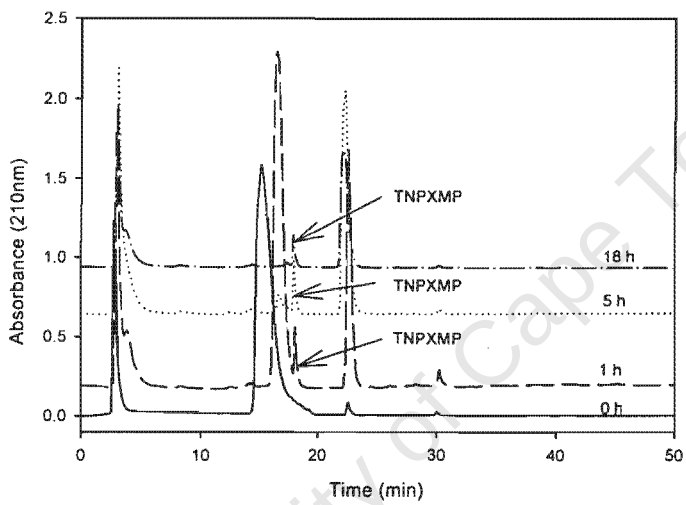

Figure 3.47 The synthesis of TNP-XMP over time. Mobile phase A= 10 mM KPi, pH 5.5; Mobile phase B= 10 mM KPi, pH5.5, 60% (v/v) acetonitrile. Detection was at 210 nm and 408 nm. Gradient (mobile phase B): 0% for 5 min, 0-100% over 30 min, 100% for 10 min, 100-0% over 5 min. Flow rate: 1ml/min.

University of Cape Town

XMP elutes at approximately 3 min, TNBS at 15 min and picrate at 23 min. A small amount of a compound with the typical Meisenheimer spectrum was identified eluting at approximately 18 min. Its amount plateaued between 1 and 5 h of reaction, and yet large amounts of XMP remained. Virtually all of the TNBS was consumed, and converted to picrate. It is clear that the reaction had stopped due to exhaustion of TNBS. Accordingly, we tried to increase the yield of TNP-XMP by supplementing the reaction with TNBS at various times. The results are shown in Figure 3.48.

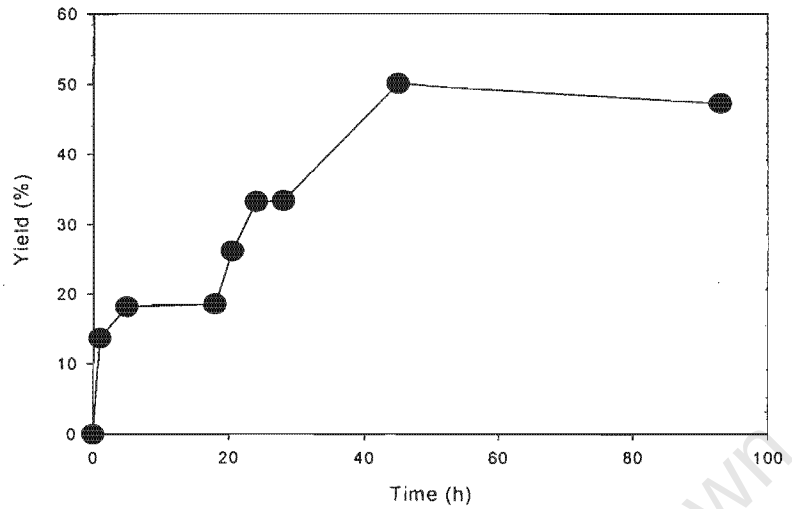

Figure 3.48 The effect of TNP-XMP synthesis supplementation with TNBS. TNP-XMP synthesis was conducted as described in Materials and Methods. After 18 h reaction, more TNBS was added (290 mg, which is the equivalent of the TNBS added at the beginning of the reaction). The reaction was allowed to proceed for 10 h, after which another 290 mg more TNBS was added. After 28 h reaction, a final amount of TNBS (290 mg) was added. The reaction was stopped after a total of 93 h incubation at room temperature. Yield was calculated using the formula Yield (%) = area under the TNP-XMP peak /area under the XMP peak at the beginning of the reaction.

The result indicates that there is a 20% yield in TNP-XMP synthesis after 5 h of reaction. Subsequent additions of TNBS improved TNP-XMP yield, however the rate of synthesis of TNP-XMP declined with each addition, which may be due to product inhibition by picrate. It may be that under these conditions, reaction equilibria and reaction kinetics are influenced by the addition of more TNBS so that the formation of picrate occurs at the expense of the formation of TNP-XMP. This may be case since the formation of picrate was rapid compared to that of TNP-XMP.

University of Cape Town

TNP-XMP was synthesised in this manner, and was purified by HPLC. An analysis of the pure compound by HPLC is shown in Figure 3.49. The spectral properties of TNP-XMP, exhibiting the typical profile of a Meisenheimer complex are shown Figure 3.50.

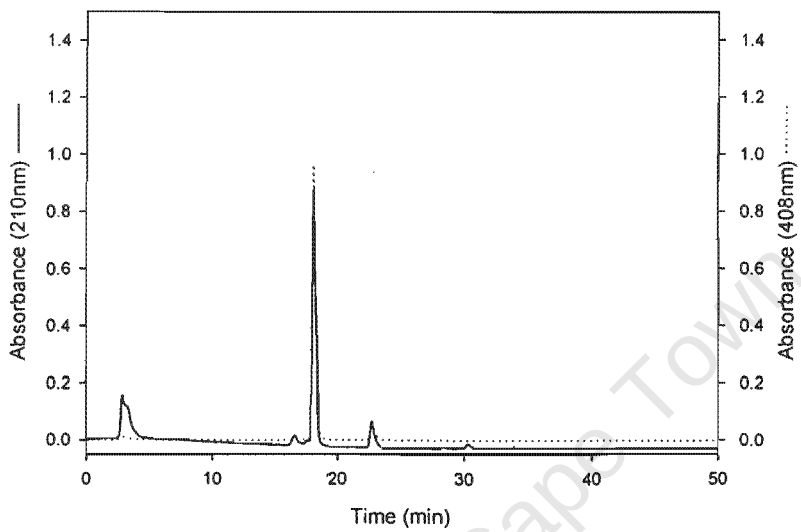

Figure 3.49 HPLC analysis of purified TNP-XMP. Mobile phase A= 10 mM KPi, pH 5.5; Mobile phase B= 10 mM KPi, pH 5.5, 60% (v/v) acetonitrile. Detection was at 210 nm and 408 nm. Gradient (mobile phase B): 0% for 5 min, 0-100% over 30 min, 100% for 10 min, 100-0% over 5 min. Flow rate: 1ml/min.

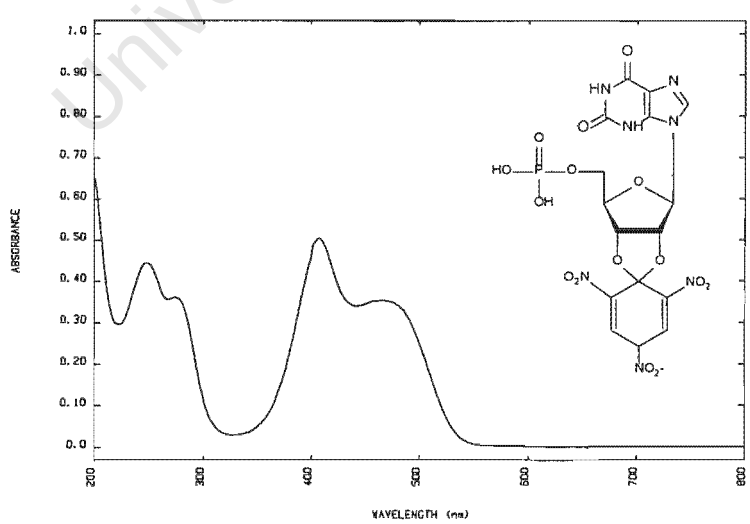

Figure 3.50 The absorption spectrum of TNP-XMP (pH 5). The inset shows the structure of TNP-XMP.

University of Cape Town

3.8.2.4 The synthesis of TNP-8-azido-xanthosine

The synthesis of TNP-8-azido-xanthosine was conducted as shown in Scheme 2B. The reaction of 8-azido-xanthosine with TNBS was conducted in the presence of DTNB. DTNB (an oxidising agent) was used to prevent sulfonic acid induced reduction of the azido group. DTNB had reportedly increased a similar trinitrophenylation reaction (Seebregts and McIntosh, 1989) Reaction was followed by HPLC analysis, and the result is shown in Figure 3.51.

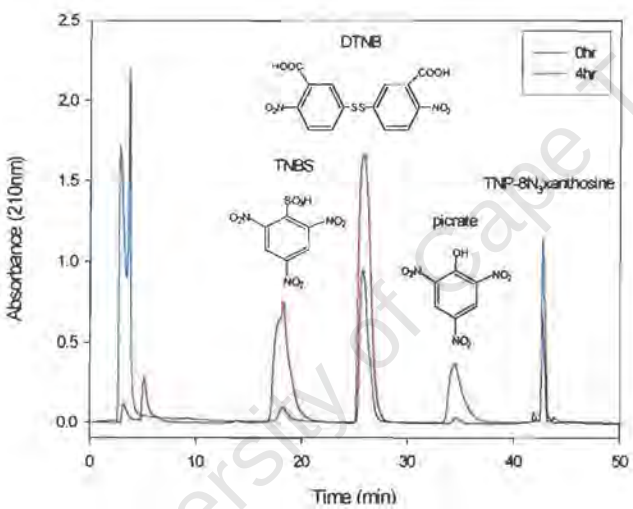

Figure 3.51 HPLC analysis of the synthesis of TNP-8-azido-xanthosine mix at 0 h (red trace) and 4 h (blue trace). Mobile phase B= 10 mM KPi, pH 5.5, 60% (v/v) acetonitrile. Detection was at 210 nm and 408 nm. Gradient (mobile phase B): 0% for 5 min, 0-30% over 30 min, 30-100% over 5 min, 100% for 5 min, 100-0% over 5 min. Flow rate: 1 ml/min.

A peak with retention time of 43 min had the typical Meisenheimer spectrum, and was presumed to be TNP-8-azidoxanthosine. Re-analysis of the product by HPLC indicated that it was not pure. It was re-purified using a different gradient system, and an analysis of this product is shown in Figure 3.52.

University of Cape Town

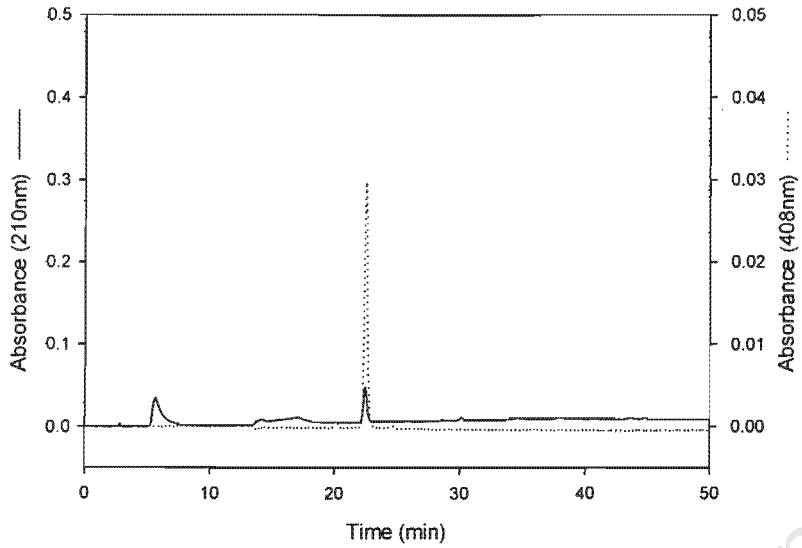

Figure 3.52 HPLC-purified TNP-8-azido-xanthosine. Mobile phase A= 10 mM KPi, pH 5.5; Mobile phase B= 10 mM KPi, pH 5.5, 60% (v/v) acetonitrile. Detection was at 210 nm and 408 nm. The mobile phase was altered for early elution of the TNP-8-azido-xanthosine. Gradient (mobile phase B): 0% for 5 min, 0-100% over 30 min, 100% for 10 min, 100-0% over 5 min. Flow rate: 1ml/min.

The changes in the spectral properties of the putative TNP-8-azido-xanthosine upon irradiation are shown in Figure 3.53. The peak at 270 nm diminished, and one at 230 nm appeared, showing that the compound was light sensitive. This characteristic coupled with the Meisenheimer spectrum allowed us to conclude that the product isolated was TNP-8-azido-xanthosine.

University of Cape Town

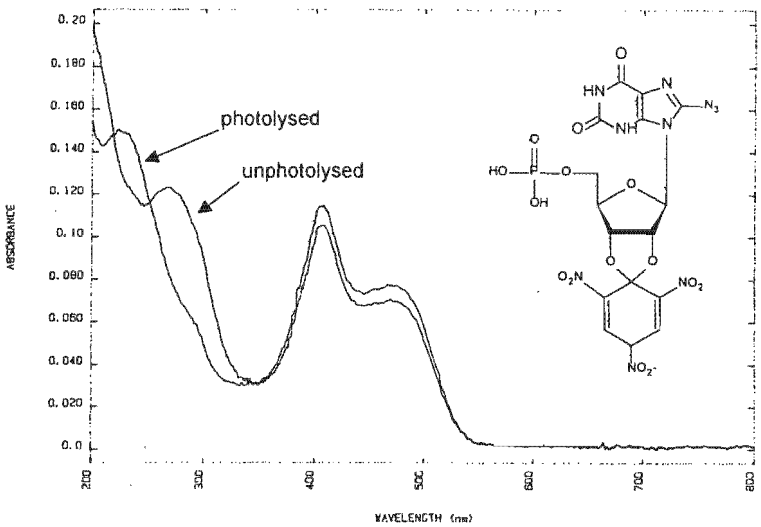

Figure 3.53 Absorption spectra of unphotolyzed and photolyzed TNP-8-azido-xanthosine. TNP-8-azido-xanthosine was irradiated for 30 s at room temperature in quartz cuvettes placed 10 cm form a Xenon light source of 150 W. The inset shows the structure of TNP-8-azido-xanthosine.

The approximate yields of the compounds synthesised are listed in Table 3.5. Those for TNP-GMP, TNP-IMP and TNP-XMP were similar and very low. The poor reaction of GMP with TNBS has been commented on by Hiratsuka (1985). However, we only needed small amounts to test their inhibitory properties on the HPRTases, and did not pursue alternative strategies.

University of Cape Town

Table 3.5 Approximate yields of compounds synthesised

Compound	Yield (%)
TNP-GMP	1.2
TNP-IMP	0.5
TNP-XMP	0.8
8-azido xanthosine	30
TNP-8-azido xanthosine	9
8-azido xanthine	6

The extinction coefficients for TNP-GMP, TNP-IMP, TNP-XMP and TNP-8-azido xanthosine at 408 nm were taken as the same as TNP-ATP, namely 26400 M^{-1} cm^{-1} (Hiratsuka, 1982). The extinction coefficient for 8-azido xanthosine at 278 nm was taken as 8900 M^{-1} cm^{-1} (Smith and Dunn, 1959), and that for 8-azido xanthine as 12700 M^{-1} cm^{-1} at 281 nm (Holmes and Robins, 1964).

3.8.3 The synthesis of nucleotide-flavonoid conjugates

3.8.3.1 The synthesis of a putative conjugate between TNP-8-azidoxanthosine and kaempferide

We explored the possibility that TNP-8-azido xanthosine may be conjugated to certain flavonoids under light. Previous results with TNP-8-azido ATP had suggested that kaempferide might be useful in this regard (unpublished results from this laboratory). A series of experiments relating to irradiation of equimolar amounts of TNP-8-azido xanthosine and kaempferide are shown in Figure 3.54.

University of Cape Town

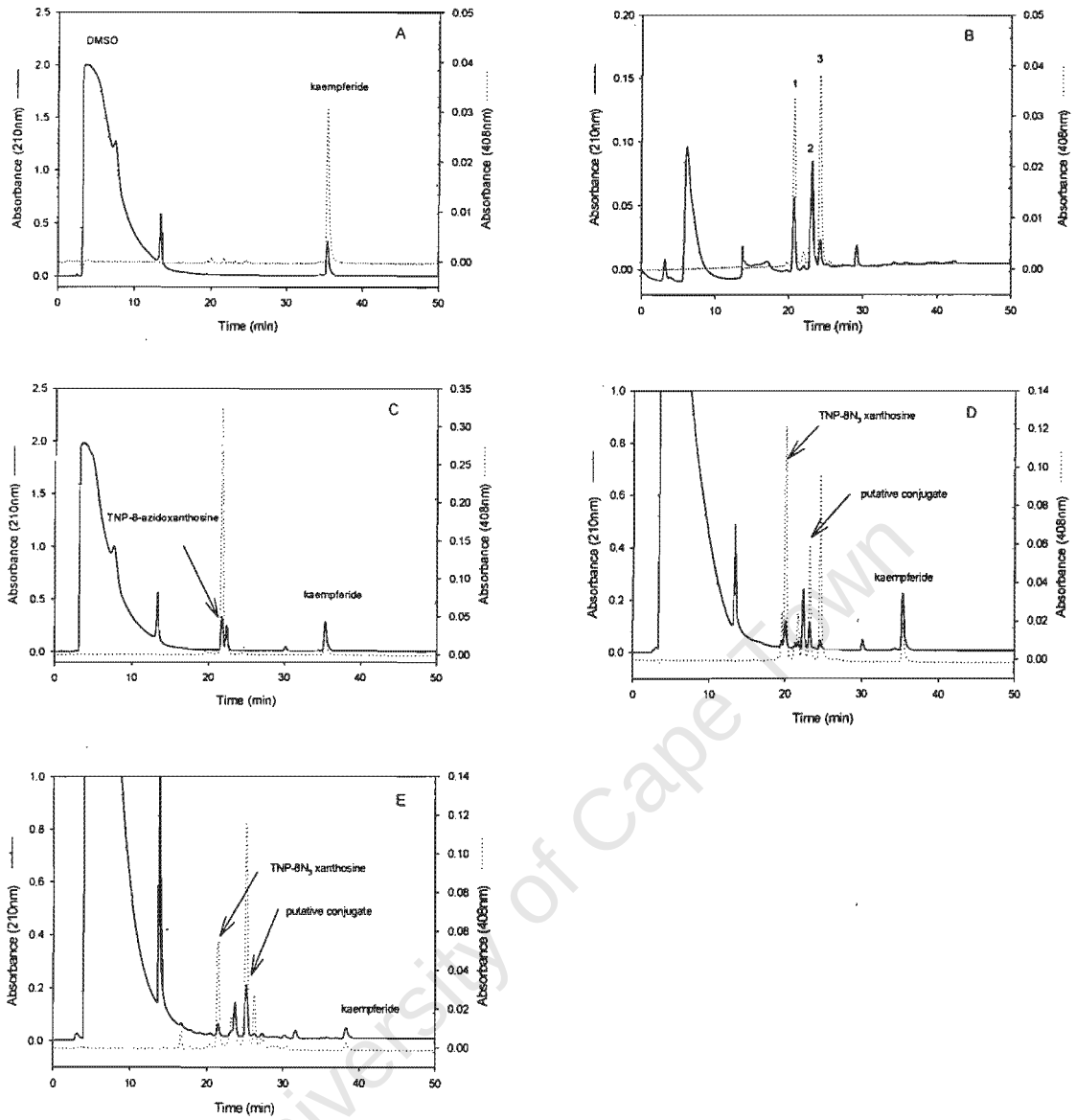

Figure 3.54 HPLC analyses of a photoinduced reaction between TNP-8-azido-xanthosine and kaempferide. A, HPLC analysis of 10 µM kaempferide; B, HPLC analysis of 10 µM TNP-8-azidoxanthosine irradiated for 30 s; C, HPLC analysis of 10 µM TNP-8-azido-xanthosine and kaempferide before irradiation; D, HPLC analysis of 10 µM TNP-8-azido-xanthosine and kaempferide irradiated for 30 s; E, HPLC analysis of 10 µMTNP-8-azido-xanthosine and kaempferide irradiated for 5 min. Mobile phase A= 1 mM KPi, pH 5.5; Mobile phase B= 1 mM KPi, pH 5.5, 60% (v/v) acetonitrile. Detection was at 210 nm and 408 nm. Gradient (mobile phase B): 0% for 5 min, 0-100% over 30 min, 100% for 10 min, 100-0% over 5 min. Flow rate: 1ml/min.

Panel A shows kaempferide with a retention time of 35 min. Panel B shows the different photolysis products from 30 s irradiation of TNP-8-azidoxanthosine alone. Three significant products were formed, with retention times of 20.5 min, 23 min and 24 min (labelled 1, 2 and 3

University of Cape Town

respectively). Panel C is a control for the reaction in the absence of light and shows the retention times of TNP-8-azido xanthosine and kaempferide. A small amount of a non-photosensitive, a possible breakdown product without the TNP group attached, and which does not absorb at 408 nm, elutes immediately after TNP-8-azido-xanthosine. Panel D shows the result of a 30 s irradiation, and that of a 5 min irradiation is shown in Panel E. The disappearance of TNP-8-azido xanthosine and kaempferide correlates with the appearance of a peak with retention time of 24 min. This peak with a unique 408 nm/ 210 nm absorbance ratio, was not seen in the photolysis of TNP-8-azido xanthosine in the absence of kaempferide (Panel B). This putative conjugate was identified on the basis of the summation of the absorbance spectra of the individual reactants, namely TNP-8-azidoxanthosine and kaempferide.

The irradiation of kaempferide alone for 5 min did not result in the degradation of kaempferide (Figure 3.55).

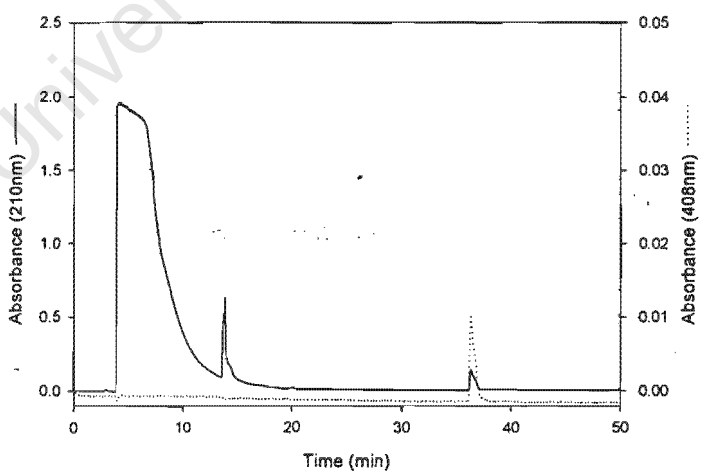

Figure 3.55 Irradiation of kaempferide in the absence of TNP-8-azido xanthosine. Kaempferide (10 µM) was irradiated in water in a quartz cuvette for 5 min using a 150 W Xenon light source. Mobile phase A= 1 mM KPi, pH 5.5; Mobile phase B= 1 mM KPi, pH 5.5, 60% (v/v) acetonitrile. Detection was at 210 nm and 408 nm. Gradient (mobile phase B): 0% for 5 min, 0-100% over 30 min, 100% for 10 min, 100-0% over 5 min. Flow rate: 1ml/min.

University of Cape Town

Similar experiments were conducted with 8-azido xanthosine and kaempferide, and the results are shown in Figure 3.56. Irradiation of 8-azido xanthosine alone appears to produce a single product that elutes early by HPLC (Panel A). Irradiation of the compounds together produced several peaks, most notably those eluting at 13 and 29 min. The efficiency of conversion was low as judged by the amount of kaempferide remaining after 5 min irradiation.

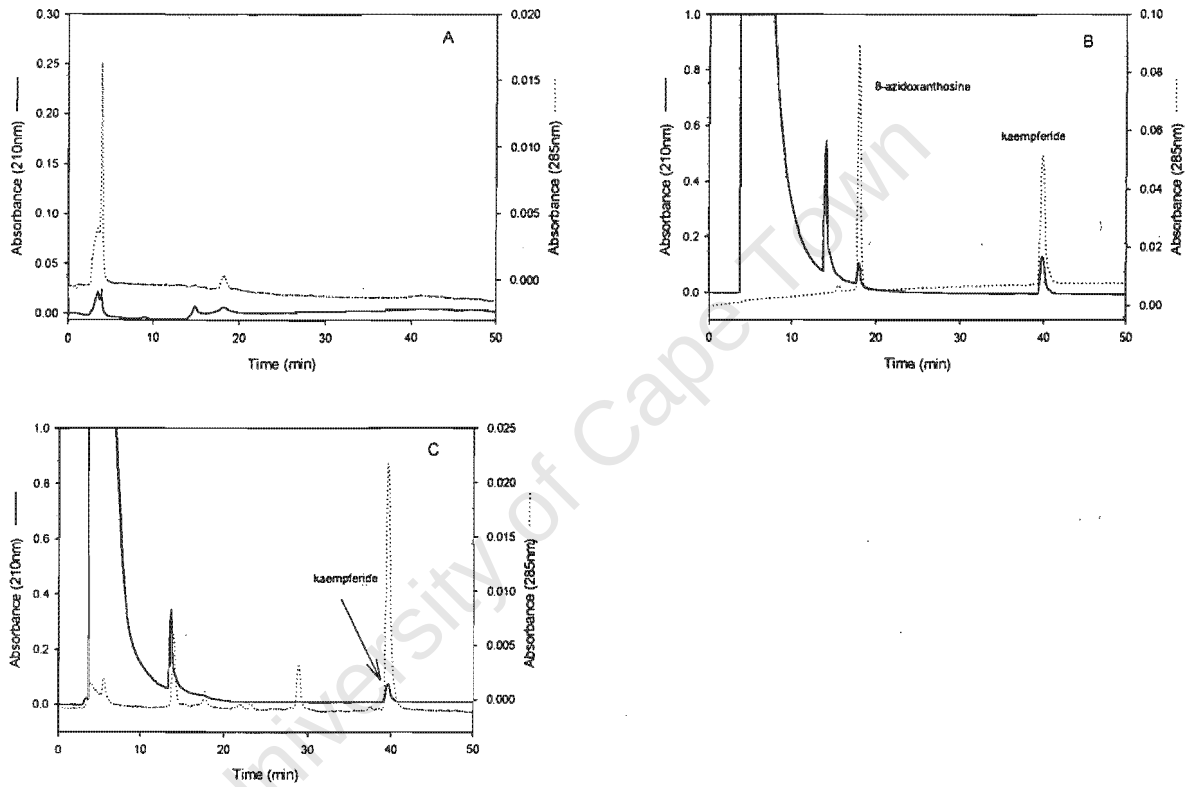

Figure 3.56 HPLC analysis of photolysis products between 8-azidoxanthosine and kaempferide. Panel A, 10 µM 8-azido-xanthosine irradiated for 5 min; Panel B, 10 µM 8-azido-xanthosine and kaempferide before irradiation; Panel C, Photolysis products from 5 min irradiation of 10 µM 8-azido-xanthosine and kaempferide. Mobile phase A= 1 mM KPi, pH 3; Mobile phase B= 50% (v/v) acetonitrile. Detection was at 210 nm and 285 nm. Gradient (mobile phase B): 0% for 5 min, 0-100% over 30 min, 100% for 10 min, 100-0% over 5 min. Flow rate: 1ml/min.

The possibility of synthesising a conjugate between 8-azidoxanthine and kaempferide was also investigated. Irradiation of the purine 8-azido xanthine with kaempferide produced a negligible amount of product as there was little change in the amount of kaempferide, and no new compound was visible by HPLC (results not shown).

University of Cape Town

Our conclusion is that the trinitrophenyl group appears to be necessary for the efficient formation of a conjugate between kaempferide and the azido compounds.

University of Cape Town

3.9 Drug screening

The compounds synthesised, and 38 flavonoids from four different classes were tested for inhibition of HPRT activity.

3.9.1 TNP derivatives

Human and malarial HPRT ($HPRT_{pfthr}$) were assayed by the continuous spectrophotometric method with 1 mM PRPP and 20 μM guanine, and screened for inhibition by TNP-GMP, TNP-IMP and TNP-XMP. The latter two were without effect, but TNP-GMP was found to selectively inhibit $HPRT_{pfthr}$. Examples of the concentration dependence of TNP-GMP on the activities of these enzymes, including *T. gondii* HPRT are shown in Figure 3.57. A large background subtraction was necessary at high TNP-GMP concentration, which gave rise to excessive noise on the trace, but the effect of TNP-GMP on the malarial enzyme and not on the others is clear.

The interaction of TNP-GMP with $HPRT_{pfthr}$ could also be demonstrated in experiments similar to Figure 3.26 by pre-incubating the enzyme for 5 min at 25 °C with and without the nucleotide (6 μM) for 5 min, and then adding the substrates (60 μM guanine and 1 mM PRPP). In the absence of TNP-GMP the enzyme showed activity on the addition of substrates because of the stabilisation afforded by the small amount of PRPP coming from the stock enzyme preparation. In the presence of TNP-GMP the enzyme was inactive after 5 min, demonstrating that the nucleotide had displaced PRPP, and rendered the protein unstable.

University of Cape Town

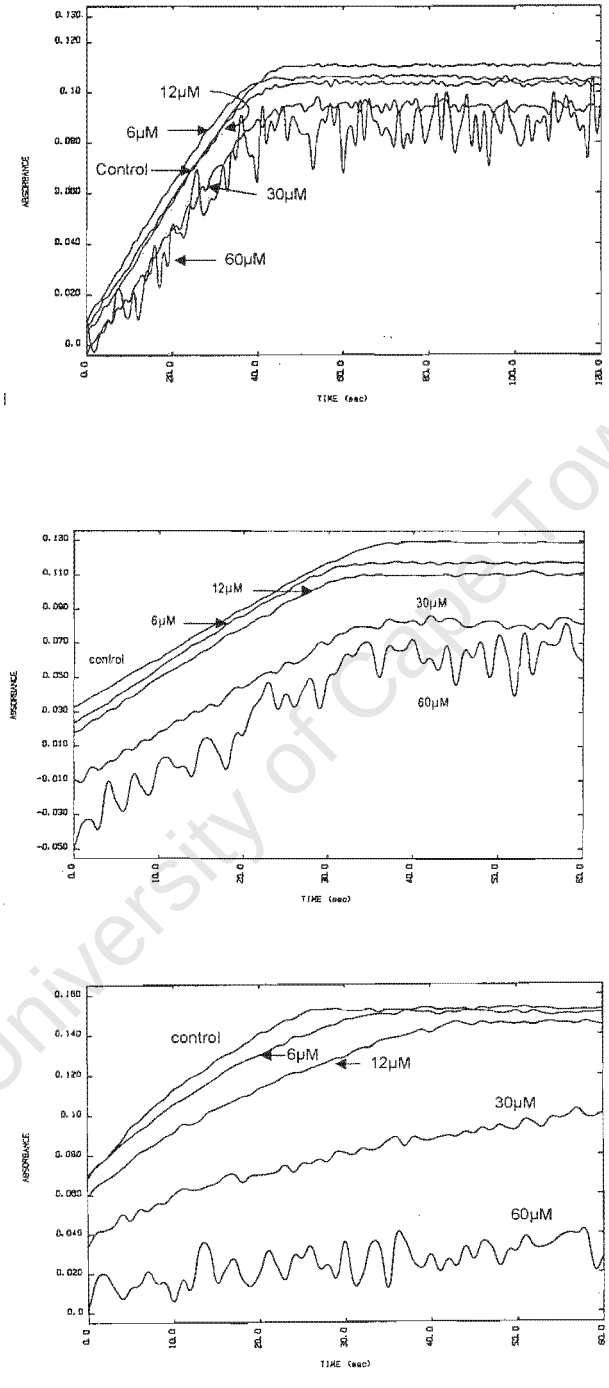

University of Cape Town

Figure 3.57 An example of the screening assay. Panel A, Human HPRT; Panel B, *T. gondii* HPRT; Panel C, $HPRT_{pfthr}$. HPRTases were incubated in the presence of 100 mM Tris/HCl, pH 8.5, 100 mM $MgCl_2$, 1 mM PRPP, 20 μM guanine and increasing concentrations of TNP-GMP at 25 °C.

The concentration dependence of activation of $HPRT_{pfthr}$ in the absence and presence of 10 μM TNP-GMP by guanine and PRPP is shown in Figure 3.58. Limitations of manual mixing prevented measurement at low guanine concentration. The result in Figure 3.58A indicates that TNP-GMP does not compete with guanine (inhibition persists at high guanine concentration), but that it possibly competes with PRPP (inhibition is abolished at high PRPP concentration; Figure 3.58B). Detailed studies to determine IC_{50} were, however, not conducted. Reversibility was not clearly demonstrated due to spectral limitations by the high absorbance of mixtures of TNP-GMP and guanine.

University of Cape Town

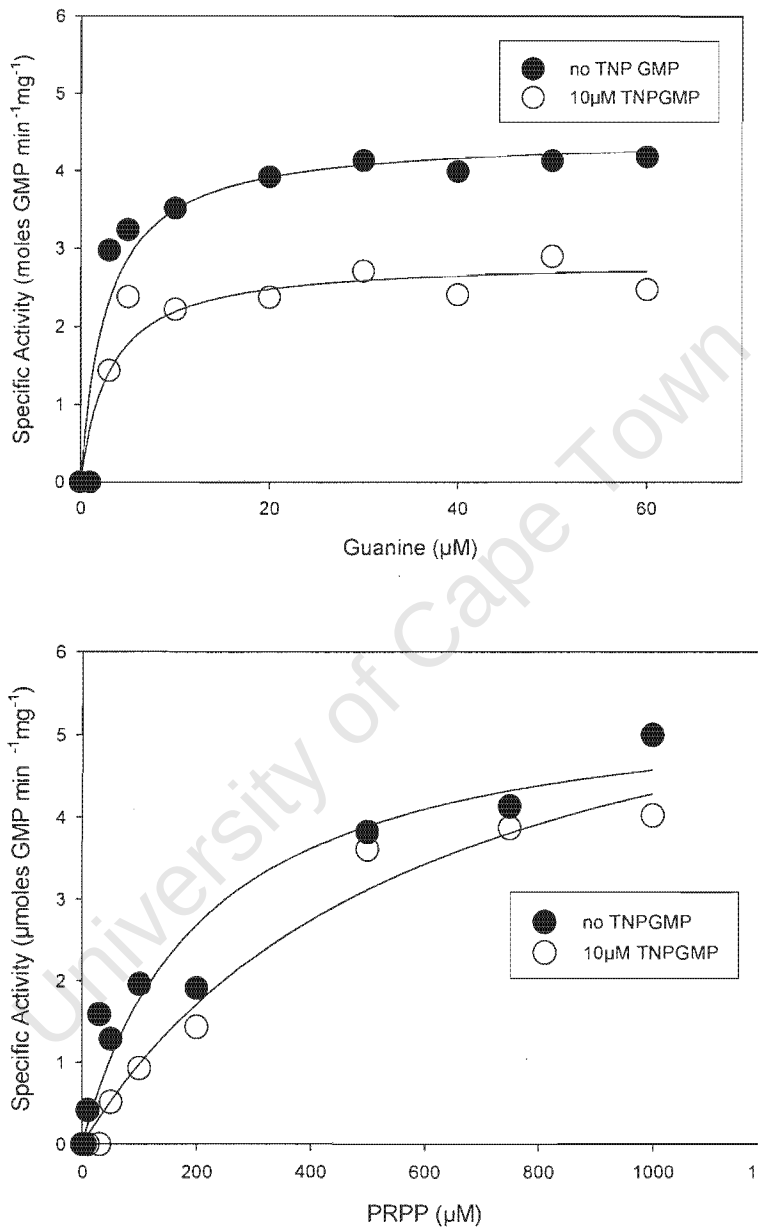

University of Cape Town

Figure 3.58 A Michaelis-Menton plot of the kinetics of $HPRT_{pfthr}$ inhibition by TNP-GMP. Panel A, guanine as substrate; Panel B, PRPP as substrate.

3.9.2 Flavonoids

A selection of flavonoids (listed in Table 3.6) was tested for inhibition of $HPRT_{pfthr}$.

Table 3.6 Flavonoids tested for inhibition of $HPRT_{pfthr}$¶

F1	4-C_6-chalcone	8-geranyl chrysin
F2	4-C_8-chalcone	4'-F-chrysin
F4	4-F-chalcone	4'-I-chrysin
Flavopyridol	4-I-chalcone	F5OH-I
Galangine	2',4',4-trihydroxychalcone	MH-48
6-prenyl-galangine	2',4',4-trihydroxy-3-prenylchalcone	CB-284
8-prenyl-galangine	Chrysin	CB-285
Kaempferide	6,8(di-DMA) chrysin	CB-286
Silybin	tectochrysin	CB-287
Dehydrosilybin	6(3,3-DMA) chrysin	CB-301
8-prenyl-dehydrosilybin	7(3,3-DMA) chrysin	
Broussochalcone A (F3)	8(1,1-DMA) chrysin	
4-C_2-chalcone	8(3,3-DMA) chrysin	
4-C_4-chalcone	6-geranyl chrysin	

¶ The structures of the flavonoids are shown in the Materials and Methods section.

$HPRT_{pfthr}$ was assayed for activity in the presence of 2 or 20 µM flavonoid. None of the flavonoids inhibited $HPRT_{pfthr}$ at the concentrations tested. However, very surprisingly, 4-I-chalcone was found to be an **activator** of $HPRT_{pfthr}$ turnover rate, as shown in Figure 3.59.

University of Cape Town

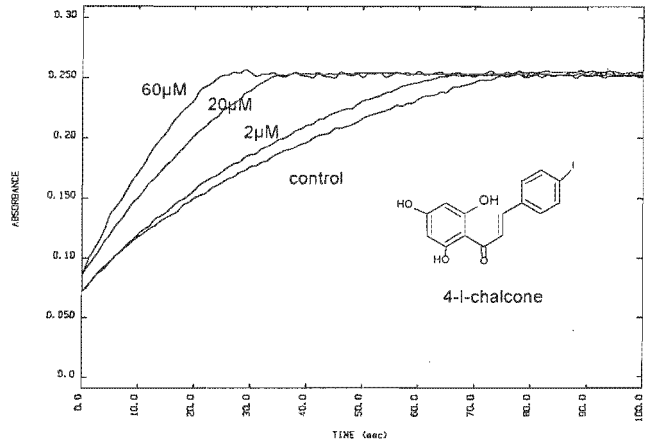

Figure 3.59 The activation of $HPRT_{pfthr}$ by 4-I-chalcone
$HPRT_{pfthr}$ was incubated in the presence of substrates and up to 60 µM of the flavonoid 4-I-chalcone at 25 °C.

The activity was increased approximately 2-fold in the presence of 60µM 4-I-chalcone (an increase form 3.0 to 5.6 and from 3.9 to 7.2 µmoles GMP min^{-1}. mg^{-1} for two different batches of enzyme). When hypoxanthine was used as the substrate, the activation was from 1.3 to 2.9 µmoles IMP min^{-1}. mg^{-1}. As with the trinitrophenylated nucleotides there was interference by high concentrations of 4-I-chalcone in the spectrophotometric assay, and it was not possible to study the effect of 4-I-chalcone at concentrations greater than 60µM. Interestingly, 4-F-chalcone was without effect.

The iodo-chalcone had no effect on the progress curve when added during the assay (Figure 3.60A), and preincubation with it caused inactivation (Figure 3.60B). It can be concluded that the iodo-chalcone provides no stabilisation of the malarial HPRT.

University of Cape Town

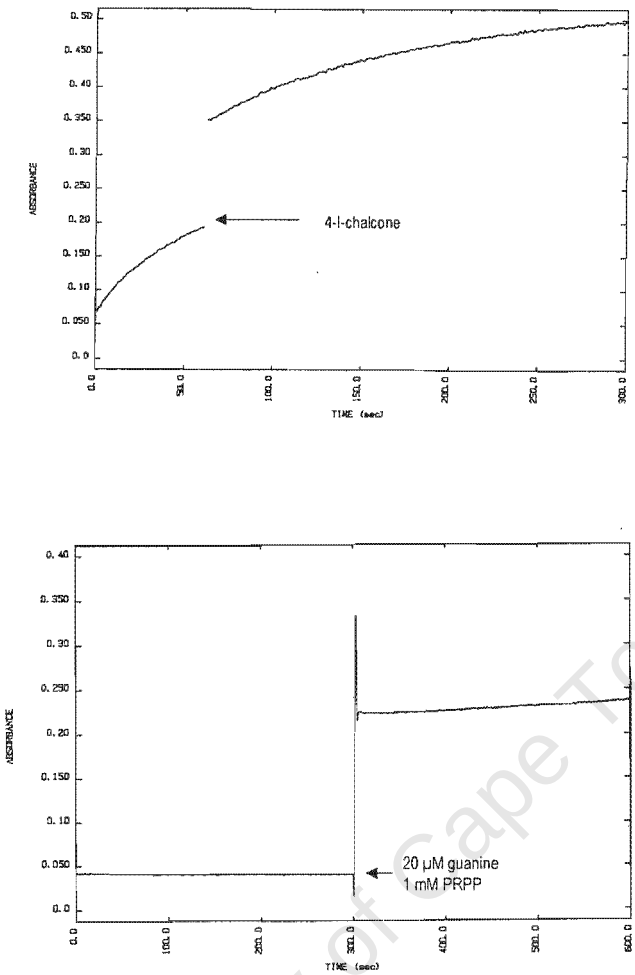

Figure 3.60 4-I-chalcone does not reverse or prevent the inactivation of $HPRT_{pfthr}$. Panel A, $HPRT_{pfthr}$ was incubated in the presence of 100 mM Tris/HCl, pH 8.5, 100 mM $MgCl_2$, 1 mM PRPP and 60 µM guanine for 1 min at 25 °C. 4-I-chalcone (20 µM) was added at the time shown, and the enzyme was incubated for a further 4 min. Panel B, $HPRT_{pfthr}$ was pre-incubated with 4-I-chalone in the presence of 100 mM Tris/HCl, pH 8.5, 100 mM $MgCl_2$ for 5 min at 25 °C. Guanine (20 µM) and PRPP (1 mM) were added as shown, and incubated for a further 5 min.

University of Cape Town

3.9.3 Putative conjugates

4-I-chalcone and TNP-8-azido xanthosine were irradiated together and the products were analysed by HPLC (Figure 3.61). Three peaks (indicated by the arrows in Panel B) that could not be ascribed to photolysis products of TNP-8-azido xanthosine alone were produced, and were presumed to be putative conjugates.

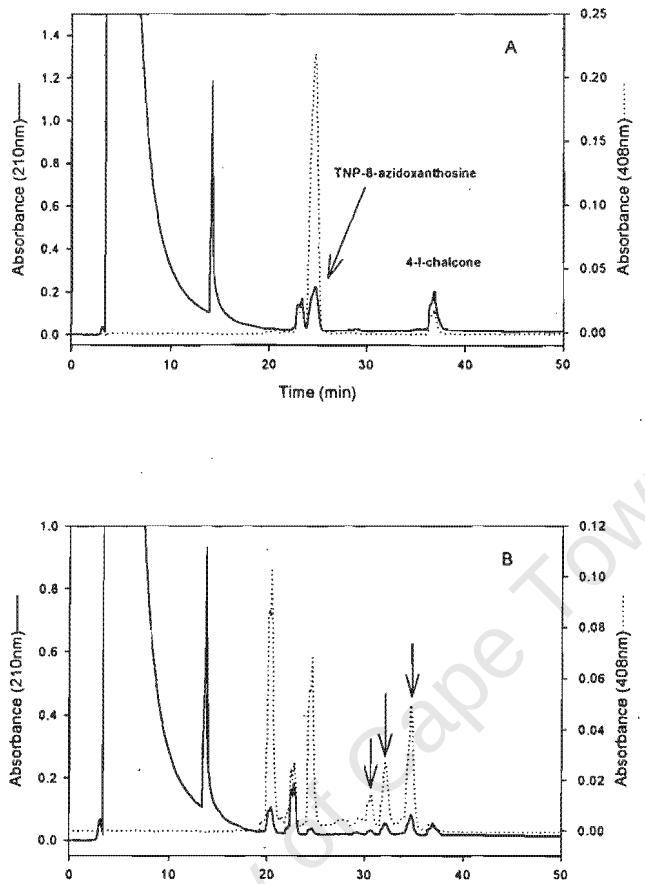

Figure 3.61 The synthesis of conjugates between TNP-8-azidoxanthosine and 4-I-chalcone Panel A, 100 µM TNP-8-azidoxanthosine and 4-I-chalcone before irradiation; Panel B, 100 µM TNP-8-azidoxanthosine and 4-I-chalcone after 5 min irradiation. Mobile phase A= 1 mM KPi, pH3; Mobile phase B= 1 mM KPi, pH 5.5, 60% (v/v) acetonitrile. Detection was at 210 nm and 408 nm. Gradient (mobile phase B): 0% for 5 min, 0-100% over 30 min, 100% for 10 min, 100-0% over 5 min. Flow rate: 1ml/min. Putative conjugates were identified on the basis of the summation of the absorbance spectra of the reactants TNP-8-azido xanthosine and 4-I-chalcone.

University of Cape Town

The effects of 8-azidoxanthosine, and TNP-8-azido xanthosine as well as those of the putative conjugate between kaempferide or 4-I-chalcone and TNP-8-azido xanthosine on $HPRT_{pfthr}$ activity were studied. The high absorbance of TNP-8-azido xanthosine and flavonoids limited the concentration to which they could be used to 10 µM and 60 µM respectively. In the case of 8-azido xanthine, 100 µM of the irradiated solution was used. No inhibition was observed under

conditions, where the azido-containing compounds were irradiated alone, or with the flavonoids to produce an array of photolysis products that could inhibit $HPRT_{pfthr}$.

3.10 Fluorescence studies

3.10.1 8-anilino 1-naphthalene-sulfonic acid (ANS) as a probe of hydrophobic pockets

ANS has been extensively used as a probe of hydrophobic pockets of proteins. It has low fluorescence in aqueous solutions, but the fluorescence can be considerably enhanced by binding to hydrophobic regions, or if it placed in organic solvents. We investigated whether the fluorescence of ANS was enhanced in the presence of $HPRT_{pfthr}$, and if inactivation caused any changes. The results are shown in Figure 3.62.

University of Cape Town

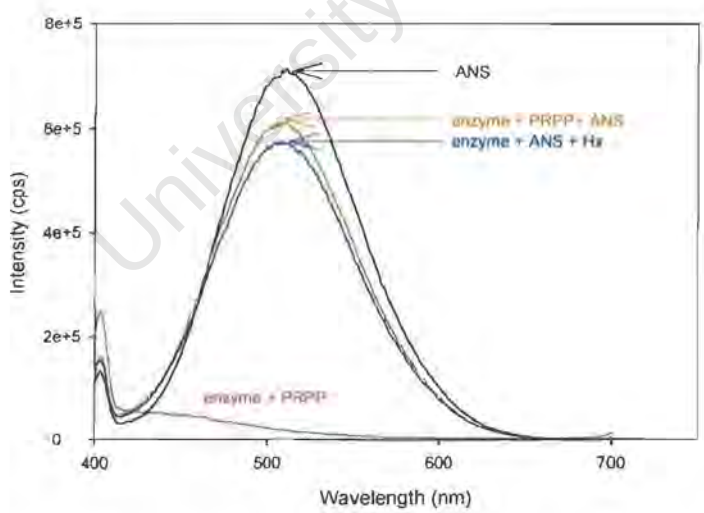

Figure 3.62 Emission scans of $HPRT_{pfthr}$ incubation with ANS. The medium contained 25 mM Tris/HCl. pH 8, 10 mM $MgCl_2$ and the additions shown as follows: enzyme (10 µg protein/ml), PRPP (0.5 mM), ANS (40 µM), Hx, hypoxanthine (50 µM). Excitation was at 290 nm.

ANS alone had a rather low fluorescence of $7x10^5$ cps. In the presence of $HPRT_{pfthr}$ and PRPP, the fluorescence was slightly decreased, and there was no change in λ_{max}. Inactivation of the enzyme by not adding PRPP to the cuvette and removing the remaining PRPP by adding hypoxanthine (via turnover) made very little difference. There was also no change in λ_{max}. The results suggest that the native protein is relatively compact with no exposed hydrophobic pockets and unfolding of the protein and the appearance of such pockets do not accompany inactivation.

3.10.2 Intrinsic tryptophan fluorescence

3.10.2.1 Intrinsic tryptophan fluorescence changes during turnover

Both the *T. gondii* and malarial HPRTs possess a single Trp residue, although in different places. That in *T. gondii* is at position 199 in the protein, and is conserved as an aromatic residue in all HPRTs, which clamps down on the purine ring of the substrate. It can be expected to change its fluorescence upon purine binding. The Trp residue in malarial HPRT is at position 181, and occurs in a loop that could be ordered to lock the hood domain onto the core domain during catalysis (Héroux *et al.*, 1999a). It is alongside Leu-180, which is replaced by Arg in the more active HPRTs. It is possible that the Trp residue may also undergo changes in fluorescence during the postulated disorder to order changes of this loop during turnover.

University of Cape Town

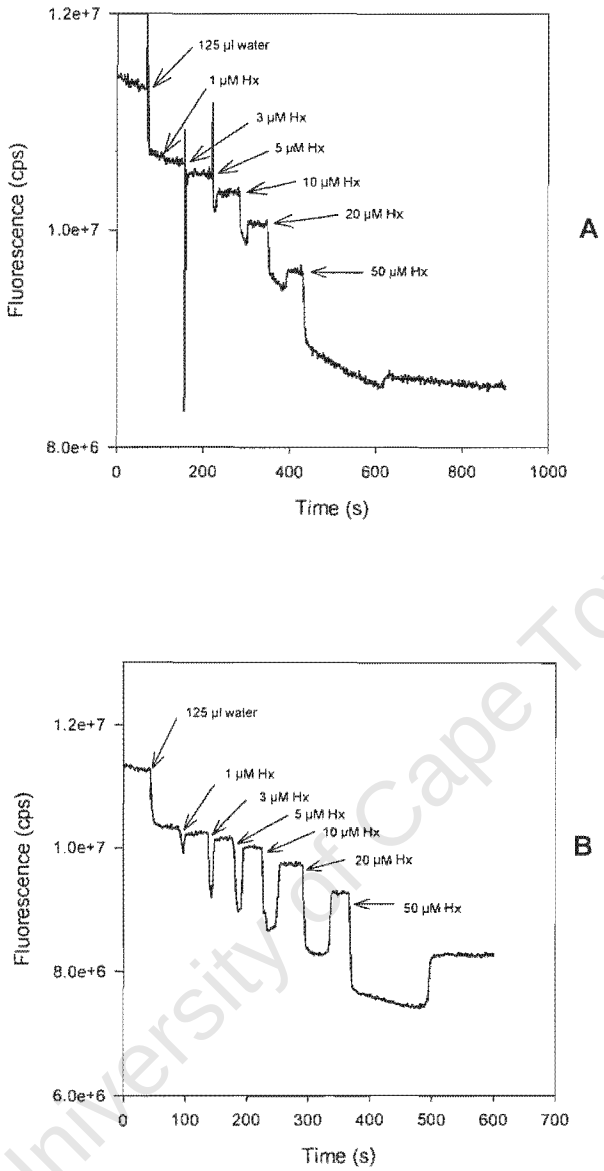

University of Cape Town

Figure 3.63 Intrinsic tryptophan fluorescence changes during turnover of (A) $HPRT_{pfthr}$ and (B) *T. gondii* HPRT. $HPRT_{pfthr}$ (1.4 µM) or *T. gondii* HPRT (0.7 µM) was incubated in the presence of 100 mM Tris/HCl, pH 8.5, 100 mM $MgCl_2$, and 500 µM PRPP at 25 °C. Excitation and emission wavelengths were 290 and 340 nm respectively. Hypoxanthine (Hx) was added as indicated in the figure from a 2 mM stock. The volumes of Hx stock added were 1.3, 3.9, 6.6, 13.2, 26.5 and 66.8 µl for the concentrations shown in the figure. The largest volume of Hx added to the reaction mix was therefore 66.8 µl and the effect of dilution on fluorescence should be taken into account.

The intrinsic fluorescence changes associated with enzyme turnover of $HPRT_{pfthr}$ and *T. gondii* HPRTs is shown in Figure 3.63. A 5% change in fluorescence is shown by the first addition of 125 µl water in 2.5 ml. Subsequently increasing concentrations of Hx are added. In the case of

the $HPRT_{pfthr}$ enzyme, the addition of 3, 5, 10, 20 and 50 μM HX resulted in a drop in fluorescence that partially recovered after longer and longer time intervals. The length of time before reversal is clearly related to the consumption of Hx. Each addition of Hx had a characteristic profile with an initial fairly large drop that seemed in part to be related to the concentration of Hx (i.e., the initial drop is larger with 50 μM Hx than with 5 μM even after dilution is taken into account), and yet the recovery of fluorescence is about the same irrespective of the amount of Hx consumed. During turnover, the level of fluorescence declines more rapidly than occurs in the absence of Hx. We considered that the initial drop in fluorescence may in part represent internal absorbance of light by Hx, but it will be seen below that this is small when the *T. gondii* enzyme is used. We will show later that the drop during turnover is related to inactivation. It is apparent that there is a reversible change in Trp fluorescence of approximately 1.25% on induction and cessation of turnover.

In the case of *T. gondii* HPRT, similar additions of Hx evoke larger fluorescence quenching effects of approximately 5% and almost all of it is reversible on depletion of Hx. The concentration of enzyme is 0.7 μM in the case of *T. gondii* HPRT, and it can be seen that 3 μM Hx produces a quench that is almost maximum. Note also that the regaining of fluorescence after depletion of substrate is rapid. Both these features are indicative of a low K_m for Hx, and this also applies to $HPRT_{pfthr}$.

University of Cape Town

3.10.2.2 The pH dependence of the intrinsic tryptophan fluorescence changes

The pH dependence of the intrinsic tryptophan fluorescence changes of $HPRT_{pfthr}$ induced by the addition of Hx is shown in Figure 3.64.

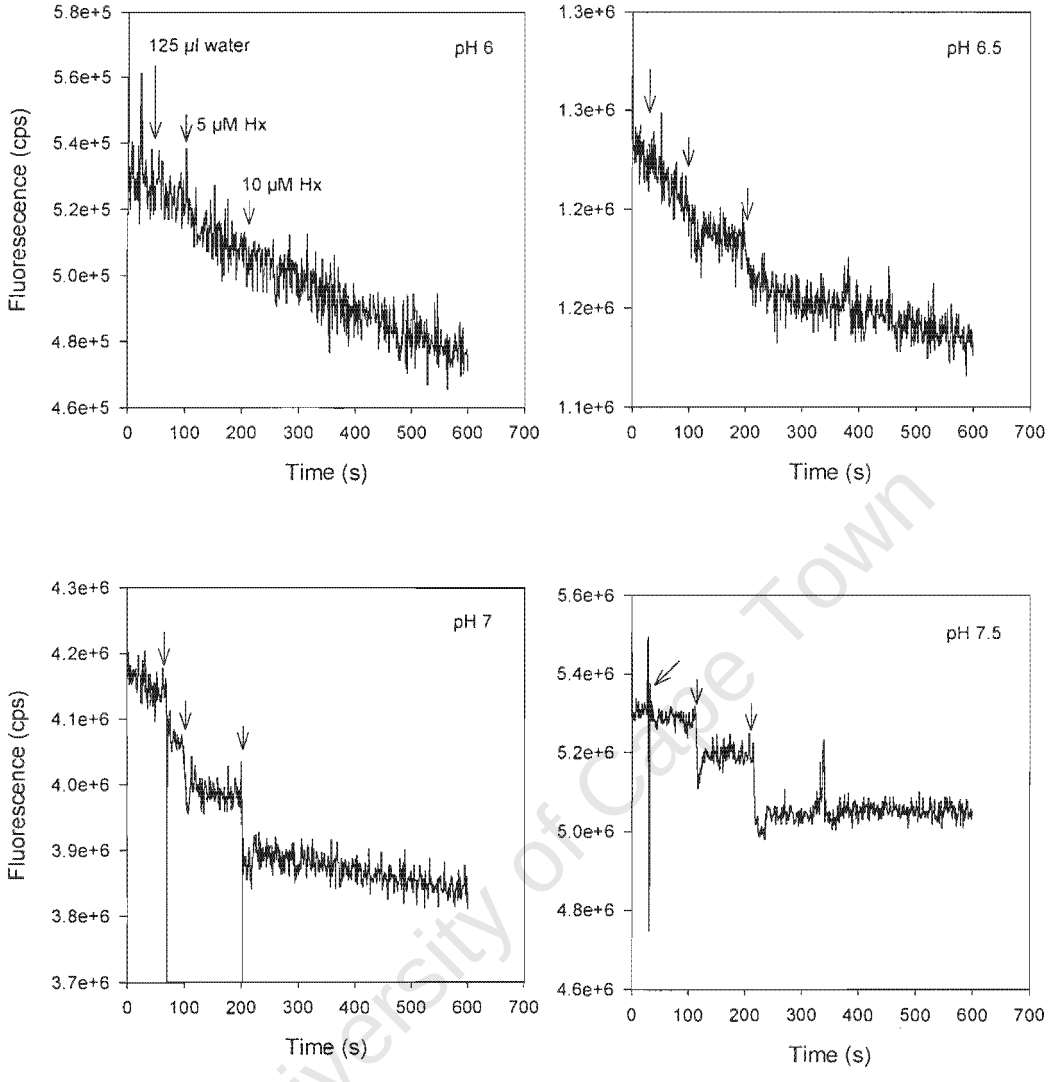

University of Cape Town

Figure 3.64 The pH-dependence tryptophan fluorescence changes on induction of $HPRT_{pfthr}$ turnover. $HPRT_{pfthr}$ (50 µg protein/ml) was incubated in the presence of 50 mM Tris/maleate buffer (pH 6 to 8) or Tris/HCl (pH 8.5 to 9.5), 100 mM $Mgcl_2$, and 500 µM PRPP in a volume of 2.5 ml at 25 °C. The arrows indicate when successive additions of water (125 µl) and hypoxanthine, Hx (5, 10 µM), as shown in the first panel. Excitation and emission wavelengths were 290 and 340 nm respectively.

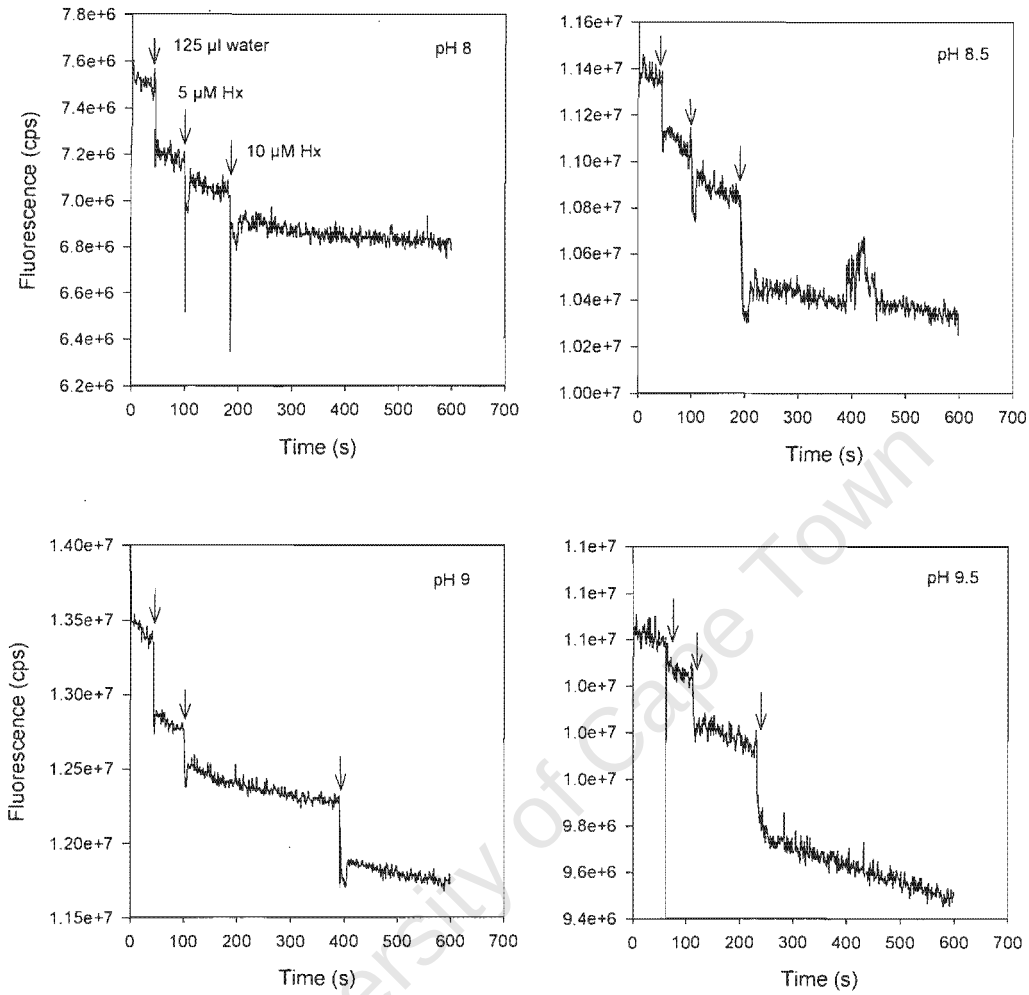

Figure 3.64 continued

University of Cape Town

At acidic pH, the total fluorescence is very low and changes induced by turnover are difficult to detect. At neutral pH and above, the addition of Hx produces clear changes in the fluorescence as seen above. At pH 8 and 8.5, the addition of 5 µM Hx produced a rapid quenching of fluorescence that that was almost completely reversible. The addition of 10 µM Hx, which needs a longer time to consume Hx, resulted in a drop that was only partially reversible, suggesting some inactivation. At pH 9 and 9.5, even addition of 5 µM Hx resulted in quench that was mostly reversible. Evidently the protein is unstable at the more alkaline pH. Thus there

are two effects produced on addition of Hx. One is reversible and is associated with steady state turnover. The other is irreversible, corresponding to inactivation.

The pH dependence of the total intrinsic tryptophan fluorescence of $HPRT_{pfthr}$ is shown in Figure 3.65 at two protein concentrations.

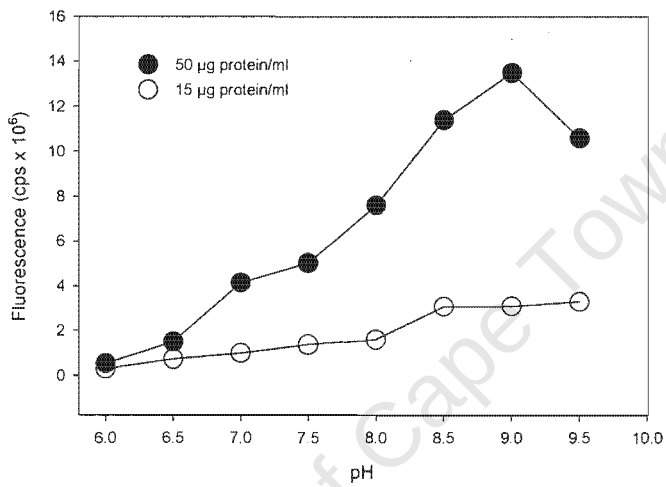

Figure 3.65 The pH-dependence of initial fluorescence levels. $HPRT_{pfthr}$ (50 or 15 µg protein/ml) was incubated in the presence of 50 mM Tris/maleate (pH 6 to 8 range) or Tris/HCl (pH 8.5 to 9.5 range), 100 mM $MgCl_2$, and 500 µM PRPP at 25 °C. Excitation and emission wavelengths were 290 and 340 nm respectively

Protonation of some residue(s) with a pK_a of approximately 7.8 could be causing the quench in fluorescence, but the data could also be due to protonation of multiple groups. There is some indication that at the higher protein concentration there may be two phases.

The above experiments suggested that the protein is highly unstable at pH 9.5, and the destabilisation can be monitored by a drop in fluorescence of 4-10%. To confirm this we tried to induce the fluorescence change purely by dilution of the PRPP and protein. The result is shown in Figure 3.66.

University of Cape Town

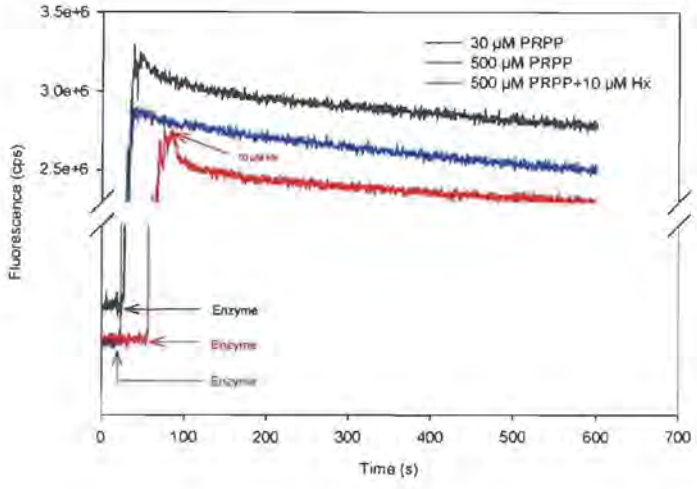

Figure 3.66 The kinetics of inactivation of $HPRT_{pfthr}$ monitored by tryptophan fluorescence. $HPRT_{pfthr}$ (50 µg protein/ml) was added to 50 mM Tris/HCl, pH 9.5 and 100 mM $MgCl_2$ at 25 °C. The amount of PRPP was varied as shown in the figure. Hypoxanthine was added to induce turnover as shown in the figure. Excitation and emission wavelengths were 290 and 340 nm respectively.

In the case of the control enzyme with 0.5 mM PRPP (blue trace) the addition of enzyme produced a rapid rise in fluorescence and then a slow, almost linear decline. If no PRPP was in the medium (black trace, final concentration of PRPP approximately 30 µM), the rise in fluorescence was followed by a rather fast decline within 100 s and then the background linear fall-off. If Hx (10 µM) is added very soon after the protein, a much faster decline is observed, as seen above, followed by the linear phase. It is clear that in the presence of low concentrations of PRPP there is a significant change in fluorescence that is probably associated with inactivation. These results should be compared with those of Figure 3.27, where a similar experiment is performed at pH 8.5, and enzyme activity is measured. In the latter experiment, the $t_{1/2}$ for inactivation is about 12 min with 30 µM PRPP, whereas in the fluorescence experiment it is around 25 s, an indication of the pronounced pH dependence of inactivation.

University of Cape Town

3.10.2.3 Effects of IMP and 4-I-chalcone on activity as monitored by intrinsic tryptophan fluorescence changes

As shown above, the turnover of malarial and *T. gondii* HPRTs can be followed by changes in intrinsic Trp fluorescence. The advantage of the fluorescence measurements, as opposed to absorbance measurements, is that they can be performed in the presence of high concentrations of IMP. We therefore sought to investigate whether activation of malarial HPRT by the flavonoid activator 4-I-chalcone was influenced by the presence of inhibitory levels of IMP. The experiment is shown in Figure 3.67.

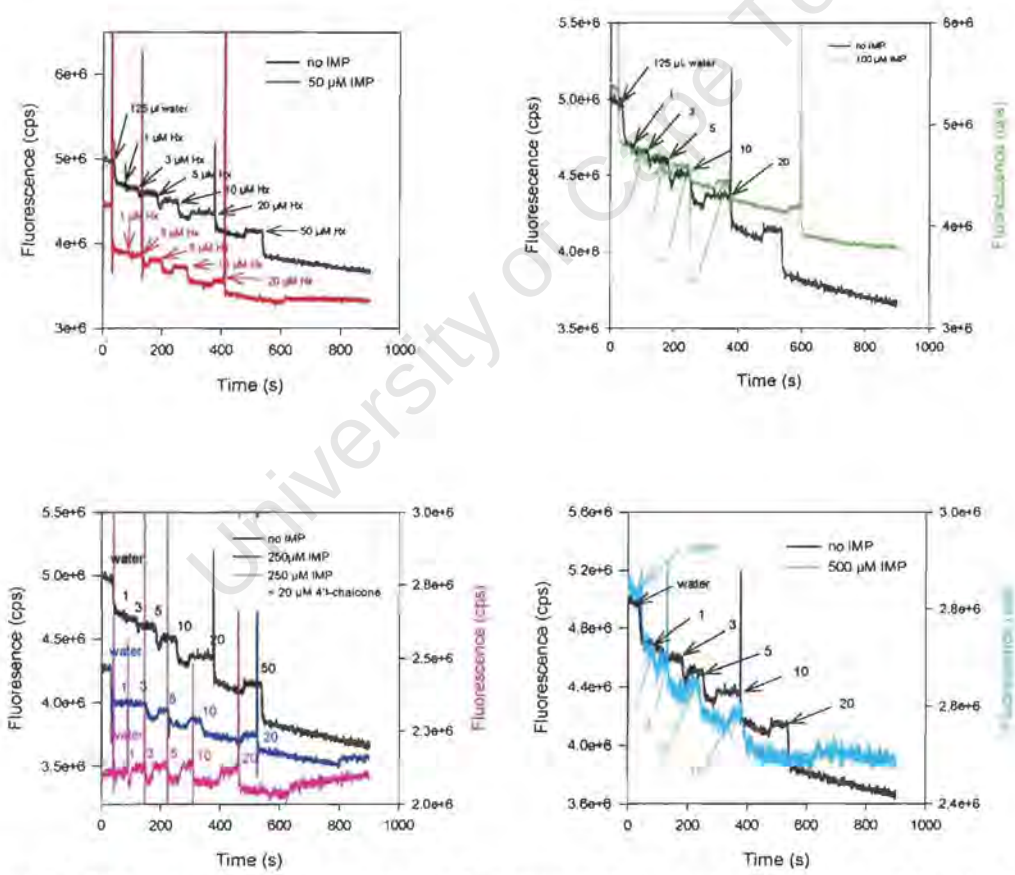

Figure 3.67 Fluorescence changes during turnover, and an assay for reversal of IMP inhibition of $HPRT_{pfthr}$ (20 µg protein/ml) activity by 4-I-chalcone. The arrows indicate when successive additions of water (125 µl) and hypoxanthine (1, 3, 5, 10, 20 and 50 µM). The excitation and emission wavelengths were 290 and 340 nm respectively.

University of Cape Town

The addition of 1, 3, 5, 10, 20 and 50 μM Hx produced the characteristically partially reversible quench of fluorescence. If increasing concentrations of IMP in the 50 to 500 μM range were present, the turnover dependent quench interval became longer for each addition of Hx. If 20 μM of the iodo-chalcone was present in addition to 250 μM IMP, the consumption of Hx was about twice as fast as without the iodo-chalcone. This is approximately the activation by 20 μM iodo-chalcone observed in the absence of IMP in the absorbance assay shown earlier in Figure 3.59. One interpretation could be that the IMP-inhibited enzyme has been fully activated, which would imply that IMP and the iodo-chalcone bind to different sites. Another possibility is that the iodo-chalcone has partially displaced the IMP, released the product inhibition and activated turnover. It is difficult to distinguish between these possibilities. The normal method to determine if the effects remain in the presence of high concentrations of the ligands (characteristic of competitive inhibition) is not possible by spectroscopic methods. As a control experiment, the same assays were carried out with the *T. gondii* HPRT (Figure 3.68). The iodo-chalcone had no effect on the inhibition produced by 250 μM IMP.

University of Cape Town

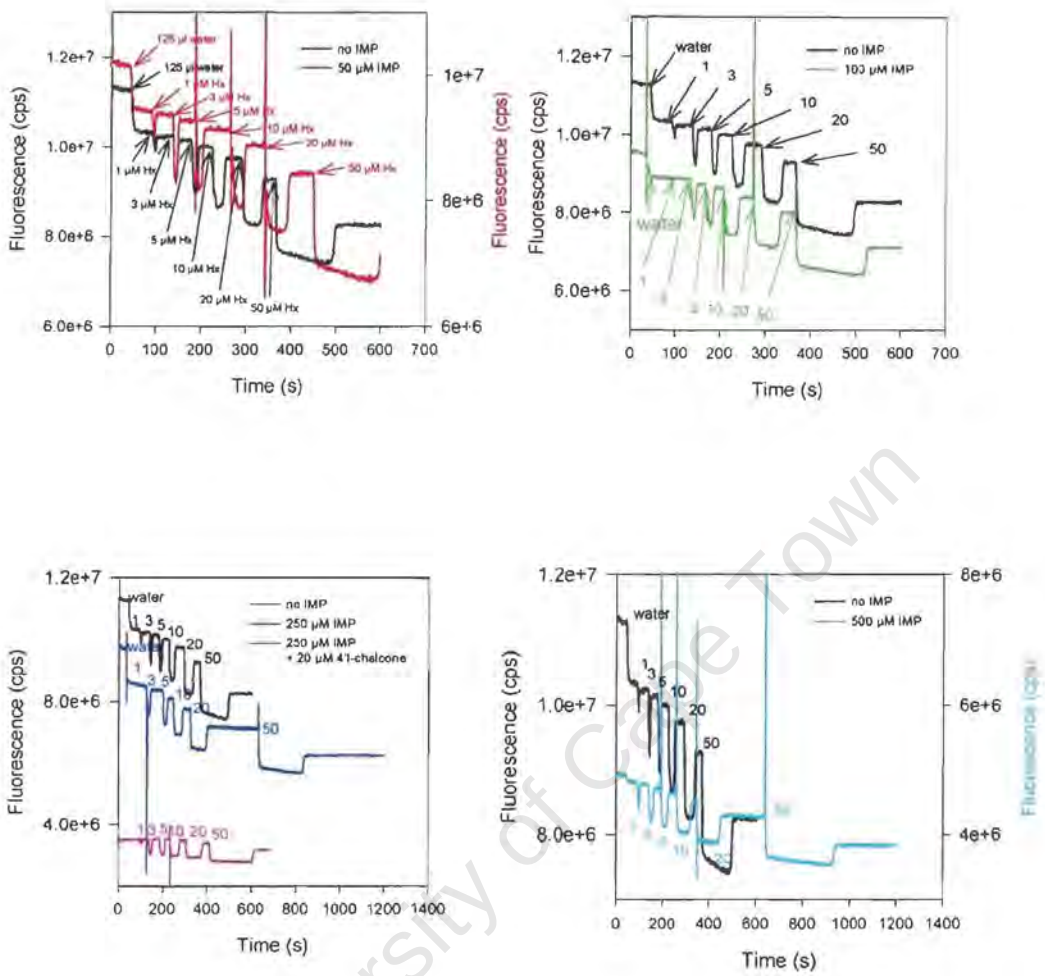

Figure 3.68 Fluorescence changes during turnover, and an assay for reversal of IMP inhibition of *T. gondii* (20 µg protein/ml) activity by 4-I-chalcone. The arrows indicate when successive additions of water (125 µl) and hypoxanthine (1, 3, 5, 10, 20 and 50 µM), as shown in the first panel. The excitation and emission wavelengths were 290 and 340 nm respectively.

University of Cape Town

CHAPTER 4 DISCUSSION

In this study, human, two forms of malarial and *T. gondii* HPRTs were expressed in *E. coli* and purified by nickel-chelate chromatography. The human and *T. gondii* enzymes were stable and active. In the case of the malarial enzymes, one, with a methionine at position 101 of the protein, was inactive. Another, where the methionine was substituted for threonine, was partially active. The latter could be substantially activated by prolonged incubation with PRPP. However, it was unstable and inactivated during turnover or removal of PRPP.

Photolabile 8-azido xanthine was synthesised from xanthosine mainly with a view to generating a diversity of xanthine analogues. However, light activation resulted in a single product where the ring appeared to be opened. Reaction of the furanose ring of GMP, IMP, XMP and 8-azido-xanthosine with TNBS produced the 2',3'-*O*-(2,4,6-trinitrophenyl) derivatives. All were screened for possible inhibition of malarial HPRT, and TNP-GMP was effective in the micromolar range. Irradiation of TNP-8-azido xanthosine in water produced a number of different TNP compounds, suggesting that it may be a path to a diversity of analogues. Thirty-eight flavonoids from several different classes were screened as well. None inhibited malarial HPRT, but one, 4-I-chalacone activated the enzyme in the micromolar range. Both TNP-GMP and the iodo-chalcone had no effect on the human enzyme. Irradiation of TNP-8-azido xanthosine in the presence of the flavonoids kaempferide and the iodo-chalcone produced conjugates which may be duplex structures with the two rings stacked. Mixtures of the conjugates did not affect malarial HPRT activity. Crude modelling suggests that the TNP moiety may be accommodated in the PPi binding site. The iodo-chalcone may assume a similar position, and stimulate the dissociation of the nucleotide.

University of Cape Town

4.1 Sequencing and expression

All four HPRTs were sequenced in the forward and reverse direction using automated sequencing. The malarial and *T. gondii* clones were sequenced as inserts in the pET-15b expression vector. The human clone was sequenced as an insert in pGEM®-T. The sequencing was performed several times to remove uncertainties.

All sequences and chromatograms from which they were derived were individually analysed and edited using the Chromas Version 1.43 software package (incorporating the Alfwin Express sequencing software package). The consensus sequences were exported in Fasta format and aligned with the published sequences using the Clustal X Version 1.81 software package (Appendices 1A-D).

Appendix 1A shows the published human HPRT sequence (Jolly *et al.*, 1983) aligned with the consensus sequence determined in his study. Part of the pGEM®-T (upstream of the CATATG *Nde*1 region) sequence is shown in the determined Human HPRT sequence, and may be compared to the vector sequence shown in Appendix 1E. The sequence of the coding region is identical to that published.

The *P. falciparum* HPRT sequence published by King and Melton (1987) is shown aligned to $HPRT_{pfmet}$ in Appendix 1B. The 6 x His tag and the thrombin cleavage site from pET-15b are shown. The codon for Met 101 is underlined. The coding regions are identical.

The *P. falciparum* HPRT sequence published by Vasanthakumar *et al.* (1989) is shown in Appendix 1C aligned with the consensus sequence determined in this study for $HPRT_{pfthr}$. The

University of Cape Town

6 x His tag and thrombin cleavage site can be seen. The Thr 101 codon is underlined, and the coding regions are identical.

The *T. gondii* HPRT published by Vasanthakumar *et al.* (1994) is aligned with that determined in this study (Tox), and is shown in Appendix 1D. As for the $HPRT_{pfmet}$ and $HPRT_{pfthr}$ sequences, the 6 x His tag and thrombin cleavage sites from pET-15b are shown., and the coding regions are identical.

A difference in the sequences obtained is in the position of the *BamH*1 restriction site after the stop codon. In $HPRT_{pfmet}$ and $HPRT_{Tgondii}$, the engineered *BamH*1 site occurs immediately after the stop codon. In the case of $HPRT_{pfthr}$ it is one amino acid (His, ATA) after the stop codon, while in Human HPRT, it is 23 bases after the stop codon. In the case of the human gene, the positioning of the *BamH*1 site was chosen so that the sequence of the designed primer incorporating this restriction site would not be very different from the template. Experience with subsequent primer designs ($HPRT_{pfmet}$) showed that the positioning of this restriction site downstream of the stop codon did not influence expression of the target gene.

Human, malarial and *T. gondii* HPRTs were expressed in *E. coli* with the pET expression system. This system has several advantages (i) the BL21 strain of *E. coli* BL21(DE3)pLysS lacks the *lon* protease and the *ompT* membrane proteases that could degrade the target protein, (ii) the strain carries a plasmid with the *lac* repressor to repress transcription of T7 polymerase by the host, which prevents low level expression of the target protein in the absence of the inducer, IPTG, (iii) the presence of small amounts of plasmid-encoded T7 lysozyme inhibits transcription by binding to T7 RNA polymerase that could be produced before

University of Cape Town

induction with IPTG, and could lead to early expression of the target protein, (iv) T7 lysozyme also assists with the lysis of cells during freeze-thaw treatment or Triton X-100 treatment.

Plasmid stability was tested before making glycerol stocks of the expression plasmid containing cDNA HPRT clone in *E. coli* BL21(DE3)pLysS. Very small colonies were observed after 16 h incubation at 37 °C on Luria agar plates supplemented with 1 mM IPTG and 100 µg/ml ampicillin, or with IPTG alone, and suggested strong induction by IPTG in cells containing both the inducible gene for T7 RNA polymerase and functional target plasmid (containing pLysS). Glycerol stocks of the expression cell lines were made, taking care to select cells that contained the plasmid by not overgrowing the cultures.

Initially we were concerned that the expression of protozoan genes in *E. coli* would present with problems. The first of these relates to differences in codon usage between the malarial parasite and the *E. coli* bacterium. The *P. falciparum* genome has an A + T content of about 82% (Pollack *et al.*, 1982; McCutchan *et al.*, 1984) whereas that for *E. coli* is about 47% (Maruyama *et al.*, 1986). The *P. falciparum* parasite shows a preference for T or A in the third position of codons (Weber, 1987). The depletion of *E. coli* tRNA pools due to the overexpression of genes with codons infrequently used by *E. coli* may result in limited or delayed in RNA expression and translation, ribosome stalling and unfavourable secondary structure of the target transcript.

Nevertheless, the expression of human, malarial ($HPRT_{pfmet}$ and $HPRT_{pfthr}$) and *T. gondii* HPRT was successful, with prominent protein bands on SDS-PAGE gels evident in the crude extract after 3 h of induction with 1 mM IPTG at 37 °C. The yields of overexpressed protein were in the region of 13% total cell protein as determined by absorbance scanning of the gels. Approximately 0.5 mg of pure HPRT was obtained from 100 ml culture.

University of Cape Town

4.2 Purification

The majority of the expressed HPRT was found in the supernatant fraction and was therefore soluble. Purification was readily achieved with the nickel-chelate columns and elution with imidazole. However, freezing the proteins in 1 M imidazole for extended periods resulted in distinct aggregates being present upon thawing. In the case of $HPRT_{pfmet}$, removal of imidazole after elution from the nickel-chelate column by gel filtration or dialysis still produced aggregates. Other strategies to remove imidazole included elution from the nickel-chelate column with EDTA or histidine. However the most satisfactory result was obtained by eluting with a lower (250 mM) imidazole concentration as the metal ion chelating properties of EDTA and contaminating histidine were not desired in the final pure protein solution. The success of the purification by nickel-chelate chromatography suggests that the 6x His tag was sufficiently free to bind to the immobilised nickel.

4.3 Activity

Purified human HPRT was active, and the activity obtained in this study is comparable with literature values (Keough *et al.*, 1999). Purified *T. gondii* HPRT had an activity of 4 to 8-fold less than published values (Héroux *et al.*, 1999a), depending on the substrate used. The reason for this difference was not identified. Changing the isolation procedure to one closely resembling that published by Héroux and colleagues did not yield *T. gondii* HPRT of higher activity. The low activity *of T. gondii* HPRT may be due to the presence of the 6 x His tail, which was not cleaved off as was done by Héroux *et al.* (1999a). Another possible explanation is that a final Superdex 200 column was not used in the purification step. $HPRT_{pfmet}$ was inactive, and changes to the expression and purification protocols did not alter this situation. Expression at lower temperatures, rapid removal of imidazole from the nickel-chelate eluant, cleavage of the His tag and isolation in the presence of PRPP did not yield active $HPRT_{pfmet}$.

University of Cape Town

The cytoplasm of *E. coli* is normally reducing, and prevents disulfide bond formation in proteins (Derman *et al.*, 1993). Seven cysteine residues occur in $HPRT_{pfmet}$, and could potentially form disulfide bonds if they came into proximity to one another in an oxidising environment such as may be present upon lysis of the *E. coli* cells. DTT has been reported to increase the activity of malarial HPRT during assay (Queen *et al.*, 1988) and provide stabilisation (Keough *et al.*, 1999). However the addition of reducing agents to the assay medium did not activate $HPRT_{pfmet}$. The rapid cross-linking of $HPRT_{pfmet}$ to high molecular weight oligomers in the presence of glutaraldehyde suggested that it was in a denatured, semi-aggregated state.

The sequence of the malarial HPRT published by Vasanthakumar and colleagues (1989; 1990), and those of the clone used by Keough and colleagues (1998, 1999) were compared to that originally published by King and Melton (1987), from whom we obtained the cDNA for $HPRT_{pfmet}$. The coding region of the original sequence differed from the latter sequences in position 101 in the protein, where the original sequence coded for methionine (ATG), and the latter sequences coded for threonine (ACG). These differences are possibly due to differences in the strains from which DNA was isolated for the construction of genomic libraries (King and Melton, 1987). $HPRT_{pfthr}$ was partially active when it was purified in the presence of PRPP, and could be activated to approximately 4-fold by incubation with PRPP over several days. The activated activity is close to that reported for the enzyme isolated by other laboratories (Keough *et al.*, 1999). It seemed therefore that the Met to Thr change has a dramatic effect on HPRT folding in *E. coli*. What is strange is that the segment around position 101 is one of the least conserved in the protein, and constitutes a loop between and α3 and β4 (Figure 4.1).

University of Cape Town

Human	87	NSDRS- --IPM	94
T.gondii	98	YSGRES SVPPF	107
P.falciparum	96	YSAVET SKPLF	106
T.cruzi		------ --VPV	72
T.foetus		------ --FQL	64

Figure 4.1 Primary structure of the loop between α3 and β4 (nomenclature for malarial HPRT according to Shi *et al.*, 1999a) in human and protozoal HPRTs. The conservatively substituted residue Thr is shaded.

The length of this loop is identical to that of *T. gondii*, but the amino acid is changed conservatively from Thr to Ser. Compared with the human and Tritrichomonas enzymes, this loop is longer in the malarial HPRT. The siting of the loop in the 3-D atomic structure is shown in Figure 4.2.

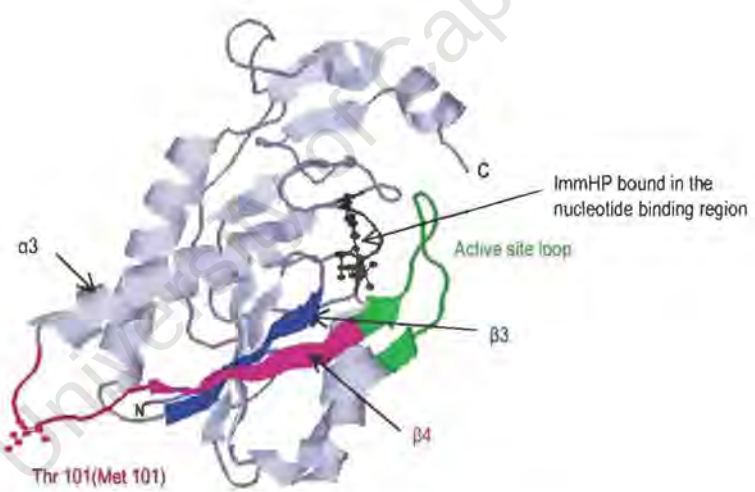

Figure 4.2 Malarial HPRT showing the position of Thr 101 (Met 101) in relation to the catalytic or active site loop. Bound immucillinHP is shown in the nucleotide-binding region (Shi *et al.*, 1999a)

It is on the edge of the core β-sheet on the opposite side of the active site. The loop could be at a rather critical position in terms of monomer folding as it leads with β4 into the beginning of the core β-sheet alongside β3. β4 is followed by the highly conserved catalytic loop, and then the largest of the most conserved segments of the protein, namely His-140 to Thr-150. Failure of

University of Cape Town

β4 to adjoin with β3 could disturb nascent core β-sheet formation. In the atomic structure the side chain of the Thr is pointing away from the protein into the medium. However, during folding, replacement of Thr with Met may set the sampling of folding pathways in the wrong direction. Site-directed mutagenesis to change the threonine in active malarial HPRT (published in the literature (Keough *et al.*, 1999)) to methionine and other residues could be conducted to verify this, and would be a possible area of exploration in the design of inhibitors that would target an area outside the active site, and possibly function by inhibiting protein folding.

Alternatively this loop might play an important role in the interaction with malarial chaperones, which may be different in *E. coli*, or absent. If this were the case, the malarial equivalent of human HPRT chaperones could be co-expressed with malarial HPRT, and could perhaps assist in folding.

The loop, and main chain Thr 101 in particular, seems to be involved in the interaction of one set of dimers. The loop is positioned alongside the α1 helix hat incorporates His-35. There may be significant interactions between these structures in the tetramer form. It is known that oligomeric interactions are required for activity of HPRTs (Héroux *et al.*, 1999a; Keough *et al.*, 1999) and the disruption of these interactions may result in inactive enzyme.

As mentioned above purified $HPRT_{pfthr}$ was fairly active. Interestingly, the crude homogenate seemed much more active if the proportion of contaminating proteins was taken into account. We estimated that the difference may be as high as 10-fold. This suggested that the pure enzyme had lost activity during the isolation procedure. Several steps in the isolation procedure were changed to try and prevent inactivation by adopting similar procedures used for the *T.*

University of Cape Town

gondii HPRT by Héroux *et al* and colleagues (1999a). These included (i) addition of sodium phosphate to the growth medium and replacing the Tris/HCl in the nickel-chelate buffer with sodium phosphate, in part to reduce phosphatase activity (ii) washing bacteria with phosphate buffered saline (iii) resuspension of cells in 10% glycerol and protease inhibitors (iv) lysis of cells by freeze thaw and sonication with lysozyme and DNase 1 without lengthy incubations (v) scavenging of Ni^{2+} ions in the nickel-chelate column eluant with 1,10-phenanthroline. In addition, the elution from the nickel-chelate column was optimised to use a lower concentration of imidazole. These changes did not yield more active $HPRT_{pfthr}$ or *T. gondii* HPRT.

Early studies reported on the stabilisation of malarial HPRT by PRPP (Queen *et al.*, 1988). Keough and colleagues (1999) found that recombinant malarial HPRT could be stabilised and activated by including PRPP, Hx (hypoxanthine) and DTT in the medium. Both PRPP and Hx were found to be important. Enzyme turnover was inhibited by excluding $MgCl_2$. High KCl concentrations inactivated the enzyme, and changed the quaternary structure from tetramer to dimer or trimer. In contrast, the human enzyme is stabilised in the active tetrameric form by a high KCl concentration (Strauss *et al.*, 1978; Holden and Kelley, 1978).

We found that the partially active $HPRT_{pfthr}$ could be maximally activated by prolonged incubation with $MgCl_2$, PRPP, DTT and 50% glycerol. DTT alone gave some activation, but not as much as in combination with PRPP. Reducing the glycerol concentration to 10% led to a similar result as with DTT alone. However, in one experiment, maximal activation was achieved in the absence of glycerol. The effects of glycerol are not clear, but it was included in the isolation and reactivation as a precaution to stabilise the enzyme and to prevent aggregation upon thawing. Glycerol is well known stabiliser, and may function by displacing "lubricating" water at the protein surface and increasing protein rigidity through minimising the protein

University of Cape Town

surface (Reisler and Eisenberg, 1969; Zaks and Klibanov, 1988a; 1988b; Cioni and Strambini, 1994) or by releasing water form the protein interior (Priev *et al.*, 1996). These events, or similar ones could bring about stabilisation and reactivation of $HPRT_{pfthr}$.

It was not possible to test the effects of Hx and PRPP as our isolation procedures, based on the work by Héroux and colleagues included $MgCl_2$, and, as will be elaborated on below, the induction of turnover inactivated the malarial enzyme. It appears from our work and that of Keough and colleagues that maximal reactivation can be accomplished by incubation with MgPRPP, DTT and glycerol, or with Hx, PRPP and DTT.

4.4 Inactivation during turnover

The most notable feature of the kinetics of the recombinant $HPRT_{pfthr}$, besides the fact that it was active, was the exponential fall-off in activity with time during assay, resulting in an inactive enzyme after 3 to 5 min ($t_{1/2} \approx 50$ s) at pH 8.5. This was in spite of adequate levels of substrates and Mg^{2+}. Cleavage of the histidine tag from $HPRT_{pfthr}$ was accomplished using thrombin, and the cleaved enzyme was assayed for activity. Some stability was afforded by the cleavage, but inactivation was still evident. The initial rate of activity of the cleaved enzyme was the same as that of the uncleaved enzyme. The limited inactivation observed during turnover of cleaved enzyme could be due to the presence of three amino acid residues at the N-terminal end (Gly, Ser, and His) that remain after cleavage (Figure 4.2). It may be possible that their presence interferes with loop folding events, or, more likely, dimer interactions. The untagged malarial HPRT of Keough *et al.* (1999) was much more stable.

Inactivation began immediately after turnover was induced, which suggests that this was not a case of product inhibition. The reaction scheme of HPRTs is as follows:

University of Cape Town

$$E \leftrightarrow E{\cdot}PRPP \leftrightarrow E{\cdot}PRPP{\cdot}Hx \leftrightarrow E{\cdot}PPi{\cdot}IMP \leftrightarrow E{\cdot}IMP \leftrightarrow E$$

The malarial malarial enzyme was stabilised and activated by MgPRPP, and clearly the E·PRPP intermediate is stable. This likely also applies to E·PRPP·Hx. Keough and colleagues established that PRPP and Hx stabilised malarial HPRT in the absence of Mg^{2+} (Keough *et al.*, 1999). In this study, lowering the concentration of PRPP by dilution, or reducing it to virtually zero by coupling dilution with Hx addition led to inactivation, indicating that unligated enzyme (E) in the presence of Mg^{2+} is unstable. The half time ($t_{1/2}$) for inactivation of this species at room temperature is approximately 12 s at pH 8.5. It was difficult to determine whether E·PPi·IMP, E·IMP and possibly E·PPi were unstable by direct spectrophotometric assay because of the high concentrations of IMP required. It was also difficult to determine the effect of protein concentration as the enzyme had to be quite dilute to achieve a reasonable rate over, say, 1 min. Secondly, the concentration of PRPP was difficult to control accurately since the stock protein was in PRPP.

Simulations of the kinetics of the reaction cycle provide some insights into the inactivation process. Xu *et al.* (1997) have published the kinetic parameters of the human enzyme at pH 7.4 and 23 °C with 12 mM $MgCl_2$, and they are shown in Figure 4.3.

University of Cape Town

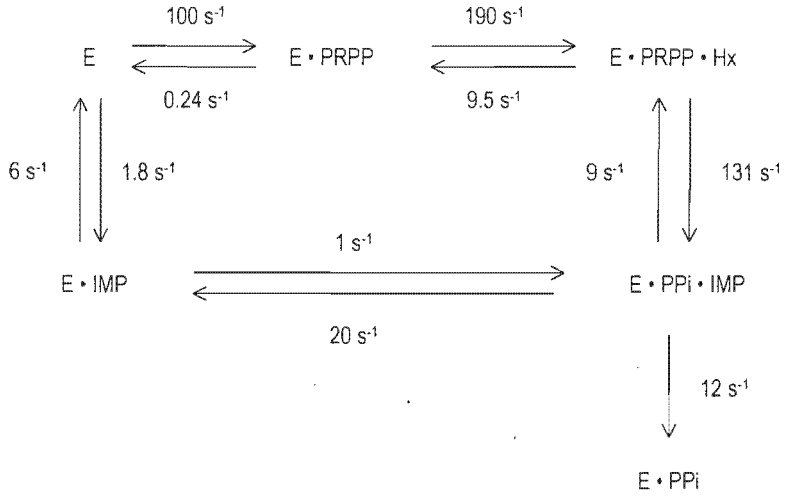

Figure 4.3 The catalytic cycle of human HPRT (Xu *et al.*, 1997). Rate constants were calculated with the concentration of PRPP and Hx at 0.5 mM and 10 μM respectively. E·PPi·IMP to E·IMP conversion and the reverse are taken to be 20 and 1 s^{-1} respectively as rates are given as >12 s^{-1} and >0.9 x 10^6 M^{-1} s^{-1} respectively in the cited reference.

Features of the cycle are rapid binding of PRPP followed by Hx, a rapid chemical interconversion step followed by the ordered release of first PPi and then IMP. In a less favoured route, IMP may leave first. The slowest step in the cycle in the forward direction is the release of IMP from E·IMP.

Simulation of this cycle over 0.2 s starting with 1 unit of enzyme, 0.5 mM PRPP and 10 μM Hx is shown in Figure 4.4.

University of Cape Town

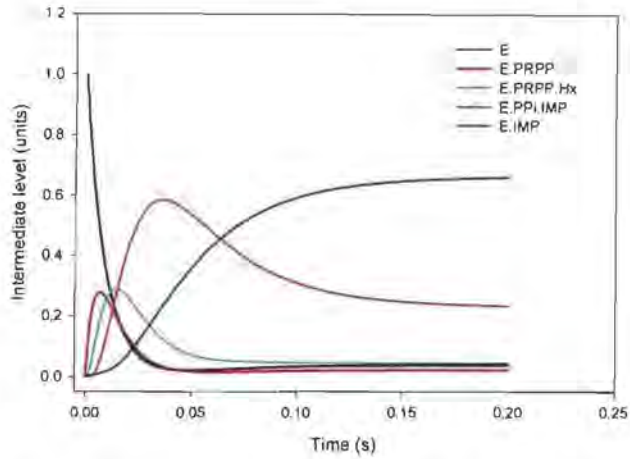

Figure 4.4 A simulation of the human HPRT enzyme catalytic cycle showing the levels of intermediates. The rates used were taken from Xu *et al.* (1997), assuming PRPP, and Hx amounts of 0.5 mM and 20 µM respectively. Simulations were performed using SimZyme! v 2.0 (Sorensen *et al.*, 2000)

In the pre-steady state, the concentration of E declines and that of the other intermediates transitorily increase until all reach their steady state levels. The rate of turnover of the enzyme, k_{cat}, is provided most easily by $k_{forward}$ [E·IMP] or $k_{forward}$ [E·PPi IMP] since the backward reactions are negligible before the development of high concentrations of either product. The simulations show that E·IMP is the most abundant intermediate during cycling and levels at 0.68 units, where E_{total} = 1 unit. Therefore $K_{cat} = 6\ s^{-1} \times 0.68 = 4\ s^{-1}$.

The possibility of one of the intermediates being unstable, for example E, can be introduced into the cycle with the scheme shown in Figure 4.5.

University of Cape Town

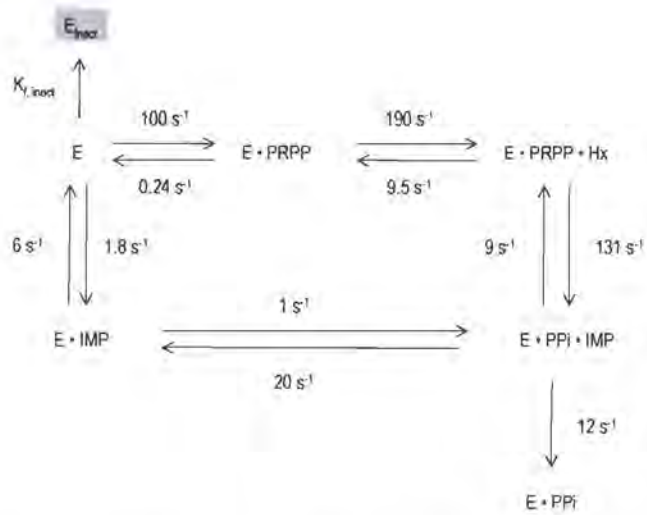

Figure 4.5 A schematic diagram to show the possibility of the conversion of the unstable intermediate E to an inactive species E_{inact} (shaded).

The simulation of this process over 500 s with a $k_{f,inact}$ (forward rate constant for inactivation) of 0.32 s^{-1} and a nominal very low $k_{r,inact}$ (reverse rate constant of inactivation) of $4x10^{-4}$ s^{-1} to produce a virtually irreversible conversion is shown in Figure 4.6.

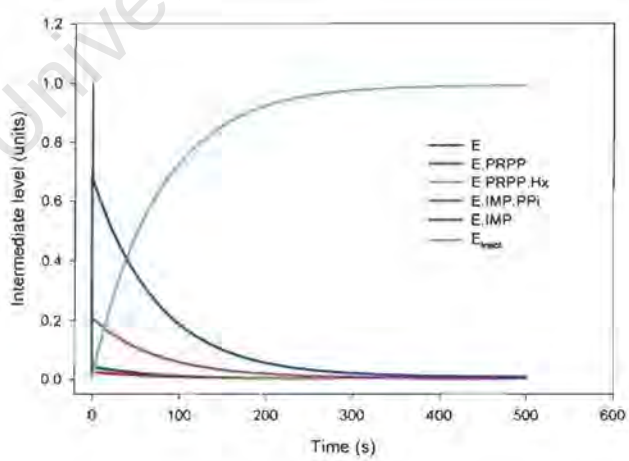

Figure 4.6 A simulation of the catalysis where E is unstable and converts to the inactive species E_{inact}. Simulations were performed using SimZyme! v 2.0 (Sorensen *et al.*, 2000).

University of Cape Town

The concentration of all cycle intermediates declines with time, and after 500 s, all the prolein is inactivated. In this example, the $t_{1/2}$ for inactivation is approximately 50 s, which is approximately what we observe for the malarial enzyme under our conditions. However, the rate for $k_{f,inact}$ of 0.32 s^{-1} is approximately 5-fold faster than experimentally observed for the malarial enzyme ($t_{1/2}$ = 12 s, $k_{f,inact}$ = 0.06 s^{-1}).

It is possible to assign other intermediates as unstable. For example, if E·IMP is as unstable as E (shown in Figure 4.7), then using the same kinetic parameters, the $t_{1/2}$ for inactivation during the assay is now 3 s instead of 50 s, because E·IMP is the most abundant intermediate during turnover.

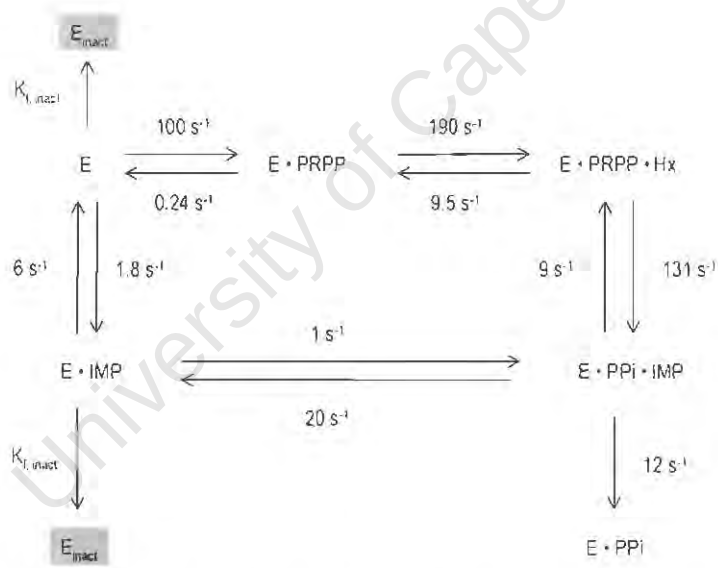

Figure 4.7 A schematic diagram to show the possibility of the conversion of the unstable intermediates E and E·IMP to an inactive species E_{inact} (shaded).

Changing $k_{f,inact}$ to 0.06 s^{-1} i.e., 5-fold slower, causes the $t_{1/2}$ for inactivation to be approximately 16 s, which is faster than the 50 s observed for the malarial enzyme. Thus it can be seen how

University of Cape Town

experimental data provides constraints for inactivation, and insights into which species are unstable.

Malarial HPRT has an activity with Hx of approximately 1.4 μmoles IMP min^{-1} mg^{-1} of protein, which yields k_{cat} of 0.6 s^{-1}, i.e. about 7-fold slower than the human enzyme measured under the somewhat different conditions of Xu and colleagues. The main difference is probably the temperature which was about 6 °C lower for the malarial enzyme, so the 7-fold slower rate may be changed to, say, 5-fold, which brings the k_{cat} to around 0.8 s^{-1}. The reason why the malarial enzyme is slower than the human and *T. gondii* enzymes is not known, but it has been speculated that it may be related to the fact that a rather critical Arg-196 or Arg-182 residue in the human or *T. gondii* enzymes respectively is a Leu-180 residue in malarial HPRT (Héroux *et al.*, 1999b). It appears that the Arg is sandwiched between two conserved carboxylates in the ternary enzyme structure, locking the hood domain onto the core domain. If this is true, then the difference in turnover rate between the malarial and other enzymes may be a slowing of the chemical step (phosphoribosyl transfer): E·PRPP·Hx to E·PPi·IMP.

If the simulation is repeated with the chemical step slowed 100-fold in both directions, then the k_{cat} becomes 0.96 s^{-1}, which is close to the 0.8 s^{-1} actually observed. It is possible to get to the latter figure by increasing the rates constant for the reverse chemical transfer step to close to the original value of 9 s^{-1} (therefore altering the equilibrium constant of the chemical step). In the circumstance where both the forward and reverse constants for the chemical step are slowed 100-fold, it is possible to get a $t_{1/2}$ of 50 s during turnover, and $k_{t,inact}$ of close to 0.06 s^{-1} if both E and E·IMP are made unstable. If only E is the unstable species then the latter needs to be at least 10-fold faster, which is incompatible with the experimental data.

University of Cape Town

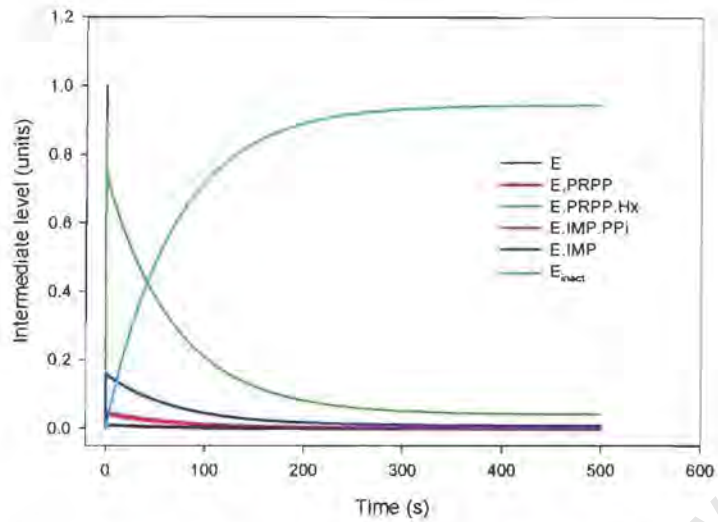

Figure 4.8 A simulation of both E and E·IMP as unstable species converted to the inactive species E_{inact}. Simulations were performed using SimZyme! v 2.0 (Sorensen *et al.*, 2000)

If E·PPi·IMP is also made unstable, the outcome of the simulation is not changed significantly as its concentration is very low.

If the chemical interconversion is unaltered in the malarial enzyme, then in order to slow turnover, the dissociation of IMP and/or PPi has to be slowed approximately 6-fold, and the intermediates E·IMP and E·PPi·IMP predominate in the cycle. If these same intermediates are as unstable as E, then $k_{f,inact}$ has to be slowed about 4 to 5-fold to get a $t_{1/2}$ for inactivation during the assay of 50 s^{-1}. This in turn raises the $k_{f,inact}$ too high to fit with the results obtained in this study. Therefore, interestingly, the chemical interconversion step has to be slowed in the malarial enzyme. As will be seen below, the characteristics of TNP-GMP inhibition and 4-I-chalcone activation of malarial HPRT are probably best explained by the nucleotide release being the slowest step in the cycle. We consider that the most likely scenario for the malarial enzyme is that both the chemical step and nucleotide release may both be slowed somewhat compared with the kinetics of the human enzyme.

University of Cape Town

4.5 Fluorescence studies

We endeavoured to further probe the inactive state by using ANS fluorescence, glutaraldehyde cross-linking and intrinsic tryptophan fluorescence. Both the native (bound with MgPRPP) and inactive malarial HPRT did not bind ANS, suggesting that there were no exposed hydrophobic pockets, and that inactivation is not the result of gross unfolding of the protein. A similar conclusion was made from the glutaraldehyde cross-linking experiments. These indicated that the inactive protein cross-linked to dimers as fast as the native PRPP-stabilised enzyme. There was a slight indication that less tetramer was formed with the inactive protein, and this could indicate instability at the dimer interface. It would be interesting to explore this with another technique like gel filtration, and sedimentation equilibrium studies.

As far as we are aware, we are the first to use natural intrinsic tryptophan changes of HPRTs to monitor catalytic activity. It is not surprising that such changes are produced in the *T. gondii* HPRT as the intrinsic tryptophan is positioned in the hood domain, and sandwiches the purine in place. In the malarial enzyme, the tryptophan residue is in a loop that locks the hood domain onto the core domain during catalysis via a disorder to order transition (Héroux *et al.*, 1999b). Evidently, the tryptophan residue responds to this change by a slight fluorescence quench, possibly by coming into a slightly more polar environment. Interestingly, there was a larger quench in the fluorescence on inactivation of $HPRT_{pfthr}$, suggesting that this loop may be displaced. The tryptophan seems to play an important role as it overlays Ile-147 of the P-loop, which in turn is vital for binding of the 5'-phosphate moiety of nucleotides. Thus any displacement of the tryptophan could affect the positioning of the absolutely conserved Asp residues of the P-loop, and could account in part for inactivation.

University of Cape Town

While addition of hypoxanthine to the PRPP-bound enzymes, $HPRT_{pfthr}$ and $HPRT_{Tgondii}$, produced a fluorescence quench, IMP had no effect. Evidently, binding of the nucleotide failed to elicit the same changes in domain and loop closure in the reverse direction of catalysis as that in the forward direction with substrates. This is readily explained if either PPi was released prior to IMP (which means that IMP binding occurs without bound PPi, and could not form a closed active site) or, if significant E·PPi is present during steady state catalysis, the reverse reaction to a closed active site is highly unfavourable. As will be discussed later, it is likely that IMP release may be rate limiting and the first possibility probably prevails.

The most significant stabilisation is brought about by PRPP. According to the *T. gondii* atomic structure, this substrate provokes large changes in the positioning of the core loop (with the peptide bond) and hood loop (residues 200–214). An extensive array of salt bridges and hydrogen bonds forms when these loops fold over the pyrophosphate moiety to close the active site at one end. Fixing of the hood domain onto the core follows binding of the purine, thereby locking the purine in place. In the absence of PRPP, the interactions between the hood and core domains are weaker, and would exacerbate a tendency to instability. The increase in freedom of movement of the hood domain would impinge on the stability of the β-strand at the interface which leads into the loop containing the tryptophan residue.

An interesting observation made with respect to the malarial HPRT, and not the others is the formation of a cross-linked species that migrates faster on SDS-PAGE. We suggest that this is an intramolecular cross-link that alters the hydrodynamic properties of the protein. Such phenomena have been described for an intramolecular glutaraldehyde cross-link formed between Lys-492 and Arg-678 of the Ca^{2+} ATPase of sarcoplasmic reticulum, and retard the mobility of the protein on SDS-PAGE (McIntosh *et al.*, 1992).

University of Cape Town

In general, changes in hydrodynamics brought about by cross-linking could be larger if the cross-linking occurred between segments widely separated in the linear sequence. We found that the putative intramolecular cross-link of $HPRT_{pfthr}$ was unaffected by PRPP or Hx, suggesting that it is not in the active site region. The inactive $HPRT_{pfthr}$ seemed to produce the putative intramolecular more readily than the native protein, perhaps suggesting increased degrees of freedom of the relevant segment of the protein.

4.6 Chemical syntheses and inhibition studies

The starting point for the synthesis of inhibitors of malarial HPRT was the finding by Queen *et al.* (1988) that this enzyme utilizes xanthine as substrate, whereas the human form does so poorly (Krentisky *et al.*, 1969; Kelley *et al.*, 1967). Other protozoan HPRTs are similar in this regard. This laboratory has extensive experience in the synthesis of 8-azido ATP and the 2',3'-*O*-(2,4,6-trinitrophenyl) derivative, and photolabelling of different proteins. It emerged from these studies that irradiation of TNP-8-azido ATP in different aqueous media could yield a large diversity of products via radical chemistry. This could be an avenue for generating an array of different and unusual xanthine analogues for inhibition screening. The development of the synthesis pathway of 8-azido xanthine was not straightforward. Irradiation of 8-azido xanthine produced a single product in a variety of media according to HPLC. This led to the notion that 8-azido xanthosine and TNP-8-azido xanthosine may be more suitable for producing product diversity upon irradiation, and this was found to be the case. Crude modelling suggested that the TNP-derivatives of nucleosides or nucleotides might fit into the HPRT catalytic site in the open unligated conformation. It had also been noted in this laboratory that the TNP-8 azido ATP readily conjugated to certain flavonoids when under the influence of light. This led to the idea that TNP-XMP-flavonoid duplex complexes might bind to the active sight in the open conformation with the flavonoid on top of the nucleotide interacting with the mobile loops.

University of Cape Town

Therefore the approach taken to synthesising inhibitors was three-pronged:

(i) the synthesis of 8-azido xanthosine and 8-azido xanthine to yield a diversity of purines

(ii) the synthesis of 2',3'-*O*-(2,4,6-trinitrophenyl)-nucleotides and nucleosides

(iii) the synthesis of 2',3'-*O*-(2,4,6-trinitrophenyl)-nucleosides conjugated to flavonoids

Attempts to synthesise 8-azido xanthosine from 8-bromo xanthosine by standard methods used for 8-azido ATP and 8-azido GTP were unsuccessful, and alternative methods were found in work done prior to this study (Cox, Hacker, Phehane, and McIntosh, unpublished results). These involved performing the substitution in NaN_3-saturated DMSO in the presence of the oxidising agent H_2O_2. The yield was close to 100%. In this study considerable difficulties were encountered in removing NaN_3-saturated DMSO. Eventually aluminium oxide chromatography proved to be a suitable means of separation. A second problem was that the 8-azido xanthosine reacted with the ammonium acetate used to elute the nucleoside from the resin.

An HPLC purification step was introduced, and the pure product was obtained. Acid cleavage of the glycosidic bond produced 8-azido xanthine. The 8-azido xanthine did not inhibit malarial HPRT. The irradiation of 8-azido xanthine resulted in its breakdown to a single product as judged by HPLC, irrespective of the aqueous medium used. The product did not absorb in the 260-280 nm wavelength range, and evidently the purine ring had opened up. The early elution of the open-ringed product on HPLC suggested a more hydrophilic compound.

In this study, only HPLC and UV spectrophotometry analytical data were obtained for the products 8-azidoxanthine and 8-azidoxanthosine. NMR, MS and HRMS were not used as

University of Cape Town

general techniques, as screening was exploratory. Large amounts of compounds would be required for NMR, and the low yields obtained prevented this. The compounds synthesised were therefore only tentatively identified.

TNP derivatives of GMP, XMP and IMP were synthesised using a method developed for ATP (Hiratsuka, 1982). The TNP-IMP and TNP-XMP derivatives had not been synthesised before. The yields of all three TNP derivatives were not high but were sufficient to test the compounds as inhibitors. It was shown that the reaction of guanosine with TNBS yields mixtures of *N*-TNP, *O*-TNP, and *N,O*-bis-TNP derivatives (Azegami and Iwai, 1964). The use TNCB avoids these side reactions and results in higher yields of *O*-TNP derivatives (Hiratsuka, 1985). If higher yields were required, this would be the route to follow.

TNP-GMP, and not TNP-IMP or TNP-XMP inhibited $HPRT_{pfthr}$. Strong inhibition was observed in the presence of 1 mM PRPP, 20 μM guanine and up to 60 μM TNP-GMP. TNP-GMP had no effect on the turnover of human or *T. gondii* HPRT. It is unclear why the inhibitor is specific for the malarial enzyme but it is possible that the latter may have a different rate limiting step from the other two. However, we found that TNP-GMP was competitive with PRPP, suggesting that it bound to the unligated enzyme. The steady state concentration of unligated enzyme is likely to be similar for all three enzymes as the K_m(PRPP) are rather similar (16-60 μM, Table 1.3). Therefore it appears that TNP-GMP may bind intrinsically tighter to the malarial HPRT. The tightness of binding may be related to differences in loop binding tightness.

Examination of the crystal structures of human (Eads *et al.*, 1994; Shi *et al.*, 1999b), malarial (Shi *et al.*, 1999a) and *T. gondii* HPRTs (Héroux *et al.*, 1999a; 1999b) suggests that the TNP moiety might be accommodated in the PPi binding site. As mentioned in the Introduction, the

University of Cape Town

TNP group interacts strongly with amines. There are two Lys residues (Lys-44 and Lys-114) and Arg-210 that may interact with the TNP group. The Lys-77 residue seems to be in a favourable position to interact with the 4-nitro group of TNP, and the Lys-114 or Arg-201 with the 2-nitro group. An amino group may interact directly with the aromatic ring. Amino-aromatic and ammonium-aromatic interactions are common in proteins (Burley and Petsko, 1986; Dougherty and Stauffer, 1990), and model studies describe the favourable interaction between benzene and ammonia (Rodham *et al.*, 1993).

There are three acidic residues that normally interact with one Mg^{2+} and indirectly with the other. It is possible that the metal sites may be occupied by Mg^{2+} ions. The Mg^{2+} ions may interact directly with the TNP ring as cation-π interactions are known to stabilise the association between a cation and the electron-rich face of an aromatic ring (Dougherty and Stauffer, 1990; Petti *et al*, 1998, see Figure 4.9), and such interactions were evident in the ion selectivity of the *shaker* channel in Drosophila (Kumpf and Dougherty, 1993). In conclusion, favourable amine-nitro, amine-nitro, amine-aromatic, and/or cation-aromatic interactions may be involved in binding the TNP functionality.

University of Cape Town

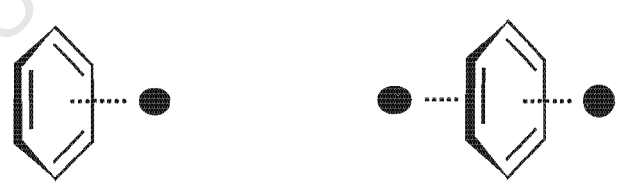

Figure 4.9 The cation-π interaction. Adapted from Kumpf and Dougherty (1993)

GMP binds ten-fold more strongly than IMP (K_D = 7 vs. 61 μM respectively in human HPRT (Xu *et al.*, 1997)). The enthalpy of binding of GMP in human HPRT is more favourable than that of IMP, and it was postulated that this may be due to hydrogen bonds formed between the

exocyclic group of GMP and peptide oxygens of Val-187 and Asp-193 of the protein. Perhaps the corresponding contacts in the parasitic HPRTs occur, and may favour the selectivity of the TNP analogue over the TNP-IMP and TNP-XMP derivatives. It is possible that the latter two compounds may be inhibitory at concentrations higher than could be used in the spectrophotometric assay.

Although the active sites of human, malarial and *T. gondii* HPRT are very similar, one difference is the high instability of the malarial form. It is possible that the instability of the $HPRT_{pfthr}$ may allow more movement to better accommodate the TNP moiety. It would be interesting to determine if the more stable untagged protein expressed by Keough *et al.* (1999) is susceptible to inhibition by TNP-GMP. Some of the residues that may be in proximity to TNP-GMP within the active site region of malarial HPRT are shown in Figure 4.10.

University of Cape Town

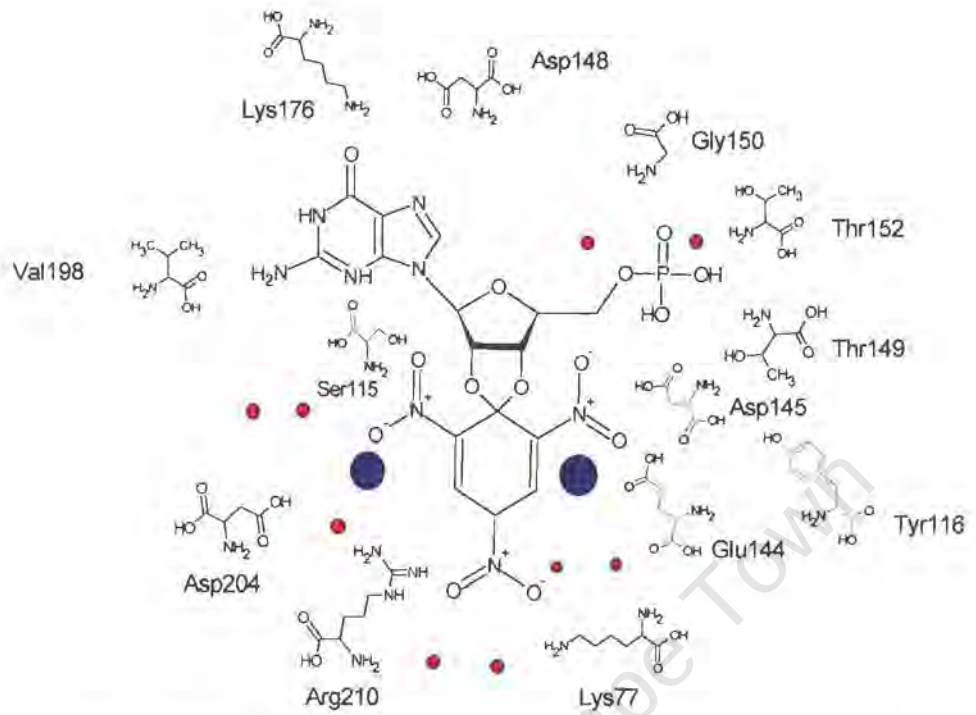

Figure 4.10 Amino acid residues in proximity of TNP-GMP placed in the active site of malarial HPRT. Blue spheres represent Mg2+ ions. Red spheres represent water molecules. The position of the residues has been taken from Shi *et al.* (1999a). It should be noted that the plane of the TNP ring should be at right angles to the plane of the ribosyl ring.

University of Cape Town

It may be possible to increase the potency or binding affinity of TNP-GMP by synthesising derivatives thereof. One approach may be to continue along the lines initially proposed in this work, which was to synthesize an 8-azido derivative as a lead compound, and generate diversity through irradiation and radical chemistry. Along these lines, TNP-8-azido xanthosine was synthesised and was shown to yield many products upon irradiation. However, none of the mixtures inhibited the enzyme. It might be worthwhile to synthesise 8-azido GMP using the method described by Nagesh and Chatterji (1999), and then to add the TNP group as has been done in this study. One potential problem is that 8-substituted nucleotides often adopt the syn conformation about the glycosidic bond, and this might hinder optimal binding in the active site.

In future studies it might be worthwhile to explore the azido derivatives as photolabels of the active site. In this regard the malarial HPRT may be particularly suitable because of the presence of Tyr-116 in an active site loop (residues 112-132). Photolabeling with a radiolabeled probe would provide a simple means of scanning compounds for binding to the active site.

We demonstrate in his study that it is possible to obtain conjugates between TNP-8-azido xanthosine and certain flavonoids, and two ideas on how this might occur are shown in Figure 4.11. Formation of the conjugate may involve stacking of the flavonoid moiety on top of the purine ring through π-π interactions and reaction with the azido group to form a link between the two. An alternative is interaction of the TNP group with the flavonoid, and reaction with the azido group. A single conjugate was produced with kaempferide, and three with 4-I-chalcone. The yield of conjugate was high in both cases (50-80%) when the reactants were present in a 1:1 molar ratio. We did not obtain conjugates with 8-azidoxanthosine or 8-azido xanthine, suggesting that the TNP moiety plays a role in conjugate formation. These observations suggest that the formation of the conjugates is predominantly through stacking of the flavonoid with the TNP moiety (as shown in Figure 4.11 below). This implies that the interactions between the TNP group and the flavonoid are substantially stronger than that between the flavonoid and the purine ring.

University of Cape Town

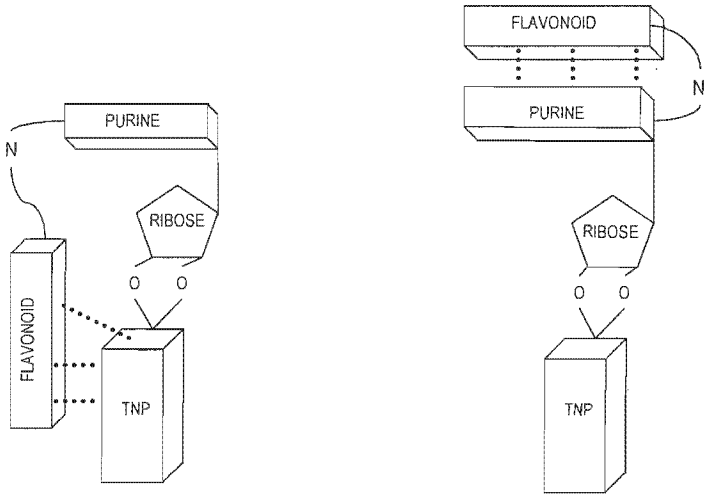

Figure 4.11 Possible flavonoid/ TNP-nucleoside conjugates

The conjugate between kaempferide and TNP-8-azido xanthosine did not inhibit $HPRT_{pfthr}$, most likely due its inability to bind in the active site. TNP-8-azido xanthosine irradiated on its own did not produce inhibitory products, and neither did 8-azido xanthosine, even when the final concentration of the irradiation mix was at 50 or 100 μM, and substrates guanine and PRPP were at 20 and 500 μM respectively. It may be possible to identify tight-binding components by passing an irradiated mixture over the enzyme immobilised to the nickel-chelate column, and look for the disappearance of photolysis products by HPLC. Obviously more conjugates need to be synthesised and investigated for inhibiting malarial HPRT activity before firm conclusions can be made as to whether such duplex structures have potential as inhibitors.

Flavonoid compounds have been previously found to inhibit ATP-dependent enzymes. P-glycoprotein (Pgp), is an ATP-dependent efflux pump that confers multidrug resistance (MDR) in tumour cells (Gottesman and Pastan, 1993) and in parasites such as *Plasmodium* (Wilson *et al.*, 1989; Foote *et al.*, 1989). Flavonoids (for example 8-(1,1-dimethylallyl)kaempferide were

University of Cape Town

shown to bind to mouse Pgp (Conseil *et al.*, 1998) and the Pgp-like multidrug transporter, and promote the accumulation of duanomycin in *Leishmania tropica* (Pérez-Victoria *et al.*, 1999). Certain flavonoids have been shown in this laboratory to bind tightly to the ATP site of recombinant nucleotide binding domains of Pgp (de Wet *et al.*, 2001).

4.7 Activation of $HPRT_{pfthr}$ by a flavonoid

Thirty-eight flavonoids from an available library were tested for possible inhibition of $HPRT_{pfthr}$. No inhibition was detected by any of the flavonoids at up to 20 μM in the presence of 20 μM guanine and 1 mM PRPP. However, one, namely, 4-I-chalcone activated the enzyme 2 to 3-fold. Activation was not seen in the human or *T. gondii* HPRTs.

There might be three possibilities for activation:

(i) An allosteric effector site, distinct from the catalytic site, binding to which may accelerate any of the partial reactions of the cycle

(ii) Binding to the PPi site and activating nucleotide release

(iii) Binding to the nucleotide site and activating PPi release

(i) It is not known which is the principal rate-limiting step in catalysis of malarial HPRT. The rate-limiting step of catalysis in human HPRT in the forward direction was determined to be the release of nucleotide (Xu *et al.*, 1997). In the simulations presented above, it was shown that the rate of turnover of malarial HPRT could be approached if the chemical interconversion step is slowed 100-fold, without changing any of the other rate constants of the human HPRT. This means that E·PRPP·Hx to E·PPi·IMP (with rate constant of 1.3 s^{-1}) becomes the principal rate-limiting step, and IMP release is 5-fold faster (with rate constant of 6 s^{-1}). Under these

University of Cape Town

circumstances, activation would come from an acceleration of the chemical interconversion step, which in turn could only come about by binding of the iodo-chalcone to an allosteric site. Activating the chemical interconversion step 5-fold increases k_{cat} from 1 s^{-1} to 2.5 s^{-1}. On the other hand, 10-fold activation of the release of IMP only increases k_{cat} to 1.1 s^{-1}.

No allosteric site has been described for any of the HPRTs as far as we know. The atomic structure of the malarial HPRT is fairly compact, but there are pockets on the surface that might form a binding site. However, how binding in these pockets could influence catalysis is unclear. The transition state requires shifting of the hood domain onto the core domain, and ordering of loops over the substrates, so that all substrates are tightly enclosed within the active site during the chemical interconversion step. If any of these interactions are stabilised by the iodo-chalcone binding, then the chemical interconversion step might be accelerated.

(ii) If GMP or IMP contributes significantly to rate limitation as in the human enzyme, then acceleration could occur by iodo-chalcone binding to the PPi site. The release of nucleotide is apparently slow because the hood domain needs to tilt backwards, and the ordered opening of loops has to occur. The departure of PPi would result in loss of the extensive hydrogen-bonding network that holds the core and hood domains together. Interactions between the purine ring and Asp-204 of loop IV (according to nomenclature by Héroux *et al.*, 1999b) would be loosened. The β-strand over the purine ring, and Phe-197 would be pulled away from the IMP. Thus the site is rather open, as discussed for the binding of TNP. The iodo-chalcone may fit here and aid the release of the hood domain. The strong possibility that TNP-GMP fits at the active site (albeit vacant), where the TNP moiety is necessarily replaced at the PPi site, argues for the iodo-chalcone being able to be accommodated here. The incoming/bound iodo-chalcone would find the intermediate in a rather loosened form. All that would be left to occur

University of Cape Town

are the opening of the phosphate binding loop and the loop that contains Leu-182 (loop III' according to nomenclature by Héroux *et al.*, 1999b). The latter loop would not have bound very tightly anyway, as the Asp-148-Leu-18-Asp-195 sandwich is not as strongly held as in the human or *T. gondii* enzymes where the Leu is an Arg. This difference may account for the selective acceleration of the malarial HPRT by the iodo-chalcone.

(iii) It is also possible that rate limitation for the malarial enzyme is PPi release. While this is not the case for the human enzyme, the pathway is not negligible (see Figure 4.7) (Xu *et al.*, 1997). PPi release requires that a peptide bond (Leu-76-Lys-77) changes from the cis to the trans configuration, and while this may be energetically favoured, there may be kinetic limitations in the malarial HPRT (i.e., high activation energy). Flavonoids have the general shape of a mononucleotide, and it is likely that the iodo-chalcone can occupy the IMP site. The iodo-chalcone resembles phthalic anhydrides that are inhibitors of *T. foetus* HPRT (Figure 4.12; Somoza *et al.*, 1998). Modelling showed that the phthalic anhydride group could fill a guanine-binding pocket, and a nitrobenzene substituent group could fill a hydrophobic pocket near the ribose phosphate-binding loop. The binding of the iodo-chalcone could accelerate cis to trans isomerisation of the peptide bond, opening of the loop containing residues 200-214, and therefore PPi release.

University of Cape Town

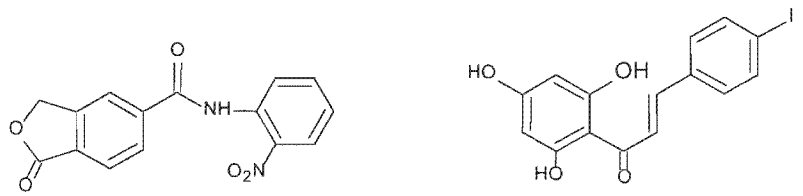

phthalic anhydride 4-I-chalcone

Figure 4.12 A comparison of the structures of a phthalic anhydride derivative and 4-I-chalcone.

The modelled active site of *T. gondii* HPRT (Héroux *et al.*, 1999b) is shown in Figure 4.13, and 4-I-chalcone is crudely placed in the PPi and nucleotide sites, and TNP in the PPi site.

University of Cape Town

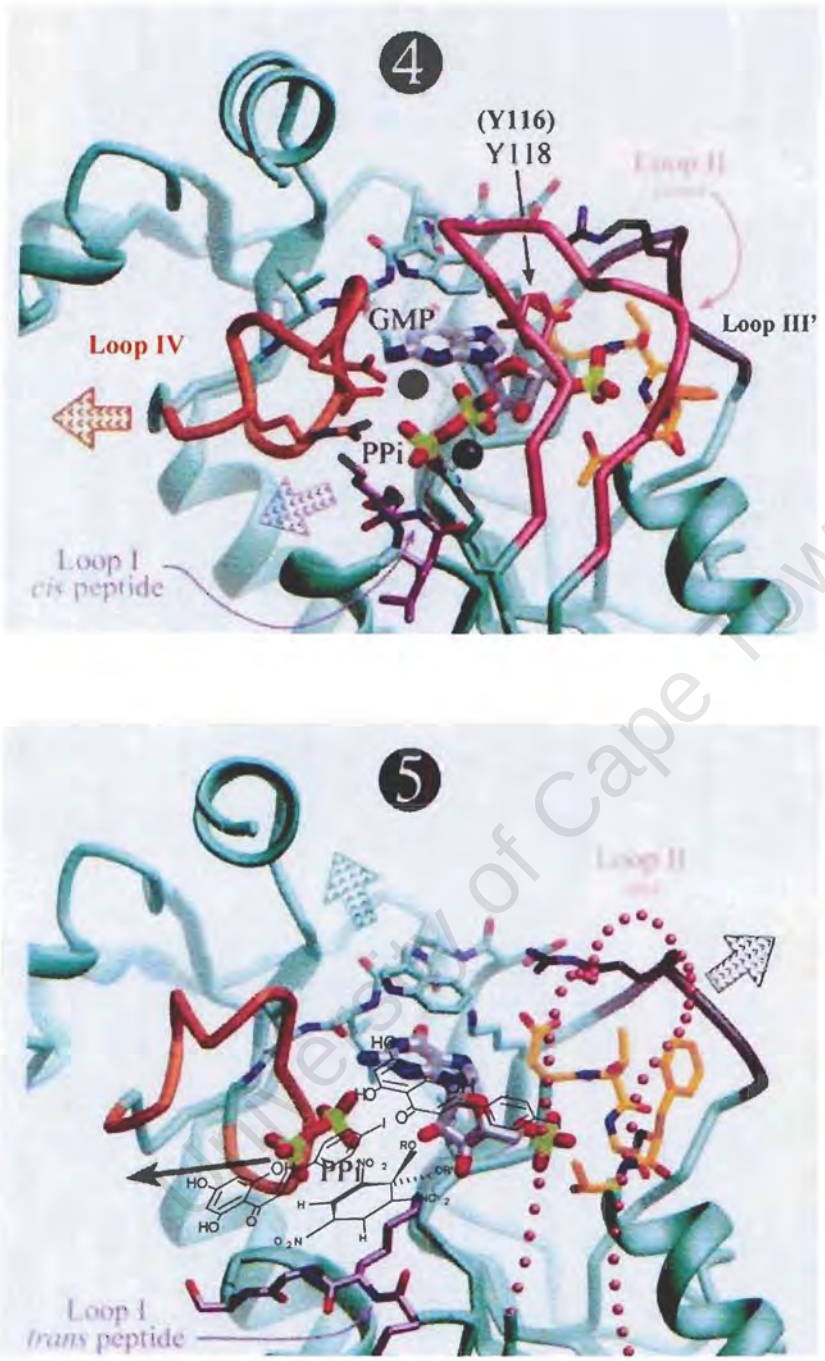

University of Cape Town

Figure 4.13 Modelled active site of *T. gondii* HPRT with GMP and PPi (Taken from Héroux *et al.*, 1999b), and possible binding sites for the TNP group and 4-I-chalcone. Panel A, Both substrates in the active region. The Y-116 residue in malarial HPRT is shown in parentheses. Panel B, Placing of 4-I-chalcone and TNP in the active site.

Which of the above possibilities actually is true cannot be decided, but two results provide some points for discussion. The first is that acceleration of turnover by the iodo-chalcone resulted in less inactivation of $HPRT_{pfthr}$ during the consumption of 20 μM guanine (Figure 3.59). This means that less time was spent in the unstable states, i.e., the steady state level of E, E·IMP and possibly E·PPi (if PPi dissociation is rate-limiting) were less. The steady state level of E is very low, due to the high concentration of PRPP during assay. The concentrations of E·IMP and possibly E·PPi must therefore have been less, and in turn suggests the release of IMP (or PPi if rate-limiting) is accelerated (the affinity is likely to be lowered). The other information we have is that using the fluorescence assay, the iodo-chalcone provided acceleration in the presence of inhibitory levels of IMP. This could be interpreted in three ways depending on whether the iodo-chalcone binds to (a) an allosteric site (no competition with IMP), (b) the PPi site (no competition with IMP) or (c) the IMP site (competition with IMP). Almost maximal acceleration was observed in the presence of 250 μM IMP, and indicates that the iodo-chalcone and IMP do not compete, supporting either (a) or (b). Taken with the above deductions regarding stability, the most likely mechanism is that IMP release is rate-limiting, and the iodo-chalcone binds to the PPi site, and accelerates the off rate of IMP. A more detailed study of the kinetics, perhaps using radiolabeled Hx so that high concentrations of IMP can be used could confirm this conclusion.

The activation seemed specific for this particular chalcone. Replacing the iodo group with a fluoro group eliminated the effect. This may be related to lipophilicity, which decreases in the series I>Br>Cl>F>OMe>OH (Hansch and Leo (1979) cited in Bois *et al.*, 1998). However, replacement with a C_2, C_4, C_6 or C_8 alkyl chain was ineffective. The iodo group is larger than the fluoro group, and this may play a role in the effects observed. None of the other flavonoids with iodo or halogenated substituents on the same ring were activators.

University of Cape Town

It may not be a coincidence that the tri-hydroxy ring of 4-I-chalcone has similarities to the TNP grouping. It is interesting that positioning the trihydroxy ring into the PPi site could place the iodo ring in proximity to the conserved Tyr-116, and that the opening of the active site loop might be favoured by π-π interactions of the two rings. It would be interesting to determine if the malarial enzyme could be crystallised with the transition analogues ImmucillinHP or ImmucillinGP and 4-I-chalcone.

It is a puzzle that the malarial parasite is so dependent on HPRT for purine salvage, and yet its activity is lower than the human enzyme. One speculative possibility in view of our results is that a natural activator similar in structure to our chalcone exists in the parasite.

University of Cape Town

APPENDIX

Appendix 1A: CLUSTAL X (1.81) multiple sequence alignment of published human HPRT and human HPRT determined in this study

```
HUMHPRT         TCTTGCTGCGCCTCCGCCTCCTCCTCTGCTCCGCCACCGGCTTCCTCCTCCTGAGCAGTC  60
Hum             ------------------------------------------------------CCGGCC   6
                                                                       * * *

HUMHPRT         AGCCCGCGCGCCGGC-CGGCTCCGTTATGGCGACCCGCAGCCCTGGCGTCGTGATTAGTG 119
Hum             GCCATGGCCGCGGGATCGGCTCCCATATGGCGACCCGCAGCCCTGGCGTCGTGATTAGTG  66
                  *  *  *** **  *******  **********************************

HUMHPRT         ATGATGAACCAGGTTATGACCTTGATTTATTTTGCATACCTAATCATTATGCTGAGGATT 179
Hum             ATGATGAACCAGGTTATGACCTTGATTTATTTTGCATACCTAATCATTATGCTGAGGATT 126
                ************************************************************

HUMHPRT         TGGAAAGGGTGTTTATTCCTCATGGACTAATTATGGACAGGACTGAACGTCTTGCTCGAG 239
Hum             TGGAAAGGGTGTTTATTCCTCATGGACTAATTATGGACAGGACTGAACGTCTTGCTCGAG 186
                ************************************************************

HUMHPRT         ATGTGATGAAGGAGATGGGAGGCCATCACATTGTAGCCCTCTGTGTGCTCAAGGGGGGCT 299
Hum             ATGTGATGAAGGAGATGGGAGGCCATCACATTGTAGCCCTCTGTGTGCTCAAGGGGGGCT 246
                ************************************************************

HUMHPRT         ATAAATTCTTTGCTGACCTGCTGGATTACATCAAAGCACTGAATAGAAATAGTGATAGAT 359
Hum             ATAAATTCTTTGCTGACCTGCTGGATTACATCAAAGCACTGAATAGAAATAGTGATAGAT 306
                ************************************************************

HUMHPRT         CCATTCCTATGACTGTAGATTTTATCAGACTGAAGAGCTATTGTAATGACCAGTCAACAG 419
Hum             CCATTCCTATGACTGTAGATTTTATCAGACTGAAGAGCTATTGTAATGACCAGTCAACAG 366
                ************************************************************

HUMHPRT         GGGACATAAAAGTAATTGGTGGAGATGATCTCTCAACTTTAACTGGAAAGAATGTCTTGA 479
Hum             GGGACATAAAAGTAATTGGTGGAGATGATCTCTCAACTTTAACTGGAAAGAATGTCTTGA 426
                ************************************************************

HUMHPRT         TTGTGGAAGATATAATTGACACTGGCAAAACAATGCAGACTTTGCTTTCCTTGGTCAGGC 539
Hum             TTGTGGAAGATATAATTGACACTGGCAAAACAATGCAGACTTTGCTTTCCTTGGTCAGGC 486
                ************************************************************

HUMHPRT         AGTATAATCCAAAGATGGTCAAGGTCGCAAGCTTGCTGGTGAAAAGGACCCCACGAAGTG 599
Hum             AGTATAATCCAAAGATGGTCAAGGTCGCAAGCTTGCTGGTGAAAAGGACCCCACGAAGTG 546
                ************************************************************

HUMHPRT         TTGGATATAAGCCAGACTTTGTTGGATTTGAAATTCCAGACAAGTTTGTTGTAGGATATG 659
Hum             TTGGATATAAGCCAGACTTTGTTGGATTTGAAATTCCAGACAAGTTTGTTGTAGGATATG 606
                ************************************************************

HUMHPRT         CCCTTGACTATAATGAATACTTCAGGGATTTGAATCATGTTTGTGTCATTAGTGAAACTG 719
Hum             CCCTTGACTATAATGAATACTTCAGGGATTTGAATCATGTTTGTGTCATTAGTGAAACTG 666
                ************************************************************

HUMHPRT         GAAAAGCAAAATACAAAGCCTAAGATGAGAGTTCAAGTTGAGTTTGGAAACATCTGGAGT 779
Hum             GAAAAGCAAAATACAAAGCCTAAGATGAGAGTTCAAGTTGAGTTTGGGA---TCCGG--- 720
                ********************************************* *   ** **

HUMHPRT         CCTATTGACATCGCCAGTAAAATTATCAATGTTCTAGTTCTGTGGCCATCTGCTTAGTAG 839
Hum             -CTGCTAACAAAGCCCGAAAGGAAGYGAKKGYG---------------------------- 752
                 **  * ***  *** * **       *  *
```

University of Cape Town

```
HUMHPRT     AGCTTTTTGCATGTATCTTCTAAGAATTTTATCTGTTTTGTACTTTAGAAATGTCAGTTG 899
Hum         ------------------------------------------------------------

HUMHPRT     CTGCATTCCTAAACTGTTTATTTGCACTATGAGCCTATAGACTATCAGTTCCCTTTGGGC 959
Hum         ------------------------------------------------------------

HUMHPRT     GGATTGTTGTTTAACTTGTAAATGAAAAAATTCTCTTAAACCACAGCACTATTGAGTGAA 1019
Hum         ------------------------------------------------------------

HUMHPRT     ACATTGAACTCATATCTGTAAGAAATAAAGAGAAGATATATTAGTTTTTTAATTGGTATT 1079
Hum         ------------------------------------------------------------

HUMHPRT     TTAATTTTTATATATGCAGGAAAGAATAGAAGTGATTGAATATTGTTAATTATACCACCG 1139
Hum         ------------------------------------------------------------

HUMHPRT     TGTGTTAGAAAAGTAAGAAGCAGTCAATTTTCACATCAAAGACAGCATCTAAGAAGTTTT 1199
Hum         ------------------------------------------------------------

HUMHPRT     GTTCTGTCCTGGAATTATTTTAGTAGTGTTTCAGTAATGTTGACTGTATTTTCCAACTTG 1259
Hum         ------------------------------------------------------------

HUMHPRT     TTCAAATTATTACCAGTGAATCTTTGTCAGCAGTTCCCTTTTAAATGCAAATCAATAAAT 1319
Hum         ------------------------------------------------------------

HUMHPRT     TCCCAAAAATTT 1331
Hum         ------------
```

Figure 1: Published Human HPRT (Jolly *et al.*, 1983) aligned to sequence determined in this study (Hum). The published sequence occurs above the determined sequence. The Met residue (ATG) is shaded. Part of the pGEM®-T vector is underlined upstream to the start region. The *Nde*1 (CATATG) and *Bam*H1 (GGATCC) restriction sites are shaded. The stop codon (TAA) is shaded. Gaps underneath the alignments show differences to the published sequence, the asterisks (*) represent identity and the dashes (-) indicate no match made.

University of Cape Town

Appendix 1B: CLUSTAL X (1.81) multiple sequence alignment of published *P. falciparum* HPRT sequence with that of $HPRT_{pfmet}$ determined in this study

```
HPRT            ------------------------------------------------------------
Pfmet           NNNNNNNNNNNNNNNNNNNNNNNNNNNNNNNNNNNNNNNNNNNNNNNNNNNNNNNNNNN 60

HPRT            ------------------------------------------------------------
Pfmet           NNMNNNNNNNWNNNNNNNNNNNRNNNNNTTTCCCNNSGNNAKTSGNNAWWNGGSCCNNCA 120

HPRT            ------------------------------------------------------------
Pfmet           MCNCCCCNKGGCCCNGGNANCCGNCCNNAKNNTCSGGGKARAGAWNGRNNTTNGTNCCGG 180

HPRT            ----TAAAAATTTTAATAATATACTTTCACCACACCAAAAACCAAAAATATATATTTAAT 56
Pfmet           NAANTAWNCNNYCCNTWAGGGGATTKKRGCGGWAACNATTCCCNNTAG-AAATANTTTGT 239
                    **          *   * *   *  * * *  **   *  * *** **  *

HPRT            TCATAATATTAAAGAAAATATATTTTTCTTTGTATATATTATTACTAT-ATATTTATA-- 113
Pfmet           TNACTTTA--GAAGGAGATWTNCCWGGGCA-GCAGNCATCATCATCATCATCACAGCAGC 296
                * *   **   *** * ** *         * *   ** ** *  ** **      *

HPRT            ----TAATATTAGA--------AAATGCCAATACCAAATAATCCAGGAGCTGGTGAAAAT 161
Pfmet           GGCCTGGTGCCGCGCGGCAGCCATATGCCAATACCAAATAATCCAGGAGCTGGTGAAAAT 356
                    *  *              * ************************************

HPRT            GCCTTTGATCCCGTTTTCGTAAAGGATGACGATGGTTATGACCTTGATTCTTTTATGATC 221
Pfmet           GCCTTTGATCCCGTTTTCGTAAAGGATGACGATGGTTATGACCTTGATTCTTTTATGATC 416
                ************************************************************

HPRT            CCTGCACATTATAAAAAATATCTTACCAAGGTCTTAGTTCCAAATGGTGTCATAAAAAAC 281
Pfmet           CCTGCACATTATAAAAAATATCTTACCAAGGTCTTAGTTCCAAATGGTGTCATAAAAAAC 476
                ************************************************************

HPRT            CGTATTGAGAAATTGGCTTATGATATTAAAAAGGTGTACAACAATGAAGAGTTTCATATT 341
Pfmet           CGTATTGAGAAATTGGCTTATGATATTAAAAAGGTGTACAACAATGAAGAGTTTCATATT 536
                ************************************************************

HPRT            CTTTGTTTGTTGAAAGGTTCTCGTGGTTTTTTCACTGCTCTCTTAAAGCATTTAAGTAGA 401
Pfmet           CTTTGTTTGTTGAAAGGTTCTCGTGGTTTTTTCACTGCTCTCTTAAAGCATTTAAGTAGA 596
                ************************************************************

HPRT            ATACATAATTATAGTGCCGTTGAGATGTCCAAACCATTATTTGGAGAACACTACGTACGT 461
Pfmet           ATACATAATTATAGTGCCGTTGAGATGTCCAAACCATTATTTGGAGAACACTACGTACGT 656
                ************************************************************

HPRT            GTGAAATCCTATTGTAATGACCAATCAACAGGTACATTAGAAATTGTAAGTGAAGATTTA 521
Pfmet           GTGAAATCCTATTGTAATGACCAATCAACAGGTACATTAGAAATTGTAAGTGAAGATTTA 716
                ************************************************************

HPRT            TCTTGTTTAAAAGGAAAACATGTATTAATTGTTGAAGATATTATTGATACTGGTAAAACA 581
Pfmet           TCTTGTTTAAAAGGAAAACATGTATTAATTGTTGAAGATATTATTGATACTGGTAAAACA 776
                ************************************************************

HPRT            TTAGTAAAGTTTTGTGAATACTTAAAGAAATTTGAAATAAAAACCGTTGCCATCGCTTGT 641
Pfmet           TTAGTAAAGTTTTGTGAATACTTAAAGAAATTTGAAATAAAAACCGTTGCCATCGCTTGT 836
                ************************************************************

HPRT            CTTTTTATTAAAAGAACACCTTTGTGGAATGGTTTTAAAGCTGATTTCGTTGGATTCTCA 701
Pfmet           CTTTTTATTAAAAGAACACCTTTGTGGAATGGTTTTAAAGCTGATTTCGTTGGATTCTCA 896
                ************************************************************
```

University of Cape Town

```
HPRT          ATTCCTGATCACTTTGTTGTTGGTTATAGTTTAGACTATAATGAAATTTTCAGAGATCTT 761
Pfmet         ATTCCTGATCACTTTGTTGTTGGTTATAGTTTAGACTATAATGAAATTTTCAGAGATCTT 956
              ************************************************************

HPRT          GACCATTGTTGTTTGGTTAATGATGAGGGAAAAAAGAAATATAAAGCAACTTCATTATAA 821
Pfmet         GACCATTGTTGTTTGGTTAATGATGAGGGAAAAAAGAAATATAAAGCAACTTCATTATAA1016
              ************************************************************

HPRT          --ATACATTTATTGAAGTGATCAAAAATGTCACAACCTTTCTATTTATATCAATTTAAAA 879
Pfmet         GGATCCGGCTGCTAACAAAGCCCGAAAGGAAGYGAKTGNYG-------------------1057
                ** *   *  * *      *  *** *     *

HPRT          AAAAAAAAAAAAAAAAAAAAAAATAGAGAAGAAAATATCTGTACCAAAAATATATATATA 939
Pfmet         ------------------------------------------------------------

HPRT          TATATATATATATATATATATATATGTATATATATATTTTATGTACATGTTATATATATT 999
Pfmet         ------------------------------------------------------------

HPRT          TATATATAACTTATAATGAACGTGAACTATATAAAAAAAAAAAAAAAAAAAAAAAAAAA 1059
Pfmet         ------------------------------------------------------------
```

Figure 2: Published *P. falciparum* HPRT (King and Melton, 1987) aligned to sequence determined in this study (Pfmet). The published sequence occurs above the determined sequence. The Met residue (ATG) is shaded. The bold regions are the 6 x His tag (bases 273-290) and thrombin cleavage (bases 300-317) regions respectively of pET-15b. The *Nde*1 (CATATG) and *Bam*H1 (GGATCC) restriction sites are shaded. The stop codon (TAA) is shaded. The Met 101 residue (ATG) is underlined. Gaps underneath the alignments show differences to the published sequence, the asterisks (*) represent identity and the dashes (-) indicate no match made.

University of Cape Town

Appendix 1C: CLUSTAL X (1.81) multiple sequence alignment of published *P. falciparum* HPRT with that of $HPRT_{pfthr}$ determined in this study

```
HPRT      AAAATTTATACAAATTTTAATATAAACTTTCACCACACCAAAAACCAAAAATATATATTT 60
Pfthr     ------------------------------------------------------------

HPRT      AATTCATAATATTAAAGAAAATATATTTTTCTTTGTATATATTATTACTATATATTTATA 120
Pfthr     -------------GCAGCAGCCATCATCATCATCAT-CACAGCAGCGGCCTGGTGCCGCG 46
                          ** *   **  *  ** *  *  * *  *      *

HPRT      TAATATTAGAAAATGCCAATACCAAATAATCCAGGAGCTGGTGAAAATGCCTTTGATCCC 180
Pfthr     CGGCAGCC--ATATGCCAATACCAAATAATCCAGGAGCTGGTGAAAATGCCTTTGATCCC 104
              *     * ***************************************************

HPRT      GTTTTCGTAAAGGATGACGATGGTTATGACCTTGATTCTTTTATGATCCCTGCACATTAT 240
Pfthr     GTTTTCGTAAAGGATGACGATGGTTATGACCTTGATTCTTTTATGATCCCTGCACATTAT 164
          ************************************************************

HPRT      AAAAAATATCTTACCAAGGTCTTAGTTCCAAATGGTGTCATAAAAAACCGTATTGAGAAA 300
Pfthr     AAAAAATATCTTACCAAGGTCTTAGTTCCAAATGGTGTCATAAAAAACCGTATTGAGAAA 224
          ************************************************************

HPRT      TTGGCTTATGATATTAAAAAGGTGTACAACAATGAAGAGTTTCATATTCTTTGTTTGTTG 360
Pfthr     TTGGCTTATGATATTAAAAAGGTGTACAACAATGAAGAGTTTCATATTCTTTGTTTGTTG 284
          ************************************************************

HPRT      AAAGGTTCTCGTGGTTTTTTCACTGCTCTCTTAAAGCATTTAAGTAGAATACATAATTAT 420
Pfthr     AAAGGTTCTCGTGGTTTTTTCACTGCTCTCTTAAAGCATTTAAGTAGAATACATAATTAT 344
          ************************************************************

HPRT      AGTGCCGTTGAGACGTCCAAACCATTATTTGGAGAACACTACGTACGTGTGAAATCCTAT 480
Pfthr     AGTGCCGTTGAGACGTCCAAACCATTATTTGGAGAACACTACGTACGTGTGAAATCCTAT 404
          ************************************************************

HPRT      TGTAATGACCAATCAACAGGTACATTAGAAATTGTAAGTGAAGATTTATCTTGTTTAAAA 540
Pfthr     TGTAATGACCAATCAACAGGTACATTAGAAATTGTAAGTGAAGATTTATCTTGTTTAAAA 464
          ************************************************************

HPRT      GGAAAACATGTATTAATTGTTGAAGATATTATTGATACTGGTAAAACATTAGTAAAGTTT 600
Pfthr     GGAAAACATGTATTAATTGTTGAAGATATTATTGATACTGGTAAAACATTAGTAAAGTTT 524
          ************************************************************

HPRT      TGTGAATACTTAAAGAAATTTGAAATAAAAACCGTTGCCATCGCTTGTCTTTTTATTAAA 660
Pfthr     TGTGAATACTTAAAGAAATTTGAAATAAAAACCGTTGCCATCGCTTGTCTTTTTATTAAA 584
          ************************************************************

HPRT      AGAACACCTTTGTGGAATGGTTTTAAAGCTGATTTCGTTGGATTCTCAATTCCTGATCAC 720
Pfthr     AGAACACCTTTGTGGAATGGTTTTAAAGCTGATTTCGTTGGATTCTCAATTCCTGATCAC 644
          ************************************************************

HPRT      TTTGTTGTTGGTTATAGTTTAGACTATAATGAAATTTTCAGAGATCTTGACCATTGTTGT 780
Pfthr     TTTGTTGTTGGTTATAGTTTAGACTATAATGAAATTTTCAGAGATCTTGACCATTGTTGT 704
          ************************************************************

HPRT      TTGGTTAATGATGAGGGAAAAAAGAAATATAAAGCAACTTCATTATAAATACATTTATTG 840
Pfthr     TTGGTTAATGATGAGGGAAAAAAGAAATATAAAGCAACTTCATTATAAATAGG---ATCC 761
          ************************************************      **
```

University of Cape Town

```
HPRT            AAGTGATCAAAAATGTCACAACCTTTCTATTTATATCAATTTACCCCCCCCCCCCCCCCC 900
Pfthr           GGCTGCYAACAAAGCCCGAAAGGAAGYGRKG---------------------------- 792
                   **   * ***   *  **

HPRT            CCTGCAGG 908
Pfthr           -------- 
```

Figure 3: Published *P. falciparum* HPRT (Vasanthakumar *et al.*, 1989) aligned to sequence determined in this study (Pfthr). The published sequence occurs above the determined sequence. The Met residue (ATG) is shaded. The bold regions are the 6 x His tag (bases 9-26) and thrombin cleavage (bases 36-53) regions respectively of pET-15b. The *Nde*I (CATATG) and *Bam*H1 (GGATCC) restriction sites are shaded. The stop codon (TAA) is shaded. The Thr 101 residue (ACG) is underlined. Gaps underneath the alignments show differences to the published sequence, the asterisks (*) represent identity and the dashes (-) indicate no match made.

University of Cape Town

Appendix 1D: CLUSTAL X (1.81) multiple sequence alignment of published *T. gondii* HPRT with that of $HPRT_{Tgondii}$ (Tox) determined in this study.

```
Tgondii         ------------------------------------------------------------
Tox             ATYGNNNNNNNNNTCGGRCGGNTACATTCCCCTCTAGAAATAATTTTGTTTAACTTTAAG 60

Tgondii         ----------------------------------------GCCTACCAACTTTTCCCTAA 20
Tox             AAGGAGATYYYCCRTGGGGSAGNAAMCATCATCATCATCATCACAGCAGCGGCCTGGTGC 120
                                                        *  * ** *       *

Tgondii         CGTGAAGCA---AAATGGCGTCCAAACCCATTGAAGACTACGGCAAGGGCAAGGGCCGTA 77
Tox             CGCGCGGCAGCCATATGGCGTCCAAACCCATTGAAGACTACGGCAAGGGCAAGGGCCGTA 180
                ** *  ***    * **************************************************

Tgondii         TTGAGCCCATGTATATCCCCGACAACACCTTCTACAACGCTGATGACTTTCTTGTGCCCC 137
Tox             TTGAGCCCATGTATATCCCCGACAACACCTTCTACAACGCTGATGACTTTCTTGTGCCCC 240
                ************************************************************

Tgondii         CCCACTGCAAGCCCTACATTGACAAAATCCTCCTCCCTGGTGGATTGGTCAAGGACAGAG 197
Tox             CCCACTGCAAGCCCTACATTGACAAAATCCTCCTCCCTGGTGGATTGGTCAAGGACAGAG 300
                ************************************************************

Tgondii         TTGAGAAGTTGGCGTATGACATCCACAGAACTTACTTCGGCGAGGAGTTGCACATCATTT 257
Tox             TTGAGAAGTTGGCGTATGACATCCACAGAACTTACTTCGGCGAGGAGTTGCACATCATTT 360
                ************************************************************

Tgondii         GCATCCTGAAAGGCTCTCGCGGCTTCTTCAACCTTCTGATCGACTACCTTGCCACCATAC 317
Tox             GCATCCTGAAAGGCTCTCGCGGCTTCTTCAACCTTCTGATCGACTACCTTGCCACCATAC 420
                ************************************************************

Tgondii         AGAAGTACAGTGGTCGTGAGTCCAGCGTGCCCCCCTTCTTCGAGCACTATGTCCGCCTGA 377
Tox             AGAAGTACAGTGGTCGTGAGTCCAGCGTGCCCCCCTTCTTCGAGCACTATGTCCGCCTGA 480
                ************************************************************

Tgondii         AGTCCTACCAGAACGACAACAGCACAGGCCAGCTCACCGTCTTGAGCGACGACTTGTCAA 437
Tox             AGTCCTACCAGAACGACAACAGCACAGGCCAGCTCACCGTCTTGAGCGACGACTTGTCAA 540
                ************************************************************

Tgondii         TCTTTCGCGACAAGCACGTTCTGATTGTTGAGGACATCGTCGACACCGGTTTCACCCTCA 497
Tox             TCTTTCGCGACAAGCACGTTCTGATTGTTGAGGACATCGTCGACACCGGTTTCACCCTCA 600
                ************************************************************

Tgondii         CCGAGTTCGGTGAGCGCCTGAAAGCCGTCGGTCCCAAGTCGATGAGAATCGCCACCCTCG 557
Tox             CCGAGTTCGGTGAGCGCCTGAAAGCCGTCGGTCCCAAGTCGATGAGAATCGCCACCCTCG 660
                ************************************************************

Tgondii         TCGAGAAGCGCACAGATCGCTCCAACAGCTTGAAGGGCGACTTCGTCGGCTTCAGCATTG 617
Tox             TCGAGAAGCGCACAGATCGCTCCAACAGCTTGAAGGGCGACTTCGTCGGCTTCAGCATTG 720
                ************************************************************

Tgondii         AAGACGTCTGGATCGTTGGTTGCTGCTACGACTTCAACGAGATGTTCCGCGACTTCGACC 677
Tox             AAGACGTCTGGATCGTTGGTTGCTGCTACGACTTCAACGAGATGTTCCGCGACTTCGACC 780
                ************************************************************

Tgondii         ACGTCGCCGTCCTGAGCGACGCCGCTCGCAAAAAGTTCGAGAAGTAAACCCTGCATATGT 737
Tox             ACGTCGCCGTCCTGAGCGACGCCGCTCGCAAAAAGTTCGAGAAGTAAGGATCCGGCTGCT 840
                ********************************************              *
```

University of Cape Town

```
Tgondii         AGAAAAGTTGTAACGTTAGTAAACGTAACACACGGGTATAATAGCCATTTAATGGCGCCG 797
Tox             AACAAAGCCCGAAAGGAAGCYGA-KTG---------------------------------- 866
                *  ****    ** *  **   *  *

Tgondii         TATATTTTTCACTCCCCCTCTCCGATAGGAGGAAGAAAGACGATCCGTCTGCGAATGTAT 857
Tox             ------------------------------------------------------------

Tgondii         ATTACATCGACCGGCCATAGTACGAGAAGTGGTGCCGGTATTGTTCTGTCCGGGGATGTA 917
Tox             ------------------------------------------------------------

Tgondii         CCATCCTATTTTTGTATATGTCGTTCTTGTCGGGGAGCAACAGCCCATCTTCCGGCTATT 977
Tox             ------------------------------------------------------------

Tgondii         GTCTCGTATCAGTTGTGAAACAGACTGCGTTTTGCCGAAAATGAGTCCTATGTCCGATGG 1037
Tox             ------------------------------------------------------------

Tgondii         CTATTTGTACCGCTTCGTACCATTTCGCTTGTCAGCTGTAATCAACCGAATTCATTTGGC 1097
Tox             ------------------------------------------------------------

Tgondii         GAGACATGATTCCGATTAAATTCTTTACTGCGA 1130
Tox             --------------------------------
```

Figure 4: Published *T. gondii* HPRT (Vasanthakumar *et al.*, 1994) aligned to sequence determined in this study (Tox). The published sequence occurs above the determined sequence. The Met residue (ATG) is shaded. The bold regions are the 6 x His tag (bases 87-104) and thrombin cleavage (bases 114-131) regions respectively of pET-15b. The *Nde*1 (CATATG) and *Bam*H1 (GGATCC) restriction sites are shaded. The stop codon (TAA) is shaded. Gaps underneath the alignments show differences to the published sequence, the asterisks (*) represent identity and the dashes (-) indicate no match made.

University of Cape Town

Appendix 1E: pGEM®-T Vector Sequence

Note: Genetic elements of Promega's plasmid vectors are quality tested for their functionality. The sequence of the multiple cloning site is confirmed using restriction enzyme digestion, but the identity of every base pair of the plasmid has not been established by DNA sequencing. As a result, minor errors may exist in the sequence information provided.

pGEM®-T Vector sequence reference points:

Base pairs	3000
T7 RNA transcription initiation site	1
SP6 RNA transcription initiation site	126
T7 RNA Polymerase promoter (-17 to +3)	2984-3
SP6 RNA Polymerase promoter (-17 to +3)	124-143
multiple cloning region	10-113
phage f1 region	2365-2820
lacZ start codon	165
lac operon sequences	2821-2981; 151-380
lac operator	185-201
beta-lactamase (Ampr) coding region	1322-2182
binding site of pUC/M13 Forward Sequencing Primer	2941-2957
binding site of pUC/M13 Reverse Sequencing Primer	161-177

The sequence supplied below is that of the circular pGEM®-5zf(+) Vector from which the pGEM®-T Vector is derived. The pGEM®-T Vector has been linearized with EcoR V at base 51 (*) and a T-residue has been added to both 3'-ends. The added T is not included in this sequence.

```
   1  GGGCGAATTG GGCCCGACGT CGCATGCTCC CGGCCGCCAT GGCCGCGGGA
  51  T*ATCACTAGTGCGGCCGCCT GCAGGTCGAC CATATGGGAG AGCTCCCAAC
 101  GCGTTGGATG CATAGCTTGA GTATTCTATA GTGTCACCTA AATAGCTTGG
 151  CGTAATCATG GTCATAGCTG TTTCCTGTGT GAAATTGTTA TCCGCTCACA
 201  ATTCCACACA ACATACGAGC CGGAAGCATA AAGTGTAAAG CCTGGGGTGC
 251  CTAATGAGTG AGCTAACTCA CATTAATTGC GTTGCGCTCA CTGCCCGCTT
 301  TCCAGTCGGG AAACCTGTCG TGCCAGCTGC ATTAATGAAT CGGCCAACGC
 351  GCGGGGAGAG GCGGTTTGCG TATTGGGCGC TCTTCCGCTT CCTCGCTCAC
 401  TGACTCGCTG CGCTCGGTCG TTCGGCTGCG GCGAGCGGTA TCAGCTCACT
 451  CAAAGGCGGT AATACGGTTA TCCACAGAAT CAGGGGATAA CGCAGGAAAG
 501  AACATGTGAG CAAAAGGCCA GCAAAAGGCC AGGAACCGTA AAAAGGCCGC
 551  GTTGCTGGCG TTTTTCCATA GGCTCCGCCC CCCTGACGAG CATCACAAAA
 601  ATCGACGCTC AAGTCAGAGG TGGCGAAACC CGACAGGACT ATAAAGATAC
 651  CAGGCGTTTC CCCCTGGAAG CTCCCTCGTG CGCTCTCCTG TTCCGACCCT
 701  GCCGCTTACC GGATACCTGT CCGCCTTTCT CCCTTCGGGA AGCGTGGCGC
```

University of Cape Town

751 TTTCTCATAG CTCACGCTGT AGGTATCTCA GTTCGGTGTA GGTCGTTCGC

801 TCCAAGCTGG GCTGTGTGCA CGAACCCCCC GTTCAGCCCG ACCGCTGCGC

851 CTTATCCGGT AACTATCGTC TTGAGTCCAA CCCGGTAAGA CACGACTTAT

901 CGCCACTGGC AGCAGCCACT GGTAACAGGA TTAGCAGAGC GAGGTATGTA

951 GGCGGTGCTA CAGAGTTCTT GAAGTGGTGG CCTAACTACG GCTACACTAG

1001 AAGAACAGTA TTTGGTATCT GCGCTCTGCT GAAGCCAGTT ACCTTCGGAA

1051 AAAGAGTTGG TAGCTCTTGA TCCGGCAAAC AAACCACCGC TGGTAGCGGT

1101 GGTTTTTTTG TTTGCAAGCA GCAGATTACG CGCAGAAAAA AAGGATCTCA

1151 AGAAGATCCT TTGATCTTTT CTACGGGGTC TGACGCTCAG TGGAACGAAA

1201 ACTCACGTTA AGGGATTTTG GTCATGAGAT TATCAAAAAG GATCTTCACC

1251 TAGATCCTTT TAAATTAAAA ATGAAGTTTT AAATCAATCT AAAGTATATA

1301 TGAGTAAACT TGGTCTGACA GTTACCAATG CTTAATCAGT GAGGCACCTA

1351 TCTCAGCGAT CTGTCTATTT CGTTCATCCA TAGTTGCCTG ACTCCCCGTC

1401 GTGTAGATAA CTACGATACG GGAGGGCTTA CCATCTGGCC CCAGTGCTGC

1451 AATGATACCG CGAGACCCAC GCTCACCGGC TCCAGATTTA TCAGCAATAA

1501 ACCAGCCAGC CGGAAGGGCC GAGCGCAGAA GTGGTCCTGC AACTTTATCC

1551 GCCTCCATCC AGTCTATTAA TTGTTGCCGG GAAGCTAGAG TAAGTAGTTC

1601 GCCAGTTAAT AGTTTGCGCA ACGTTGTTGC CATTGCTACA GGCATCGTGG

1651 TGTCACGCTC GTCGTTTGGT ATGGCTTCAT TCAGCTCCGG TTCCCAACGA

1701 TCAAGGCGAG TTACATGATC CCCCATGTTG TGCAAAAAAG CGGTTAGCTC

1751 CTTCGGTCCT CCGATCGTTG TCAGAAGTAA GTTGGCCGCA GTGTTATCAC

1801 TCATGGTTAT GGCAGCACTG CATAATTCTC TTACTGTCAT GCCATCCGTA

1851 AGATGCTTTT CTGTGACTGG TGAGTACTCA ACCAAGTCAT TCTGAGAATA

1901 GTGTATGCGG CGACCGAGTT GCTCTTGCCC GGCGTCAATA CGGGATAATA

1951 CCGCGCCACA TAGCAGAACT TTAAAAGTGC TCATCATTGG AAAACGTTCT

2001 TCGGGGCGAA AACTCTCAAG GATCTTACCG CTGTTGAGAT CCAGTTCGAT

2051 GTAACCCACT CGTGCACCCA ACTGATCTTC AGCATCTTTT ACTTTCACCA

2101 GCGTTTCTGG GTGAGCAAAA ACAGGAAGGC AAAATGCCGC AAAAAAGGGA

2151 ATAAGGGCGA CACGGAAATG TTGAATACTC ATACTCTTCC TTTTTCAATA

2201 TTATTGAAGC ATTTATCAGG GTTATTGTCT CATGAGCGGA TACATATTTG

University of Cape Town

```
2251 AATGTATTTA GAAAAATAAA CAAATAGGGG TTCCGCGCAC ATTTCCCCGA
2301 AAAGTGCCAC CTGATGCGGT GTGAAATACC GCACAGATGC GTAAGGAGAA
2351 AATACCGCAT CAGGAAATTG TAAGCGTTAA TATTTTGTTA AAATTCGCGT
2401 TAAATTTTTG TTAAATCAGC TCATTTTTTA ACCAATAGGC CGAAATCGGC
2451 AAAATCCCTT ATAAATCAAA AGAATAGACC GAGATAGGGT TGAGTGTTGT
2501 TCCAGTTTGG AACAAGAGTC CACTATTAAA GAACGTGGAC TCCAACGTCA
2551 AAGGGCGAAA AACCGTCTAT CAGGGCGATG GCCCACTACG TGAACCATCA
2601 CCCTAATCAA GTTTTTTGGG GTCGAGGTGC CGTAAAGCAC TAAATCGGAA
2651 CCCTAAAGGG AGCCCCCGAT TTAGAGCTTG ACGGGGAAAG CCGGCGAACG
2701 TGGCGAGAAA GGAAGGGAAG AAAGCGAAAG GAGCGGGCGC TAGGGCGCTG
2751 GCAAGTGTAG CGGTCACGCT GCGCGTAACC ACCACACCCG CCGCGCTTAA
2801 TGCGCCGCTA CAGGGCGCGT CCATTCGCCA TTCAGGCTGC GCAACTGTTG
2851 GGAAGGGCGA TCGGTGCGGG CCTCTTCGCT ATTACGCCAG CTGGCGAAAG
2901 GGGGATGTGC TGCAAGGCGA TTAAGTTGGG TAACGCCAGG GTTTTCCCAG
2951 TCACGACGTT GTAAAACGAC GGCCAGTGAA TTGTAATACG ACTCACTATA
```

Figure 5: pGEM®-T Vector Sequence (Promega website http:\\www.promega.com) © 1995-2001, Promega Corporation). The shaded region appears in the human sequence determined in this study, and shows the region where the human HPRT cDNA was inserted within pGEM®-T.

University of Cape Town

Appendix 1F: NCBI Entrez entry for Human HPRT

```
LOCUS       HUMHPRT 1331 bp    mRNA    linear   PRI 08-NOV-1994
DEFINITION  Human hypoxanthine phosphoribosyltransferase (HPRT) mRNA, complete
            cds.
ACCESSION   M31642 J00205 V00530
VERSION     M31642.1  GI:184349
KEYWORDS    hypoxanthine phosphoribosyltransferase; transferase.
SOURCE      Human, cDNA to mRNA.
ORGANISM    Homo sapiens
            Eukaryota; Metazoa; Chordata; Craniata; Vertebrata; Euteleostomi;
            Mammalia; Eutheria; Primates; Catarrhini; Hominidae; Homo.
REFERENCE   1  (bases 1 to 1331)
AUTHORS     Jolly,D.J., Okayama,H., Berg,P., Esty,A.C., Filpula,D., Bohlen,P.,
            Johnson,G.G., Shively,J.E., Hunkapillar,T. and Friedmann,T.
TITLE       Isolation and characterization of a full-length expressible cDNA
            for human hypoxanthine phosphoribosyl transferase
JOURNAL     Proc. Natl. Acad. Sci. U.S.A. 80 (2), 477-481 (1983)
MEDLINE     83169681
PUBMED      6300847
FEATURES             Location/Qualifiers
     source          1..1331
                     /organism="Homo sapiens"
                     /db_xref="taxon:9606"
                     /map="Xq26.1"
     gene            1..1331
                     /gene="HPRT"
     mRNA            <1..1331
                     /gene="HPRT"
     CDS             86..742
                     /gene="HPRT"
                     /note="hypoxanthine phosphoribosyltransferase"
                     /codon_start=1
                     /protein_id="AAA52690.1"
                     /db_xref="GI:306885"
                     /db_xref="GDB:G00-119-317"
                     /translation="MATRSPGVVISDDEPGYDLDLFCIPNHYAEDLERVFIPHGLIMD
                     RTERLARDVMKEMGGHHIVALCVLKGGYKFFADLLDYIKALNRNSDRSIPMTVDFIRL
                     KSYCNDQSTGDIKVIGGDDLSTLTGKNVLIVEDIIDTGKTMQTLLSLVRQYNPKMVKV
                     ASLLVKRTPRSVGYKPDFVGFEIPDKFVVGYALDYNEYFRDLNHVCVISETGKAKYKA
                     "
BASE COUNT      385 a    237 c    281 g    428 t
ORIGIN          Chromosome Xq26.
        1 tcttgctgcg cctccgcctc ctcctctgct ccgccaccgg cttcctcctc ctgagcagtc
       61 agcccgcgcg ccggccggct ccgttatggc gacccgcagc cctggcgtcg tgattagtga
      121 tgatgaacca ggttatgacc ttgatttatt ttgcatacct aatcattatg ctgaggattt
      181 ggaaagggtg tttattcctc atggactaat tatggacagg actgaacgtc ttgctcgaga
      241 tgtgatgaag gagatgggag gccatcacat tgtagccctc tgtgtgctca agggggggcta
      301 taaattcttt gctgacctgc tggattacat caaagcactg aatagaaata gtgatagatc
      361 cattcctatg actgtagatt ttatcagact gaagagctat tgtaatgacc agtcaacagg
      421 ggacataaaa gtaattggtg gagatgatct ctcaacttta actggaaaga atgtcttgat
      481 tgtggaagat ataattgaca ctggcaaaac aatgcagact ttgctttcct tggtcaggca
      541 gtataatcca aagatggtca aggtcgcaag cttgctggtg aaaaggaccc cacgaagtgt
      601 tggatataag ccagactttg ttggatttga aattccagac aagtttgttg taggatatgc
      661 ccttgactat aatgaatact tcagggattt gaatcatgtt tgtgtcatta gtgaaactgg
      721 aaaagcaaaa tacaaagcct aagatgagag ttcaagttga gtttggaaac atctggagtc
      781 ctattgacat cgccagtaaa attatcaatg ttctagttct gtggccatct gcttagtaga
      841 gctttttgca tgtatcttct aagaatttta tctgttttgt actttagaaa tgtcagttgc
      901 tgcattccta aactgtttat ttgcactatg agcctataga ctatcagttc cctttgggcg
      961 gattgttgtt taacttgtaa atgaaaaaat tctcttaaac cacagcacta ttgagtgaaa
```

University of Cape Town

```
1021 cattgaactc atatctgtaa gaaataaaga gaagatatat tagtttttta attggtattt
1081 taatttttat atatgcagga aagaatagaa gtgattgaat attgttaatt ataccaccgt
1141 gtgttagaaa agtaagaagc agtcaatttt cacatcaaag acagcatcta agaagttttg
1201 ttctgtcctg gaattatttt agtagtgttt cagtaatgtt gactgtattt tccaacttgt
1261 tcaaattatt accagtgaat ctttgtcagc agttcccttt taaatgcaaa tcaataaatt
1321 cccaaaaatt t
```

Figure 6: NCBI Entrez entry for human HPRT. The translation of the nucleotide is shown. The start codon of the coding region of the nucleotide sequence (atg) and the stop codon (taa) are shaded.

University of Cape Town

Appendix 1G: Entrez entry for *P. falciparum* HPRT (King and Melton, 1987)

```
LOCUS       PFHPRT 1059 bp    mRNA    linear   INV 12-SEP-1993
DEFINITION  Plasmodium mRNA for hypoxanthine-guanine phosphoribosyltransferase
            (HPRT).
ACCESSION   Y00519
VERSION     Y00519.1  GI:9901
KEYWORDS    hypoxanthine-guanine phosphoribosyltransferase.
SOURCE      Plasmodium falciparum.
ORGANISM    Plasmodium falciparum
            Eukaryota; Alveolata; Apicomplexa; Haemosporida; Plasmodium.
REFERENCE   1  (bases 1 to 1059)
AUTHORS     King,A.
TITLE       Direct Submission
JOURNAL     Submitted (11-DEC-1987) King A., Dept. Molecular Biology, Edinburgh
            University, Mayfield Road, Edinburgh, EH9 3JR, U.K
REFERENCE   2  (bases 1 to 1059)
AUTHORS     King,A. and Melton,D.W.
TITLE       Characterisation of cDNA clones for hypoxanthine-guanine
            phosphoribosyltransferase from the human malarial parasite,
            Plasmodium falciparum: comparisons to the mammalian gene and
            protein
JOURNAL     Nucleic Acids Res. 15 (24), 10469-10481 (1987)
MEDLINE     88096579
PUBMED      3320967
COMMENT     It is proposed that the run of 28 'A' residues at the 3' end of the
            HPRT mRNA is not a polyA tail but a polyA tract in the 3'
            untranslated region.
            Data kindly reviewed (03-FEB-1988) by King A.
FEATURES             Location/Qualifiers
     source          1..1059
                     /organism="Plasmodium falciparum"
                     /strain="K1"
                     /db_xref="taxon:5833"
     CDS             126..821
                     /note="HPRT (AA 1 - 231)"
                     /codon_start=1
                     /protein_id="CAA68573.1"
                     /db_xref="GI:9902"
                     /db_xref="SWISS-PROT:P07833"
                     /translation="MPIPNNPGAGENAFDPVFVKDDDGYDLDSFMIPAHYKKYLTKVL
                     VPNGVIKNRIEKLAYDIKKVYNNEEFHILCLLKGSRGFFTALLKHLSRIHNYSAVEMS
                     KPLFGEHYVRVKSYCNDQSTGTLEIVSEDLSCLKGKHVLIVEDIIDTGKTLVKFCEYL
                     KKFEIKTVAIACLFIKRTPLWNGFKADFVGFSIPDHFVVGYSLDYNEIFRDLDHCCLV
                     NDEGKKKYKATSL"
BASE COUNT      425 a    120 c    143 g    371 t
ORIGIN
        1 taaaaatttt aataatatac tttcaccaca ccaaaaacca aaaatatata tttaattcat
       61 aatattaaag aaaatatatt tttctttgta tatattatta ctatatattt atataatatt
      121 agaaaatgcc aataccaaat aatccaggag ctggtgaaaa tgcctttgat cccgttttcg
      181 taaaggatga cgatggttat gaccttgatt cttttatgat ccctgcacat tataaaaaat
      241 atcttaccaa ggtcttagtt ccaaatggtg tcataaaaaa ccgtattgag aaattggctt
      301 atgatattaa aaaggtgtac aacaatgaag agtttcatat tctttgtttg ttgaaaggtt
      361 ctcgtggttt tttcactgct ctcttaaagc atttaagtag aatacataat tatagtgccg
      421 ttgagatgtc caaaccatta tttggagaac actacgtacg tgtgaaatcc tattgtaatg
      481 accaatcaac aggtacatta gaaattgtaa gtgaagattt atcttgttta aaaggaaaac
      541 atgtattaat tgttgaagat attattgata ctggtaaaac attagtaaag ttttgtgaat
      601 acttaaagaa atttgaaata aaaaccgttg ccatcgcttg tctttttatt aaaagaacac
      661 ctttgtggaa tggttttaaa gctgatttcg ttggattctc aattcctgat cactttgttg
      721 ttggttatag tttagactat aatgaaattt tcagagatct tgaccattgt tgtttggtta
```

University of Cape Town

```
 781 atgatgaggg aaaaaagaaa tataaagcaa cttcattata aatacattta ttgaagtgat
 841 caaaaatgtc acaacctttc tatttatatc aatttaaaaa aaaaaaaaaa aaaaaaaaaa
 901 aatagagaag aaaatatctg taccaaaaat atatatatat atatatatat atatatatat
 961 atatgtatat atatatttta tgtacatgtt atatatattt atatataact tataatgaac
1021 gtgaactata taaaaaaaaa aaaaaaaaaa aaaaaaaaa
```

Figure 7: NCBI Entrez entry for *P. falciparum* HPRT (King and Melton, 1987). The translation of the nucleotide is shown, and the Met 101 residue (M) is shaded. The start codon of the coding region of the nucleotide sequence (atg) is shaded. The codon for the Met 101 residue (atg) is underlined. The stop codon (taa) is shaded.

University of Cape Town

Appendix 1H: Entrez entry for *P. falciparum* HPRT (Vasanthakumar *et al.*, 1989)

```
LOCUS       PFLACZR  908 bp    mRNA    linear   INV 12-SEP-1993
DEFINITION  Plasmodium falciparum lacZ mRNA for hypoxanthine-guanine
            phosphoribosyltransferase.
ACCESSION   X16279
VERSION     X16279.1  GI:9913
KEYWORDS    hypoxanthine-guanine phosphoribosyltransferase; lacZ gene.
SOURCE      Plasmodium falciparum.
ORGANISM    Plasmodium falciparum
            Eukaryota; Alveolata; Apicomplexa; Haemosporida; Plasmodium.
REFERENCE   1  (bases 1 to 908)
AUTHORS     Vasanthakumar,G.
TITLE       Direct Submission
JOURNAL     Submitted (17-AUG-1989) Vasanthakumar G., Southern Research
            Institute, Biochemistry Research Department, 2000 Ninth Avenue
            South, P O Box 55305, Birmingham AL 35255-5305, UK
REFERENCE   2  (bases 1 to 908)
AUTHORS     Vasanthakumar,G., Davis,R.L. Jr., Sullivan,M.A. and Donahue,J.P.
TITLE       Nucleotide sequence of cDNA clone for hypoxanthine-guanine
            phosphoribosyltransferase from Plasmodium falciparum
JOURNAL     Nucleic Acids Res. 17 (20), 8382 (1989)
MEDLINE     90045974
PUBMED      2682528
COMMENT     see also X16279 for Plasmodium falciparum HPRT mRNA.
FEATURES             Location/Qualifiers
     source          1..908
                     /organism="Plasmodium falciparum"
                     /strain="FCR-3, Gambia"
                     /db_xref="taxon:5833"
                     /clone="pRD500"
                     /clone_lib="puc9, JM106"
     CDS             133..828
                     /note="hypoxanthine-guanine phosphoribosyltransferase (AA
                     1-231)"
                     /codon_start=1
                     /protein_id="CAA34355.1"
                     /db_xref="GI:9914"
                     /db_xref="SWISS-PROT:P20035"
                     /translation="MPIPNNPGAGENAFDPVFVNDDDGYDLDSFMIPAHYKKYLTKVL
                     VPNGVIKNRIEKLAYDIKKVYNNEEFHILCLLKGSRGFFTALLKHLSRIHNYSAVETS
                     KPLFGEHYVRVKSYCNDQSTGTLEIVSEDLSCLKGKHVLIVEDIIDTGKTLVKFCEYL
                     KKFEIKTVAIACLFIKRTPLWNGFKADFVGFSIPDHFVVGYSLDYNEIFRDLDHCCLV
                     NDEGKKKYKATSL"
BASE COUNT      318 a    136 c    135 g    319 t
ORIGIN
        1 aaaatttata caaattttaa tataaacttt caccacacca aaaaccaaaa atatatattt
       61 aattcataat attaaagaaa atatattttt ctttgtatat attattacta tatatttata
      121 taatattaga aaatgccaat accaaataat ccaggagctg gtgaaaatgc ctttgatccc
      181 gttttcgtaa acgatgacga tggttatgac cttgattctt ttatgatccc tgcacattat
      241 aaaaaatatc ttaccaaggt cttagttcca aatggtgtca taaaaaaccg tattgagaaa
      301 ttggcttatg atattaaaaa ggtgtacaac aatgaagagt ttcatattct ttgtttgttg
      361 aaaggttctc gtggtttttt cactgctctc ttaaagcatt taagtagaat acataattat
      421 agtgccgttg agacgtccaa accattattt ggagaacact acgtacgtgt gaaatcctat
      481 tgtaatgacc aatcaacagg tacattagaa attgtaagtg aagatttatc ttgtttaaaa
      541 ggaaaacatg tattaattgt tgaagatatt attgatactg gtaaaacatt agtaaagttt
      601 tgtgaatact taaagaaatt tgaaataaaa accgttgcca tcgcttgtct ttttattaaa
      661 agaacacctt tgtggaatgg ttttaaagct gatttcgttg gattctcaat tcctgatcac
      721 tttgttgttg gttatagttt agactataat gaaatttttca gagatcttga ccattgttgt
```

University of Cape Town

```
781 ttggttaatg atgagggaaa aaagaaatat aaagcaactt cattataaat acatttattg
841 aagtgatcaa aaatgtcaca acctttctat ttatatcaat ttacccccccc ccccccccccc
901 cctgcagg
```

Figure 8: Entrez entry for *P. falciparum* HPRT (Vasanthakumar *et al.*, 1989). The Thr 101 residue (T) is shaded. The start codon of the coding region of the nucleotide sequence (atg) is shaded. The codon for the Thr 101 residue (acg) is underlined. The stop codon (taa) is shaded.

University of Cape Town

Appendix 1I: Entrez entry for *T.gondii* HPRT

```
LOCUS       TGU09219  1130 bp    mRNA    linear   INV 13-DEC-1994
DEFINITION  Toxoplasma gondii RH hypoxanthine-guanine phosphoribosyltransferase
            mRNA, complete cds.
ACCESSION   U09219
VERSION     U09219.1  GI:501059
SOURCE      Toxoplasma gondii.
ORGANISM    Toxoplasma gondii
            Eukaryota; Alveolata; Apicomplexa; Coccidia; Eimeriida;
            Sarcocystidae; Toxoplasma.
REFERENCE   1  (bases 1 to 1130)
AUTHORS     Vasanthakumar,G., van Ginkel,S. and Parish,G.
TITLE       Isolation and sequencing of a cDNA encoding the
            hypoxanthine-guanine phosphoribosyltransferase from Toxoplasma
            gondii
JOURNAL     Gene 147 (1), 153-154 (1994)
MEDLINE     94374703
PUBMED      8088544
REFERENCE   2  (bases 1 to 1130)
AUTHORS     Vasanthakumar,G.
TITLE       Direct Submission
JOURNAL     Submitted (26-APR-1994) G. Vasanthakumar, Southern Research
            Institute, Biological Chemistry, 2000 9th Avenue South, Birmingham,
            AL 35255-5305, USA
FEATURES             Location/Qualifiers
     source          1..1130
                     /organism="Toxoplasma gondii"
                     /strain="RH"
                     /db_xref="taxon:5811"
                     /clone="C1"
                     /clone_lib="Toxoplasma gondii lambda ZAPII cDNA library"
                     /dev_stage="trophozoite"
     CDS             32..724
                     /codon_start=1
                     /product="hypoxanthine-guanine phosphoribosyltransferase"
                     /protein_id="AAA57068.1"
                     /db_xref="GI:501060"
                     /translation="MASKPIEDYGKGKGRIEPMYIPDNTFYNADDFLVPPHCKPYIDK
                     ILLPGGLVKDRVEKLAYDIHRTYFGEELHIICILKGSRGFFNLLIDYLATIQKYSGRE
                     SSVPPFFEHYVRLKSYQNDNSTGQLTVLSDDLSIFRDKHVLIVEDIVDTGFTLTEFGE
                     RLKAVGPKSMRIATLVEKRTDRSNSLKGDFVGFSIEDVWIVGCCYDFNEMFRDFDHVA
                     VLSDAARKKFEK"
     polyA_site      1130
                     /note="19 A residues"
BASE COUNT      273 a    311 c    262 g    284 t
ORIGIN
        1 gcctaccaac ttttccctaa cgtgaagcaa aatggcgtcc aaacccattg aagactacgg
       61 caagggcaag ggccgtattg agcccatgta tatccccgac aacaccttct acaacgctga
      121 tgactttctt gtgccccccc actgcaagcc ctacattgac aaaatcctcc tccctggtgg
      181 attggtcaag gacagagttg agaagttggc gtatgacatc cacagaactt acttcggcga
      241 ggagttgcac atcatttgca tcctgaaagg ctctcgcggc ttcttcaacc ttctgatcga
      301 ctaccttgcc accatacaga agtacagtgg tcgtgagtcc agcgtgcccc ccttcttcga
      361 gcactatgtc cgcctgaagt cctaccagaa cgacaacagc acaggccagc tcaccgtctt
      421 gagcgacgac ttgtcaatct ttcgcgacaa gcacgttctg attgttgagg acatcgtcga
      481 caccggtttc accctcaccg agttcggtga gcgcctgaaa gccgtcggtc ccaagtcgat
      541 gagaatcgcc accctcgtcg agaagcgcac agatcgctcc aacagcttga agggcgactt
      601 cgtcggcttc agcattgaag acgtctggat cgttggttgc tgctacgact tcaacgagat
      661 gttccgcgac ttcgaccacg tcgccgtcct gagcgacgcc gctcgcaaaa agttcgagaa
      721 gtaaaccctg catatgtaga aaagttgtaa cgttagtaaa cgtaacacac gggtataata
```

University of Cape Town

```
 781 gccatttaat ggcgccgtat atttttcact ccccctctcc gataggagga agaaagacga
 841 tccgtctgcg aatgtatatt acatcgaccg gccatagtac gagaagtggt gccggtattg
 901 ttctgtccgg ggatgtacca tcctatttt gtatatgtcg ttcttgtcgg ggagcaacag
 961 cccatcttcc ggctattgtc tcgtatcagt tgtgaaacag actgcgtttt gccgaaaatg
1021 agtcctatgt ccgatggcta tttgtaccgc ttcgtaccat ttcgcttgtc agctgtaatc
1081 aaccgaattc atttggcgag acatgattcc gattaaattc tttactgcga
```

Figure 9: NCBI Entrez entry for *T.gondii* HPRT. The translation of the nucleotide is shown. The start codon (atg) and the stop codon (taa) of the coding region of the nucleotide sequence are shaded.

University of Cape Town

Appendix 1J: SEQUENCING PRIMERS

The primers used for sequencing are presented below:

Sequencing within pGEM®-T

T7 promoter primer 5' TCGCCCTATAGTGAGTCGTATTA 3'

SP6 promoter primer 5' TTTAGGTGACACTATAGAATAC 3'

Sequencing within pET-15b

T7 promoter primer 5' TAATACGACTCACTATAGGG 3'

T7 terminator primer 5' CCGCTGAGCAATAACTAGC 3'

SP6 promoter primer 5' GCTAGTTATTGCTCAGCGG 3'

M13 Forward Primer 5' QCGCCAGGGTTTTCCCAGTCACGAC 3'

M13 Reverse Primer: 5' QGAGCGGATAACAATTTCACACAGG 3'

Q= Cy5 fluorescent label.

Unresolved bases and codes assigned by sequencing software are tabled below (Table 1a)

Table 1a Unresolved bases and associated codes

CODE	UNRESOLVED BASES
M	AC
R	AG
W	AT
S	CG
Y	CT
K	GT
V	ACG
H	ACT
D	AGT
B	CGT
N	ACGT

The sequences obtained are presented unedited. ALF-Express sequence analysis software has been used. Capital letters: unresolved bases, small case letters: unclear whether there is a base at that position or not. The table of unresolved bases was used in conjunction with the sequence viewed in Chromas Version 1.43 (© 1996-1997, McCarthy, C, Griffith University, Brisbane, Australia) when verifying sequences.

University of Cape Town

Additional sequencing information

Instruments: ALFexpress DNA Automated Sequencer.
Amersham Pharmacia Biotech AB (APBiotech)
ABI Prism 3100 Analyser

Sequencing kit and reaction: (dye terminator sequencing, primer walking)

Amersham Pharmacia Biotech Cy5™ Thermo Sequenase Dye Terminator Kit
Thermo Sequenase fluorescent labelled primer cycle sequencing kit with 7-deaza-dGTP (Amersham Pharmacia Biotech).

The chain termination technique of (Sanger *et al.*, 1977) which employs dideoxy cycle sequencing reactions using Thermo Sequenase™ DNA polymerase was used.

All reactions were performed according to the manufacturer's instructions and cycle sequenced.

Amplifier: GeneAmp PCR System 9700, Perkin Elmer, Applied Biosystems

Gelmix: 1) Reprogel Long Read (7%) (APBiotech)
2) 5% Long Ranger gel solution (FMC, BioProducts)

Electrophoresis:
7% or 5% gel: Run according to the manufacturer's operating procedure for 13 h at 55 °C, using a standard gel cassette, 0.5mm spacers and controlled by ALFwin 2.1 software (Amersham Pharmacia Biotech).

Strain of bacterial strain used for expression

E. coli BL21(DE3)pLysS is a lysogen of bacteriophage λDE3, and contains the T7 bacteriophage gene. This gene is controlled by the *lac* UV5 promoter, and encodes T7 RNA polymerase. The pLysS plasmid contains the gene for T7 lysozyme, which lowers the background expression levels of target genes, but does not suppress expression of genes once induction with IPTG has commenced. Bacterial strains containing the plysS plasmid tolerate toxic target proteins, and are easily lysed by freezing and thawing, or the addition of Triton X.

University of Cape Town

Bibliography

Achidi, E.A., Salimonu, L.S., Asuzu, M.C., Berzins, K., and Walker, O. (1996). Studies on *Plasmodium falciparum* parasitemia and development of anemia in Nigerian infants during their first year of life. Am. J. Trop. Med. Hyg. *55*, 138-43.

Ah-Kow, G., Terrier, F., Pouet M-J., and Simonnin M-P (1980). Meisenheimer Spiro Picryl Complex of adenosine. An example of a stereoselective dioxalane ring opening in an acidic medium. J. Org. Chem *45*, 4399-4404.

Allen, T.E. and Ullman, B. (1993). Cloning and expression of the hypoxanthine-guanine phosphoribosyltransferase gene from *Trypanosoma brucei*. Nucleic. Acids. Res. *21*, 5431-8.

Allen, T.E. and Ullman, B. (1994). Molecular characterization and overexpression of the hypoxanthine-guanine phosphoribosyltransferase gene from *Trypanosoma cruzi*. Mol. Biochem. Parasitol. *65*, 233-45.

Aronov, A.M., Munagala, N.R., Ortiz De Montellano, P.R., Kuntz, I.D., and Wang, C.C. (2001). Rational design of selective submicromolar inhibitors of *Tritrichomonas foetus* hypoxanthine-guanine-xanthine phosphoribosyltransferase. Biochemistry *39*, 4684-91.

Azegami M and Iwai K (1964). Specific modification of nucleic acids and their constituents with trinitrophenyl group. J. Biochem. *55*, 346-8.

Bayley, H. and Knowles, J.R. (1977). Photoaffinity labeling. Methods Enzymol. *46*, 69-114.

Berman, P.A., Human, L., and Freese, J.A. (1991). Xanthine oxidase inhibits growth of *Plasmodium falciparum* in human erythrocytes in vitro. J. Clin. Invest. *88*, 1848-55.

Bloor, S.J. (2001). Overview of methods for analysis and identification of flavonoids. Methods Enzymol. *335*, 3-14.

Bois, F., Beney, C., Boumendjel, A., Mariotte, A.M., Conseil, G., and Di Pietro, A. (1998). Halogenated chalcones with high-affinity binding to P-glycoprotein: potential modulators of multidrug resistance. J. Med. Chem. *41*, 4161-4.

Bruce-Chwatt, L. (1985). Essential malariology (London: William Heinemann).

Bugg, C.E., Thomas, J.M., Sundaralingam, M., and Rao, S.T. (1971). Stereochemistry of nucleic acids and their constituents. X. Solid-state base-stacking patterns in nucleic acid constituents and polynucleotides. Biopolymers *10*, 175-219.

Burley, S.K. and Petsko, G.A. (1986). Amino-aromatic interactions in proteins. FEBS Lett. *203*, 139-43.

Campagna, A.C. (1997). Pulmonary toxoplasmosis. Semin. Respir. Infect. *12*, 98-105.

Carlton, J.M., Fidock, D.A., Djimde, A., Plowe, C.V., and Wellems, T.E. (2001). Conservation of a novel vacuolar transporter in Plasmodium species and its central role in chloroquine resistance of *P. falciparum*. Curr. Opin. Microbiol. *4*, 415-20.

University of Cape Town

Carruthers, V.B. (2002). Host cell invasion by the opportunistic pathogen *Toxoplasma gondii*. Acta Trop. *81*, 111-22

Cassady, J.M., Baird, W.M., and Chang, C.J. (1990). Natural products as a source of potential cancer chemotherapeutic and chemopreventive agents. J. Nat. Prod. *53*, 23-41.

Chen, M., Christensen, S.B., Blom, J., Lemmich, E., Nadelmann, L., Fich, K., Theander, T.G., and Kharazmi, A. (1993). Licochalcone A, a novel antiparasitic agent with potent activity against human pathogenic protozoan species of *Leishmania*. Antimicrob. Agents Chemother. *37*, 2550-6.

Cioni, P. and Strambini, G.B. (1994). Pressure effects on protein flexibility monomeric proteins. J. Mol. Biol. *242*, 291-301.

Clarke, R., van den Berg, H.W., and Murphy, R.F. (1990). Reduction of the membrane fluidity of human breast cancer cells by tamoxifen and 17 beta-estradiol. J. Natl. Cancer Inst. *82*, 1702-5.

Conseil, G., Baubichon-Cortay, H., Dayan, G., Jault, J.M., Barron, D., and Di Pietro, A. (1998). Flavonoids: a class of modulators with bifunctional interactions at vicinal ATP- and steroid-binding sites on mouse P-glycoprotein. Proc. Natl. Acad. Sci. U. S. A. *95*, 9831-6.

Cowman, A.F., Morry, M.J., Biggs, B.A., Cross, G.A., and Foote, S.J. (1988). Amino acid changes linked to pyrimethamine resistance in the dihydrofolate reductase-thymidylate synthase gene of *Plasmodium falciparum*. Proc. Natl. Acad. Sci. U. S. A. *85*, 9109-13.

Cox, A.J. (1993). Synthesis of 8-azido xanthosine and an assay to test purine analogues as antimalarial analogues. BSc (Med) Honours Thesis, University of Cape Town, South Africa.

Craig, S.P., 3rd and Eakin, A.E. (2000). Purine phosphoribosyltransferases. J. Biol. Chem. *275*, 20231-4.

Crampton, M.R. (1969). Meisenheimer Complexes. In Advances in Physical Organic Chemistry. Gold V, ed. (London: Academic Press), pp. 211-257.

Critchfield, J.W., Welsh, C.J., Phang, J.M., and Yeh, G.C. (1994). Modulation of adriamycin accumulation and efflux by flavonoids in HCT-15 colon cells. Activation of P-glycoprotein as a putative mechanism. Biochem. Pharmacol. *48*, 1437-45.

Czarnecki, J., Geahlen, R., and Haley, B. (1979). Synthesis and use of azido photoaffinity analogs of adenine and guanine nucleotides. Methods Enzymol. 56, 642-53.

Czarnecki, J.J. (1984). Tautomerism of 2-azidoadenine nucleotides. Effects on enzyme kinetics and photoaffinity labeling. Biochim. Biophys. Acta *800*, 41-51.

Davanloo, P., Rosenberg, A.H., Dunn, J.J., and Studier, F.W. (1984). Cloning and expression of the gene for bacteriophage T7 RNA polymerase. Proc. Natl. Acad. Sci. U. S. A. *81*, 2035-9.

Dayan, G., Baubichon-Cortay, H., Jault, J.M., Cortay, J.C., Deleage, G., and Di Pietro, A. (1996). Recombinant N-terminal nucleotide-binding domain from mouse P-glycoprotein. Overexpression, purification, and role of cysteine 430. J. Biol. Chem. *271*, 11652-8.

University of Cape Town

Derman, A.I., Prinz, W.A., Belin, D., and Beckwith, J. (1993). Mutations that allow disulfide bond formation in the cytoplasm of *Escherichia coli*. Science *262*, 1744-7.

de Wet, H., McIntosh, D.B., Conseil, G, Baubichon-Cortay, H., Krell, T., Jault, J.M., Daskiewicz, J.B., Barron, D., and Di Pietro, A. (2001). Sequence requirements for the ATP-binding site within the C-terminal nucleotide-binding domain of mouse P-glycoprotein: structure-activity relationships for flavonoid binding. Biochemistry *40*, 10382-91

Dormán, G. and Prestwich, G.D. (2000). Using photolabile ligands in drug discovery and development. Trends. Biotechnol. *18*, 64-77.

Dougherty, D.A. (1996). Cation-pi interactions in chemistry and biology: a new view of benzene, Phe, Tyr, and Trp. Science *271*, 163-168.

Dougherty, D.A. and Stauffer, D.A. (1990). Acetylcholine binding by a synthetic receptor: implications for biological recognition. Science *250*, 1558-60.

Dubey, J.P. (1986). Toxoplasmosis. J. Am. Vet. Med. Assoc. 189, 166-70.

Dubey, J.P. (1998). Advances in the life cycle of *Toxoplasma gondii*. Int. J. Parasitol. *28*, 1019-24.

Dupont, Y., Chapron, Y., and Pougeois, R. (1982). Titration of the nucleotide binding sites of sarcoplasmic reticulum Ca^{2+} -ATPase with 2',3'-O-(2,4,6-trinitrophenyl) adenosine 5'-triphosphate and 5'-diphosphate. Biochem. Biophys. Res. Commun. *106*, 1272-9.

Eads, J.C., Scapin, G., Xu, Y., Grubmeyer, C., and Sacchettini, J.C. (1994). The crystal structure of human hypoxanthine-guanine phosphoribosyltransferase with bound GMP. Cell *78*, 325-334.

English, M., Marsh, V, Amukoye, E., Lowe, B., Murphy, S., and Marsh, K. (1996). Chronic salicylate poisoning and severe malaria. Lancet *347*, 1736-7.

Fitzgerald, P.R. (1986). Bovine trichomoniasis. Vet. Clin. North Am. Food Anim. Pract. *2*, 277-82.

Fleet, G.W.J., Porter, R.R., Rodney, R. and Knowles, J.R. (1969). Affinity labelling of antibodies with aryl nitrene as reactive group. Nature (London) *224*, 511-512.

Focia, P.J., Craig, S.P., Nieves-Alicea, R., Fletterick, R.J., and Eakin, A.E. (1998b). A 1.4 A crystal structure for the hypoxanthine phosphoribosyltransferase of *Trypanosoma cruzi*. Biochemistry *37*, 15066-75.

Foote, S.J., Galatis, D., and Cowman, A.F. (1990a). Amino acids in the dihydrofolate reductase-thymidylate synthase gene of *Plasmodium falciparum* involved in cycloguanil resistance differ from those involved in pyrimethamine resistance. Proc. Natl. Acad. Sci. U. S. A. *87*, 3014-7.

Foote, S.J., Kyle, D.E., Martin, R.K., Oduola, A.M., Forsyth, K., Kemp, D.J., and Cowman, A.F. (1990b). Several alleles of the multidrug-resistance gene are closely linked to chloroquine resistance in *Plasmodium falciparum*. Nature *345*, 255-8.

Foote, S.J., Thompson, J.K., Cowman, A.F., and Kemp, D.J. (1989). Amplification of the multidrug resistance gene in some chloroquine-resistant isolates of *P. falciparum*. Cell *57*, 921-30

University of Cape Town

Fung, H.B. and Kirschenbaum, H.L. (1996). Treatment regimens for patients with toxoplasmic encephalitis. Clin. Ther. *18*, 1037-56.

Garcia-Zapata, M.T.A., McGreevy, P.B., and Marsden, P.D. (1991). Hunter's Tropical Medicine. Strickland GT, ed. (Philadelplhia: The WB Saunders Co), pp. 628-637.

Garin, J., Boulay, F., Issartel, J.P., Lunardi, J., and Vignais, P.V. (1986). Identification of amino acid residues photolabeled with 2-azido[alpha-32P]adenosine diphosphate in the beta subunit of beef heart mitochondrial F1-ATPase. Biochemistry *25*, 4431-7.

Giacomello, A. and Salerno, C. (1978). Human hypoxanthine-guanine phosphoribosyltransferase. Steady state kinetics of the forward and reverse reactions. J. Biol. Chem. *253*, 6038-44.

Goitein, R.K., Chelsky, D., and Parsons, S.M. (1978). Primary ^{14}C and alpha secondary ^{3}H substrate kinetic isotope effects for some phosphoribosyltransferases. J. Biol. Chem. *253*, 2963-71.

Gottesman, M.M. and Pastan, I. (1993). Biochemistry of multidrug resistance mediated by the multidrug transporter. Annu. Rev. Biochem. *62:385-427*. 385-427.

Grammer, J.C., Kuwayama, H., and Yount, R.G. (1993). Photoaffinity labeling of skeletal myosin with 2-azidoadenosine triphosphate. Biochemistry *32*, 5725-32.

Gullivan, J.P. and Dougherty, D.A. (1999). Cation-pi interactions in structural biology. Proc. Natl. Acad.Sci. U.S.A. *96*, 9459-64.

Hacker, H.I. (1994). Synthesis and evaluation of xanthine analogues as antimalarial agents.
BSc (Med) Honours Thesis, University of Cape Town, South Africa.

Hanahan, D. (1985). DNA cloning. Glover D, ed. (London: IRL Press Ltd),

Hansch, C., Leo, A. (1979). Substituent constants for correlation analysis in chemistry and biology. (New York), pp. 23-49.

Harborne, J.B. and Williams, C.A. (2000) Advances in flavonoid research since 1992. Phytochemistry *55*, 481-504.

Hassan, H.F. and Coombs, G.H. (1988). Purine and pyrimidine metabolism in parasitic protozoa. FEMS Microbiol. Rev. *4*, 47-83.

Henderson, J.F., Brox, L.W., Kelley, W.N., Rosenbloom, F.M., and Seegmiller, J.E. (1968). Kinetic studies of hypoxanthine-guanine phosphoribosyltransferase. J. Biol. Chem. *243*, 2514-22.

Hèroux, A., White, E.L., Ross, L.J., and Borhani, D.W. (1999a). Crystal structures of the Toxoplasma gondii hypoxanthine-guanine phosphoribosyltransferase-GMP and -IMP complexes: comparison of purine binding interactions with the XMP complex. Biochemistry *38*, 14485-94.

Hèroux, A., White, E.L., Ross, L.J., Davis, R.L., and Borhani, D.W. (1999b). Crystal structure of *Toxoplasma gondii* hypoxanthine-guanine phosphoribosyltransferase with XMP, pyrophosphate, and two Mg(2+) ions bound: insights into the catalytic mechanism. Biochemistry *38*, 14495-14506.

University of Cape Town

Héroux, A., White, E.L., Ross, L.J., Kuzin, A.P., and Borhani, D.W. (2000). Substrate deformation in a hypoxanthine-guanine phosphoribosyltransferase ternary complex: the structural basis for catalysis. Structure. Fold. Des.*8*, 1309-18.

Higgins, C.F. (1992). ABC transporters: from microorganisms to man. Annu. Rev. Cell Biol. *8*, 67-113.

Hiratsuka, T. (1982). Biological activities and spectroscopic properties of chromophoric and fluorescent analogs of adenine nucleoside and nucleotides, 2',3'-O-(2,4,6-trinitrocyclohexadienylidene) adenosine derivatives. Biochim. Biophys. Acta *719*, 509-17.

Hiratsuka, T. (1985). A chromophoric and fluorescent analog of GTP, 2',3'-O-(2,4,6-trinitrocyclohexadienylidene)-GTP, as a spectroscopic probe for the GTP inhibitory site of liver glutamate dehydrogenase. J. Biol. Chem. *260*, 4784-90.

Hiratsuka, T. and Uchida, K. (1973). Preparation and properties of 2'(or 3')-O-(2,4,6-trinitrophenyl) adenosine 5'-triphosphate, an analog of adenosine triphosphate. Biochim. Biophys. Acta *320*, 635-47.

Holden, J.A. and Kelley, W.N. (1978). Human hypoxanthine-guanine phosphoribosyltransferase. Evidence for tetrameric structure. J. Biol. Chem. *253*, 4459-63.

Holmes, R.E. and Robins, R.K. (1964). Purine Nucleosides. VII. Direct Bromination of Adenosine, Deoxyadenaosine, Guanosine, and Related Purine Nucleosides. J. Am. Chem Soc. *86*, 1242-45.

Hunter, C.A. (1993). Sequence-dependent DNA structure. The role of base stacking interactions. J. Mol. Biol. *230*, 1025-54.

Hyatt, J.A. and Swenton,. J.S. (1972a). Facile synthesis of 9H-pyrimido [4,5-b] indole via photolysis of 4-azido-5-phenylpyrimidine. J. Heterocycl. Chem. *9*, 409-10

Hyatt, J.A. and Swenton,. J.S. (1972b). Facile synthesis of 9H-pyrimido [4,5-b] indoles from photolysis of 8-phenyltetrazolo [1,5-c] pyrimidines in acidic media. J. Org. Chem. *37*, 3216-9

Ikehara, M., Uesugi, S., and Yoshida, K. (1972). Studies on the conformation of purine nucleosides and their 5'-phosphates. Biochemistry *11*, 830-6.

Jakobsen, P.H., Bate, C.A., Taverne, J., and Playfair, J.H. (1995). Malaria: toxins, cytokines and disease. Parasite Immunol. *17*, 223-31.

Janse, C.J., van der Klooster, P.F., van der Kaay, H.J., van der Ploeg, M., and Overdulve, J.P. (1986). DNA synthesis in *Plasmodium berghei* during asexual and sexual development. Mol. Biochem. Parasitol. *20*, 173-82.

Jolly, D.J., Okayama, H., Berg, P., Esty, A.C., Filpula, D., Bohlen, P., Johnson, G.G., Shively, J.E., Hunkapillar, T., and Friedmann, T. (1983). Isolation and characterization of a full-length expressible cDNA for human hypoxanthine phosphoribosyl transferase. Proc. Natl. Acad. Sci. U. S. A. *80*, 477-81.

University of Cape Town

Kelley, W.N., Rosenbloom, F.M., Henderson, J.F., and Seegmiller, J.E. (1967). Xanthine phosphoribosyltransferase in man: relationship to hypoxanthine-guanine phosphoribosyltransferase. Biochem. Biophys. Res. Commun. *28*, 340-5.

Keough, D.T., Ng, A.L., Emmerson, B.T., and de Jersey, J. (1998). Expression and properties of recombinant *P. falciparum* hypoxanthine-guanine phosphoribosyltransferase. Adv. Exp. Med. Biol. *431*, 735-9.

Keough, D.T., Ng, A.L., Winzor, D.J., Emmerson, B.T., and de Jersey, J. (1999). Purification and characterization of *Plasmodium falciparum* hypoxanthine-guanine-xanthine phosphoribosyltransferase and comparison with the human enzyme. Mol. Biochem. Parasitol. *98*, 29-41.

King, A. and Melton, D.W. (1987). Characterisation of cDNA clones for hypoxanthine-guanine phosphoribosyltransferase from the human malarial parasite, *Plasmodium falciparum*: comparisons to the mammalian gene and protein. Nucleic. Acids. Res. *15*, 10469-81.

Kioka, N., Hosokawa, N., Komano, T., Hirayoshi, K., Nagata, K., and Ueda, K. (1992). Quercetin, a bioflavonoid, inhibits the increase of human multidrug resistance gene (MDR1) expression caused by arsenite. FEBS Lett. *301*, 307-9.

Knight, K.L. and McEntee, K. (1985). Tyrosine 264 in the recA protein from *Escherichia coli* is the site of modification by the photoaffinity label 8-azidoadenosine 5'-triphosphate. J. Biol. Chem. *260*, 10185-91.

Knowles, J.R .(1972). Photogenerated reagents for biological receptor-site labelling. Accounts of chemical research *5*, 155-60.

Kotyba-Hibert, F., Kapfer, I., and Goeldner, M. (1995). Recent Trends in Photoaffinity Labelling. Angew. Chem. Int. Engl. *34*, 1296-1312.

Kraft, R., Tardiff, J., Krauter, K.S., and Leinwand, L.A. (1988). Using mini-prep plasmid DNA for sequencing double stranded templates with Sequenase. Biotechniques *6*, 544-6, 549.

Krenitsky, T.A., Papaioannou, R., and Elion, G.B. (1969). Human hypoxanthine phosphoribosyltransferase. I. Purification, properties, and specificity. J. Biol. Chem. *244*, 1263-70.

Kumpf, R.A. and Dougherty, D.A. (1993). A mechanism for ion selectivity in potassium channels: computational studies of cation-pi interactions. Science *261*, 1708-10.

Kyle, D.E., Oduola, A.M., Martin, S.K., and Milhous, W.K. (1990). *Plasmodium falciparum*: modulation by calcium antagonists of resistance to chloroquine, desethylchloroquine, quinine, and quinidine in vitro. Trans. R. Soc. Trop. Med. Hyg. *84*, 474-8.

Laemmli, U.K. (1970). Cleavage of structural proteins during the assembly of the head of bacteriophage T4. Nature *227*, 680-5.

Lesch, M. and Nyhan, W.L .(1964). A familial disorder of uric acid metabolism and central nervous system function. Am. J. Med *36*, 561-70.

University of Cape Town

Levy, R.M., Bredesen, D.E., and Rosenblum, M.L. (1985). Neurological manifestations of the acquired immunodeficiency syndrome (AIDS): experience at UCSF and review of the literature. J. Neurosurg. *62*, 475-95.

Li, Y-Z., Kirby, J.P., George, M.W., Poliakoff, M., and Schuster, G.B. (1988). 1,2-Didehydroazepines from the photolysis of substituted aryl azides: analysis of their chemical and physical properties by time-resolved spectroscopic methods. J Am Chem Soc *110*, 8092-8.

Li, C.M., Tyler, P.C., Furneaux, R.H., Kicska, G., Xu, Y., Grubmeyer, C., Girvin, M.E., and Schramm, V.L. (1999). Transition-state analogs as inhibitors of human and malarial hypoxanthine-guanine phosphoribosyltransferases. Nat. Struct. Biol. *6*, 582-7.

Long, R.A., Robins, R.K., and Townsend, L.B .(1967). Purine Nucleosides. XV. The Synthesis of 8-Amino- and 8-Substituted Aminopurine Nucleosides. J. Am. Chem. Soc *32*, 2751-6.

Looareesuwan, S., Ho, M., Wattanagoon, Y., White, N.J., Warrell, D.A., Bunnag, D., Harinasuta, T., and Wyler, D.J. (1987). Dynamic alteration in splenic function during acute falciparum malaria. N. Engl. J. Med. *317*, 675-9.

Luft, B.J., Brooks, R.G., Conley, F.K., McCabe, R.E., and Remington, J.S. (1984). Toxoplasmic encephalitis in patients with acquired immune deficiency syndrome. JAMA *252*, 913-7.

Ma, J.C. and Dougherty, D.A. (1997). The cation-pi interaction. Chem . Rev. *97*, 1303-24.

MacPherson, G.G., Warrell, M.J., White, N.J., Looareesuwan, S., and Warrell, D.A. (1985). Human cerebral malaria. A quantitative ultrastructural analysis of parasitized erythrocyte sequestration. Am. J. Pathol. *119*, 385-401.

Martin, S.K., Oduola, A.M., and Milhous, W.K. (1987). Reversal of chloroquine resistance in *Plasmodium falciparum* by verapamil. Science *235*, 899-901.

Maruyama, T., Gojobori, T., Aota, S., and Ikemura, T. (1986). Codon usage tabulated from the GenBank genetic sequence data. Nucleic. Acids. Res. *14 Suppl*, r151-97.

Mayinger, P. and Klingenberg, M. (1992). Labeling of two different regions of the nucleotide binding site of the uncoupling protein from brown adipose tissue mitochondria with two ATP analogs. Biochemistry *31*, 10536-43.

McCutchan, T.F., Dame, J.B., Miller, L.H., and Barnwell, J. (1984). Evolutionary relatedness of Plasmodium species as determined by the structure of DNA. Science *225*, 808-11.

McIntosh, D.B., Woolley, D.G., and Berman, M.C. (1992). 2',3'-O-(2,4,6-trinitrophenyl)-8-azido-AMP and -ATP photolabel Lys-492 at the active site of sarcoplasmic reticulum Ca(2+)-ATPase. J. Biol. Chem. *267*, 5301-9.

McIntosh, D.B., Woolley, D.G., Vilsen, B., and Andersen, J.P. (1996). Mutagenesis of segment 487Phe-Ser-Arg-Asp-Arg-Lys492 of sarcoplasmic reticulum Ca2+-ATPase produces pumps defective in ATP binding. J. Biol. Chem. *271*, 25778-89.

University of Cape Town

Middleton E and Kandaswami C (1994). The impact of plant flavonoids on mammalian biology: implications for immunity, inflammation and cancer. In The flavonoids: advances in research since 1986. J. Harborne, ed. (London: Chapman and Hall), pp. 619-52.

Munagala, N.R., Chin, M.S., and Wang, C.C. (1998). Steady-state kinetics of the hypoxanthine-guanine-xanthine phosphoribosyltransferase from *Tritrichomonas foetus*: the role of threonine-47. Biochemistry *37*, 4045-51.

Murray HW (1991). Harrison'e Principals of Internal Medicine. Wilson JD, Braunwald E, Esselbacher KJ, Petersdorf RG, Martin JB, Fauci AS, and Root RK, eds. (New York: McGraw-Hill), pp. 795-9.

Musick, W.D. (1981). Structural features of the phosphoribosyltransferases and their relationship to the human deficiency disorders of purine and pyrimidine metabolism. CRC Crit. Rev. Biochem. *11*, 1-34.

Nagesh N and Chatterji D (1997). A useful method for the synthesis of 8 azido-guanosine tri- and tetraphosphate: important substrates for many enzymatic reactions. J. Biochem. Biophys. Meth. *35*, 61-6.

Nakamoto, R.K. and Inesi, G. (1984). Studies of the interactions of 2',3'-O-(2,4,6-trinitrocyclohexyldienylidine)adenosine nucleotides with the sarcoplasmic reticulum (Ca2++ Mg2+)-ATPase active site. J. Biol. Chem. *259*, 2961-70.

Nomura, T., Carlton, J.M., Baird, J.K., del Portillo, H.A., Fryauff, D.J., Rathore, D., Fidock, D.A., Su, X., Collins, W.E., McCutchan, T.F., Wootton, J.C., and Wellems, T.E. (2001). Evidence for different mechanisms of chloroquine resistance in 2 Plasmodium species that cause human malaria. J. Infect. Dis. *183*, 1653-61.

Parsonson, I.M., Clark, B.L., and Dufty, J. (1974). The pathogenesis of *Tritrichomonas foetus* infection in the bull. Aust. Vet. J. *50*, 421-3.

Perez-Victoria, J.M., Chiquero, M.J., Conseil, G., Dayan, G., Di Pietro, A., Barron, D., Castanys, S., and Gamarro, F. (1999). Correlation between the affinity of flavonoids binding to the cytosolic site of *Leishmania tropica* multidrug transporter and their efficiency to revert parasite resistance to daunomycin. Biochemistry *38*, 1736-43.

Peterson, D.S., Walliker, D., and Wellems, T.E. (1988). Evidence that a point mutation in dihydrofolate reductase-thymidylate synthase confers resistance to pyrimethamine in falciparum malaria. Proc. Natl. Acad. Sci. U. S. A. *85*, 9114-8.

Peterson, D.S., Milhous, W.K., and Wellems, T.E. (1990). Molecular basis of differential resistance to cycloguanil and pyrimethamine in *Plasmodium falciparum* malaria. Proc. Natl. Acad. Sci. U. S. A. *87*, 3018-22.

Petti, M.A., Shepodd, T.J., Barrans, R.E.,Jr., and Dougherty, D.A. (1988). Hygroscopic binding of water-soluble guests by high-symmetry, chiral hosts. An electron-rich receptor site with a general affinity for quaternary compounds and electron-deficient π systems. J. Am. Chem. Soc *110*, 6825-40.

Phehane, V.N. (1995). Synthesis and evaluation of xanthine analogues as antimalarials. BSc (Med) Honours Thesis, University of Cape Town, South Africa.

University of Cape Town

Pierpont, W.S. (1986). Flavonoids in Biology and Medicine: Biochemical Pharmacological ans structure-activity relationships. Cody, V., Middleton, E., and Harborne, J.B., eds. (New York: Alan R Liss), pp. 124-40.

Pietta, P.G. (2000). Flavonoids as antioxidants. J. Nat. Prod. *63*, 1035-42.

Pollack, Y., Katzen, A.L., Spira, D.T., and Golenser, J. (1982). The genome of *Plasmodium falciparum*. I. DNA base composition. Nucleic. Acids. Res. *10*, 539-46.

Priev, A., Almagor, A., Yedgar, S., and Gavish, B. (1996). Glycerol decreases the volume and compressibility of protein interior. Biochemistry *35*, 2061-6.

Queen, S.A., Vander Jagt, D., and Reyes, P. (1988). Properties and substrate specificity of a purine phosphoribosyltransferase from the human malaria parasite, *Plasmodium falciparum*. Mol. Biochem. Parasitol. *30*, 123-33.

Queen, S.A., Jagt, D.L., and Reyes, P. (1990). In vitro susceptibilities of *Plasmodium falciparum* to compounds which inhibit nucleotide metabolism. Antimicrob. Agents Chemother. *34*, 1393-8.

Reed, M.B., Saliba, K.J., Caruana, S.R., Kirk, K., and Cowman, A.F. (2000). Pgh1 modulates sensitivity and resistance to multiple antimalarials in *Plasmodium falciparum*. Nature *403*, 906-9.

Reiser, A., Willets, F.W., Terry, G.C., Williams, V., and Marley, R. (1968). Photolysis of aromatic azides. IV. Lifetimes of aromatic nitrenes and absolute rates of some of their reactions. Trans Faraday Soc. *64*, 3265-75

Reiser, A. and Leyshon, L .(1970). Correlation between negative charge on nitrogen and the reactivity of aromatic nitrenes. J. Am. Chem Soc. *92*, 7487

Reisler, E. and Eisenberg, H. (1969). Interpretation of equilibrium sedimentation measurements of proteins in guanidine hydrochloride solutions. Partial volumes, density increments, and the molecular weight of the subunits of rabbit muscle aldolase. Biochemistry *8*, 4572-8.

Rice-Evans, C. (2002). Flavonoid antioxidants. Curr. Med. Chem. 2001. Jun;8(7):797-807.

Rodham, D.A., Suzuki, S., Suenram, R.D., Lovas, F.J., Dasgupta, S., Goddard, W.A., and Blake, G.A. (1993). Hydrogen bonding in the benzene-ammonia dimer. Nature *362*, 735-7.

Rosenthal, P.J. (1998). Proteases of malaria parasites: new targets for chemotherapy. Emerg. Infect. Dis. *4*, 49-57.

Roullet, E. (1999). Opportunistic infections of the central nervous system during HIV-1 infection (emphasis on cytomegalovirus disease). J. Neurol. *246*, 237-43.

Sanger, F., Nicklen, S., and Coulson, A.R. (1977). DNA sequencing with chain-terminating inhibitors. Proc. Natl. Acad. Sci. U. S. A. *74*, 5463-7.

Sasaki, T., Kanematsu, K., and Murata, M. (1971). Heteroaromaticity. XLIX. Tetrazolo-azido iomerization in heteroaromatics. I. Syntheses and reactivities of some tetrazolopolyazines. J. Org Chem. *36*, 446-9.

University of Cape Town

Scalbert, A. and Williamson, G. (2000) Dietary intake and bioavailability of polyphenols. J. Nutr. 130, 2073S-20785S

Scambia, G., Ranelletti, F.O., Panici, P.B., De Vincenzo, R., Bonanno, G., Ferrandina, G., Piantelli, M., Bussa, S., Rumi, C., Cianfriglia, M., *et al.* (1994). Quercetin potentiates the effect of adriamycin in a multidrug-resistant MCF-7 human breast-cancer cell line: P-glycoprotein as a possible target. Cancer Chemother. Pharmacol. *34*, 459-64.

Schumacher, M.A., Carter, D., Ross, D.S., Ullman, B., and Brennan, R.G. (1996). Crystal structures of *Toxoplasma gondii* HGXPRTase reveal the catalytic role of a long flexible loop. Nat. Struct. Biol. *3*, 881-7.

Schuster, G.B. and Platz, M.S. (1992). Photochemistry of phenyl azide. Adv. Photochem. *17*, 69-143.

Sculley, D.G., Dawson, P.A., Emmerson, B.T., and Gordon, R.B. (1992). A review of the molecular basis of hypoxanthine-guanine phosphoribosyltransferase (HPRT) deficiency. Hum. Genet. *90*, 195-207.

Seebregts, C.J. and McIntosh, D.B. (1989). 2',3'-O-(2,4,6-trinitrophenyl)-8-azido-adenosine mono-, di-, and triphosphates as photoaffinity probes of the Ca2+-ATPase of sarcoplasmic reticulum. Regulatory/superfluorescent nucleotides label the catalytic site with high efficiency. J. Biol. Chem. *264*, 2043-52.

Seitz, H.M. and Trammer, T. (1998). Opportunistic infections caused by protozoan parasites. Tokai J. Exp. Clin. Med. *23*, 249-57.

Shapiro, A.B. and Ling, V. (1997a). Effect of quercetin on Hoechst 33342 transport by purified and reconstituted P-glycoprotein. Biochem. Pharmacol. *53*, 587-96.

Shapiro, A.B. and Ling, V. (1997b). Positively cooperative sites for drug transport by P-glycoprotein with distinct drug specificities. Eur. J. Biochem. *250*, 130-7.

Sherman, I.W. (1979). Biochemistry of Plasmodium (malarial parasites). Microbiol. Rev. *43*, 453-95.

Sherman, I.W. (1998). Purine and pyrimidine metabolism of asexual stages. In Malaria. Parasite biology pathogenesis and protection. Sherman IW, ed. (Washington DC: American Society for Microbiology), pp. 177-184.

Shi, W., Li, C.M., Tyler, P.C., Furneaux, R.H., Cahill, S.M., Girvin, M.E., Grubmeyer, C., Schramm, V.L., and Almo, S.C. (1999a). The 2.0 Å structure of malarial purine phosphoribosyltransferase in complex with a transition-state analogue inhibitor. Biochemistry *38*, 9872-80.

Shi, W., Li, C.M., Tyler, P.C., Furneaux, R.H., Grubmeyer, C., Schramm, V.L., and Almo, S.C. (1999b). The 2.0 Å structure of human hypoxanthine-guanine phosphoribosyltransferase in complex with a transition-state analog inhibitor. Nature Structural Biology *6*, 588-93.

Shoemaker, M.T. and Haley, B.E. (1993). Identification of a guanine binding domain peptide of the GTP binding site of glutamate dehydrogenase: isolation with metal-chelate affinity chromatography. Biochemistry *32*, 1883-90.

University of Cape Town

Sirawaraporn, W., Sathitkul, T., Sirawaraporn, R., Yuthavong, Y., and Santi, D.V. (1997). Antifolate-resistant mutants of *Plasmodium falciparum* dihydrofolate reductase. Proc. Natl. Acad. Sci. U. S. A. *94*, 1124-9.

Smith, J.D. and Dunn, D.B. (1959). Occurrence of methylated guanines in ribonucleic acids from several sources. Biochem. J. *72*, 294-301.

Smith, J.D. and Matthews, R.E.F. (1957). The metabolism of 8-azapurines. Biochem J *66*, 323-33.

Somoza, J.R., Chin, M.S., Focia, P.J., Wang, C.C., and Fletterick, R.J. (1996). Crystal structure of the hypoxanthine-guanine-xanthine phosphoribosyltransferase from the protozoan parasite *Tritrichomonas foetus*. Biochemistry *35*, 7032-40.

Somoza, J.R., Skillman, A.G., Jr., Munagala, N.R., Oshiro, C.M., Knegtel, R.M., Mpoke, S., Fletterick, R.J., Kuntz, I.D., and Wang, C.C. (1998). Rational design of novel antimicrobials: blocking purine salvage in a parasitic protozoan. Biochemistry *37*, 5344-8.

Sorensen, T.L., Dupont, Y., Vilsen, B., and Andersen, J.P. (2000). Fast kinetic analysis of conformational changes in mutants of the Ca(2+)-ATPase of sarcoplasmic reticulum. J. Biol. Chem. *275*, 5400-8.

Sponer, J., Leszczynski, J., and Hobza, P. (1996). Hydrogen bonding and stacking of DNA bases: a review of quantum-chemical *ab initio* studies. J. Biomol. Struct. Dyn. *14*, 117-35.

Strauss, M., Behlke, J., and Goerl, M. (1978). Evidence against the existence of real isozymes of hypoxanthine phosphoribosyltransferase. Eur. J. Biochem. *90*, 89-97.

Studier, F.W. and Moffatt, B.A. (1986). Use of bacteriophage T7 RNA polymerase to direct selective high-level expression of cloned genes. J. Mol. Biol. *189*, 113-30.

Sussman, J.L., Harel, M., Frolow, F., Oefner, C., Goldman, A., Toker, L., and Silman, I. (1991). Atomic structure of acetylcholinesterase from *Torpedo californica*: a prototypic acetylcholine-binding protein. Science *253*, 872-9.

Tao, W., Grubmeyer, C., and Blanchard, J.S. (1996). Transition state structure of *Salmonella typhimurium* orotate phosphoribosyltransferase. Biochemistry *35*, 14-21.

Toyoshima, C., Nakasako, M., Nomura, H., and Ogawa, H. (2000). Crystal structure of the calcium pump of sarcoplasmic reticulum at 2.6 A resolution. Nature. *405*, 647-55.

Tran, C.M., Huston, E.E., and Farley, R.A. (1994). Photochemical labeling and inhibition of Na,K-ATPase by 2-Azido-ATP. Identification of an amino acid located within the ATP binding site. J. Biol. Chem. *269*, 6558-65.

Trang, T.T., Phu, N.H., Vinh, H., Hien, T.T., Cuong, B.M., Chau, T.T., Mai, N.T., Waller, D.J., and White, N.J. (1992). Acute renal failure in patients with severe falciparum malaria. Clin. Infect. Dis. *15*, 874-80.

Vasanthakumar, G., Davis, R.L., Jr., Sullivan, M.A., and Donahue, J.P. (1989). Nucleotide sequence of cDNA clone for hypoxanthine-guanine phosphoribosyltransferase from *Plasmodium falciparum*. Nucleic. Acids. Res. *17*, 8382.

University of Cape Town

Vasanthakumar, G., Davis, R.L., Jr., Sullivan, M.A., and Donahue, J.P. (1990). Cloning and expression in *Escherichia coli* of a hypoxanthine-guanine phosphoribosyltransferase-encoding cDNA from *Plasmodium falciparum*. Gene *91*, 63-69.

Vasanthakumar, G., van Ginkel, S., and Parish, G. (1994). Isolation and sequencing of a cDNA encoding the hypoxanthine-guanine phosphoribosyltransferase from *Toxoplasma gondii*. Gene *147*, 153-154.

Waksman, G., Kominos, D., Robertson, S.C., Pant, N., Baltimore, D., Birge, R.B., Cowburn, D., Hanafusa, H., Mayer, B.J., Overduin, M., *et al.* (1992). Crystal structure of the phosphotyrosine recognition domain SH2 of v-src complexed with tyrosine-phosphorylated peptides. Nature *358*, 646-53.

Walter, R.D. and Königk, E. (1974). Hypoxanthine-guanine phosphoribosyltransferase and adenine phosphoribosyltransferase from *Plasmodium chabaudi*, purification and properties. Tropenmed. Parasitol. *25*, 227-35.

Wang, F., Shi, W., Nieves, E., Angeletti, R.H., Schramm, V.L., and Grubmeyer, C. (2001). A transition-state analogue reduces protein dynamics in hypoxanthine-guanine phosphoribosyltransferase. Biochemistry *40*, 8043-54.

Watanabe, T. and Inesi, G. (1982). The use of 2',3'-O-(2,4,6-trinitrophenyl) adenosine 5'-triphosphate for studies of nucleotide interaction with sarcoplasmic reticulum vesicles. J. Biol. Chem. *257*, 11510-6.

Weber, J.L. (1987). Analysis of sequences from the extremely A + T-rich genome of *Plasmodium falciparum*. Gene *52*, 103-109.

Wellems, T.E. and Plowe, C.V. (2001). Chloroquine-resistant malaria. J. Infect. Dis.*184*, 770-6.

White, E.L., Ross, L.J., Davis, R.L., Héroux A., Borhani, D. (1999). Manuscript in preparation, as cited in Héroux *et al.*,(1999a)

White, E.L., Ross, L.J., Davis, R.L., Zywno-Van Ginkel, S., Vasanthakumar, G., and Borhani, D.W. (2000). The two *Toxoplasma gondii* hypoxanthine-guanine phosphoribosyltransferase isozymes form heterotetramers. J. Biol. Chem. *275*,19218-23.

White, N.J., Warrell, D.A., Chanthavanich, P., Looareesuwan, S., Warrell, M.J., Krishna, S., Williamson, D.H., and Turner, R.C. (1983). Severe hypoglycemia and hyperinsulinemia in falciparum malaria. N. Engl. J. Med. *309*, 61-6.

White, N. and Ho, M. (1992). The pathophysiology of malaria. In Advances in parasitology. R.M.J.R.Baker, ed. (London: Academic press), pp. 84-175.

Williams, O.J., McEwan, D., Bertram, J.D., and Gilfedder, J. (1987). Treatment of Trichomoniasis. Aust. Vet. J. *64*, 159-60.

Wilson, C.M., Serrano, A.E., Wasley, A., Bogenschutz, M.P., Shankar, A. H. and Wirth, D.F. (1989). Amplification of a gene related to mammalian mdr genes in drug-resistant *Plasmodium falciparum*. Science. *244*, 1184-86

University of Cape Town

Wilson, C.M., Volkman, S.K., Thaithong, S., Martin, R.K., Kyle, D.E., Milhous, W.K., and Wirth, D.F. (1993). Amplification of pfmdr 1 associated with mefloquine and halofantrine resistance in *Plasmodium falciparum* from Thailand. Mol. Biochem. Parasitol. *57*, 151-60.

Xu, Y., Eads, J., Sacchettini, J.C., and Grubmeyer, C. (1997). Kinetic mechanism of human hypoxanthine-guanine phosphoribosyltransferase: rapid phosphoribosyl transfer chemistry. Biochemistry *36*, 3700-12.

Xue, Z.X., Miller, C.G., Zhou, J.M., and Boyer, P.D. (1987). Catalytic and noncatalytic nucleotide binding sites of chloroplast F1 ATPase. Photoaffinity labeling and peptide sequencing. FEBS Lett. *223*, 391-4.

Yuan, L., Craig, S.P., 3rd, McKerrow, J.H., and Wang, C.C. (1992). Steady-state kinetics of the schistosomal hypoxanthine-guanine phosphoribosyltransferase. Biochemistry *31*, 806-10.

Zaks, A. and Klibanov, A.M. (1988a). The effect of water on enzyme action in organic media. J. Biol. Chem. *263*, 8017-21.

Zaks, A. and Klibanov, A.M. (1988b). Enzymatic catalysis in nonaqueous solvents. J. Biol. Chem. *263*, 3194-201.

Zolg, J.W., Plitt, J.R., Chen, G.X., and Palmer, S. (1989). Point mutations in the dihydrofolate reductase-thymidylate synthase gene as the molecular basis for pyrimethamine resistance in *Plasmodium falciparum*. Mol. Biochem. Parasitol. *36*, 253-62.

Zhong, W., Gullivan, J.P., Zhang,. Y., Li, L., Lester, H.A., and Dougherty, D.A. (1998). From *ab initio* quantum mechanics to molecular neurobiology: a cation-pi binding site in the nicotinic receptor. Proc. Natl. Acad. Sci. U.S.A. *95*, 12088-93.

University of Cape Town